Heterotypic interactions between endothelial and cancer cells in breast cancer progression

Sarah Sophie Steinhäuser

Thesis for the degree of Philosophiae Doctor

Supervisor:
Prof. Dr. Þórarinn Guðjónsson

Co-supervisor:
Dr. Gunnhildur A. Traustadóttir

Doctoral committee:
Dr. Sævar Ingþórsson
Dr. Þórður Óskarsson
Dr. Margrét Helga Ögmundsdóttir

August 2019

UNIVERSITY OF ICELAND
SCHOOL OF HEALTH SCIENCES
FACULTY OF MEDICINE

Samskipti æðaþels og þekjuvefjar í framþróun brjóstakrabbameina

Sarah Sophie Steinhäuser

Ritgerð til doktorsgráðu

Umsjónarkennari og leiðbeinandi:
Prof. Dr. Þórarinn Guðjónsson

Meðleiðbeinandi:
Dr. Gunnhildur A. Traustadóttir

Doktorsnefnd:
Dr. Sævar Ingþórsson
Dr. Þórður Óskarsson
Dr. Margrét Helga Ögmundsdóttir

Ágúst 2019

UNIVERSITY OF ICELAND
SCHOOL OF HEALTH SCIENCES
FACULTY OF MEDICINE

Thesis for a doctoral degree at the University of Iceland. All right reserved. No part of this publication may be reproduced in any form without the prior permission of the copyright holder.

© Sarah Sophie Steinhäuser 2019

ISBN 978-9935-9455-8-7

Printing by Háskólaprent ehf.

Reykjavik, Iceland 2019

Ágrip

Það verður sífellt ljósara að umhverfi krabbameinsfruma, þ.m.t. frumuríkur stoðvefur, spilar lykilhlutverk í stuðningi við framþróun æxlisvaxtar. Það er mikilvægt að rannsaka samskipti milli krabbameinsfruma og stoðvefjar til að skilja betur hvernig ákveðnar frumutegundir í stoðvef styðja við vöxt æxlis og auðvelda meinvarpamyndun. Kirtilgangar og kirtilber brjósta eru umlukin æðaþelsríkum stoðvef og hafa rannsóknir sýnt fram á að æðaþelsfrumur stuðla að vexti og sérhæfingu þekjufruma í brjóstkirtli. Jafnframt er velþekkt að nýmyndun æða er nauðsynlegt skref fyrir framþróun æxlisvaxtar.

Markmið þessa verkefnis var að rannsaka víxlverkandi samskipti milli eðlilegra- og illkynja þekju- og æðaþelsfruma með því að notast við frumulínurnar D492, D492M (sem hvorug myndar æxli í músum) og D492HER2 (sem er æxlismyndandi). D492 er eðlileg brjóstaþekjufrumulína með stofnfrumueiginleika sem í samrækt með æðaþeli undirgekkst bandvefsumbreytingu þekjufruma (e. epithelial-to-mesenchymal transition) og myndaði þannig D492M. D492HER2 var mynduð með yfirtjáningu á HER2 krabbameinsgeninu í D492 og hefur eiginleika illkynja æxlisfruma og sýnir að hluta til svipgerð bandvefsfruma.

Æðaþelsfrumur sem ræktaðar voru í sermislausu æti frá D492HER2 frumum sýndu aukna myndun æðanets í samburði við D492 og D492M. Frumuæti frá æðaþelsfrumum sem áður höfðu verið ræktaðar í frumuæti frá D492HER2 auka frumuskrið D492HER2 fruma, sem gefur til kynna hugsanlega afturvirkni (e. feedback). Með samanburðarkortlagningu á próteinmengi (e. secretome) ætis sem D492 og D492HER2 frumur höfðu verið ræktaðar í greindum við próteinin ECM1 og YKL-40 í D492HER2 frumuætinu sem kandidata fyrir æðasprotamyndun í frumurækt. Með því að slá út ECM1 í D492HER2 dró úr eiginleikum D492HER2 til að stuðla að æðasprotamyndun og afturvirknisáhrif á frumuskrið og ífarandi hegðun D492HER2 voru hindruð. Æðaþelsfrumur sem ræktaðar voru í sermislausu æti frá D492HER2 frumum með „recombinant“ ECM1 (rECM1) sýndu aukna tjáningu á NOTCH1 og NOTCH3. Bæling á NOTCH boðleiðinni í æðaþelsfrumum hindraði aukningu á æðasprotamyndun í frumurækt af völdum rECM1 og hindraði einnig afturvirknisáhrif á frumuskrið og ífarandi hegðun krabbameinsfruma. Niðursláttur (e. knockdown) á ECM1 í D492HER2 leiddi ennfremur til minnkaðrar tjáningar á basalfrumu svipgerð og aukningar á tjáningu GATA3

umritunarþáttarins sem er lykilþáttur í sérhæfingu kirtilþekjufruma og sem er einnig tengdur betri lífslíkum. Niðursláttur á YKL-40 dró einnig úr getu D492HER2 til að stuðla að æðasprotamyndun í frumurækt, dró úr frumuskriði og ífarandi hegðun og myndun berjaklasa formgerðar í þrívíðri rækt.

Niðurstöðurnar sýna að krabbameinsfrumur, í þessu tilfelli HER2 yfirtjáandi brjóstaþekjufrumur, hafa áhrif á æðarnar umhverfis þær með því að seyta ECM1 sem hvatar æðavöxt og ýtir undir afturverkandi áhrif frá æðaþelsfrumunum á krabbameinsfrumurnar þannig að æxlismyndandi eiginleikar þeirra aukast. Ennfremur sýna niðurstöðurnar að ECM1 getur miðlað boðum í gegnum GATA3 og NOTCH boðleiðina í æðaþeli. YKL-40 ýtir hugsanlega undir illkynja hegðun krabbameina með því að auka frumuskrið, ífarandi hegðun og eiginleikann til að stuðla að æðasprotamyndun. Niðurstöður þessarar rannsóknar benda til þess að meðferðarúrræði sem beinast gegn víxlverkandi samskiptum krabbameinsfruma og æðaþelsfruma gætu reynst góð í baráttunni gegn krabbameini.

Lykilorð:

Brjóstakrabbamein, formeðhöndlað æti, æðaþelsvist, ECM1, YKL-40

Abstract

The microenvironment is increasingly being recognized as a key player in supporting cancer progression. Therefore, investigating heterotypic interactions between cancer cells and their microenvironment is important for improving our understanding of how specific cell types support tumor growth and facilitates metastasis. The intralobular breast stroma is highly vascularized and endothelial cells (ECs) are a major cell type in breast cancer microenvironment.

Here, we analyze crosstalk between non-tumorigenic and tumorigenic breast epithelial cells and endothelial cells (ECs) using the cellular model of D492, D492M (both non-tumorigenic) and D492HER2 (tumorigenic). D492 is a breast epithelial cell-line that in co-culture with ECs underwent epithelial-to-mesenchymal-transition and gave rise to D492M. D492HER2 was generated by overexpressing the HER2-oncogene in D492.

Treatment with conditioned medium (CM) from D492HER2 increased endothelial network formation and induced an endothelial feedback increasing cancer cell migration and invasion. Secretome analysis identified extracellular matrix protein 1 (ECM1) and chitinase-3-like protein 1 (CHI3L1/YKL-40) as pro-angiogenic candidates in CM from D492HER2. ECM1 knockdown in D492HER2 reduced the pro-angiogenic properties of D492HER2 and prevented endothelial feedback induction. ECs treated with D492HER2-CM and recombinant ECM1 (rECM1) showed upregulated expression of NOTCH1 and NOTCH3. Inhibition of endothelial NOTCH signaling blocked the increase in endothelial network formation upon rECM1 treatment as well as the induction of the feedback promoting cancer cell migration and invasion. Knockdown of ECM1 in D492HER2 further led to decreased basal marker expression and upregulation of GATA-binding protein 3 (GATA3), which is associated with better prognosis. Knockdown of YKL-40 also reduced pro-angiogenic properties of D492HER2, as well as migration, invasion and formation of grape-like structures in 3D.

These data show that cancer cells affect their vascular niche through secretion of ECM1, resulting in induction of an endothelial feedback enhancing cancer cell tumorigenicity. Further, these data suggest ECM1 as a novel mediator of GATA3 and of endothelial NOTCH signaling. YKL-40 may contribute to cancer aggressiveness by increasing migration, invasion and

pro-angiogenic properties. Targeting the crosstalk between cancer cells and their vascular niche may provide opportunities for improved treatment and development of novel cancer treatments.

Keywords:

Breast cancer, conditioned medium, vascular niche, ECM1, YKL-40

Acknowledgements

The core of the work presented in this thesis was carried out at the Stem Cell Research Unit (SCRU) as part of the Biomedical Center at the University of Iceland, Háskóli Íslands. In this chapter, I would like to thank the many people that have contributed to this work and helped and supported me on all different levels during my PhD project.

First of all, I would like to thank my supervisor **Þorarinn Guðjónsson** for giving me the opportunity to to perform this project in his lab. It has been a privilege working with you. Thank your for your guidance, support and understanding during this time, both on a professional and personal level.

Next, I would like to thank my advisor and dear collueage **Gunnhildur Ásta Traustadóttir** for all the help. You always had an open ear for any kind of lab issues, took the time for critical discussions and gave very valuable advise throughout the time of the project. Thank you for being a great mentor and dear friend.

Also, I would like to thank the other members of my doctoral committee, **Sævar Ingþórsson, Þórður Óskarsson** and **Margret Helga Ögmundsdóttir**. Thank you for your support and valuable input during the committee meeting and beyond. In this context, I would also like to thank **Magnús Karl Magnússon** for his valuable ideas and discussions in the initial phase of my project.

Many thanks go to **Þórður Óskarsson** and all members of his lab at the DKFZ in Heidelberg, **Angi, Maren, Jacob** and **Kristin** as well as **Jasmin** and **Aileen** for all the support and great times during my stay there. Also I want to thank **Gunhild Mælandsmo** for giving me the opportunity to visit her lab at the Radium Hospital in Oslo and for conducting the *in vivo* studies.

Importantly, I would like to thank all current and former members of the Stem Cell Research Unit. **Amaranta (guapa), Zuzan(it)a** and **Erika**, thank you for great scientific discussions during my project but even more for being very close friends outside of the lab. I will miss the great times we spend together! **Alex**, thank you for great discussions and for making the lab an even more enjoyable place with your humor, understanding and positivity. **Anna Karin, Jennifer, Ari, Sævar, Bryndis, Jon Pétur, Kata, Jón Þór, Tobias, Bylgja** and **Eirikur**, thank you for all advise and support! Also **Halla**

and **Sigga**, thank you for great company in and outside of the lab. I would also like to thank **Óttar Rólfsson** and everybody from the Systems Biology lab at the University of Iceland, especially **Qiong** for all her help with the secretome analysis and great times together also outside of work. Thanks also to everybody else at the Biomedical Center, Department of Pathology and Landspitali. In this context, I also want to thank **Valerie H. Meier** and **Ólafur S. Andrésson** for their special support.

In the end, I would like to thank my family in Germany and Iceland for all their support from near and far through good and tough times during my PhD and beyond.

Contents

Ágrip **3**
Abstract **5**
Acknowledgements **7**
Contents **9**
List of abbreviations **13**
List of figures **17**
List of tables **19**
List of original papers **21**
Declaration of contribution **22**
1 Introduction **25**
1.1 The human mammary gland 25
1.2 Epithelial-stromal interactions 27
1.2.1 Cell-matrix interactions 27
1.2.2 Cell-cell interactions 28
1.2.3 Epithelial-to-mesenchymal transition (EMT) 29
1.3 Breast Cancer as major cause of mortality 32
1.4 Epithelial-stromal interactions in breast cancer 34
1.4.1 Cell-matrix interactions in breast cancer 34
1.4.2 Cell-cell interactions in breast cancer 35
1.5 D492 as cellular model for mammary gland development and breast cancer progression 37
2 Aims **41**
3 Materials and methods **43**
3.1 Cell culture 43
3.1.1 2D cell culture 43
3.1.2 3D cell culture 44
3.2 Migration and invasion assay 44
3.3 Conditioned medium (CM) and mass spectrometry 45
3.4 Transient knockdown (KD) using siRNA 46
3.5 Generation of stable knockdown (KD) and overexpression (OE) cell lines using CRISPRi/CRISPRa 46
3.6 RNA microarray 49
3.7 RNA, cDNA and RT-qPCR 49
3.8 Protein isolation and western blotting 50

3.9 Immunofluorescence (IF) and immunohistochemistry (IHC) 51
3.10 Mouse xenografts 52
3.11 Statistical analysis 52

4 Results and Discussion 53

4.1 Context matters - ECM composition affects expression profile of breast epithelial cells 53
4.2 Cancer-endothelial interactions 55
4.2.1 CM from D492HER2 increases endothelial network formation…. 55
4.2.2 D492HER2-CM induced endothelial feedback on D492HER2 migration and invasion 57
4.2.3 Enrichment of pro-angiogenic factors in D492HER2 transcriptome 59
4.2.4 Identification of ECM1 and YKL-40 as pro-angiogenic factors in the D492HER2 secretome 62
4.3 HER2-overexpressing breast cancer cells secrete ECM1 generating a vascular niche that further accelerates cancer cell migration and invasion (manuscript #I) 65
4.3.1 Recombinant ECM1 and overexpression enhance tube formation and induce endothelial feedback 65
4.3.2 ECM1 upregulates endothelial NOTCH1 and NOTCH3 71
4.3.3 Blocking endothelial NOTCH signaling interrupts increase in network formation and feedback induction 74
4.4 ECM1 knockdown in HER2-expressing breast cancer decreases basal characteristics and promotes better outcome by re-expression of GATA3 (Manuscript #II) 75
4.4.1 ECM1 knockdown leads to loss of basal characteristics and gain of GATA3 expression, associated with better outcome…… 76
4.5 Role of ECM1 in tumor growth and metastatic potential *in vivo* 83
4.5.1 ECM1 in tumor growth 83
4.5.2 ECM1 in metastasis formation 86
4.6 YKL-40/CHI3L1 facilitates migration and invasion in HER2 overexpressing breast epithelial progenitor cells and generates a niche for capillary-like network formation (manuscript III, Morera et al.) 87
4.6.1 YKL-40 expression in D492HER2 is linked to vascular network formation 87
4.6.2 Knockdown of YKL-40 in D492HER2 inhibits migration and invasion 90

4.6.3 YKL-40 affects morphology of D492 cell lines when cultured in 3D culture ... 93

5 Technical considerations ... 95

5.1 Conditioned medium ... 95

5.1.1 Controlled conditions and consistency ... 95

5.1.2 Growth factors ... 96

5.1.3 Storage conditions ... 96

5.2 Endothelial network formation ... 97

5.2.1 Endothelial model system ... 97

5.2.2 Matrigel lot variability ... 98

5.2.3 Conditioned medium treatment ... 99

5.3 Western Blotting ... 99

5.3.1 Protein isolation ... 99

5.3.2 Antibody optimization ... 100

5.4 CRISPRa and CRISPRi ... 101

5.5 Summary ... 102

6 Summary and Conclusions ... 103

References ... 107

Original publications ... 121

... 123

... 179

... 205

List of abbreviations

2D	2-dimensional
3D	3-dimensional
ANGPTL4	Angiopoietin-related protein 4
ACTA2	Smooth muscle actin
Blast	Blasticidin
BMP	Bone morphogenic protein
BMPER	BMP-binding endothelial regulator
BRENCs	Breast endothelial cells
cDNA	Complementary deoxyribonucleic acid
CAF	Cancer-associated fibroblast
CCL5	CC-chemokine ligand 5
CD31	Cluster of differentiation 31 (PECAM gene)
CDH3	P-cadherin
CHI3L1/YKL-40	Chitinase 3-like protein 1
CM	Conditioned medium
COL-I/COL-IV	Collagen I/Collagen IV
CRISPR	Clustered regularly interspaced short palindromic repeats
CRISPRa	CRISPR activation
CRISPRi	CRISPR interference
CSF1	Colony-stimulating factor 1
CXCR4	CXC chemokine receptor 4
CXCL12	CXC chemokine ligand 12
DDR2	Discoidin domain receptor 2
DLL	Delta-like

DNMT1	DNA methyl transferase-1
ECs	Endothelial cells
ECM1	Extracellular matrix protein 1
EGFR	Epithelial growth factor receptor
EMT	Epithelial-to-mesenchymal transition
EPCAM	Epithelial cell adhesion molecule
ER	Estrogen receptor
ERK1/2	Extracellular signal-regulated kinases 1/2
FAK	Focal adhesion kinase
FBS	Fetal bovine serum
FGF2/bFGF	Fibroblast growth factor 2
FOX	Forkhead box protein
FN	Fibronectin
GATA3	GATA-binding protein 3
GO	Gene ontology
GPR124	G-protein coupled receptor 124
GREM1	Gremlin 1
HER2	Human epithelial growth factor receptor 2
HGF	Hepatocyte growth factor
HUVECs	Human umbilical vascular endothelial cells
Hygro	Hygromycin
IF	Immunofluorescence
IL-6	Interleukin 6
ITGB4	Integrin beta 4
JAG	Jagged
KD	Knockdown
KLF8	Kruppel-like factor 8
KRT/CK	Keratin

LAMA1	Laminin 1
LEC	Lymphatic endothelial cell
LFQ	Label-free quantification
lncRNA	long non-coding RNA
LOX	Lysyl oxidase
LV	Left venticle
MET	Mesenchymal-to-epithelial transition
miR/miRNA	microRNA
MMP	Matrix metallopeptidase
MUC1	Mucin 1
NECD	NOTCH extracellular domain
NICD	NOTCH intracellular domain
NR4A1	Nuclear receptor superfamily 4
NTMIC	NOTCH transmembrane intracellular domain
OE	Overexpression
PBS	Phosphate-buffered saline
PDGF	Platelet-derived growth factor
PR	Progesterone receptor
RASGRP3	Ras guanyl releasing protein 3
rBM	Reconstituted basement membrane
rECM1	Recombinant ECM1
RNA	Ribonucleic acid
RT-qPCR	Real-time quantitative polymerase chain reaction
SERPINE1	Plasminogen activator inhibitor 1
sgRNA	Single guide RNA
siRNA	Small interfering RNA
SNAI1/SNAIL	Zink finger transcription factor SNAIL homolog 1
SNAI2/SLUG	Zink finger transcription factor SNAIL homolog 2

SOX	SRY-related HMG-box
STAT5	Signal transducer and activator of transcription 5
TAM	Tumor-associated macrophage
TDLU	Terminal duct lobular unit
TGF-b1	Transforming growth factor b1
TIGD5	Tigger transposable element derived 5
TM4SF18	Transmembrane L 4 six family member 18
TN	Triple-negative
TNC	Tenascin C
TNF-a	Tumor necrosis factor alpha
TNFSF18	TNF superfamily member 18
TWIST1	TWIST family BHLH transcription Factor 1
VEGF	Vascular endothelial growth factor
VEGFR	VEGF Receptor
WB	Western blot
ZEB1/2	Zinc finger E-Box binding homeobox 1/2
zeo	Zeocin
ZNF283	Zinc finger protein 283

List of figures

Figure 1. Structure of the human breast gland. 25
Figure 2. Epithelial-to-mesenchymal transition (EMT). 29
Figure 3. Epithelial-to-mesenchymal transition (EMT) in cancer. 31
Figure 4. Molecular subtypes in breast cancer. 33
Figure 5. D492 cellular model. 39
Figure 6. Schematic setup of transwell migration/invasion assays. 45
Figure 7. Schematic workflow of CRISPRi and CRISPRa. 47
Figure 8. Collagen IV-rich environment promotes basal-like phenotype in breast epithelial cells. 54
Figure 9. D492HER2-CM enhances endothelial network. 56
Figure 10. D492HER2-CM induces endothelial feedback increasing migration and invasion.. 57
Figure 11. D492HER2 shows increased affinity to ECs in 2D and 3D. 58
Figure 12. Enrichment of pro-angiogenic factors in D492HER2. 60
Figure 13. GREM1 knockdown inhibits enhancing effect of D492HER2-CM on endothlial network formation. 61
Figure 14. Identification of ECM1 and YKL-40 as pro-angiogenic candidates in D492HER2 63
Figure 15. Recombinant ECM1 enhances endothelial network. 65
Figure 16. Recombinant ECM1 induces endothelial feedback increasing D492HER2 migration and invasion. 66
Figure 17. CM from MDA-MB-231 enhances endothelial network and induces endothelial feedback increasing MDA-MB-231 migration. 67
Figure 18. ECM1 knockdown inhibits pro-angiogenic effect of D492HER2- and MDA-MB-231-CM. 69
Figure 19. ECM1 knockdown prevents induction of endothelial feedback on D492HER2 migration and invasion. 70

Figure 20. Mildly increased gene expression of candidates in ECs upon treatment with D492HER2-CM compared to CM from D492HER2-kdECM1. 72
Figure 21. ECM1 upregulates endothelial NOTCH1 and NOTCH3 gene and protein expression..... 73
Figure 22. Inhibition of ECM1-induced NOTCH1 and NOTCH3 in ECs prevents increased tube formation and endothelial feedback induction..... 74
Figure 23. ECM1 knockdown leads to loss of basal characteristics in D492HER2. 77
Figure 24. ECM1 knockdown leads to gain of GATA3 expression, associated with better outcome. 78
Figure 25. ECM1 knockdown decreases D492HER2 migration and invasion. 80
Figure 26. Transient KD of ECM1 decreases MDA-MB-231 and D492HER2 migration and invasion. 82
Figure 27. Role of ECM1 in tumor growth and metastatic potential. 85
Figure 28. YKL-40 is higher expressed and secreted by D492HER2. 87
Figure 29. YKL-40 increases endothelial network formation. 88
Figure 30. YKL-40 mediates VEGF-A and VEGF-C expression and increases endothelial proliferation. 90
Figure 31. YKL-40 expression is associated with increased migration and invasion i*n vitro*. 92
Figure 32. KD of YKL-40 affects D492HER2 3D phenotype. 93
Figure 33. Schematic summary of ECM1 inducing an endothelial feedback promoting cancer cell migration and invasion. 103
Figure 34. Schematic summary of ECM1 knockdown decreasing tumorigenic properties of D492HER2. 105

List of tables

Table 1: Cell lines used in this project. 43
Table 2. Plasmids and sgRNAs used for ECM1 KD and OE with CRISPRi/CRISPRa. 48
Table 3. SYBR Green RT-qPCR primers used in this study. 50
Table 4. Antibodies used in this study. 51

List of original papers

This thesis is based on the following original publications, which are referred to in the text by their Roman numerals (I - III):

I. **ECM1 secreted by HER2-overexpressing breast cancer cells promotes formation of a vascular niche accelerating cancer cell migration and invasion.** Steinhaeuser SS, Morera E, Budkova Z, Wang Q, Rolfsson O, Riedel A, Krueger A, Ingthorsson S, Traustadottir GA, Oskarsson T, Gudjonsson T. *Submitted for publication and revised in [Laboratory Investigations].*

II. **ECM1 knockdown in HER2-expressing breast cancer promotes loss of basal characteristics and re-expression of GATA3.** Steinhaeuser SS, Sigurdarsdottir AK, Budkova Z, Hilmarsdottir B, Traustadottir GA, Maelandsmo G, Gudjonsson T. *Manuscript in preparation.*

III. **YKL-40/CHI3L1 facilitates migration and invasion in HER2 overexpressing breast epithelial progenitor cells and generates a niche for capillary-like network formation.** Morera E, Steinhaeuser SS, Budkova Z, Ingthorsson S, Kricker J, Krueger A, Traustadottir GA, Gudjonsson T. *Accepted for publication in [In Vitro Cellular & Developmental Biology].*

In addition, unpublished data are presented:

Context matters - ECM composition affects expression profile of breast epithelial cells. Steinhaeuser SS, Ingthorsson S, Hilmarsdottir B, Gudjonsson T. *unpublished data*.

All accepted manuscripts are reprinted by kind permission of the publishers.

Declaration of contribution

Manuscript #I: ECM1 secreted by HER2-overexpressing breast cancer cells promotes formation of a vascular niche accelerating cancer cell migration and invasion. Manuscript #I is the main manuscript of my thesis and represents the core outcome of my PhD project. It describes the identification of ECM1 as breast cancer-secreted protein that has pro-angiogenic properties and induces an endothelial feedback promoting cancer cell migration and invasion by increasing endothelial NOTCH1/3 expression. Here, I performed experiments with conditioned medium (CM) from D492, D492M and D492HER2 to determine endothelial network formation and feedback induction. I further prepared CM samples for secretome analysis using mass spectrometry and analysed the secretome data, in collaboration with Q. Wang and O. Rolfsson. Next, I generated ECM1 KD and OE cell lines in collaboration with the T. Oskarsson lab. and performed CM experiments to determine its involvement in angiogenesis and feedback induction. *In vivo* studies were performed at the G. Maelandsmo lab. at the Radium Hospital in Oslo, where I prepared the cells for injection and assisted during the procedure of the tumor formation assay. I wrote the manuscript while my supervisor and co-supervisor provided critical reviews and correntions, as well as the other co-authors.

Manuscript #II: ECM1 knockdown in HER2-expressing breast cancer promotes loss of basal characteristics and re-expression of GATA3. This manuscript is in preparation and is a continuation of the main manuscript #1 where I am also the first author. In this manuscript we describe that ECM1 KD leads to GATA3 re-expression in D492HER2, associated with improved outcome according to Kaplan Meier survival analysis. As mentioned in manuscript #1, I generated the ECM1 KD and OE cell lines used also in this manuscript. I performed gene expression analysis and IF stainings, followed by functional analysis of migration and invasion. *In vivo* studies were performed at the G. Maelandsmo lab. at the Radium Hospital in Oslo, where AK Sigurdarsdottir prepared the cells and assisted during the injection for the metastasis assay. IHC stainings of mouse xenografts were done by AK Sigurdarsdottir. I wrote the manuscript in collaboration with the critical reviews from my supervisor and co-supervisor.

Manuscript #III: YKL-40/CHI3L1 facilitates migration and invasion in

HER2 overexpressing breast epithelial progenitor cells and generates a niche for capillary-like network formation. In this manuscript, which represents the main outcome of a PhD project of my colleague E. Morera, I am second author. This manuscipt describes the identification of CHI3L1/YKL-40 as pro-tumorigenic protein upregulated in D492HER2, which is involved in angiogenesis, cancer cell migration and invasion. For this manuscript, I have performed migration and invasion assays for cell lines with OE and KD of YKL-40. I further generated the CM samples for secretome analysis and identification of YKL-40 as highly secreted protein by D492HER2. Also, I generated the volcano plot for representation of the secretome data. I was further involved in writing and correction of the manuscript.

1 Introduction

1.1 The human mammary gland

The female human breast gland is a complex and dynamic organ that undergoes significant cellular changes throughout development that are connected to sexual maturation and reproduction. Mammary gland development consists of distinct stages including embryonic, prepubertal, pubertal, pregnancy, lactation and involution (Henninghausen & Robinson, 2001; Macias & Hinck, 2012). Each developmental stage is characerized by distinct gene expression profiles and extrinsic signaling factors including epidermal growth factor (EGF), growth hormone (GH) and insulin-like growth factor 1 (IGF1) as well as estrogen (ER), progesterone (PR) and prolactin (Henninghausen & Robinson, 2001; Macias & Hinck, 2012). Epithelium and surrounding stroma are the two cellular compartments contributing to the mammary gland, which are derived from ectoderm and mesoderm during embryonic development (Henninghausen & Robinson, 2001). The epithelium consists of a branching ductal system that develops initially during puberty and further extend into a lobuloalveolar compartment during pregnancy (Henninghausen & Robinson, 2001).

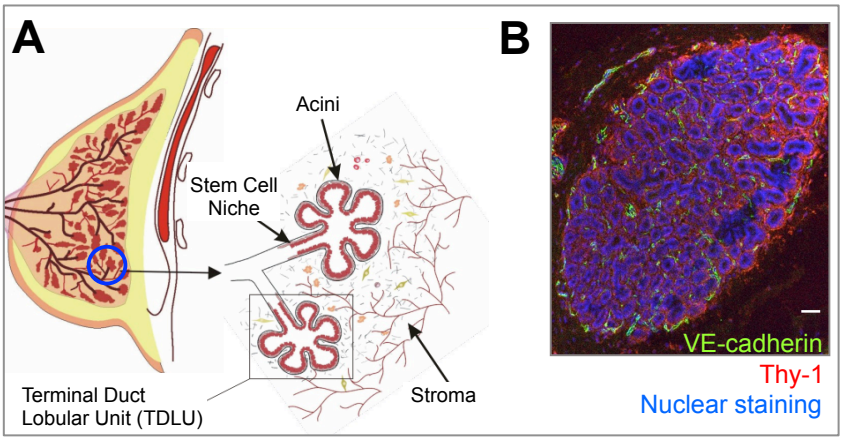


Figure 1. Structure of the human breast gland. Left: Schematic overview over the human breast gland morphology showing the branching ductal system embedded in stroma, ending in the terminal duct lobular units (TDLUs). Right: Representative TDLU (schematic and cross section), composed of luminal and myoepithelial cells and surrounded by basement membrane and stroma containing microvessels, fibroblasts, adipocytes and other cell types. Endothelial VE-cadherin IF-staining (red) shows close proximity of the epithelium and the vasculature. Scale bar = 50 µm. (Sigurdsson et al., 2011).

Mediators of the drastic changes occuring during mammary gland development, maturation and reproduction are a specialized subpopulation of mammary stem cells, able to generate progenitors for both luminal and myoepithelial cells (Gudjonsson et al., 2002; Macias & Hinck, 2012). These tissue-specific stem cells are responsible for continuous tissue remodeling and regeneration during branching morphogenesis in pregnancy, lactation and eventual involution (Henninghausen & Robinson, 2001; Macias & Hinck, 2012). Starting from the nipple as collection of ducts, the ductal system branches further inwards into increasingly smaller ductules and terminates in lobules. The lobules are composed of clusters of acini, connecting to the collective ducts (Fig. 1). These clusters represent the functional milk-producing units of the breast gland, the terminal duct lobular units (TDLUs). As in most branched organs the goal is to achieve as high surface area as possible, maximizing milk production. TDLUs are composed of secretory luminal epithelial cells producing the milk and a surrounding layer of contractile myoepithelial cells pumping the milk through the ductal system towards the nipple.

Phenotypically, luminal and myoepithelial cells can be distinguished by their specific marker expression. Among characteristic luminal markers are Mucin 1 (MUC1), epithelial cell adhesion molecule (EpCAM) and GATA3 as well as luminal cytokeratins including keratin 8 (KRT8), keratin18 (KRT18) and keratin 19 (KRT19) (Gudjonsson et al., 2002). In contrast, myoepithelial cells express high levels of P-cadherin (CDH3), alpha 2 smooth-muscle actin (ACTA2), vimentin and p63 as well as myoepithelial keratins such as keratin 5 (KRT5), keratin 14 (KRT14) and keratin 17 (KRT17) (Gudjonsson et al., 2002). The transcription factor p63 is thereby expressed in the basal layer of the epithelium and vital for maintaining mammary stem cells during development, pregnancy and lactation (Hilmarsdottir et al., 2015).

The epithelial compartment ending in TDLUs is surrounded by basement membrane and embedded in cellular rich stroma, commonly referred to as microenvironment. It consists of extracellular matrix (ECM), rich in filamentous proteins such as collagen, fibronectin and laminin, and multiple cell types including fibroblasts, immune cells and endothelial cells (ECs). Numerous studies suggest that there is constant crosstalk between epithelium and surrounding vascular-rich stroma that plays a significant role in regulating epithelial differentiation during branching morphogenesis in the breast (Bissell et al., 1982; Ghajar et al., 2013; Gudjonsson et al., 2003; Hovey et al., 2001; Ingthorsson et al., 2010; Rossiter et al., 2007).

1.2 Epithelial-stromal interactions

During embryonic development and during puberty, stroma plays an important role in directing epithelial differentiation and rudimentary duct formation in the developing mammary gland (Macias & Hinck, 2012). Thereby, components of the ECM itself as well as other stromal cell types can be essential regulators of mammary development.

1.2.1 Cell-matrix interactions

Matrix proteins are essential components of cell regulation and developmental programs in various tissues through the body. Consisting of structural proteins such as laminins, collagens, fibronectin and others, the matrix provides support and structure to tissues and also interacts with other cells through a variety of specific receptors. Thereby, the ECM is involved in mediating various processes such as cell survival, proliferation or migration (Muschler & Streuli, 2010; Sternlicht, 2006).

The ECM surrounding epithelial cells, vascular endothelial cells and adipocytes in the mammary gland consists of glycoproteins and proteoglycans, constructed around laminin polymers and crosslinked collagen IV fibrils. This ECM is commonly referred to as the basement membrane (BM). The main isoforms of laminins in the BM surrounding the epithelium in the breast are laminin-111, -322, -511 and -521 (Muschler & Streuli, 2010). The most-studied group of receptors through which ECM proteins interact with mammary epithelial cells are integrins. Integrins are heterodimers consisting of an alpha and beta chain. They include receptors for collagen (α1β1 and α2β1), for laminin-111, -511 and -521 (α3β1, α6β1, and α6β4), for laminin-322 (α3β1 and α6β4) and fibronectin and vitronectin (α5β1 and α5β3). Studies using 3D cultures of mammary epithelial cells and Madin-Darby Canine Kidney (MDCK) cells indicate that laminin-111 and β1-integrins play central roles in establishing apical-basal polarity, which is a key mechanism for lumen formation (Muschler & Streuli, 2010; Yu et al., 2005) Furthermore, loss of β1 integrin results in reduced mammary outgrowth and lactation failure through loss of signal transducer and activator of transcription 5 (STAT5) activity (Naylor et al., 2005). Specific blocking antibodies for laminin-1 inhibited branching in the breast, lung, salivary gland and pancreas (Kleinman et al., 2003). Also, extracellular collagens are essential contributors during mammary development. So far, 28 different types of collagens have been identified, divided into fibrilar and non-fibrilar collagens (Egeblad et al., 2010; Insua-Rodriguez & Oskarsson, 2016). Whereas collagen I is involved in directing proper branch orientation, involvement of

collagen IV has been shown in regulation of ERa expression and function (Zhu et al., 2014). Collagen IV is found at the basal surface of epithelial and endothelial cells and is also required for maintainance of tissue polarity (Egeblad et al., 2010; Insua-Rodriguez & Oskarsson, 2016; Kalluri, 2003).

Apart from ECM components themselves, several other cell types present in the stroma are also involved in mediating mammary gland development and epithelial differentiation.

1.2.2 Cell-cell interactions

Wiesen et al. (1999) reported that signaling through stromal EGFR plays an important role in ductal growth and morphogenesis (Wiesen et al., 1999). Epithelial-secreted amphregulin (AREG) binds to stromal EGFR and activates downstream signaling through matrix metallopeptidases MMP14 and MMP2, promoting mammary ductal elongation (Sternlicht, 2006). Depletion of EGFR in stromal but not epithelial cells significantly disrupted ductal development, suggesting an important contribution of stromal signaling to mammary gland development and morphogenesis (Wiesen et al., 1999).

Schwertfeger and colleagues reported that macrophages as part of the surrounding stroma play a significant role during mammary development (Schwertfeger et al., 2006). Macrophages are thought to promote branching morphogenesis via secretion of the macrophage growth factor CSF1 during postnatal mammary gland development through to lactation (Gouon-Evans et al., 2002). Also, fibroblasts as stromal components are important contributors to gland development. Morsing and colleagues have recently demonstrated that TDLU-associated fibroblasts differ in their expression profile from ductal fibroblasts and are able to efficiently stimulate branching morphogenesis (Morsing et al., 2016). Ucar and colleagues identified the microRNAs miR212 and miR132 as essential for epithelial-stromal interactions during pre-pubertal development of the mammary gland in mice. The expression of miR212 and miR132 appears to be restricted to the mammary gland stroma, especially fibroblasts (Ucar et al., 2010). Knockout mice for miR212 showed significantly impaired ductal outgrowth, indicating that these stromal microRNAs are essential mediators of epithelial-stromal signaling during development of mammary epithelial structures.

Another cell type present in mammary stroma are endothelial cells (ECs). They are the major components forming organ-specific vasculature and are therefore already important during organ development by providing ways for delivering oxygen and nutrients. However, studies indicate that their role is

actually far beyond that. In a 3-dimensional *in vitro* model of breast morphogenesis, the presence of breast endothelial cells strongly enhanced the ability of breast epithelial cells to form TDLU-like structures (Ingthorsson et al., 2010; Sigurdsson et al., 2011). Furthermore, ECs have been shown to induce a process called epithelial-to-mesenchymal transition (EMT) in breast epithelial cells (Briem et al., 2019; Sigurdsson et al., 2011).

1.2.3 Epithelial-to-mesenchymal transition (EMT)

During the process of EMT, epithelial cells undergo phenotypic changes resulting in loss of epithelial characteristics such as adhesion and downregulation of epithelial markers (e.g. E-cadherin) and epithelial cytokeratins on both gene and protein expression level (Fig. 2). At the same time, mesenchymal markers such as N-cadherin and vimentin are upregulated and cells show increased migration ability (Kalluri & Weinberg, 2009; Thiery et al., 2009).

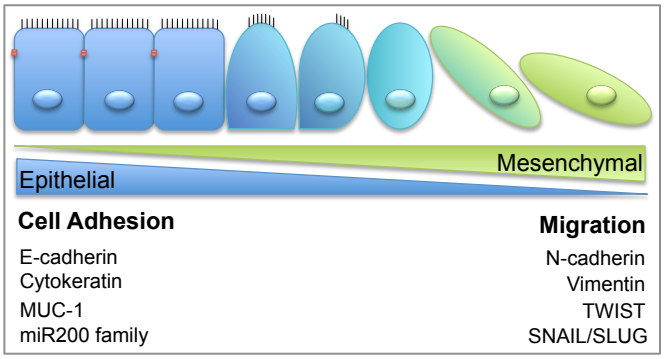


Figure 2. Epithelial-to-mesenchymal transition (EMT). Epithelial cells loose epithelial characteristics (e.g. adhesion) and epithelial marker expression while gaining mesenchymal characteristics (e.g. migration) and mesenchymal marker expression.

1.2.3.1 EMT in embryogenesis, development and wound healing

EMT plays an important role during embryogenesis, normal organ development and wound healing. During embryonic development, EMT plays an important role during gastrulation for the formation of the three germ layers (Kalluri & Weinberg, 2009). Later on, epithelial cells of the neuroectoderm undergo EMT and give rise to migratory neural crest cells. These cells then dissociate from the neural folds, become motile and travel to different parts of the embryo, where they undergo further differentiation. On the molecular level, this process is characterized by upregulated expression of EMT transcription factors such as SRY-related HMG-box (SOX), zink

finger transcription factors SNAI1 and SNAI2 and forkhead box protein FOXD3 in the premigratory neural crest cells. Subsequently, these cells undergo EMT and gain mesenchymal characteristics before they undergo the reverse process of mesenchymal-to-epithelial transition (MET), where they re-gain epithelial characteristics and differentiate (Kalluri & Weinberg, 2009). In addition to its role during development, EMT also is involved in the physiological response to injury. During wound healing, keratinocytes loose adhesion and gain the ability to migrate as individual cells in order to close the wound. This is characterized by upregulated SLUG expression at the migratory front (Thiery et al., 2009). In addition to transcription factors as direct regulators of downstream marker expression in EMT, post-transcriptional regulation by non-coding RNAs plays a major role in enhancing or suppressing EMT/MET marker expression. The major classes of non-coding RNAs are miRNAs (micro RNAs) and lncRNAs (long non-coding RNAs), which are increasingly investigated and recognized as important regulators of gene expression both during development and disease. One fundamental regulator during EMT is the miR200 family, which plays an essential role in maintaining E-cadherin expression and epithelial integrity (Briem et al., 2019; Hilmarsdottir et al., 2015).

1.2.3.2 EMT in cancer progression

Numerous studies have shown that cancer cells are able to hijack the EMT process in the context of cancer progression, metastasis formation and chemotherapy resistance (Fig. 3). Various *in vitro* and *in vivo* studies have demonstrated that cancer cells can acquire mesenchymal characteristics, followed by loss of adhesion, intravasation and transport through the blood vessels, extravasation and formation of micro- and ultimately macrometastases in distant organs (Kalluri & Weinberg, 2009; Thiery et al., 2009; Yang & Weinberg, 2008). Although the exact role of EMT in metastasis formation is still debated, it is considered a key process during cancer progression. One of the major challenges is to distinguish tumor cells that have undergone EMT from the resident fibroblasts and/or myofibroblasts.

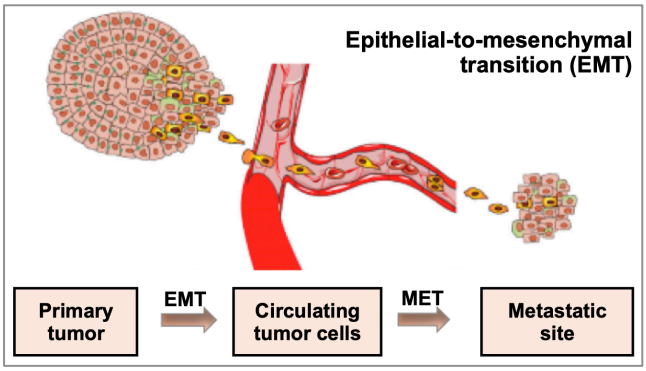


Figure 3. Epithelial-to-mesenchymal transition (EMT) in cancer. Cancer cells at the primary tumor site loose cell adhesion, gain migratory capacity and leave the primary tumor, invade the blood vessels and travel as circulating tumor cells to distant sites. After leaving the circulatory system, they undergo the reverse process of mesenchymal-to-epithelial transition (MET) and re-gain epithelial characteristics, allowing them to attach and proliferate and form metastases (Fabregat et al., 2016).

In colon carcinoma, EMT is especially frequent at the invasive front of tumors as a result of deregulated WNT signaling, which leads to the generation of single mesenchymal-like cells with high migratory capacity and loss of E-cadherin expression (Thiery et al., 2009). This phenomenon is also seen in other types of cancer. Recent studies show that the invasive fronts in papillary thyroid carcinoma and some breast carcinomas also exhibit an EMT expression profile and in cervical carcinoma, cells at the invasive front show increased vimentin expression and loss of E-cadherin (Thiery et al., 2009). Since the invasive front is the immediate interface between tumor and stroma, this points out the potential importance of stromal signals in EMT induction and therefore cancer progression. Indeed, studies have shown that secreted factors from tumor-associated stroma such as hepatocyte growth factor (HGF), EGF, platelet-derived growth factor (PDGF) and transforming growth factor b1 (TGF-b1) are involved in the induction of EMT-modulating transcription factors such as SNAI1, SNAI2, zink finger E-box binding homeobox 1/2 (ZEB1/2), Kruppel-like factor 8 (KLF8), TWIST and FOXC2 in carcinoma cells (Kalluri & Weinberg, 2009; Thiery, 2002; Thiery et al., 2009; Yang & Weinberg, 2008). KFL8 has been shown to induce EMT and tumor invasion in breast cell lines after directly binding to the E-cadherin promoter through GT boxes (Thiery et al., 2009; Wang et al., 2007). Tran and colleagues reported that endogenous expression of SNAI1 in breast cancer mouse models was restricted to primary tumors and was required and sufficient for breast cancer metastasis (Santamaria et al., 2017; Tran et al., 2014). In a spontaneous SCC mouse model, upregulation of TWIST1

expression promoted invasive carcinoma progression and dissemination into the bloodstream (Santamaria et al., 2017; Tsai et al., 2012).

One major challenge in cancer treatment is tumor heterogeneity and development of drug resistance. Recent studies provide evidence that cancer cells are able to undergo EMT only partially, hence to varying degrees, which leads to the existence of distinct cell populations within one tumor (Saitoh, 2018). The presence of multiple cell populations could contribute to drug resistance followed by later relapse of that particular tumor. The ability to go through EMT/MET indicates a high degree of cellular plasticity, often in response to changes in the microenvironment. Further elucidating the role of the microenvironment in regulation of phenotypic plasticity, EMT/MET and beyond can therefore give novel insights in the underlying mechanisms of cancer progression.

1.3 Breast Cancer as major cause of mortality

According to the World Health Organization, cancer is one of the leading causes of death worldwide being responsible for 9.6 million deaths in the year 2018 (https://www.who.int/news-room/fact-sheets/detail/cancer, 4.2.19). For women, breast cancer is the most common type of cancer and the most frequent cause of cancer-related deaths, as reported by The Cancer Atlas (http://canceratlas.cancer.org/the-burden/breast-cancer/, 4.2.19). Despite new methods in assessing the genetic background of cancers (next-generation sequencing), metastatic diseases remain largely incurable and are still one of the main causes of cancer related deaths (Turajlic et al., 2016).

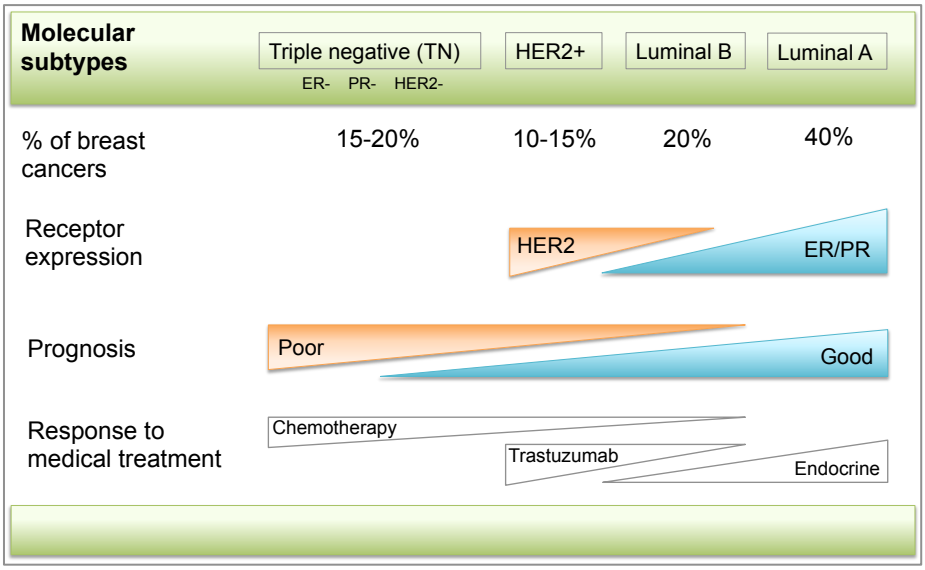


Figure 4. Molecular subtypes in breast cancer. Devision of breast cancer into distinct subgroups of triple-negative (TN), HER2-positive, luminal A and luminal B subtype, according to Perou and Sorlie (2000). Percentage of total breast cancers is presented for each subgroup as well as receptor expression, prognosis and response to chemotherapy. Schematic adapted from McMaster Pathophysiology Review, http://www.pathophys.org/breast-cancer/breastcancer-copy/ (4.2.19).

There are multiple ways of subtyping breast cancer. Using cDNA microarrays derived from primary tumor samples, Perou and Sorlie grouped breast tumors using hierarchical clustering into distinct subgroups (Perou et al., 2000; Sorlie et al., 2001; Sorlie et al., 2003). Herein, the most prominent groups were Luminal A, Luminal B, triple-negative (TN), HER2-enriched and Normal-like breast cancer, with the last one resembling in signature to that of normal breast gland (Fig. 4). Whereas luminal A and B tumors are estrogen receptor (ER) positive, HER2-enriched tumors show high expression of the HER2/ERBB2 (human epidermal growth factor receptor 2) receptor. HER2-enriched tumors are usually ER-negative and more prone to form metastasis due to high heterogeneity. They can be treated using Trastuzumab (Herceptin), a monoclonal antibody inhibiting the function of the HER2 receptor (Baselga et al., 1998), which can greatly increase survival of HER2 breast cancer patients. However, in many cases tumor cells can develop resistance against trastuzumab, which leads to relapse after initial improvement (Lee et al., 2014c).

TN tumors are characterized by low expression of epithelial cadherins and keratins and are believed to originate from the least differentiated progenitor

populations of the breast (Perou, 2011). The majority of TN breast cancers show basal characteristics and are referred to as basal-like (Gazinska et al., 2013; Rakha & Ellis, 2009). Basal-like breast cancer is more common in young women and has high rates of metastasis, as cancer cells are more invasive. Due to lack of targetable receptor expression, basal-like breast cancer has been difficult to treat and therefore has the worst prognosis. However, basal characteristics are not only associated with worse outcome in TN breast cancer. Martin-Castillo and colleagues have suggested the existence of a subpopulation of HER2+ cancer cells with increased basal or stem-like signature that is prone to acquire trastuzumab resistance in contrast to a more luminal trastuzumab-sensitive subpopulation (Martin-Castillo et al., 2013). Through high heterogeneity, populations of HER2+ cells are able to enter or exit the trastuzumab-sensitive stage and therefore escape therapy (Martin-Castillo et al., 2013). In addition to intrinsic pathways, Martin-Castillo et al. also suggest the involvement of microenvironmental signaling in mediating the induction of stem-like characteristics, underlining the potential impact of the stroma in cancer progression (Roswall et al., 2018).

1.4 Epithelial-stromal interactions in breast cancer

In addition to its role during normal development, recent studies provide evidence that signals from the microenvironment can be an important factor in malignant growth that goes beyond their role in EMT induction. The interaction between cancer cells and the microenvironment leads to generation of niches that support tumor growth, both at the primary site and at distant metastatic sites. The stromal niche surrounding a tumor can have profound effects on tumor cell behavior, facilitate tumor growth and progression, and possibly even initiate malignant transformation (Erler & Weaver, 2009; Ghajar et al., 2013; Hoye & Erler, 2016; Ingthorsson et al., 2010; Insua-Rodriguez & Oskarsson, 2016; Lowy & Oskarsson, 2015). Both the ECM and different cell types in the stroma have been shown to affect tumorigenic properties of cancer cells.

1.4.1 Cell-matrix interactions in breast cancer

One protein of interest in the context of cell-matrix interactions is the ECM protein tenascin C (TNC), which is significantly expressed during embryonic development. In adult tissues, TNC expression is restricted, but is highly induced in the context of tissue regeneration and cancer. Studies have shown that TNC is overexpressed across different cancer types, indicating

substantial ECM remodeling within the tumor tissue. TNC further enhances migratory and invasive cell behavior, angiogenesis and cancer cell viability under stress, thereby promoting tumor progression (Lowy & Oskarsson, 2015; Oskarsson et al., 2011). The Erler research lab has showed that tumor-secreted lysyl oxidase (LOX) participates in crosslinking collagen IV at distant sites and thereby mediates the formation of a pre-metastatic niche promoting the invasion of metastatic tumor cells (Erler et al., 2009). Furthermore, Zhang and colleagues reported that binding of type I collagen to the discoidin domain receptor 2 (DDR2) stimulates the activity of mitogen-activated protein kinase ERK2. Activation of ERK2 then leads to phosphorylation and nuclear accumulation of SNAIL1, promoting breast cancer cell invasion and metastasis (Zhang et al., 2013). In addition, there is growing evidence that laminin-332 and -511 may be involved in cancer progression by increasing cancer cell migration and invasion (Insua-Rodriguez & Oskarsson, 2016). In contrast, laminin-111 may function as an inhibitor of dissemination in breast cancer. In 3-dimensional cultures of breast cancer cells, laminin-111 prevented methylation of the E-cadherin promoter by decreasing expression of DNA methyl transferase-1 (DNMT1). This resulted in increasing expression levels of E-cadherin and therefore increased cell-cell adhesion, preventing cancer cell dissemination from the primary tumor (Benton et al., 2009; Insua-Rodriguez & Oskarsson, 2016).

These and many more studies provide evidence that the microenvironment surrounding a tumor can contribute to a large extent to its progression or regression and therefore plays an essential role in patient prognosis. In addition to the ECM as a player in cancer cell communication, also stromal cells are involved in the crosstalk with cancer cells.

1.4.2 Cell-cell interactions in breast cancer

In addition to direct cell-matrix interactions, many studies have focused on exploring the role of immune cells and fibroblasts in cancer progression (Komohara et al., 2014; Komohara & Takeya, 2017; Pollard, 2008; Shan et al., 2017; Zhang et al., 2017). Komohara and research colleagues have described that tumor-associated macrophages (TAMs) induced by tumor-secreted cytokines promote tumor growth by suppressing anti-tumor immunity as well as inducing angiogenesis, invasion and metastasis (Komohara et al., 2014). In addition to TAMs, cancer-associated fibroblasts (CAFs) have also been reported to drive invasion and tumor progression (Komohara & Takeya, 2017; Shan et al., 2017). Zang et al. showed that activation of resting fibroblasts leads to loss of exosomal miR320a, which

contributes to increased proliferation and metastasis in hepatocellular carcinoma (Zhang et al., 2017).

More recent studies, however, suggest that in addition to immune cells and fibroblasts also endothelial cells play a role in cancer progression that is far beyond delivering oxygen and nutrients (Ghajar, 2015; Ghajar et al., 2013; Lee et al., 2014a; Lee et al., 2014b, 2015a; Moser et al., 2003). There is evidence that the endothelium plays a key role in cancer progression by either preventing or supporting tumor growth and metastasis formation. An intact vasculature can keep metastatic cells in a dormant and non-proliferative state whereas a sprouting vasculature in contrast supports metastatic outgrowth (Franses et al., 2011; Franses et al., 2013; Ghajar et al., 2013). The Ghajar research group found that endothelial-derived thrombospondin-1 induces cancer cell dormancy in breast cancer and therefore prevents outgrowth of metastasis in lung and bones (Ghajar et al., 2013). However, in the presence of sprouting neovasculature this suppressive effect was lost and the endothelium now appeared to promote tumor outgrowth via TGF-b1 and periostin (Ghajar et al., 2013). Recently, Hoshino and colleagues provided evidence that cancer-derived exosomes taken up by brain endothelial cells induce the formation of a pre-metastatic niche supporting brain metastasis (Hoshino et al., 2015). Therefore, an essential question to ask is how cancer cells interact with endothelial cells in order to promote the generation of a vascular niche, enhancing tumor growth and cancer progression. Dr. Laughner and colleagues were able to show that HER2 signaling in breast cancer cells could increase HIF1a-mediated VEGF expression resulting in increased tumor angiogenesis (Laughner et al., 2001). Lee and research group have showed that by increased interleukin 6 (IL-6) secretion breast cancer cells induce secretion of CC-chemokine ligand 5 (CCL5) in lymphatic endothelial cells (LEC), which in return enhances cancer cell migration (Lee et al., 2014a). Furthermore, cancer cell-secreted IL-6 increases VEGF expression in LECs, which enhances lung vascular permeability and lymph node angiogenesis and thereby promotes metastatic outgrowth (Lee et al., 2014a; Lee et al., 2015a). These data suggest that targeting the interaction between cancer cells and their niches may provide additional means to understanding and inhibiting cancer progression.

To date, a number of molecular mediators of angiogenesis have been identified (Ucuzian et al., 2010). The most commonly described candidates include VEGF, FGF2, TNF-a, TGF-b1, PDGF as well as angiopoietins. However, recently also the NOTCH signaling pathway has been linked to angiogenesis (Guo et al., 2013; Murtas et al., 2015; Ucuzian et al., 2010). In

general, NOTCH signaling is an evolutionary conserved mechanism of cell-to-cell interaction that plays a fundamental role during development by controlling cellular responses to extrinsic and intrinsic developmental cues (Artavanis-Tsakonas et al., 1999). In mammals, the NOTCH family consists of four transmembrane receptors (NOTCH1-4) that can be activated through an interaction with one of the five NOTCH ligands, namely Delta-like (DLL) 1, 3 and 4 and Jagged (JAG) 1 and 2. The native NOTCH polypeptide consists of two domains, an extracellular domain (NECD) and a transmembrane intracellular domain (NTMIC). Upon ligand activation, the NOTCH intracellular domain (NICD) is released into the cytoplasm and translocates to the nucleus, where it regulates transcription of target genes (De Francesco et al., 2018). However, there is also evidence for non-canonical NOTCH signaling through DLK1 and DLK2, which bind to NOTCH1 and act as antagonists and therefore affect tissue development in mammals (Traustadottir et al., 2016). The NOTCH signaling pathway regulates cell differentiation, proliferation and apoptotic programs during organ formation and morphogenesis (Artavanis-Tsakonas et al., 1999). However, Murtas et al. have reported increased NOTCH1 expression by tumor endothelium in cutaneous melanoma, linked to increasing microvascular density (Murtas et al., 2015). Guo and colleagues report that overexpression of NOTCH1 in myeloma cells leads to increased VEGF secretion, promoting tumor angiogenesis (Guo et al., 2013). However, only recently research has started to focus on whether NOTCH signaling in endothelial cells may also be involved generating cancer-supporting vascular niches in the context of cancer progression (Wieland et al., 2017).

1.5 D492 as cellular model for mammary gland development and breast cancer progression

Previously, a breast epithelial cell line with stem cell properties referred to as D492 has been established in the Gudjonsson research group, (Briem et al., 2019; Gudjonsson et al., 2002; Sigurdsson et al., 2011; Villadsen et al., 2007). D492 was generated from a MUC1-negative and EPCAM-positive suprabasal epithelial cell population isolated from reduction mammoplasty tissue (Gudjonsson et al., 2002). D492 is ER-negative but expresses both luminal KRT19 and myoepithelial KRT14 and can generate both luminal- and myoepithelial cells. In 3D rBM culture, it forms branching structures reminiscent of TDLU *in vivo* (Fig. 5) and therefore presents a valuable model for studying branching morphogenesis *in vitro*. One major focus in this context has been to establish and investigate co-culture systems of D492

with breast endothelial cells (BRENCs) in order to better understand the impact of the surrounding stroma on mammary gland development. In a 3D rBM culture of D492, the presence of BRENCs significantly increased epithelial proliferation and branching (Ingthorsson et al., 2010). Interestingly, BRENCs seeded into rBM remained as single non-proliferating cells but were metabolically active.

In addition, upon 3D co-culture with BRENCs, a subpopulation of D492 underwent EMT and formed spindle-like mesenchymal colonies (Fig. 5), giving rise to a new derivative cell line with a stable mesenchymal but non-tumorigenic phenotype, D492M (Sigurdsson et al., 2011). D492M has lost expression of E-cadherin and epithelial keratins, while N-cadherin and vimentin expression is upregulated. D492 and D492M have extensively been used to study miRNA expression during EMT. Among the most downregulated miRNAs in D492M are members of the miR200 family, miR203a and miR205. Reexpression of miR141/miR200c restores expression of luminal epithelial markers in D492M, supporting the important role of this miRNA family for epithelial integrity (Hilmarsdottir et al., 2015).

In addition to modeling branching morphogenesis and endothelial-induced EMT, D492 has also been used to study oncogene-induced EMT in the context of breast cancer progression. By overexpression of the ErbB2/HER2 oncogene, D492 underwent oncogene-induced EMT and generated a third derivative cell line, D492HER2 (Ingthorsson et al., 2015). In 3D rBM culture, D492HER2 forms both spindle-like and grape-like structures (Fig. 5). In contrast to D492M, D492HER2 shows tumorigenic increased proliferation, migration and invasion *in vitro,* and tumorigenic properties when transplanted into mice where the cells form large tumors *in vivo*. Due to the implementation process of the HER2 oncogene, D492HER2 is GFP fluorescent.

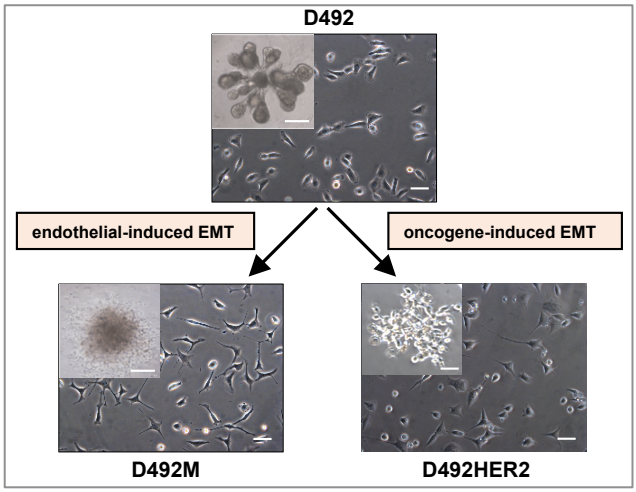


Figure 5. D492 cellular model. D492 as normal breast epithelial cell line with stem cell properties forms branching epithelial structures in 3D culture. Upon co-culture with ECs, a subpopulation underwent EMT, which gave rise to mesenchymal but non-tumorigenic D492M. D492M only forms spindle-like structures in 3D. Overexpression of the HER2 oncogene in D492 also gave rise to a mesenchymal derivate cell line, which in addition has tumorigenic properties and forms spindle- and grape-like structures in 3D. Scale bar = 50 µm.

In my PhD project, I have used the D492 cellular system to study the interaction of tumorigenic vs. non-tumorigenic epithelial cells with endothelial cells. The goal of my project was to investigate cellular crosstalk and identify novel mechanisms through which cancer cells may affect their environment to support cancer growth and progression. The system of the D492 cell lines offers the advantage of being able to directly compare how the interaction of the cancerous D492HER2 line with the stroma differs from that of the normal epithelial parental D492 line.

2 Aims

The interaction between cancer cells and their microenvironment leads to generation of cancer-associated niches that support tumor growth and progression as well as formation of metastasis in distant organs. As an essential part of the cancer microenvironment, endothelial cells play an important role that is greatly beyond delivering oxygen and nutrient rich blood to the tumor. The primary aim of my PhD study was to investigate heterotypic interactions between breast cancer cells and endothelial cells in order to understand how a cancer-associated vascular niche contributes to cancer progression and metastasis formation. This may provide additional means for cancer treatment.

In order to elucidate the underlying mechanisms in more detail, the aims were (1) To analyze the ability of cancer cells to affect the vascular niche and (2) To analyze how cancer-induced endothelial cells provide a positive feedback to the cancer cells.

Specific aims:

1) To analyze the ability of cancer cells to affect the vascular niche.
    a. Effect of cancer-conditioned medium (CM) on proliferation and tube formation of endothelial cells.
    b. Identification of cancer-secreted factors affecting the vascular niche and generation of transient and stable knockdown of candidate genes in cancer cells.
    c. Characterization of the phenotypic and functional consequences of knocking down genes identified in 1b.
2) To analyze how cancer-induced endothelial cells provide a positive feedback to the cancer cells.
    a. Effect of CM from cancer-induced endothelial cells on the cancer cells.
    b. Identification of factors secreted by cancer-induced endothelial cells that promote cancer cell proliferation, migration and invasion.

3 Materials and methods

In this chapter, the main methods used in this project will be covered. The primary focus is thereby on methods for functional characterization of ECs in the context of cancer cell crosstalk and cancer cell tumorigenicity. Futher, molecular methods for knockdown and overexpression of candidate genes and characterization will be covered. More detailed descriptions can be found in the corresponding manuscripts.

3.1 Cell culture

In this chapter, the used cell culture methods for the used cell lines as well as primary ECs will be described. Subchapters cover 2D culture methods and 3D methods for both mono- and co-culture setups.

3.1.1 2D cell culture

D492, D492M and D492HER2 cells were maintained in H14 medium (Ingthorsson et al., 2010) in tissue culture treated T25 Falcon flasks (BD Biosciences (BD)) coated with collagen I (Advanced Biomatrix), as described previously (Ingthorsson et al., 2015; Sigurdsson et al., 2011). The cells were grown at 37°C and 5% CO_2 and subcultured 1-2 times per week in a ratio of 1:10 (D492), 1:5 (D492M) or 1:15 (D492HER2). MDA-MB-231 and MCF-7 were cultured in Gibco™ RPMI 1640 medium containing 10% fetal bovine serum (FBS) (Invitrogen). Both cell lines were subcultured 1-2 per week at a ratio of 1:10. HEK293 cells were cultured in Gibco™ DMEM high glucose GlutaMax™ Supplement, pyruvate (Thermo Fisher Scientific).

Table 1: Cell lines used in this project.
Overview of cell lines and primary cells that have been used or generated in this study and their corresponding cell culture medium.

Cell lines	Culture media
D492	H14
D492M	H14
D492HER2	H14
MCF7	RPMI+10%FBS
MDA-MB-231	RPMI+10%FBS
Generated cell lines	
D492-ECM1	H14
D492M-ECM1	H14
D492HER2-kdECM1	H14
Primary cells	
HUVEC	EGM2+5%FBS

HUVEC primary ECs were obtained from the National University Hospital Reykjavik (ethical permission #35/2013) and cultured up to passage 8 in EGM2 medium (Lonza) supplemented with growth factors and 5% FBS, further referred to as EGM5. HUVECs were subcultured 1-2 times per week at a ratio of 1:10. Culture medium was changed three times per week and routinely checked for mycoplasma contamination.

For 2D co-culture with ECs, 200.000 cells of the D492 lines were seeded together with 200.000 ECs in a T25 cell culture flask (Falcon) and incubated for 24 h. Cells were then fixed in 3.7% formaldehyde solution (PFA) (Sigma Aldrich) for 5 minutes and blocked using 10% normal goat serum (Life Technologies) in 1x PBS for 5 minutes.

3.1.2 3D cell culture

For 3D culture, cells were seeded in reconstituted basement membrane gel (matrigel, BD Biosciences), further referred to as rBM (Lee et al., 2007). A total of 5000 cells were seeded in 100 µl gel in each well of a 96-well plate (Falcon). Fresh H14 was added every 2-3 days and cultures were imaged on day 7, day 14 and day 21. The cultures were obtained for 3 weeks. For 3D co-culture with ECs, 10.000 D492 line cells were seeded with 100.000 ECs in EGM5 on top of 300 µl solidified rBM in a 24-well plate setting. Medium was changed every 2-3 days and cultures were imaged every day for 5 days.

3.2 Migration and invasion assay

Migration and invasion was analyzed using transwell-filter units for 24-well plates with 8 µm pore size. 30.000 cells were seeded on top of the filter in 250 µl culture medium. For invasion assay, filters were pre-coated with 1:10 rBM in H14 for 30 minutes at 37°C (Fig. 6). For migration assay, cells were incubated for 20 h and for 48 h in invasion assay. For migration towards ECs (Fig. 6), HUVECs were grown in 500 µl EGM5 to 80% confluence in 24-well plate. Then, medium was changed to H14 + EGM5 (1:1) and D492 line cells were seeded on top of filter units (triplicates) in H14 + EGM5 (1:1). As positive control, 10% FBS was added to the medium below the filter instead of HUVECs and as negative control, medium above and below the filter unit was identical (H14 + EGM5, 1:1). For migration of D492HER2 treated with CM of induced vs. non-induced ECs, 30.000 D492HER2 cells were seeded in 250 µl H14 on top of the filter units (triplicates) and 500 µl H14 containing 10% FBS as attractant was added below.

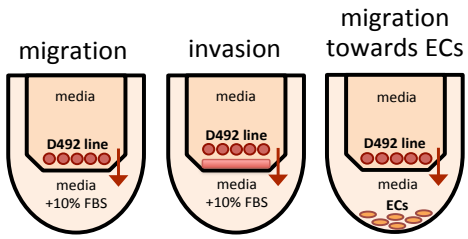


Figure 6. Schematic setup of transwell migration/invasion assays. Cells were seeded onto transwell filter inserts (rBM-coated for invasion) and placed in 24-well plates for 24 h (48 h for invasion). Below the filter, 10% FBS was added as attractant or ECs were grown to 80% confluence for migration towards ECs.

Filters were incubated for 20 h. Non-migratory cells were removed from the top of the filter using Q-tips, migratory cell below the filter were fixed for 5 minutes with 3.7% PFA and stained for 30 minutes with 1:5000 diluted DAPI nuclear staining (20 mg/ml) (Sigma). Using an EVOS FL Auto 2 Cell Imaging System (Thermo Fisher Scientific), three images per replicate were taken at 10x magnification. Images were imported into ImageJ software and converted to 8-bit. In the threshold-adjusted and binary-converted images, migratory cells were counted using the “analyze particles” function.

3.3 Conditioned medium (CM) and mass spectrometry

D492, D492M and D492HER2 were grown in H14 medium until 70-80% confluence. Cells were washed with 1x PBS and half of the original volume of fresh H14 was added in order to enrich for secreted factors. After 48 h incubation at 37°C conditioned medium (CM) was collected, centrifuged at 2000rpm for 3 minutes and sterile filtered through 0.22 µm filter unit. For endothelial network formation in 3D culture, 30.000 HUVECs were seeded in freshly collected CM (or unconditioned control H14) and fresh EGM5 medium (ratio 1:1) on a 96-well angiogenesis plate (#89646, Ibidi) on top of 10 µl solidified rBM. For recombinant protein experiments, rECM1 (#TP723147, Origene) was added to the medium in a final concentration of 15, 30, 60 or 120 ng/ml. 60 ng/ml was then chosen as concentration for further experiments. For endothelial NOTCH inhibition, gamma-secretase inhibitor DAPT (#D5942, Sigma-Aldrich) was added to the medium in a final concentration of 20µM. Recombinant YKL-40 protein (rY) (#11227H08H5, Thermo Fisher Scientific) was added to the medium at a final concentration of 100 ng/mL. Phase-contrast images of the establishing endothelial network were taken after 4 h, 24 h and 48 h using an EVOS FL Auto 2 Cell Imaging System (Thermo Fisher Scientific). Images were converted to RGB color and analyzed using ImageJ Angiogenesis Analyzer macro. For mass

spectrometry, D492 lines were grown in T175 flasks and CM was collected as described above, concentrated for 55 minutes using EMD Millipore Amicon™ Ultra-15 Centrifugal Filter Units (Merck Millipore) followed by buffer exchange to 100 mM TRIS/HCL buffer. Samples (triplicates) were stored at -80°C. Label Free relative protein quantification by nLC MS/MS after trypsin digestion was performed using LTQ-Orbitrap Velos MS system (Thermo Fisher Scientific) at the FingerPrints Proteomics Facility, University of Dundee and raw data were analyzed using MaxQuant software (version 1.6.2.1). Quantitative and statistical analysis was performed using XLStat (version 2018.1). Data were p-value corrected (significance level 0.05) and sorted based on ≥ 2-fold higher secretion (LFQ intensity) by D492HER2 compared to both D492 and D492M. The resulting candidate list of 77 proteins was used for GO term analysis using PANTHER database (statistical overrepresentation test). As annotation data set we used “GO biological process complete” with Bonferroni correction for multiple testing. To investigate feedback effects of conditioned/induced endothelial cells, CM from D492 lines was added to 40-50% confluent HUVECs (as described above) and incubated for 48 h. Cells were washed with 1x PBS and fresh EGM5 (half volume) was added to collect conditioned endothelial-secreted factors. After 48 h, CM from induced vs. non-induced HUVECs was collected, centrifuged (2000 rpm, 3 minutes) and filtered (0.22 µm) and added to 40% confluent D492HER2 together with fresh H14 (ratio 1:1) for 48 h.

3.4 Transient knockdown (KD) using siRNA

Knockdown (KD) was performed in 24-well plate using pre-designed Silencer® Select human ECM1 siRNA (#s4441, Thermo Fisher Scientific) compared to a scrambled negative control (Silencer Select negative control No. 1, Thermo Fisher Scientific, #4390843). Cells were reverse transfected for 48 h according to the manufacture’s protocol using a siRNA concentration of 10 nM. Proliferation was monitored using an IncuCyte ZOOM 2016B System. KD was confirmed using RT-qPCR and western blotting. After 48 h, medium was changed to normal H14 and incubated for another 48 h for collection of CM as described above. Endothelial network formation was analyzed as previously described for HUVECs treated with CM from D492HER2siECM1 compared to ctrl D492HER2.

3.5 Generation of stable knockdown (KD) and overexpression (OE) cell lines using CRISPRi/CRISPRa

In order to generate stable ECM1 KD in D492HER2 and OE in D492 and D492M, we used the novel CRISPRi (inhibition) and CRISPRa (activation) system. In contrast to the original CRISPR/Cas9 approach, the CRISPRi/CRISPRa system is working with a functionally inactivated Cas9 (dCas9) that is either fused to an inhibitory KRAB domain for expression inhibition or an activatory VP64 domain for expression activation. The dCas9 complex is then guided to the gene of interest with a specifically designed sgRNA (Fig. 7).

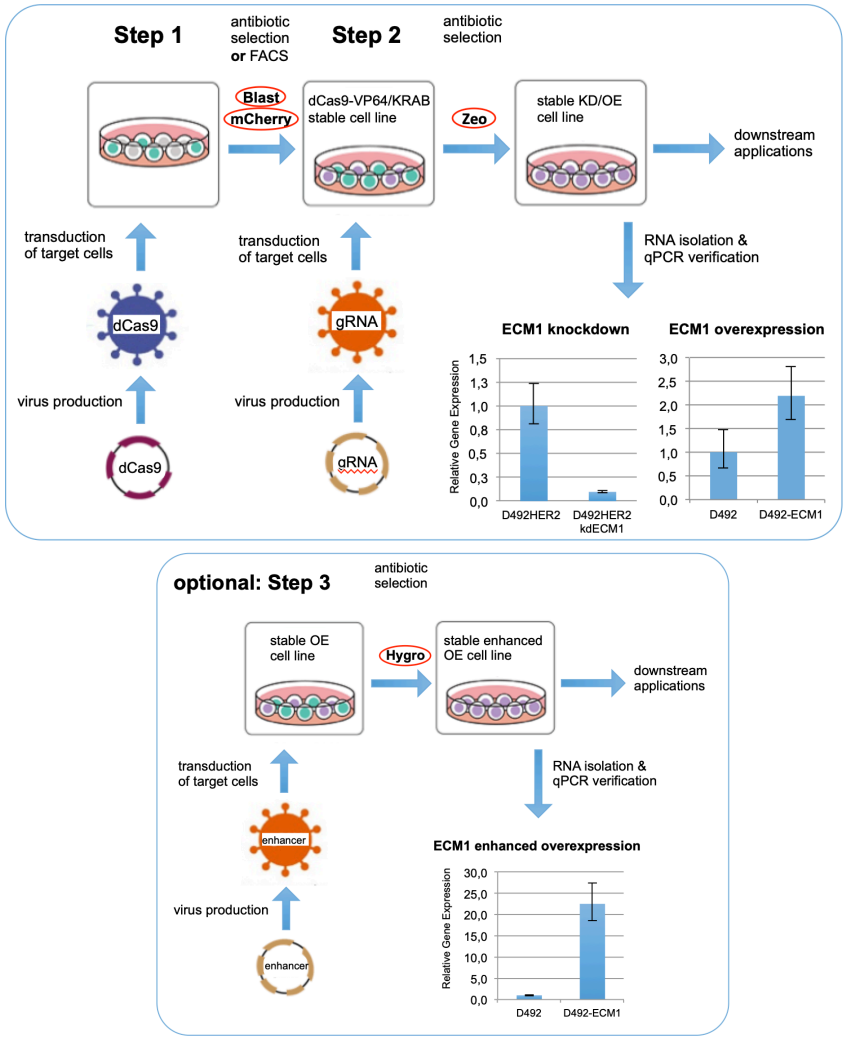


Figure 7. Schematic workflow of CRISPRi and CRISPRa. Top: Step 1 with virus production and viral transduction of target cells to insert activatory (dCAS9-VP64-Blast) or inhibitory (pHR-SFFV-KRAB-dCas9-P2A-mCherry) plasmid, followed by antibiotic selection for blasticidin or FACS selection for mCherry. Step 2 with virus

production and viral transduction of target cells to incert sgRNA(MS2)_zeo plasmid containing sgRNA for the target gene, followed by 12-14 days zeocin selection. Eventual RNA isolation for RT-qPCR validation of KD or OE and downstream applications. Bottom: Optional step 3 for OE enhancement with with virus production and viral transduction of target cells with the MS2-P65-HSF1 Hygro enhancer plasmid, followed by hygromycin selection for 10-12 days, RT-qPCR validation of enhanced overexpression and downstream applications.

sgRNA plasmids were purchased from Genscript. For ECM1 OE and KD, a combination of two sgRNAs was used. Overexpression sgRNAs were pre-design and located between 1-200 bp upstream of the ECM1 transcription start site and knockdown sgRNAs custom-designed to bind between 1-200 bp downstream (Tab. 2). sgRNAs were cloned into the plenti sgRNA(MS2)_zeo plasmid (Genscript). As negative control, an empty plenti sgRNA(MS2)_zeo plasmid was used (Genscript).

Table 2. Plasmids and sgRNAs used for ECM1 KD and OE with CRISPRi/CRISPRa. Names of plasmid from different companies used containing antibiotic of fluorescent selection markers listed, based on their use for KD and OE. sgRNA names and sequences used for KD and OE.

Overexpression		
plasmids	lenti dCAS9-VP64-Blast	Addgene
	plenti sgRNA(MS2)_zeo	Genscript
	lenti MS2-P65-HSF1_Hygro	Genscript
sgRNAs (NM_001202858)	ECM1 SAM guide RNA 1 (Genscript)	CATCTACAGGCTGCCTTCTG
	ECM1 SAM guide RNA 2 (Genscript)	GAAACTGAGGCACAAACTAG
Knockdown		
plasmids	pHR-SFFV-KRAB-dCas9-P2A-mCherry	Addgene
	plenti sgRNA(MS2)_zeo	Genscript
sgRNAs (NM_001202858)	ECM1 custom gRNA 1 (Genscript)	GTGGTCAGTTGCCCCAGGAT
	ECM1 custom gRNA 2 (Genscript)	GCCGGCCACTGAAGCTTGTC

For production of lentiviral particles, HEK293 cells were used and virus was collected 48 h and 72 h after transfection. D492 and D492M were first transduced with plenti dCAS9-VP64-Blast plasmid for transcriptional activation and selected with 2 µg/ml blasticidin for 7-10 days (Sellekchem, #S7419). D492HER2 was transduced with pHR-SFFV-KRAB-dCas9-P2A-mCherry plasmid for repression and sorted for mCherry expression (Fig. 7). Next, transduction with lentivirus containing sgRNA plasmids for OE (D492 and D492M containing dCas9-VP64 cassette) and KD (D492HER2 containing dCas9-KRAB cassette) was performed and cells were selected with 400 µg/ml (D492, D492M) or 600 µg/ml (D492HER2) zeocin (Thermo Fisher, #R25005) for 12-14 days. For enhancement of ECM1 OE, D492 and D492M were then transduced with lenti MS2-P65-HSF1 Hygro plasmid,

containing enhancer domains MS2, P65 and HSP1 that bind to VP64 and enhance its activation activity. Cells were selected with 100 µg/ml hygromycin (Sellekchem, #S2908) for 10-12 days (Fig. 7). ECM1 KD or OE were validated on gene expression level using RT-qPCR.

3.6 RNA microarray

For RNA microarray analysis, D492, D492M and D492HER2 with and without ECM1 OE/KD were grown until 80% confluence, fresh H14 medium was added and CM was collected after 48 h. HUVEC endothelial cells were grown to 40% confluence, washed with 1x PBS and CM was added together with fresh EGM5 (ratio 1:1). After 24 h, RNA was extracted using the RNeasy Mini Kit (Qiagen). Sample concentration and quality was analyzed using the Agilent 2100 Bioanalyzer System (Agilent). RNA microarray and raw data analysis was performed at the sequencing core facility, DKFZ Heidelberg, Germany using Afimetrix Clariom S, human Assay. Microarray candidates were validated using RT-qPCR.

3.7 RNA, cDNA and RT-qPCR

Total RNA was extracted with Trizol (Life Technologies) and reverse transcribed with hexanucleotides using the SuperScript® IV First-Strand Synthesis System (Invitrogen). Resulting cDNA (10 ng per reaction) was used for quantitative real-time PCR, in master mix (Life Technologies) with pre-designed primer pairs for target and reference genes (Tab. 3). Experiments were carried out in triplicate on 7500 Real Time PCR System (Life Technologies). Expression levels were normalized to the reference gene and relative mRNA differences were calculated with the ΔΔCt method according to the MIQE guidelines (Bustin et al., 2009).

Table 3. SYBR Green RT-qPCR primers used in this study. List of gene IDs for target genes and corresponding primer IDs of pre-designed primers (IDT) used in this study.

Gene	primer (IDT)
B2M	Hs.PT.58v.18759587
ECM1	Hs.PT.58.20438560
NOTCH1	Hs.PT.58.23074795
NOTCH2	Hs.PT.58.28296019
NOTCH3	Hs.PT.58.38492200
HEY1	Hs.PT.58.4299267
HEY2	Hs.PT.58.582440
CDH3	Hs.PT.58.39234242
ITGB4	Hs.PT.58.3714621
KRT14	Hs.PT.58.4592110
KRT17	Hs.PT.58.20464487
GATA3	Hs.PT.58.19431110
KRT7	Hs.PT.58.3835469
KRT19	Hs.PT.58.4188708
LAMA1	Hs.PT.58.15231709
FN	Hs.PT.58.40005963
FABP4	Hs.PT.58.20106818
TM4SF18	Hs.PT.58.20686588
ZNF283	Hs.PT.58.27732356
TNFSF18	Hs.PT.58.667787
RASGRP3	Hs.PT.58.39820682
TIGD5	Hs.PT.58.20476293
ANGPTL4	Hs.PT.58.25480012
FGF2	Hs.PT.58.24613308
GPR124	Hs.PT.58.20760365
GREM1	Hs.PT.58.21084086
HIF1A	Hs.PT.58.534274
SERPINE1	Hs.PT.58.3938488.g
BMPER	Hs.PT.58.3315719
NR4A1	Hs.PT.58.39997829

3.8 Protein isolation and western blotting

Proteins were isolated using RIPA lysis buffer supplemented with both phosphatase and protease inhibitor cocktails (Life Technologies). For western blotting, 5 µg protein was used per lane, unless otherwise stated. Samples were denatured using 10% ß-mercaptoethanol at 95 °C for 5 min and run on NuPage 10% Bis-Tris gels (Life Technologies) in 2-(N-morpholino) ethanesulfonic acid (MES) running buffer. Samples were then transferred to Immobilon FL PVDF membranes (Millipore). Membranes were blocked in Li-cor blocking buffer and primary antibodies were incubated overnight at 4°C. Proteins were detected using IRDye secondary antibodies and near-infrared fluorescence visualization was measured using Odyssey CLx scanner (Li-Cor, Cambridge, UK). As loading controls actin or tubulin were used for quantification.

3.9 Immunofluorescence (IF) and immunohistochemistry (IHC)

For IF staining, cells were grown on 8 Chamber Polystyrene Vessels (Falcon) and fixed in 3.7% formaldehyde for 5 minutes, followed by permeabilization with 0.1% Triton-X for 10 minutes and blocking using 10% normal goat serum (Life Technologies, Carlsbad, CA, USA) in 1x PSB for 5 minutes. Samples were incubated with primary antibody overnight at 4°C and then stained with isotype specific secondary fluorescent Alexa Fluor goat antibodies (Life Technologies) and counterstained with 4',6-diamidino-2-phenylindole (DAPI) (Sigma-Aldrich, St Louis, MO, USA).

Table 4. Antibodies used in this study. List of primary antibodies (protein IDs, company and order IDs for western blotting and IF/IHC staining for candidate proteins.

Protein	Ref. Nr.	Company
	Western Blot	
Tubulin beta	#ab6046	Abcam
Actin	#ab3280	Abcam
Histone H3	#CS4499S	Cell Signaling
E-cadherin	#BD610182	BD Biosciences
P-cadherin	#CS2130	Cell Signaling
Vimentin	#M0725	Dako
ECM1	#sc-515843	Santa Cruz
	IF/IHC staining	
E-cadherin	#BD610182	BD Biosciences
N-cadherin	#BD610921	BD Biosciences
F-actin	#A22283	Life Technologies
Occludin	#331500	Invitrogen
P-cadherin	#CS2130	Cell Signaling
Vimentin	#M0725	Dako
CK18	#M7010	Dako
p63	#ab124762	Abcam
CD31	#M0823	Dako
ECM1	#HPA027241	Sigma Aldrich
NOTCH1	#sc-376403	Santa Cruz
NOTCH3	#ab23426	Abcam
GATA3	#CS5852	Cell Signaling
CK19	#ab7754	Abcam
FN	#ab6328	Abcam

Visualization was done using a FV1200 Olympus inverted confocal microscope. For IHC staining, paraffin-embedded tumor tissue samples were processed in xylene and ethanol in order to remove paraffin and then rehydrated in dH_2O. Following rehydration, high-temperature antigen retrieval was performed and samples were stained with primary antibody for 30

minutes and secondary antibody (Dako EnVision+ System- HRP labelled Polymer Anti-mouse, #K4000) and DAB Chromogen. Counterstaining was done with filtered hematoxylin for 1-2 minutes.

3.10 Mouse xenografts

To assess tumorigenicity and metastatic potential of D492HER2 and D492HER2 with KD of ECM1, cells were injected subcutaneously into NSG mice independent assays for tumorigenicity and metastatic potential (ethical application FOTS IDs: 12080 and 12097). In tumor assay, 5×10^5 cells in 100 µl of 1:1 mixture of PBS and Matrigel were injected per injection site and for metastasis assay 1×10^6 cell by LV (left ventricle) injection Tumor growth was measured two times per week. Tumors where measured by calipers and the tumor volume was calculated according to the formula 0.5 x length x width^2. In the tumorigenicity assay, mice were sacrificed between day 46 and 62 due to high tumor burden and in the metastasis assay after 65 days. After the experimental period, tumors and metastatic organs (brain, spine, lungs and liver) were dissected. As D492HER2 already expresses GFP due to the HER2 overexpression procedure, metastatic organs were imaged for fluorescent marker GFP using IVIS *in vivo* imaging system, fixed in PFA and embedded in paraffin. Tumors were fixed in PFA and from each mouse, one tumor was frozen in liquid nitrogen or the other one embedded in paraffin for later RNA extraction and IHC staining.

3.11 Statistical analysis

All experiments were performed in triplicates. Graphs were generated in Microsoft Excel 2015. Error bars represent standard deviation of the mean. Statistical analysis was performed in R 3.3.3. (R Development Core team, 2013). Data were checked for normal distribution and Students t-test or ANOVA followed by Tukey's honest significant difference test on linear models (lm) was performed when normally distributed whereas Kruskal-Wallis chi-squared test was used when not normally distributed. The significance level was 0,05.

4 Results and Discussion

In the following chapter I will summarize the acquired data during my PhD project. I will focus on submitted as well as other unpublished data and discuss them within the scientific context. I will start by describing a preliminary study analyzing the effects of different ECM components on the expression profile of breast epithelial cells (unpublished data). From there, I will shift the focus on how the secretome of HER2-overexpressing breast epithelial cells affects endothelial cells (ECs) and what factors have been identified as mediators during this process. I will then describe and discuss the role of the identified factors ECM1 (manuscripts I and II) and YKL-40 (manuscript III) in the context of tumorigenicity and interaction with ECs. All three manuscripts are attached at the end of the thesis.

4.1 Context matters - ECM composition affects expression profile of breast epithelial cells

In an attempt to determine how the microenvironment can affect breast epithelial cells with a non-cancerous phenotype, I characterized epithelial marker expression in normal epithelial D492 grown on two different extracellular matrix (ECM) proteins, collagen type I vs. collagen type IV. Collagen type I (Col-I) is the most abundant collagen in the human mammary gland and found in the interstitial stroma. Type IV collagen (Col-IV) is non-fibrillar and a key component of the basement membrane (BM), which is found at the basal surface of epithelial and endothelial cells and is essential for maintenance of tissue polarity (Egeblad et al., 2010; Insua-Rodriguez & Oskarsson, 2016; Sage & Bornstein, 1982; Sage et al., 1982).

Cell culture flasks or chamber slides were coated with either Col-I or Col-IV and D492 cells were seeded onto the coated chamber slides and grown to about 80% confluence. Cells were then further processed for protein extraction or IF staining (see methods). Protein expression of luminal and basal/myoepithelial markers was assessed and quantified using western blotting and IF staining.

Expression characterization revealed upregulation of basal markers such as p63, P-cadherin and vimentin on the protein expression level in D492 cells grown on Col-IV compared to Col-I (Fig. 8A and B). Simultaneously, E-

cadherin protein expression was decreased in cells grown on Col-IV (Fig. 8A and B).

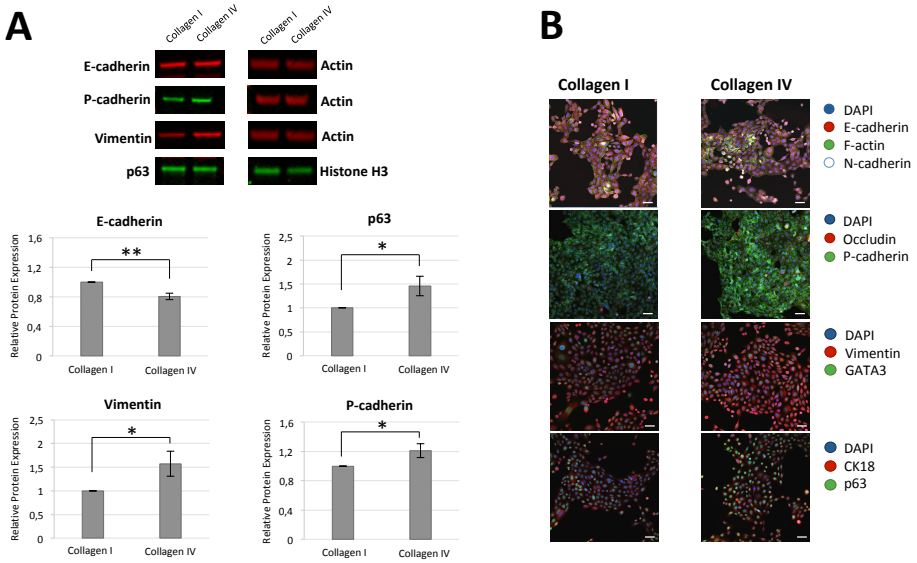


Figure 8. Collagen IV-rich environment promotes basal-like phenotype in breast epithelial cells. A) Quantification of protein expression of E-cadherin, P-cadherin, vimentin and p63 in D492 grown on Col-I vs. Col-IV using western blot. Loading contol (intracellular): actin, loading control (nuclear): histone H3. Student´s t-test (*** $p < 0.001$, ** $p < 0.01$, * $p < 0.05$). B) IF staining of D492 grown on Col-I vs. Col-IV for epithelial markers (nuclear staining: DAPI (blue)). Scale bar = 50 µm.

These data indicate that culturing breast epithelial cells in an environment rich in Col-IV rather than Col-I seems to induce an expression shift in favor of the basal epithelial phenotype. Interestingly, other studies also report an effect of Col-IV presence in the ECM on marker expression in normal breast epithelial and also breast cancer cells (Espinosa Neira & Salazar, 2012; Xiao et al., 2015). Espinosa et al. report that type IV collagen is capable of inducing a shift from epithelial to mesenchymal characteristics in the breast epithelial cell line MCF10A. While epithelial markers such as E-cadherin were downregulated in response to native Col-IV, they found mesenchymal markers such as vimentin to be upregulated (Espinosa Neira & Salazar, 2012). These data concur with our findings on changed marker expression in the presence of Col-IV.

The outcome of this initial study underlines the role of the microenvironment in affecting breast epithelial cell fate and how the composition of the microenvironment can alter the epithelial expression profile. However, not only ECM proteins as such are capable of affecting the

epithelium. Proteins secreted by other cell types can also influence characteristics and behavior of epithelial cells (Gouon-Evans et al., 2002; Ingthorsson et al., 2010; Wiesen et al., 1999). Studies have shown that ECs surrounding the branching epithelial ducts of the mammary gland are capable of enhancing epithelial growth and affecting cell phenotype (Ingthorsson et al., 2010; Sigurdsson et al., 2011). Hence, cellular crosstalk between different cell types can play an important role during normal development as well as in the context of breast cancer (Ghajar et al., 2013; Lee et al., 2014a; Lee et al., 2014b, 2015a; Oskarsson et al., 2011). Understanding how cancer cells can induce cell in their microenvironment to secrete factors supporting cancer growth and progression has therefore been the focus of my PhD project. Whereas much research has focused on cancer-induced fibroblasts and macrophages, cancer-induced ECs only recently came into attention with regard to cancer-supportive crosstalk (Ghajar et al., 2013; Lee et al., 2014a; Lee et al., 2014b, 2015a).

Using the cellular model of normal epithelial D492, mesenchymal D492M (non-tumorigenic) and mesenchymal D492HER2 (tumorigenic), I aimed to elucidate heterotypic interactions of cancer cells with ECs.

4.2 Cancer-endothelial interactions

In order to investigate crosstalk of D492, D492M and D492HER2 with ECs, conditioned medium (CM) from all cell lines was collected and its effect on endothelial network formation *in vitro* was analyzed (Fig. 9A). Further, CM from induced vs. non-induced ECs was collected in order to determine a possible feedback effect on cancerous D492HER2.

4.2.1 CM from D492HER2 increases endothelial network formation

ECs were seeded in CM from all D492 cell lines on top of rBM (matrigel) and network formation was imaged and analyzed after 4 h, 24 h and 48 h. Numbers of master junctions, master segments, meshes and total master segment length were quantified using ImageJ Angiogenesis Analyzer. The analysis revealed significantly increased network formation upon treatment with CM from D492HER2 but not D492 or D492M after 4 h (Fig. 9B and C). All quantified parameters were also significantly higher upon treatment with D492HER2-derived CM after 24 h and 48 h indicating persistence of the pro-angiogenic effect of D492HER2-CM over time (Manuscript #1, suppl. Fig. S1).

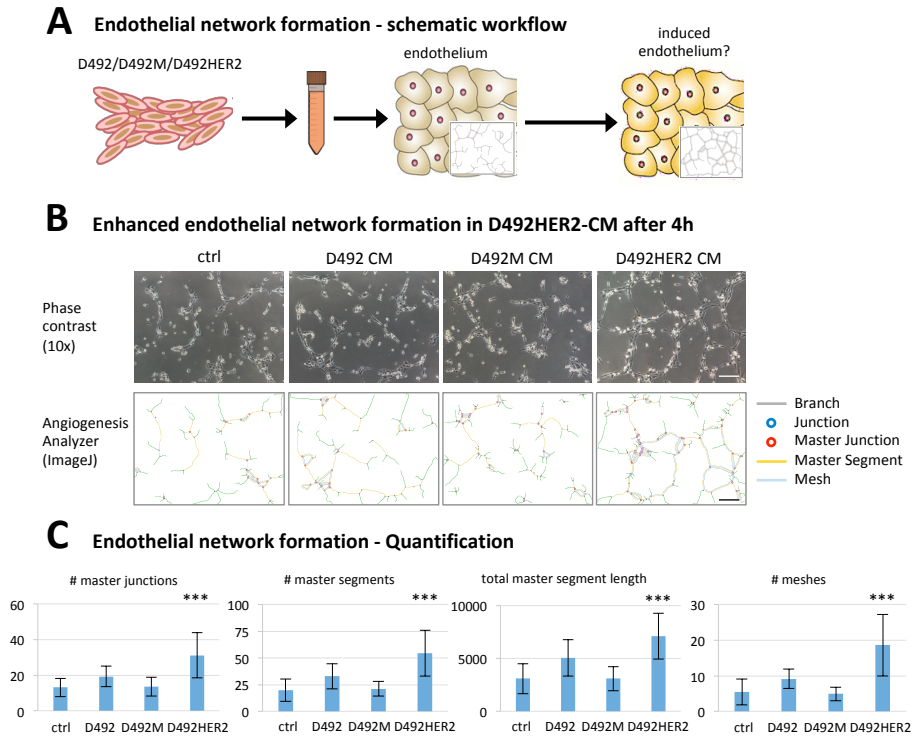


Figure 9. D492HER2-CM enhances endothelial network. A) Endothelial network formation - schematic workflow. Schematic illustration of the main research aim asking whether CM from D492, D492M or D492M increases endothelial network formation. B) Enhanced endothelial network formation in D492HER2-CM after 4 h. Top: Representative phase-contrast images of HUVEC endothelial network after 4 h on top of matrigel in control (unconditioned) medium (= H14) and conditioned medium from D492, D492M and D492HER2, 10x magnification. Bottom: Corresponding angiogenesis images (ImageJ, angiogenesis analyser plugin) showing branches, junctions, master junctions, master segments and meshes. C) Endothelial network formation - Quantification. Quantification of master junctions, master segments, total master segment length and meshes (angiogenesis analyzer). Statistical analysis performed in R, one-way ANOVA, *** $p < 0.001$, ** $p < 0.01$, * $p < 0.05$. Scale bar = 50 µm.

The results suggesting a pro-angiogenic effect of HER2+ overexpressing breast cancer cell lines go hand in hand with other studies. Throughout different cancer types, one of the main mechanisms by which HER2 promotes angiogenesis is by upregulation of VEGF signaling (Arteaga et al., 2011; Kumar & Yarmand-Bagheri, 2001; Li et al., 2017). Increased VEGF expression and secretion by tumor cells leads to increased endothelial tube formation and endothelial proliferation in this context. However, more recently other pathways have also been suggested to be involved in HER2-mediated increase in angiogenesis. In this context, Leford and colleagues suggest an

involvement of the CXCR4/CXCL12 axis in HER2-mediated angiogenesis. Targeting this pathway thereby leads to significant reduction of tumor growth and metastasis dissemination in HER2+ but not in triple-negative breast cancer (Lefort et al., 2017). However, apart from promoting effects of HER2+ breast cancer on endothelial tube formation and proliferation, there is little knowledge on whether and how cancer cells manipulate ECs in their environment molecularly, inducing a cancer-promoting feedback.

4.2.2 D492HER2-CM induced endothelial feedback on D492HER2 migration and invasion

After identifying the enhancing effect of D492HER2 on endothelial network formation, I collected CM from D492HER2-induced ECs for treatment of D492HER2 in order to investigate a possible feedback response (Fig. 10A). Remarkably, treatment of D492HER2 with CM from D492HER2-induced ECs but not D492-induced ECs resulted in increased migration and invasion compared to control D492HER2 (Fig. 10B).

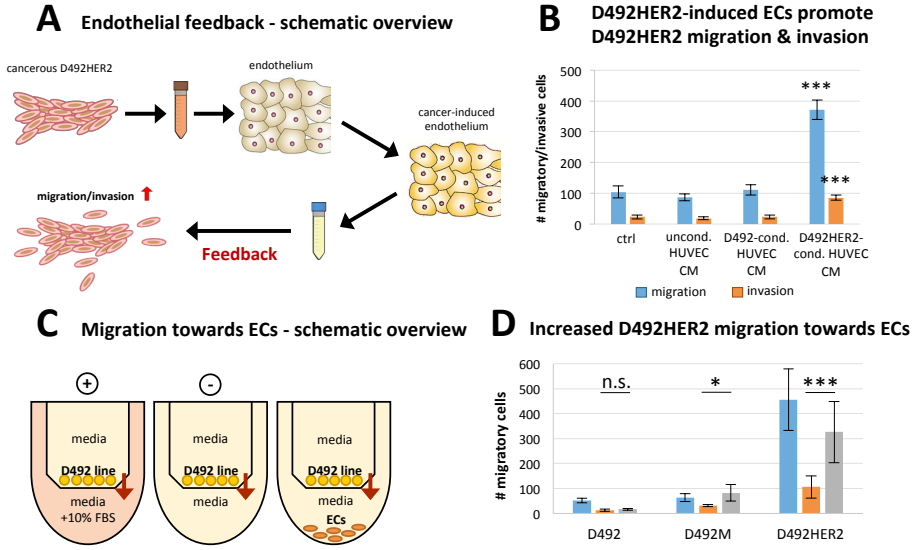


Figure 10. D492HER2-CM induces endothelial feedback increasing migration and invasion. A) Endothelial feedback - schematic overview. Work-flow of conditioning ECs (see methods). B) D492HER2-induced ECs promote D492HER2 migration and invasion. Transwell-migration and invasion assays of D492HER2 treated with unconditioned medium, unconditioned HUVEC-CM, D492-conditioned HUVEC-CM and D492HER2-conditioned HUVEC-CM. Number of migratory/invasive cells shown for different treatments (Student´s t-Test, *** $p < 0.001$, ** $p < 0.01$, * $p < 0.05$). C) Migration towards ECs - schematic overview. Setup of transwell-migration assay of D492, D492M and D492HER2 towards HUVECs below the transwell filter. Migration towards HUVECs (in H14 + EGM1) was compared with migration towards 10% FBS in H14 + EGM5 (pos. ctrl) and plane H14 + EGM5 (neg. ctrl). D) Increased

D492HER2 migration towards ECs. Migration of D492, D492M and D492HER2 towards HUVECs. Number of migratory cells shown for different treatments (Student´s t-Test, *** $p < 0.001$, ** $p < 0.01$, * $p < 0.05$).

Furthermore, I investigated whether migration of D492HER2 cells was directed towards the endothelium or rather undirected. In this context, I set up an indirect co-culture of D492, D492M and D492HER2 in a transwell assay with or without ECs present below the filter (Fig. 10C). Interestingly, the number of migratory cells indicated an increased migratory phenotype of D492HER2 specifically (Fig. 10D), supporting the hypothesis of increased migration towards the endothelium mediated by induced ECs. In agreement with these data, I could also see significantly more D492HER2 than D492 or D492M cells associated with ECs in a 2D and 3D co-culture setup with ECs (Fig. 11A and B).

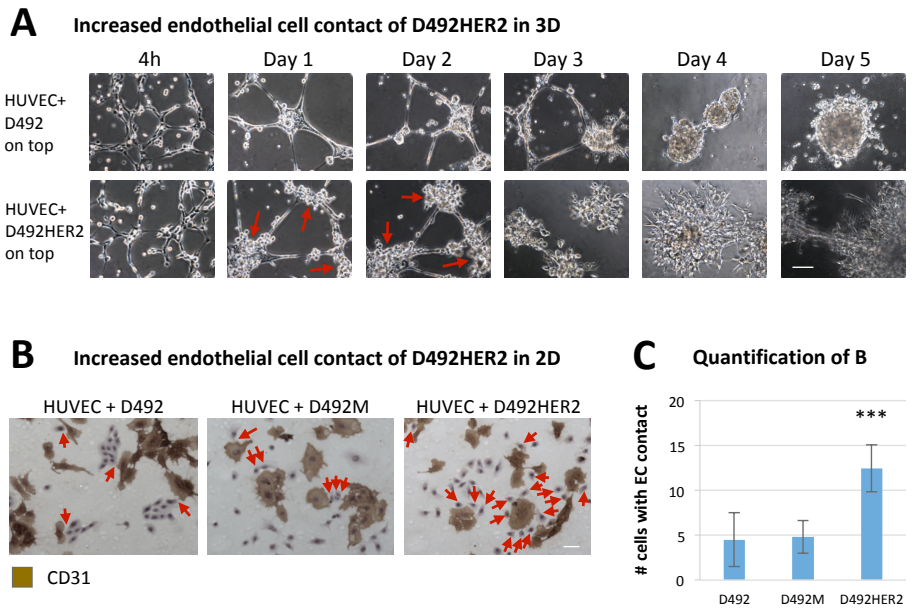


Figure 11. D492HER2 shows increased affinity to ECs in 2D and 3D. A) Increased endothelial cell contact of D492HER2 in 3D. 3D co-culture of D492 and D492HER2 with HUVEC on top of matrigel. Red arrows mark cells attached to branching points of the endothelial network. Scale bar = 50 µm. B) Increased endothelial cell contact of D492HER2 in 2D. 2D co-culture of D492, D492M and D492HER2 with HUVEC (brown: DAB staining for CD31) after 24h. Red arrows mark cells attached to brown ECs. Scale bar = 50 µm. C) Quantification of B. Mean number of cells attached to HUVEC. Statistical analyses for C) performed in R, one-way ANOVAs, *** $p < 0.001$, ** $p < 0.01$, * $p < 0.05$.

These data show that D492HER2 not only promotes endothelial network formation but also is capable of inducing a feedback response in ECs that

leads to further increased cancer cell migration and invasion ability. Only recently, research has started focusing on cancer-associated ECs as potential supporters of cancer progression and metastasis formation in addition to their role in angiogenesis. The Ghajar research lab suggested that a stable vasculature secretes factors such as thrombospondin-1 promoting cancer cell dormancy while this effect is lost in sprouting vasculature leading to metastatic outgrowth (Ghajar et al., 2013). Lee and colleagues showed that by increased IL-6 secretion triple-negative breast cancer cells induce secretion of CCL5 in lymphatic endothelial cells (LEC), which in turn enhances cancer cell migration (Lee et al., 2014a). However, due to the complex nature of cellular crosstalk the underlying molecular mechanisms involved in cancer-induced endothelial feedback are still largely unknown.

4.2.3 Enrichment of pro-angiogenic factors in D492HER2 transcriptome

In order to identify factors in D492HER2 that mediate its pro-angiogenic effect and its ability to induce a cancer-promoting endothelial feedback, I first looked into transcriptomic data of all three D492 lines. I selected all genes that were at least 10-fold upregulated in D492HER2 compared to D492 and performed enrichment analysis for gene ontology (GO) term functional group using the PANTHER database (Mi et al., 2013). The analysis revealed significant enrichment of 16-fold of the functional group “sprouting angiogenesis“ (GO:0002040). I performed RT-qPCR to validate the genes which were part of this group (Fig. 12A and B) and decided to further focus on Gremlin 1 (GREM1) (Fig. 12B). GREM1 showed strong upregulation in D492HER2 and its strong fold difference compared to both D492 and D492M indicated that it might be linked to HER2-induced tumorigenicity rather than the EMT phenotype.

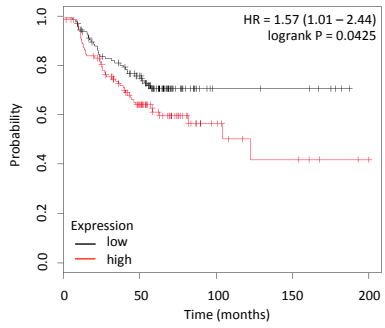
Secreted GREM1 functions as a BMP antagonist and is involved in regulating BMP-mediated actions especially during limb and kidney formation (Brazil et al., 2015). In addition, GREM1 has also gained attention in cancer research as a promoter of cancer progression by e.g. regulation of cancer stem cell maintenance (Jang et al., 2017; Karagiannis et al., 2015; Sato et al., 2016; Yin et al., 2017). Mitola and colleagues identified GREM1 as novel activator of endothelial VEGFR2 resulting in pro-angiogenic responses (Mitola et al., 2010). Survival analysis revealed significantly decreased relapse-free survival (RFS) for patients with GREM1+/HER2+ breast tumors (Fig. 12C). Therefore, GREM1 appeared to be an interesting candidate for

further investigation that might give new insights into cancer-endothelial crosstalk and offer the possibility for development of novel cancer treatments.

A **Pro-angiogenic candidates (D492HER2 transcriptome)**

Gene ID	Gene name	Family
FGF2	Fibroblast growth factor 2; FGF2;ortholog	FIBROBLAST GROWTH FACTOR 2 (PTHR11486:SF100)
GPR124	G-protein coupled receptor 124; GPR124;ortholog	G-PROTEIN COUPLED RECEPTOR 124 (PTHR12011:SF358)
GREM1	Gremlin-1;GREM1;ortholog	GREMLIN-1 (PTHR15283:SF11)
ANGPTL4	Angiopoietin-related protein 4; ANGPTL4;ortholog	ANGIOPOIETIN-RELATED PROTEIN 4 (PTHR19143:SF261)
HIF1A	Hypoxia-inducible factor 1-alpha; HIF1A;ortholog	HYPOXIA-INDUCIBLE FACTOR 1-ALPHA (PTHR23043:SF35)
SERPINE1	Plasminogen activator inhibitor 1; SERPINE1;ortholog	PLASMINOGEN ACTIVATOR INHIBITOR 1 (PTHR11461:SF246)
BMPER	BMP-binding endothelial regulator protein;BMPER;ortholog	BMP-BINDING ENDOTHELIAL REGULATOR PROTEIN (PTHR11339:SF334)
NR4A1	Nuclear receptor subfamily 4 group A member 1;NR4A1;ortholog	NUCLEAR RECEPTOR SUBFAMILY 4 GROUP A MEMBER 1 (PTHR24085:SF8)

C **RFS in GREM1+/HER2+ patients**



B **qPCR verification of candidates**

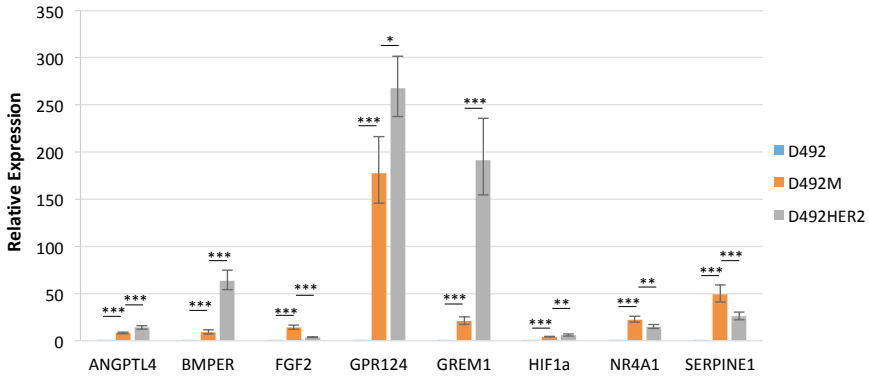


Figure 12. Enrichment of pro-angiogenic factors in D492HER2. A) Pro-angiogenic candidates (D492HER2 transcriptome). Enrichment of angiogenesis-related candidates among ≥ 10-fold upregulated genes in D492HER2 compared to D492. Statistical overrepresentation test (Panther DB) was performed for two independent transcriptomic data sets (RNA seq) using "GO biological process complete" as annotation data set with Bonferroni correction for multiple testing. B) RT-qPCR verification of transcriptome candidates (RQ = relative expression values, n = 3). One-way ANOVA, *** $p < 0.001$, ** $p < 0.01$, * $p < 0.05$. C) RFS in GREM1+/HER2+ patients. Kaplan-Meier plot of GREM1 in HER2+ tumors showing correlation of high expression with decreased relapse-free survival (RFS).

In the next step, I therefore performed transient knockdown of GREM1 in D492HER2 using siRNA. Knockdown was confirmed on the mRNA level by RT-qPCR (Fig. 13A) and functional analysis was performed. Interestingly,

GREM1 knockdown seemed to slow down D492HER2 proliferation and decrease the pro-angiogenic effect of D492HER2-CM (Fig. 13B to D).

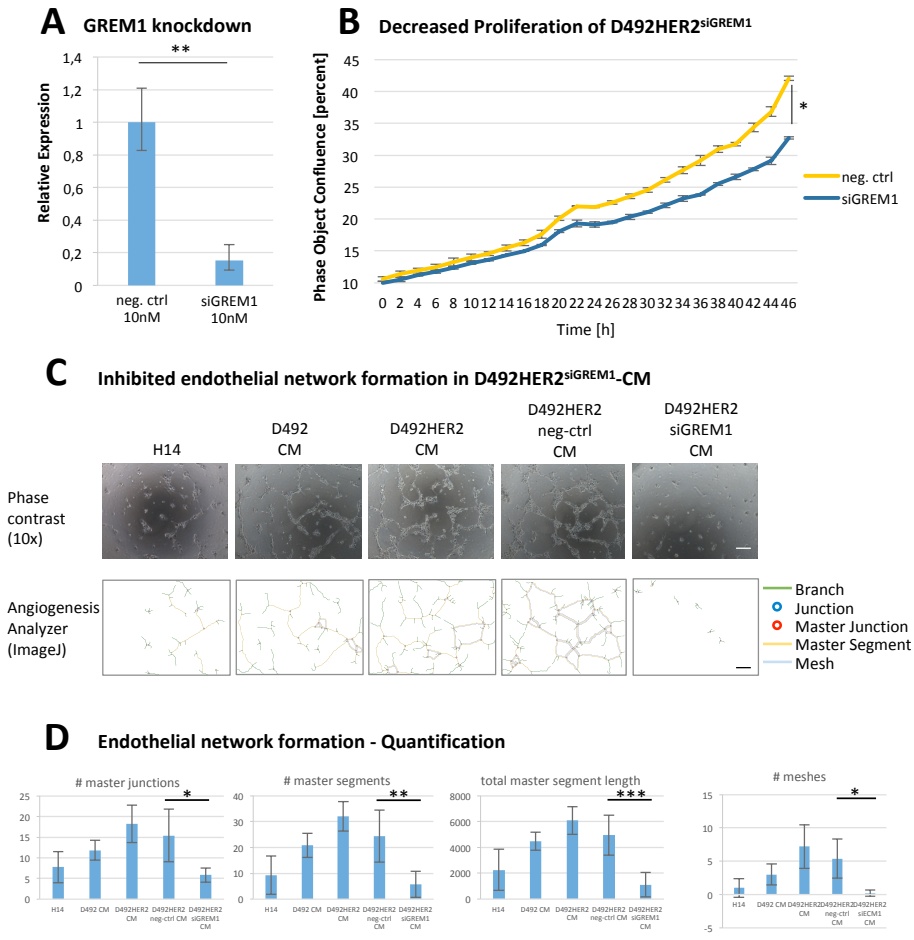


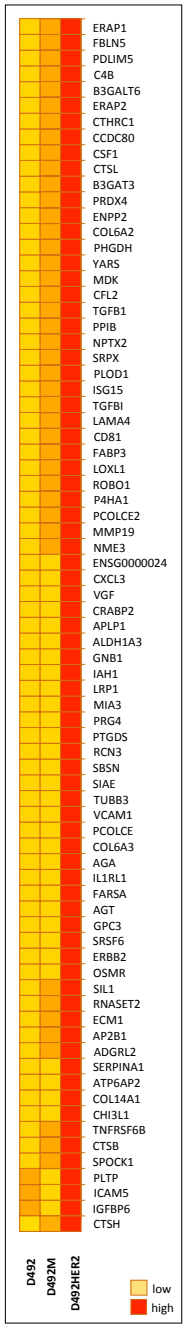
Figure 13. GREM1 knockdown inhibits enhancing effect of D492HER2-CM on endothlial network formation. A) GREM1 knockdown. RT-qPCR confirmation of transient knockdown of GREM1 in D492HER2 (10 nM siRNA). Student´s t-Test, *** $p < 0.001$, ** $p < 0.01$, * $p < 0.05$. B) Decreased proliferation of D492HER2^{siGREM1}. Proliferation of D492HER2^{siGREM1} compared to neg. ctrl (scrambled siRNA). Phase object confluence [%] over time [h] (n = 2). Student´s t-Test, *** $p < 0.001$, ** $p < 0.01$, * $p < 0.05$. C) Inhibited endothelial network formation in D492HER2^{siGREM1} after 4h. Top: Representative phase-contrast images of endothelial network on top of matrigel in control medium (H14) and CM from untreated D492HER2 and controls (lipo. ctrl = lipofectamine control without siRNA, neg. ctrl = scrambled siRNA and pos. GAPDH ctrl = siRNA for GAPDH), 10x magnification. Bottom: Corresponding angiogenesis images of branches, junctions, master junctions, master segments and meshes. Scale bar = 50 µm. D) Endothelial network formation - Quantification. Angiogenesis analyzer. One-way ANOVA, *** $p < 0.001$, ** $p < 0.01$, * $p < 0.05$.

However, these results on proliferation and endothelial network formation could only be replicated once to twice due to high variation between independent experiments. Therefore, I decided to perform label-free mass spectrometry on CM from all three D492 cell lines to be able to specify actually secreted factors more clearly. After p-value correction and ranking of the secreted proteins based on high secretion levels in D492HER2 compared to both D492 and D492M (2-fold threshold), I indeed discovered that GREM1 was below the actual detection level. Looking back at the transcriptome data, we noticed that even though the fold change difference for GREM1 between D492HER2 and D492 was very large, the actual expression level in D492HER2 still remained very low. Therefore, GREM1 was dropped as a candidate mediating the endothelial feedback and further focus put on the secretome data.

4.2.4 Identification of ECM1 and YKL-40 as pro-angiogenic factors in the D492HER2 secretome

After p-value correction and ranking of the mass spectrometry data, I determined a total of 77 proteins with higher secretion by D492HER2 compared to both D492 and D492M (Fig. 14A). With the list of corresponding gene names, I then performed enrichment analysis for functional gene groups (GO terms), similar to the analysis performed with the transcriptome data. Enrichment analysis revealed a 6.7-fold enrichment for the GO term group named “regulation of angiogenesis” (GO:0045765) among D492HER2-secreted candidates (Fig. 14B). This GO group consists of 7 gene members (Fig. 14C). I then compared secretion levels of these 7 candidates in the secretome data set and identified two proteins with the most prominent secretion profile, extracellular matrix protein 1 (ECM1) and chitinase-3-like 1 (CHI3L1 or YKL-40) (Fig. 14D). Interestingly, commonly recognized angiogenesis inducers did not show significantly elevated secretion levels in our cell lines. There have been numerous studies in the past years showing that VEGF signaling plays an important role in cancer-mediated induction of angiogenesis and endothelial proliferation (Arteaga et al., 2011; Kumar & Yarmand-Bagheri, 2001; Li et al., 2017). Also FGF2 and PDGF have previously been identified as mediators of angiogenesis in the context of cancer progression (Aparicio et al., 2005; Shibata et al., 2002; Ucuzian et al., 2010). Interestingly, these factors did not show elevated expression or secretion levels in our cellular model for HER2-overexpressing breast cancer. This suggests that these pathways may not be the drivers of the observed increase in endothelial network formation and the induced feedback on cancer migration and invasion in our system.

A 77 candidates



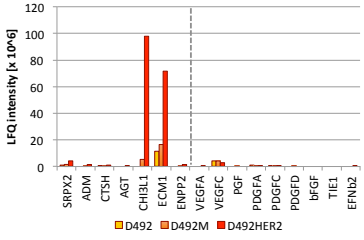
B Enrichment of angiogenesis-regulating genes in D492HER2 secretome (GO terms)

GO biological process complete	Expected Genes	Actually present Genes	Fold Enrichment	P-value
ossification involved in bone remodeling (GO:0043932)	0,01	2	> 100	2,00E-04
positive regulation of protein catabolic process in the vacuole (GO:1904352)	0,02	2	> 100	2,79E-04
cellular response to thyroid hormone stimulus (GO:0097067)	0,06	3	50,58	4,50E-05
chondrocyte morphogenesis (GO:0090171)	0,07	3	44,96	6,14E-05
growth plate cartilage chondrocyte morphogenesis (GO:0003429)	0,07	3	44,96	6,14E-05
chondrocyte morphogenesis involved in endochondral bone morphogenesis (GO:0003414)	0,07	3	44,96	6,14E-05
growth plate cartilage morphogenesis (GO:0003422)	0,07	3	42,6	7,09E-05
chondrocyte development involved in endochondral bone morphogenesis (GO:0003433)	0,09	3	35,19	1,19E-04
growth plate cartilage chondrocyte differentiation (GO:0003418)	0,09	3	33,72	1,33E-04
response to thyroid hormone (GO:0097066)	0,1	3	31,13	1,65E-04
cartilage morphogenesis (GO:0060536)	0,1	3	28,9	2,02E-04
chondrocyte differentiation involved in endochondral bone morphogenesis (GO:0003413)	0,11	3	27,91	2,23E-04
peptide catabolic process (GO:0043171)	0,11	3	26,98	2,44E-04
regulation of superoxide metabolic process (GO:0090322)	0,12	3	25,29	2,91E-04
aorta development (GO:0035904)	0,18	4	22,48	4,07E-05
collagen metabolic process (GO:0032963)	0,21	4	19,27	7,17E-05
chondrocyte differentiation (GO:0002062)	0,3	5	16,45	1,76E-05
positive regulation of animal organ morphogenesis (GO:0110110)	0,32	5	15,68	2,19E-05
organ growth (GO:0035265)	0,34	5	14,5	3,13E-05
artery development (GO:0060840)	0,3	4	13,32	2,78E-04
extracellular matrix organization (GO:0030198)	1,17	15	12,85	1,06E-12
extracellular structure organization (GO:0043062)	1,33	17	12,77	2,95E-14
regulation of morphogenesis of an epithelium (GO:1905330)	0,49	5	10,3	1,49E-04
regulation of animal organ morphogenesis (GO:2000027)	0,79	8	10,18	1,53E-06
cartilage development (GO:0051216)	0,64	6	9,36	5,28E-05
connective tissue development (GO:0061448)	0,82	7	8,51	2,21E-05
negative regulation of peptidase activity (GO:0010466)	0,89	7	7,87	3,58E-05
regulation of peptidase activity (GO:0052547)	1,55	11	7,12	4,79E-07
blood vessel development (GO:0001568)	1,77	12	6,77	2,30E-07
regulation of angiogenesis (GO:0045765)	1,05	7	6,7	9,63E-05
vasculature development (GO:0001944)	1,86	12	6,46	3,76E-07
cardiovascular system development (GO:0072358)	1,9	12	6,32	4,71E-07
regulation of vasculature development (GO:1901342)	1,15	7	6,09	1,70E-04
cellular amino acid metabolic process (GO:0006520)	1,18	7	5,94	1,99E-04
blood vessel morphogenesis (GO:0048514)	1,47	8	5,45	1,22E-04
inflammatory response (GO:0006954)	1,73	9	5,21	6,29E-05
circulatory system development (GO:0072359)	3,11	16	5,14	7,40E-08
tube morphogenesis (GO:0035239)	2,35	12	5,11	4,16E-06

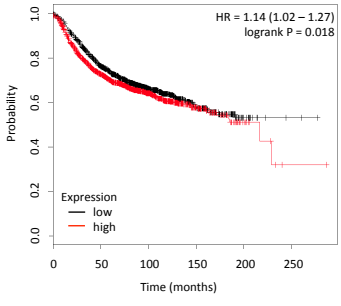
C GO:0045765 gene members

Regulation of angiogenesis (GO:0045765)		
UniProtKB	**Gene name**	**PANTHER family**
O60687	SRPX2	Sushi repeat-containing protein
P35318	ADM	ADM
P09668	CTSH	Pro-cathepsin H
P01019	AGT	Angiotensinogen
P36222	CHI3L1	Chitinase-3-like protein 1
Q16610	ECM1	Extracellular matrix protein 1
Q13822	ENPP2	Ectonucleotide pyrophosphatase/ phosphodiesterase family member 2

D Highest secretion levels of ECM1 & CHI3L1



E RFS in YKL-40+ patients



F DMFS in ECM1+/HER2+ patients

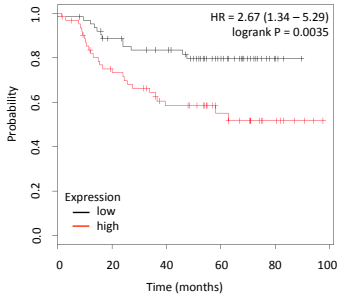


Figure 14. Identification of ECM1 and YKL-40 as pro-angiogenic candidates in D492HER2. A) 77 candidates. Heat map of 77 proteins with higher secretion by D492HER2 compared to both D492 and D492M (label-free mass spectrometry

secretome data, p < 0.05, treshold fold change ≥ 2-fold). B) Enrichment of angiogenesis-regulating genes in D492HER2 secretome (GO terms). Enrichment of „Regulation of Angiogenesis“ GO group GO:0045765 among D492HER2 secretome. Statistical overrepresentation test (Panther DB) was performed using “GO biological process complete” as annotation data set with Bonferroni correction for multiple testing. C) GO:0045765 gene members. Proteins part of GO group GO:0045765 (Regulation of Angiogenesis). D) Highest secretion levels of ECM1 and CHI3L1. Secretion levels (label-free quntification LFQ) of 7 candidates from C (left of dotted line) compared to levels of common angiogenesis inducers (right of dotted line). E) RFS in YKL-40+ patients. Kaplan-Meier plot of YKL-40+ tumors showing correlation of high expression with decreased relapse-free survival (RFS). F) DMFS in ECM1+/ HER2+ patients. Kaplan-Meier plot of ECM1 in HER2+ tumors showing correlation of high expression with decreased distant metastasis-free survival (DMFS).

ECM1 is a secreted glycoprotein, which was first identified in the mouse osteogenic stromal cell line MN7 (Mathieu et al., 1994). It was initially described as modulator of proliferation and differentiation of epidermal keratinocytes and basement membrane reconstitution in the skin (Oyama & Merregaert, 2017). However, it has also been linked to angiogenesis and malignant transformation (Han et al., 2001; Lee et al., 2015b; Lee et al., 2014c; Oyama & Merregaert, 2017; Sercu et al., 2008a; Sercu et al., 2008b; Wang et al., 2003). CHI3L1, also known as YKL-40, is a secreted glycoprotein that is associated with a number of biological functions and also in diseases such as cancer (Kastrup, 2012; Rosenblat et al., 2015; Vignon, 2001). For both genes, Kaplan-Maier survival analysis revealed a significant correlation of gene expression with poor clinical outcome (Fig. 14E and F). However, whereas in the case of YKL-40 this correlation is not specifically associated with a certain cancer subtype, ECM1 expression is significantly correlated with decreased distant metastasis-free survival (DMSF) in patients with HER2+ and generally ER- breast tumors (Fig. 14F) (Lee et al., 2014c). For this reason, the main focus of the further work has been on the role of ECM1. YKL-40 was investigated further in the context of D492HER2 tumorigenicity, 3D phenotype and angiogenesis in connection with oncogene-induced EMT in contrast to endothelial-induced EMT in D492M, which is not tumorigenic (manuscript #III, Morera et al.).

In the next subchapters, I will now focus on manuscripts #I and #II where I have analyzed the role of ECM1 in endothelial crosstalk in more detail. After that, I will summarize the data acquired on the role of YKL-40 in D492HER2 tumorigenicity (manuscript #III).

4.3 HER2-overexpressing breast cancer cells secrete ECM1 generating a vascular niche that further accelerates cancer cell migration and invasion (manuscript #I)

In order to address the potential role of D492HER2-secreted ECM1 in endothelial network formation and induction of the endothelial feedback in our system, I initially investigated whether recombinant ECM1 (rECM1) is able to induce similar responses in ECs. In addition, I generated stable cell lines with overexpression of ECM1 in D492 and D492M.

4.3.1 Recombinant ECM1 and overexpression enhance tube formation and induce endothelial feedback

To analyze whether ECM1 directly affects angiogenesis, I used recombinant ECM1 (rECM1) in an *in vitro* angiogenesis assay. ECs were treated with 15, 30, 60 and 120 ng/ml of rECM1 in fresh endothelial medium (EGM5) and H14 mixed in a ratio of 1:1 and seeded on top of rBM for network formation analysis. Endothelial network was analyzed as described previously. Indeed, rECM1 significantly increased the endothelial network after 4 h and 24 h as quantified by numbers of master junctions, meshes, master segments and total master segment length (Fig. 15A and B). Hereby, the strongest effect was observed for treatment with 15, 30 and 60 ng/ml rECM1 (Fig. 15B). This indicates that the system may already be saturated at these concentrations rather than rECM1 having a dose-dependent effect.

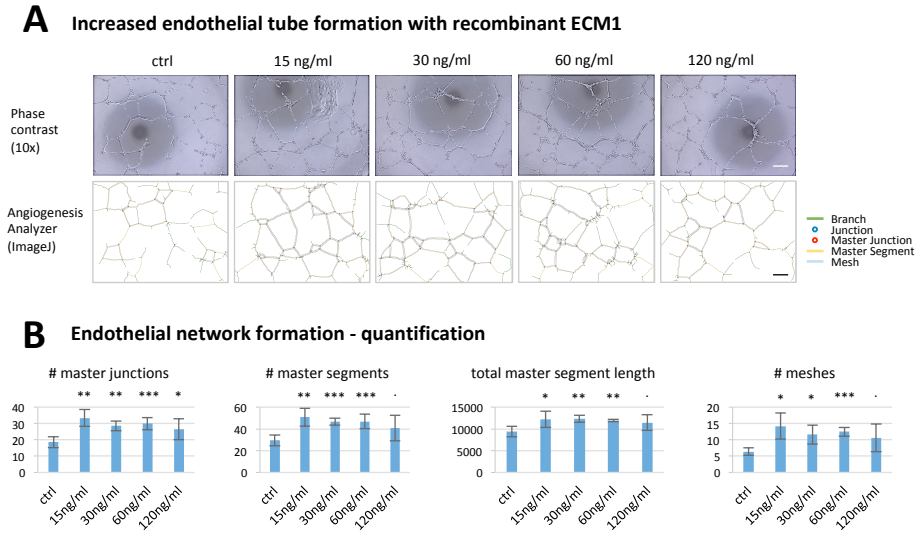


Figure 15. Recombinant ECM1 enhances endothelial network. A) Increased endothelial tube formation with recombinant ECM1. Top: Endothelial network on top of rBM in different concentrations of rECM1 (phase contrast imaging after 24 h, 10x

magnification). Bottom: Corresponding angiogenesis images (ImageJ angiogenesis analyser). Scale bar = 50 µm. B) Endothelial network formation - quantification. Quantification of master junctions, master segments, total master segment length and meshes (angiogenesis analyzer). One-way ANOVA, *** $p < 0.001$, ** $p < 0.01$, * $p < 0.05$, · $p < 0.1$.

Additionally, CM from D492 and D492M stably overexpressing ECM1 showed pro-angiogenic properties (Fig. 18A and B), confirming an involvement of ECM1 in the observed increase in angiogenesis network formation in. These results go hand in hand with previous studies linking ECM1 to increased angiogenesis (Han et al., 2001; Sercu et al., 2008a). However, the exact molecular mechanism behind this has not been elucidated completely. Furthermore, an involvement of ECM1 in the induction of an endothelial feedback promoting cancer progression has not been reported previously. Therefore, I decided to investigate whether rECM1 alone was also capable of inducing ECs to increase D492HER2 migration and invasion. I collected CM from rECM1-induced ECs for treatment of D492HER2 (Fig. 16A). Interestingly, CM from ECM1-induced ECs significantly increased D492HER2 migration and invasion, suggesting an involvement of ECM1 in endothelial feedback induction (Fig. 16B).

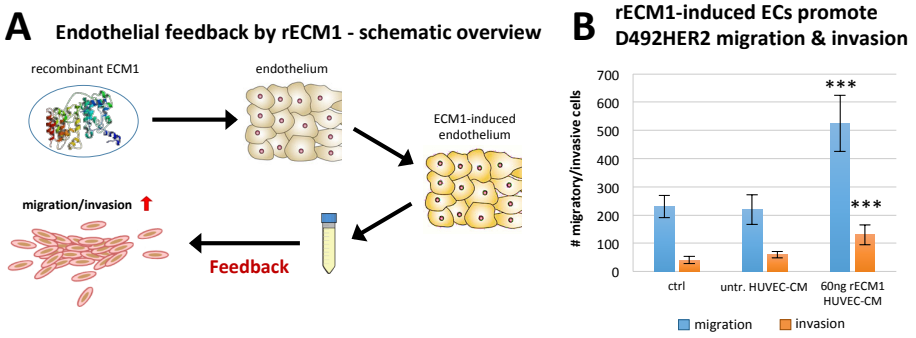


Figure 16. Recombinant ECM1 induces endothelial feedback increasing D492HER2 migration and invasion. A) Endothelial feedback by rECM1 - schematic overview. Schematic work flow of conditioning ECs using 60 ng/ml rECM1. B) rECM1-induced ECs promote D492HER2 migration/invasion. Transwell migration and invasion assays of D492HER2 treated with unconditioned medium, unconditioned HUVEC-CM and 60ng rECM1 treated HUVEC-CM. Number of migratory/invasive cells shown for different treatments (Student´s t-Test, *** $p < 0.001$, ** $p < 0.01$, * $p < 0.05$).

To determine whether these results also apply in other types of breast cancer than HER2+, we used the GOBO database (Lund University, Sweden) to identify other breast cancer cell lines expressing ECM1. Gene set analysis revealed MDA-MB-231 among others as a triple-negative breast

cancer cell line expressing high levels of ECM1. RT-qPCR confirmed similar gene expression levels of ECM1 in MDA-MB-231 as in D492HER2 (Fig. 17A). Survival analysis suggested that high ECM1 expression is not only correlated with worse outcome in patients with HER2+ breast cancer but also patients with triple-negative and generally ER- breast cancer (Fig. 17B). Interestingly, CM from MDA-MB-231 also leads to an increase in endothelial network formation in contrast to CM from MCF-7, which does not express ECM1 (Fig. 17C and D). Additionally, treatment of MDA-MB-231 with CM from rECM1-induced ECs also resulted in an increased migratory phenotype compared to untreated MDA-MB-231 and MDA-MB-231 treated with CM from non-induced ECs (Fig. 17E and F).

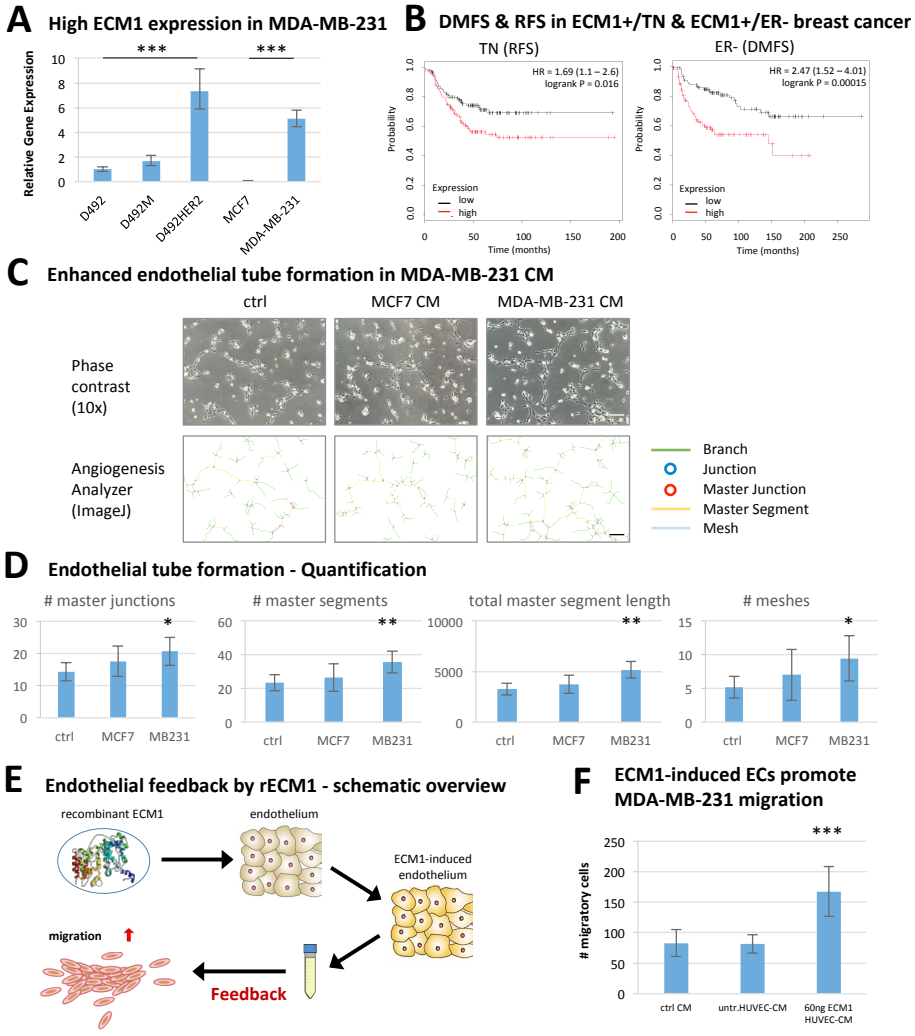


Figure 17. CM from MDA-MB-231 enhances endothelial network and induces

endothelial feedback increasing MDA-MB-231 migration. A) High ECM1 expression in MDA-MB-231. Relative Gene expression of ECM1 in MDA-MB-231 compared to MCF7 and D492 compared to D492HER2. Student´s t-Test , *** $p < 0.001$, ** $p < 0.01$, * $p < 0.05$. B) DMFS and RFS in ECM1+/TN and ECM1+/ER- breast cancer. ECM1 expression correlates with worse relapse-free survival (RFS) in triple-negative (TN) breast cancer patients and with worse distant metastasis-free survival (DMFS) in ER- breast cancer patients. C) Enhanced endothelial tube formation in MDA-MB-231 CM. Top: HUVEC endothelial network after 4h in R10F, MCF7-CM and MDA-MB-231-CM (phase contrast). Bottom: Angiogenesis images. Scale bar = 50 µm. D) Endothelial tube formation - Quantification. Quantification of master junctions, master segments total master segment length and meshes. One-way ANOVA, *** $p < 0.001$, ** $p < 0.01$, * $p < 0.05$. E) Endothelial feedback by rECM1 - schematic overview. Schematic work flow of conditioning of ECs using 60 ng/ml rECM1. F) ECM1-induced ECs promote MDA-MB-231 migration. Transwell-migration assay of MDA-MB-231 treated with unconditioned medium (RPMI+10%FBS), unconditioned HUVEC-CM and 60 ng rECM1-treated HUVEC-CM. Number of migratory cells shown for the different treatments. Student´s t-Test , *** $p < 0.001$, ** $p < 0.01$, * $p < 0.05$.

In the next step, I generated transient and stable knockdown (KD) of ECM1 in D492HER2 using siRNA and CRISPRi, respectively (see methods). Both transient and stable KD was above 90%, as confirmed on gene and protein expression level. The results showed that treatment with CM from D492HER2-kdECM1 resulted in significantly lower tube formation compared to control D492HER2 (Fig. 18A and B). These results go hand in hand with the observed effects of rECM1 and ECM1 overexpression in D492 and D492M. Similar results were obtained with CM from D492HER2 as well as MDA-MB-231 using transient ECM1 KD (Fig. 18C).

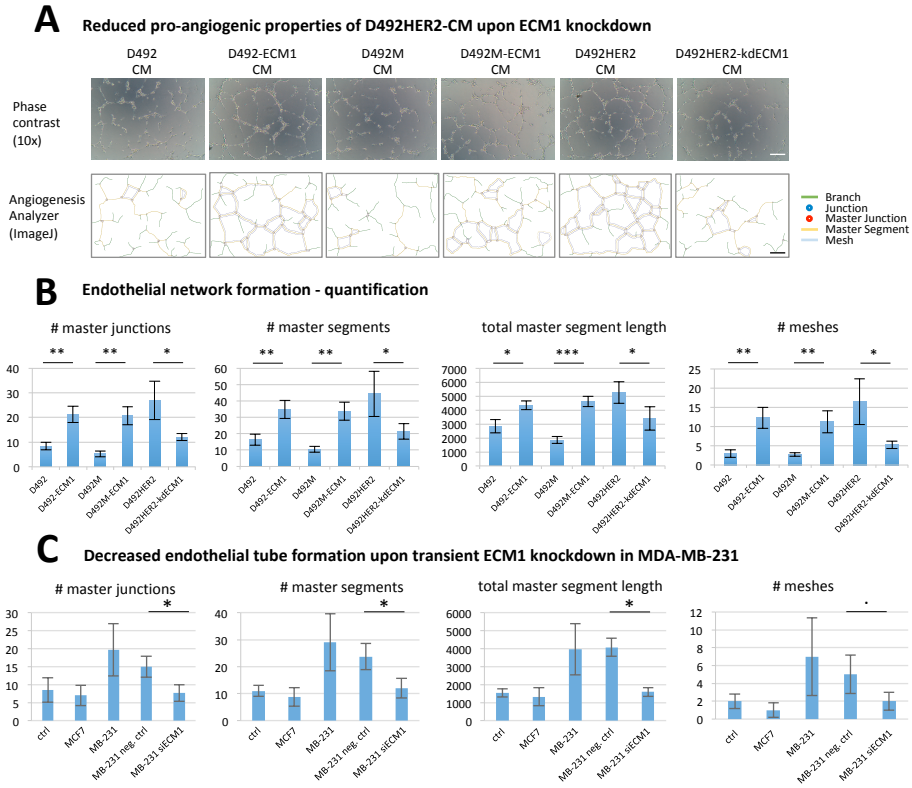


Figure 18. ECM1 knockdown inhibits pro-angiogenic effect of D492HER2- and MDA-MB-231-CM. A) Reduced pro-angiogenic properties of D492HER2-CM upon ECM1 knockdown. Top: Endothelial network in CM from D492 and D492M with ECM1 overexpression and D492HER2 with ECM1 KD compared to empty control (after 4h). Bottom: Corresponding angiogenesis images (ImageJ angiogenesis analyzer). Scale bar = 50 µm. B) Endothelial network formation - quantification. Quantification of master junctions, master segments, total master segment length and meshes (angiogenesis analyzer). One-way ANOVA, *** $p < 0.001$, ** $p < 0.01$, * $p < 0.05$. C) Decreased endothelial tube formation upon ECM1 knockdown in MDA-MB-231. Quantification of endothelial network after 4h in ctrl medium (RPMI+10%FBS), MCF7-CM, ctrl MDA-MB-231-CM, siRNA neg. ctrl MDA-MB-231-CM and siECM1 MDA-MB-231-CM. One-way ANOVA, *** $p < 0.001$, ** $p < 0.01$, * $p < 0.05$, · $p < 0.1$.

The data further showed that treatment of ECs with CM from D492HER2-kdECM1 did not induce an endothelial response increasing D492HER2 migration and invasion (Fig. 19A and B). Also, the observed increased migratory phenotype of D492HER2 towards ECs was lost upon ECM1 KD, supporting the mediating role of ECM1 in induction of an endothelial feedback promoting cancer cell migration towards the endothelium (Fig. 19C and D).

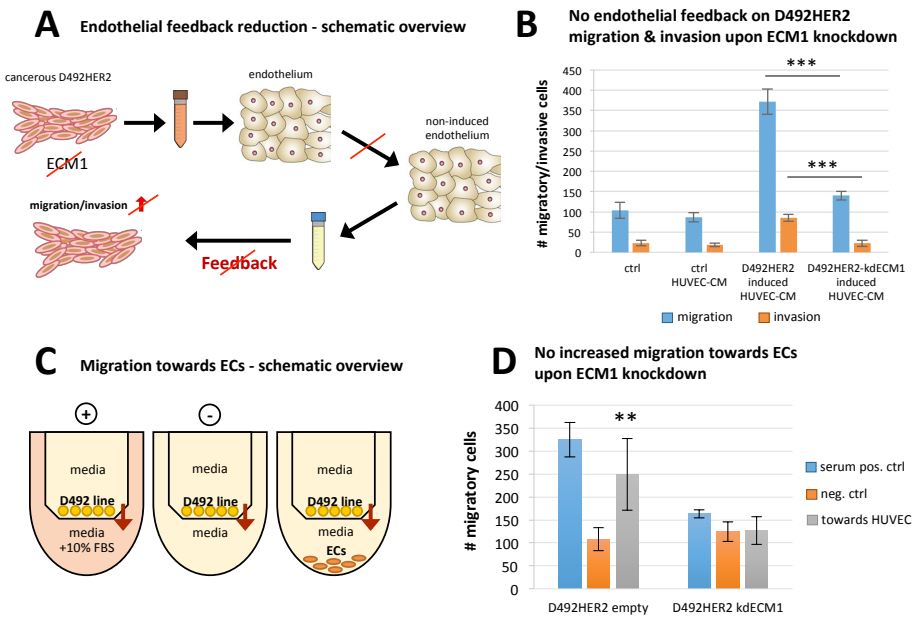


Figure 19. ECM1 knockdown prevents induction of endothelial feedback on D492HER2 migration and invasion. A) Endothelial feedback reduction - schematic overview. Work flow of treating ECs with CM from D492HER2-kdECM1. B) No endothelial feedback on D492HER2 migration/invasion upon ECM1 knockdown. Migration/invasion assays of D492HER2 treated with D492HER2-induced HUVEC-CM vs. D492HER2-kdECM1-induced HUVEC-CM. Number of migratory/invasive cells for different treatments (Student´s t-Test, *** $p < 0.001$, ** $p < 0.01$, * $p < 0.05$). C) Migration towards ECs - schematic overview. Setup of migration assay of D492HER2 ctrl. and D492HER2-kdECM1 towards ECs as described previously. D) No increased migration towards ECs upon ECM1 KD. Migration of D492HER2 ctrl. and D492HER2-kdECM1 towards ECs. Number of migratory cells for different treatments (Student´s t-Test, *** $p < 0.001$, ** $p < 0.01$, * $p < 0.05$).

To summarize, my work has identified ECM1 as a glycoprotein secreted by D492HER2 and MDA-MB-231 that appears to be involved in mediating pro-angiogenic properties. Furthermore, the data link ECM1 to the induction of an endothelial feedback that further increases tumorigenic properties as measured by increased migration and invasion both in D492HER2 and MDA-MB-231. ECM1 has been linked to tumor progression and metastasis formation in previous studies (Chen et al., 2016; Gan et al., 2017; Lee et al., 2015b; Lee et al., 2014c; Sercu et al., 2008a; Wu et al., 2018). Lee and colleagues showed that ECM1 influences resistance to trastuzumab, the major agent for chemotherapy of HER2+ breast cancer (Lee et al., 2014c). Wu and research group very recently linked ECM1 to breast cancer progression by suggesting a role in facilitating metastasis through increased invasion and adhesion capacity of ECM1-expressing cancer cells (Wu et al.,

2018). However, a driving role of cancer-secreted ECM1 in cancer progression through endothelial crosstalk and induction of a cancer-promoting feedback has not been shown yet. To follow up, I then focused on investigating which molecular mechanisms ECM1 is inducing in ECs that mediate the observed endothelial response promoting tumorigenicity.

4.3.2 ECM1 upregulates endothelial NOTCH1 and NOTCH3

Next, an Affymetrix human Clariom S RNA microarray was performed at the German Cancer Research Center (DKFZ) Heidelberg, on ECs treated with CM from D492HER2 ctrl and D492HER2-kdECM1. The goal was to identify upregulated endothelial genes upon treatment with D492HER2-CM but not with CM from D492HER2-kdECM1. That data were analyzed using Chipster high-throughput data analysis software v3.12. After p-value correction and setting the fold change cut-off to 2-fold, analysis revealed 18 genes upregulated in ECs treated with D492HER2-CM compared to ECs treated with CM from D492HER2-kdECM1 (top 10 genes shown in Fig. 20A+B). However, the observed changes in gene expression were rather mild. One of the mildly higher expressed genes in ECs treated with D492HER2-CM encoded fatty acid binding protein 4 or FABP4. Tumor endothelial FABP4 has recently been linked to cancer progression in ovarian and prostate cancer (Harjes et al., 2017; Huang et al., 2017). Harjes et al. (2017) identified FABP4 as a protein secreted by tumor-associated ECs that was associated with increased metastasis formation. Expression of FABP4 was shown to be induced by NOTCH1 signaling (Harjes et al., 2017). Therefore, I decided to focus on FABP4 and the NOTCH receptors 1-4 in order to analyze whether NOTCH signaling could be the responding signaling pathway in ECs treated with ECM1. RT-qPCR and IF staining revealed increased NOTCH1 and NOTCH3 gene and protein expression in ECs treated with D492HER2-CM or rECM1 but not with CM from D492HER2-kdECM1 compared to untreated ECs (Fig. 21B and C). However, despite sufficient primer efficiency, FABP4 expression could not be confirmed by RT-qPCR as upregulated compared to untreated ECs.

A **Top 10 up- and downregulated genes in HUVECs treated with D492HER2/D492HER2-kdECM1 CM**

chip.microarray 001.cel	Gene Symbol	Description	D492HER2 CM	D492HER2-kdECM1 CM	p-value adjusted	log2 FC	FC
100287728_at	**LOC100287728**	uncharacterized LOC100287728	↑	↓	0	-1,06	0,48
2167_at	**FABP4**	fatty acid binding protein 4, adipocyte	↑	↓	5,00E-06	-0,85	0,56
84948_at	**TIGD5**	tigger transposable element derived 5	↑	↓	0,000565	-0,71	0,61
116441_at	**TM4SF18**	transmembrane 4 L six family member 18	↑	↓	0,009003	-0,61	0,65
25780_at	**RASGRP3**	RAS guanyl releasing protein 3 (calcium and DAG-regulated)	↑	↓	0,018059	-0,58	0,67
135924_at	**OR9A2**	olfactory receptor, family 9, subfamily A, member 2	↑	↓	0,018059	-0,58	0,67
8995_at	**TNFSF18**	tumor necrosis factor (ligand) superfamily, member 18	↑	↓	0,019042	-0,58	0,67
56911_at	**MAP3K7CL**	MAP3K7 C-terminal like	↑	↓	0,02629	-0,56	0,68
284349_at	**ZNF283**	zinc finger protein 283	↑	↓	0,029553	-0,56	0,68
359787_at	**DPPA3**	developmental pluripotency associated 3	↑	↓	0,030925	-0,55	0,68
597_at	**BCL2A1**	BCL2-related protein A1	↓	↑	0,015665	0,59	1,51
51351_at	**ZNF117**	zinc finger protein 117	↓	↑	0,015046	0,59	1,51
3078_at	**CFHR1**	complement factor H-related 1	↓	↑	0,011634	0,60	1,52
6407_at	**SEMG2**	semenogelin II	↓	↑	0,009003	0,61	1,53
414189_at	**AGAP6**	ArfGAP with GTPase domain, ankyrin repeat and PH domain 6	↓	↑	0,008609	0,62	1,54
256586_at	**LYSMD2**	LysM, putative peptidoglycan-binding, domain containing 2	↓	↑	0,007606	0,63	1,54
345778_at	**MTX3**	metaxin 3	↓	↑	0,002965	0,66	1,58
56999_at	**ADAMTS9**	ADAM metallopeptidase with thrombospondin type 1 motif, 9	↓	↑	0,000989	0,69	1,61
79324_at	**OR51G1**	olfactory receptor, family 51, subfamily G, member 1 (gene/pseudogene)	↓	↑	0,00061	0,71	1,63
5473_at	**PPBP**	pro-platelet basic protein (chemokine (C-X-C motif) ligand 7)	↓	↑	0,000565	0,72	1,64

B **Validation of cadidates from A with RT-qPCR**

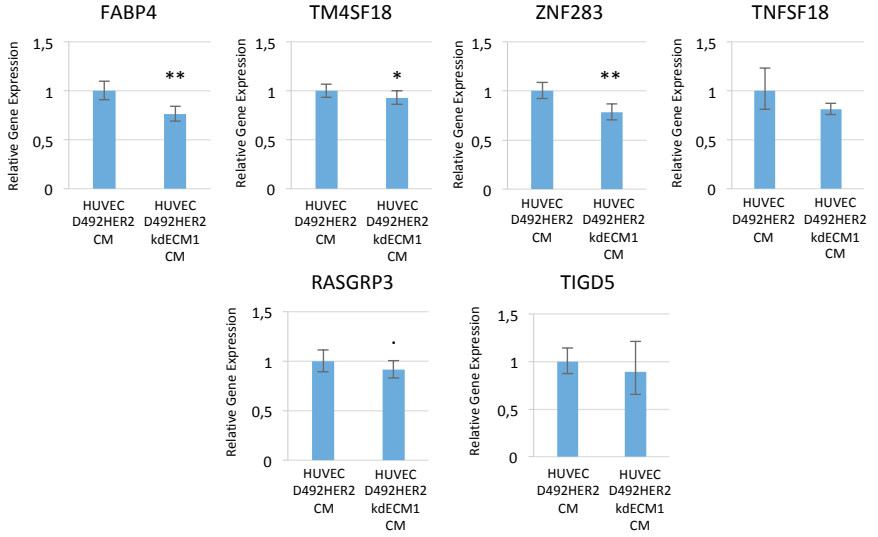


Figure 20. Mildly increased gene expression of candidates in ECs upon treatment with D492HER2-CM compared to CM from D492HER2-kdECM1. A) Top 10 up- and downregulated genes in HUVECs treated with CM from D492HER2 vs. CM from D492HER2-kdECM1. Affymetrix human Clariom S microarray, 2-fold change threshold, p-value adjusted. B) RT-qPCR validation of candidates from A). Kruskal-Wallis Test (R), *** $p < 0.001$, ** $p < 0.01$, * $p < 0.05$, · $p < 0.1$.

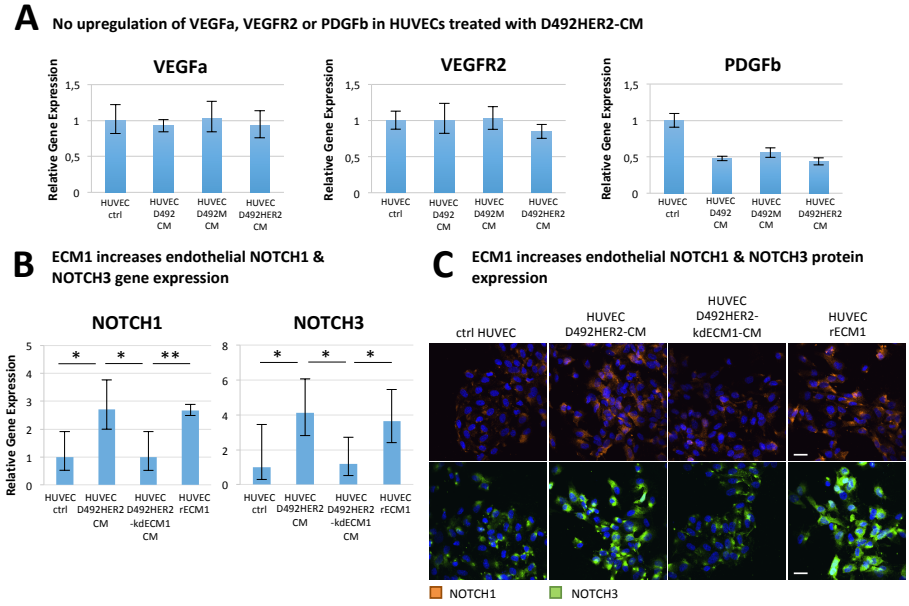


Figure 21. ECM1 upregulates endothelial NOTCH1 and NOTCH3 gene and protein expression. A) No upregulation of VEGFa, VEGFR2 or PDGFb in HUVECs treated with D492HER2-CM. RT-qPCR testing of common endothelial angiogenesis-regulating genes in response to CM treatment. B) ECM1 increases endothelial NOTCH1 and NOTCH3 gene expression. RT-qPCR for NOTCH1 and NOTCH3 in HUVECs treated with D492HER2-CM and rECM1 but not D492HER2-kdECM1-CM.Kruskal-Wallis Test, *** $p < 0.001$, ** $p < 0.01$, * $p < 0.05$. C) ECM1 increases endothelial NOTCH1 and NOTCH3 protein expression. IF staining for NOTCH1 and NOTCH3 in HUVECs treated with D492HER2-CM and rECM1 but not D492HER2-kdECM1-CM. Scale bar = 50 µM.

This indicates that whereas endothelial NOTCH signaling might indeed be involved in the observed endothelial response to ECM1, it remains unclear whether the downstream signaling cascade involves FABP4. I therefore decided to move the focus from FABP4 to NOTCH1 and 3 in general. In a previous experiment, I investigated whether treatment with D492HER2-CM upregulates commonly known angiogenesis modulators in ECs, VEGFa, VEGFR2 and PDGFb. However, none of these markers showed increased expression upon treatment with D492HER2-CM (Fig. 21A), supporting the idea of NOTCH rather than other signaling pathways being involved. Indeed, recent studies link NOTCH1 itself to induction of tumor angiogenesis and therefore tumor progression in cutaneous melanoma and myeloma (Guo et al., 2013; Kalucka et al., 2018; Murtas et al., 2015). I therefore aimed to determine how blocking of endothelial NOTCH signaling could affect both endothelial network formation and feedback induction.

4.3.3 Blocking endothelial NOTCH signaling interrupts increase in network formation and feedback induction

ECs were treated with rECM1 with or without addition of gamma-secretase inhibitor DAPT, a commonly used NOTCH inhibitor. Remarkably, blocking endothelial NOTCH signaling interrupted both the increase in network formation and feedback induction. While treatment with rECM1 significantly increased numbers of master junctions, master segments, total master segment length and number of meshes, the addition of DAPT counteracted this effect (Fig. 22A and B). Furthermore, whereas CM of rECM1-induced ECs increased cancer cell migration and invasion, this effect was no longer visible upon DAPT addition while conditioning the ECs (Fig. 22C and D).

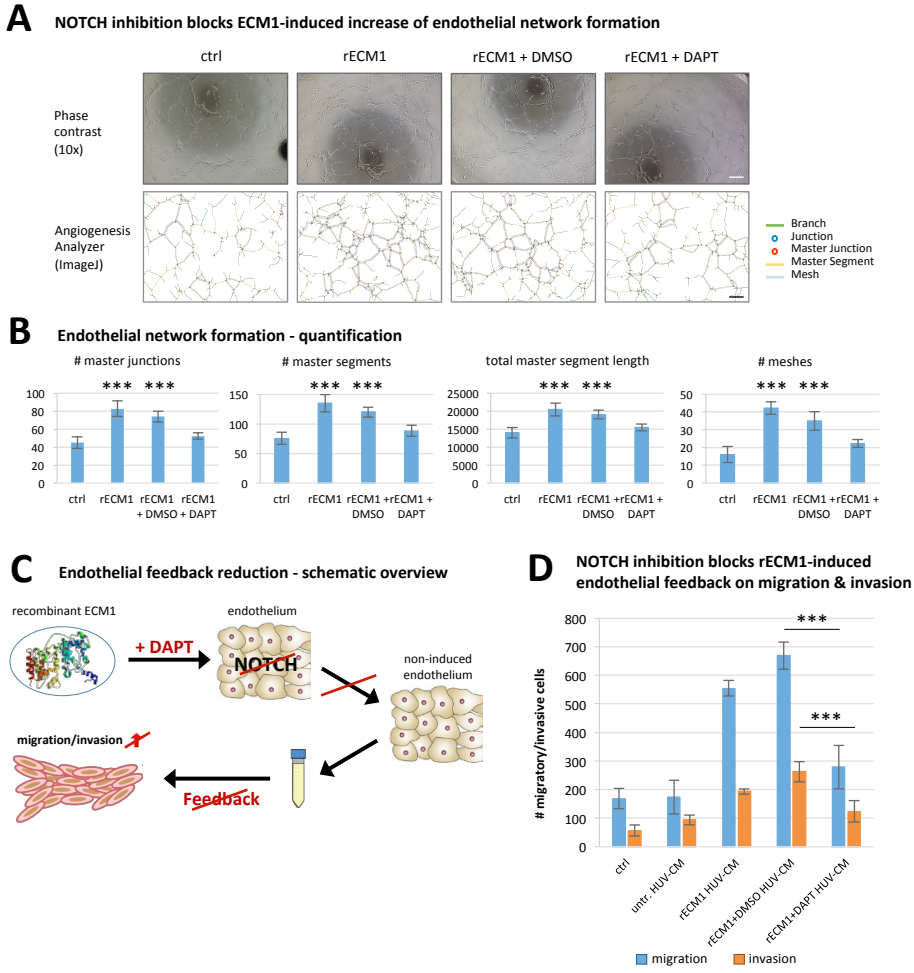


Figure 22. Inhibition of ECM1-induced NOTCH1 and NOTCH3 in ECs prevents

increased tube formation and endothelial feedback induction. A) NOTCH inhibition blocks ECM1-induced increase of endothelial network formation. Top: HUVEC endothelial network in H14 (ctrl), 60 ng/ml rECM1, 60 ng/ml rECM1 + DMSO and 60 ng/ml rECM1 + DAPT (20 µM) after 4 h, 10x magnification. Bottom: Corresponding angiogenesis images (ImageJ angiogenesis analyser). Scale bar = 50 µm. B) Endothelial network formation - quantification. Comparison between each treatment and ctrl. One-way ANOVA, *** $p < 0.001$, ** $p < 0.01$, * $p < 0.05$.. C) Endothelial feedback reduction - schematic overview. Schematic work flow of treating ECs using 60ng/ml rECM1 and blocking NOTCH signaling using DAPT (20 µM). D) NOTCH inhibition blocks rECM1-induced endothelial feedback on migration and invasion. Migration and invasion assays of D492HER2 treated with unconditioned medium, unconditioned HUVEC-CM and 60 ng rECM1 treated HUVEC-CM, 60 ng rECM1 + DMSO treated HUVEC-CM and 60 ng rECM1 + DAPT treated HUVEC-CM (NOTCH inhibition). Number of migratory/invasive cells shown for different treatments (Student´s t-Test, *** $p < 0.001$, ** $p < 0.01$, * $p < 0.05$).

In summary, I have identified ECM1 as a cancer-secreted pro-angiogenic factor involved in inducing the endothelial niche to support cancer progression through increased cancer cell migration and invasion. Further, my data indicate a novel role of ECM1 in mediating endothelial NOTCH signaling, which appears to be involved in promoting induction of the cancer-promoting endothelial feedback. ECM1 has been associated with EGF signaling (Lee et al., 2014c), ITGB4/FAK/SOX2/HIF1a (Gan et al., 2017) and WNT1/ß-catenin (Lee et al., 2015b) pathways but a mediating role in NOTCH signaling has not been described. Taken together, these findings might open up new possibilities for targeted cancer treatment by improving our understanding of how an activated vascular niche provides positive feedback to the cancer.

In addition to the role of ECM1 in mediating cancer-endothelial crosstalk, I also wanted to further understand its molecular role and contribution to tumorigenic properties of cancer cells themselves. This is the topic of manuscript II, which focuses on the effect of ECM1 knockdown on the tumorigenic properties of D492HER2.

4.4 ECM1 knockdown in HER2-expressing breast cancer decreases basal characteristics and promotes better outcome by re-expression of GATA3 (Manuscript #II)

The focus of the second manuscript as part of my PhD project was to investigate the function of ECM1 in regulating tumorigenic properties of D492HER2 cells. Previous research indicates that ECM1 expression correlates with worse prognosis for patients with HER2+ breast cancer and that KD of ECM1 may therefore have beneficial consequences (Lee et al., 2014c). Previous studies on hepatocellular carcinoma and breast cancer

have linked ECM1 both to increased EMT and stemness of cancer cells (Chen et al., 2016; Lee et al., 2015b). Therefore, I aimed to characterize the phenotype of D492HER2-kdECM1 by gene expression profiling of EMT and basal/luminal markers in comparison to D492HER2 ctrl cells.

4.4.1 ECM1 knockdown leads to loss of basal characteristics and gain of GATA3 expression, associated with better outcome

Initial characterization of D492HER2 cells with KD of ECM1 revealed reduced expression of basal/myoepithelial KRT14 and increase in luminal KRT19 (Fig. 23A). However, neither a significant upregulation of the key epithelial marker E-cadherin (CDH1) nor downregulation of mesenchymal N-cadherin (CDH2) upon ECM1 KD was observed. KRT19 however is a known luminal epithelial marker, which led the initial focus from EMT towards a possible connection with luminal differentiation. I therefore profiled expression of further selected luminal and myoepithelial/basal markers.

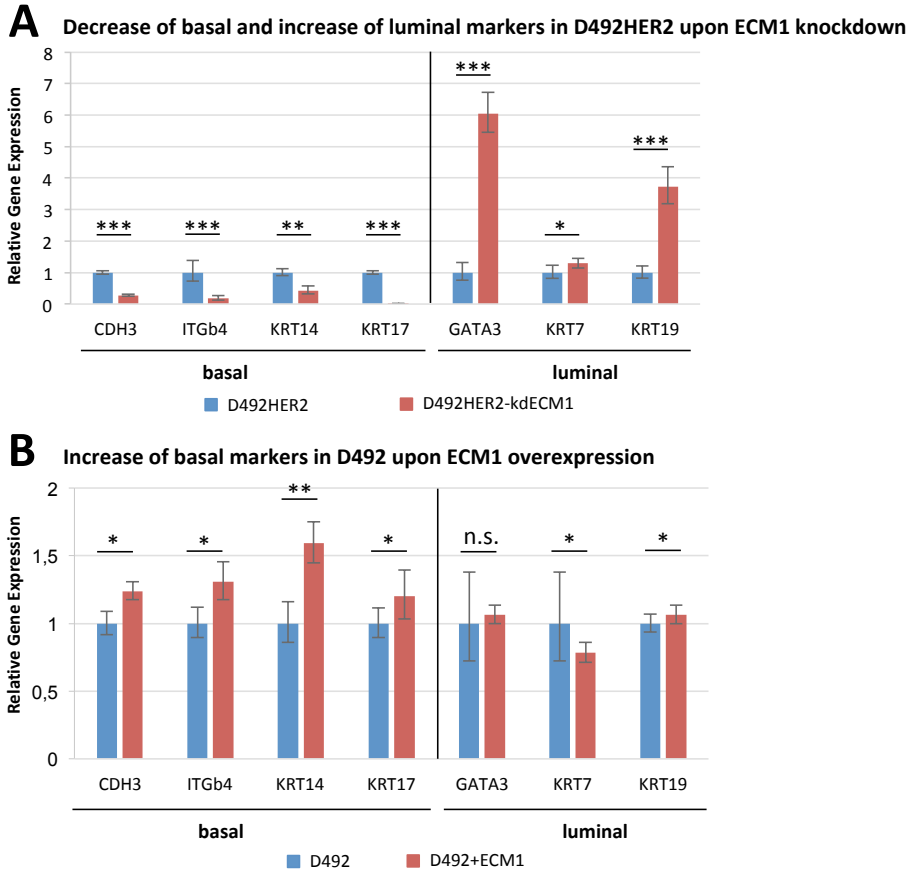


Figure 23. ECM1 knockdown leads to loss of basal characteristics in D492HER2. A) Decrease of basal and increase of luminal markers in D492HER2 upon ECM1 knockdown. Relative gene expression of luminal/basal markers in D492HER2 empty ctrl vs. D492HER2-kdECM1 (RT-qPCR). Kruskal-Wallis Test, *** $p < 0.001$, ** $p < 0.01$, * $p < 0.05$. B) Increase of basal markers in D492 upon ECM1 overexpression. Relative gene expression in D492 empty ctrl vs. D492+ECM1 (RT-qPCR).Kruskal-Wallis Test, *** $p < 0.001$, ** $p < 0.01$, * $p < 0.05$.

Further expression analysis revealed a decrease of basal markers P-cadherin (CDH3), ITGB4, and KRT17 in addition to KRT14 (Fig. 23A). In accordance to these data, expression of these basal markers was upregulated in D492 overexpressing ECM1 (Fig. 23B). Additionally, expression of luminal KRT7 and transcription factor GATA3, a key regulator of luminal differentiation (Kouros-Mehr et al., 2008), was upregulated in D492HER2 with ECM1 KD (Fig. 23A). Expression of KRT7 was also downregulated in D492 overexpressing ECM1, however downregulation of GATA3 could not be observed (Fig. 23B). This indicates that KD of ECM1 is

sufficient to upregulate GATA3 expression but ECM1 overexpression alone is not sufficient to downregulate GATA3.

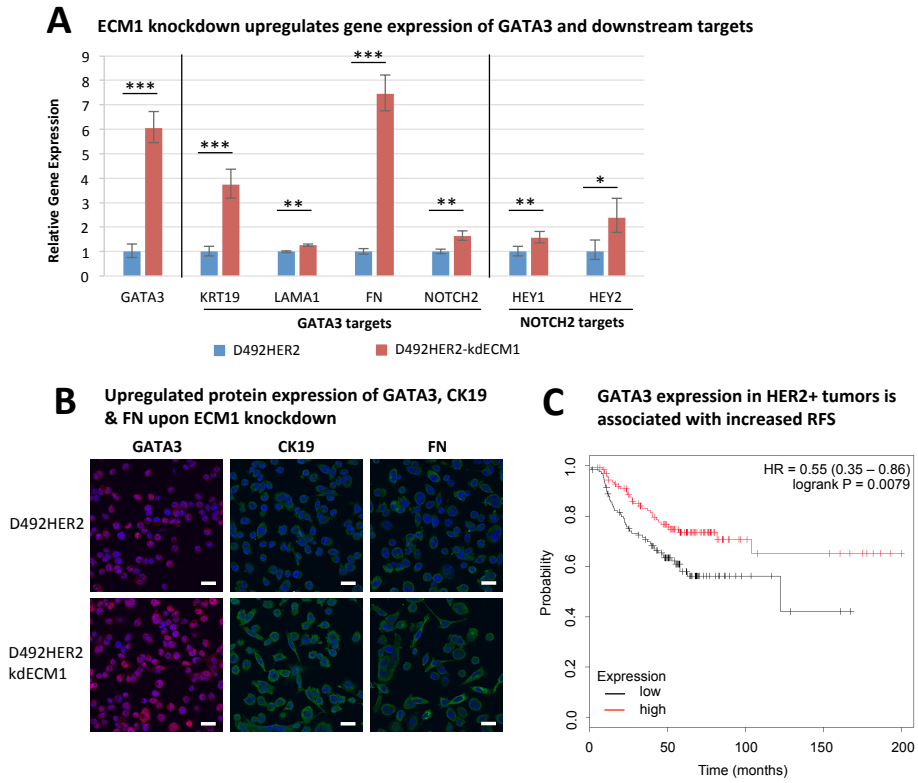


Figure 24. ECM1 knockdown leads to gain of GATA3 expression, associated with better outcome. A) ECM1 knockdown upregulates gene expression of GATA3 and downstream targets. Relative gene expression of GATA3 and downstream targets in D492HER2 ctrl vs. D492HER2-kdECM1 (RT-qPCR). Kruskal-Wallis Test, *** $p < 0.001$, ** $p < 0.01$, * $p < 0.05$. B) Upregulated protein expression of GATA3, CK19 and FN upon ECM1 knockdown. IF staining of GATA3 and selected downstream targets in D492HER2 empty ctrl vs. D492HER2-kdECM1. Scale bar = 50 µM. C) GATA3 expression in HER2+ tumors is associated with increased RFS. Kaplan-Meier plot (KM-plotter) showing relapse-free survival in patients with HER2+ breast cancer with and without GATA3 expression.

GATA3 is known to regulate KRT19 expression (Harmonizome, CHEA Transcription Factor Targets Dataset) (Rouillard et al., 2016). In order to determine whether GATA3 downstream signaling was indeed active, I analyzed expression of further GATA3 downstream targets. Downstream targets were selected based on literature (Ralston et al., 2010). RT-qPCR analysis showed additional upregulation of LAMA1, FN, NOTCH2 and NOTCH2 downstream targets HEY1 and HEY2 upon ECM1 KD in D492HER2 (Fig. 24A). The strongest upregulation in gene and protein

expression was thereby quantified for GATA3, KRT19 and FN (Fig. 24A and B). These data indicate that KD of ECM1 in D492HER2 indeed leads to upregulation of GATA3 expression and downstream GATA3 target genes. Interestingly, survival analysis revealed that GATA3 expression is associated with better outcome in patients with HER2+ breast cancer (Fig. 24C). This goes hand in hand with previous findings on GATA3 inhibiting cancer progression and metastasis formation and therefore improving survival (Yan et al., 2010; Yoon et al., 2010). However, a reverse correlation between ECM1 and GATA3 expression has not been shown previously.

Next, I analyzed the effect of ECM1 KD on tumorigenic properties of D492HER2 by quantification of migration and invasion capacity. Transwell migration and invasion assays revealed significantly reduced numbers of migratory and invasive D492HER2 cells with ECM1 KD compared to empty vector control cells (Fig. 25). Similar results were seen for transient KD of ECM1 in D492HER2 using siRNA (Fig. 26A). This confirms reduced tumorigenic properties of D492HER2 upon ECM1 KD *in vitro*. In addition to changes in tumorigenicity of D492HER2 with KD of ECM1, I also investigated migration and invasion ability of normal epithelial D492 with stable ECM1 overexpression. Quantification of migratory and invasive cells revealed increased cell numbers of D492 cells upon ECM1 overexpression compared to ctrl D492 (Fig. 26B). These results go hand in hand with the results for ECM1 KD in D492HER2.

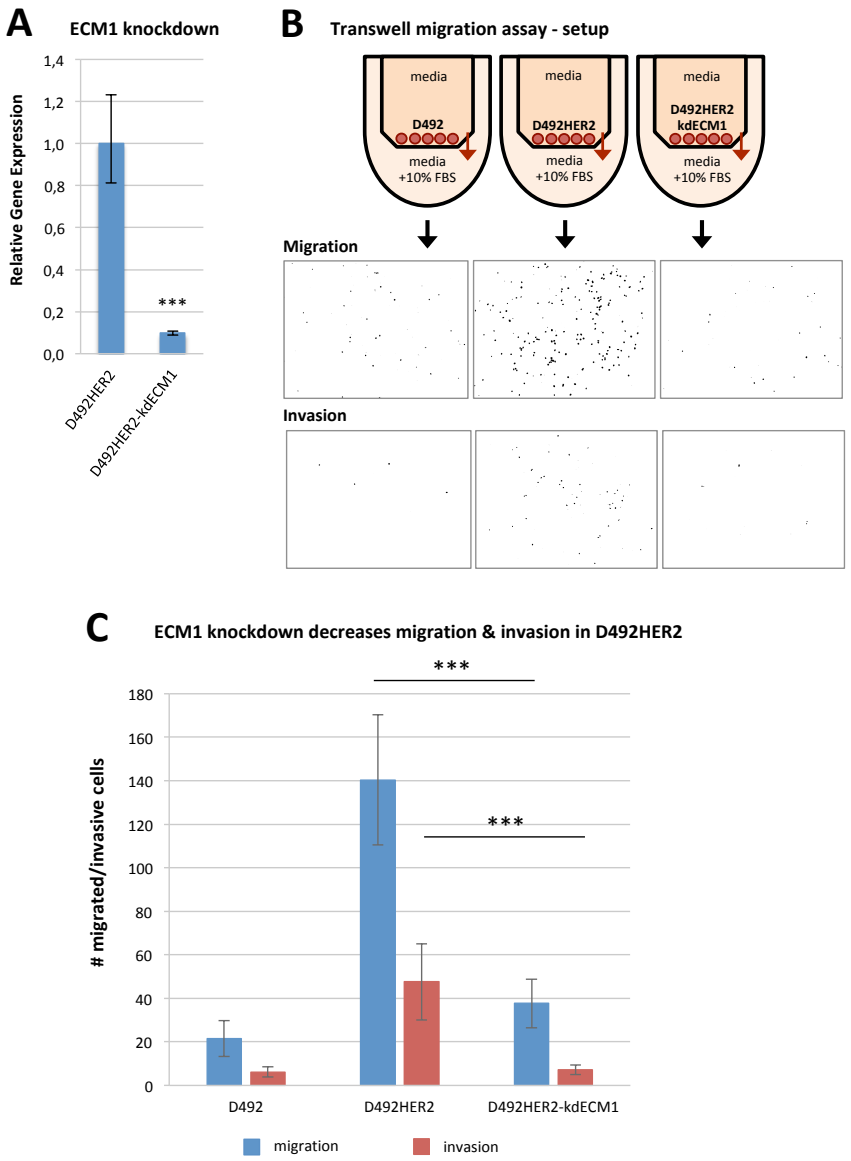


Figure 25. ECM1 knockdown decreases D492HER2 migration and invasion. A) ECM1 knockdown. Relative gene expression of ECM1 in D492HER2 empty ctrl vs. D492HER2-kdECM1 as confirmation of successful stable knockdown (RT-qPCR). Student´s t-test, *** $p < 0.001$, ** $p < 0.01$, * $p < 0.05$. B) Transwell migration assay - setup. Top: Schematic setup of transwell assays. Bottom: Representative binary images of DAPI-stained migratory and invasive cells below the transwell filter after removal of non-migratory/non-invasive cells on top. C) ECM1 knockdown decreases migration and invasion in D492HER2. Quantification of number of migratory/invasive cells on images as shown in B) (n = 3). Student´s t-test, *** $p < 0.001$, ** $p < 0.01$, * $p < 0.05$.

In order to determine whether KD of ECM1 also leads to reduction of tumorigenic properties in other breast cancer types, I also investigated migration and invasion properties in the triple-negative (TN) cell line MDA-MB-231. MDA-MB-231 expresses high levels of ECM1 as well (Fig. 17A) and survival analysis shows also for TN breast cancer that ECM1 expression correlates with worse outcome (Figs. 26E).

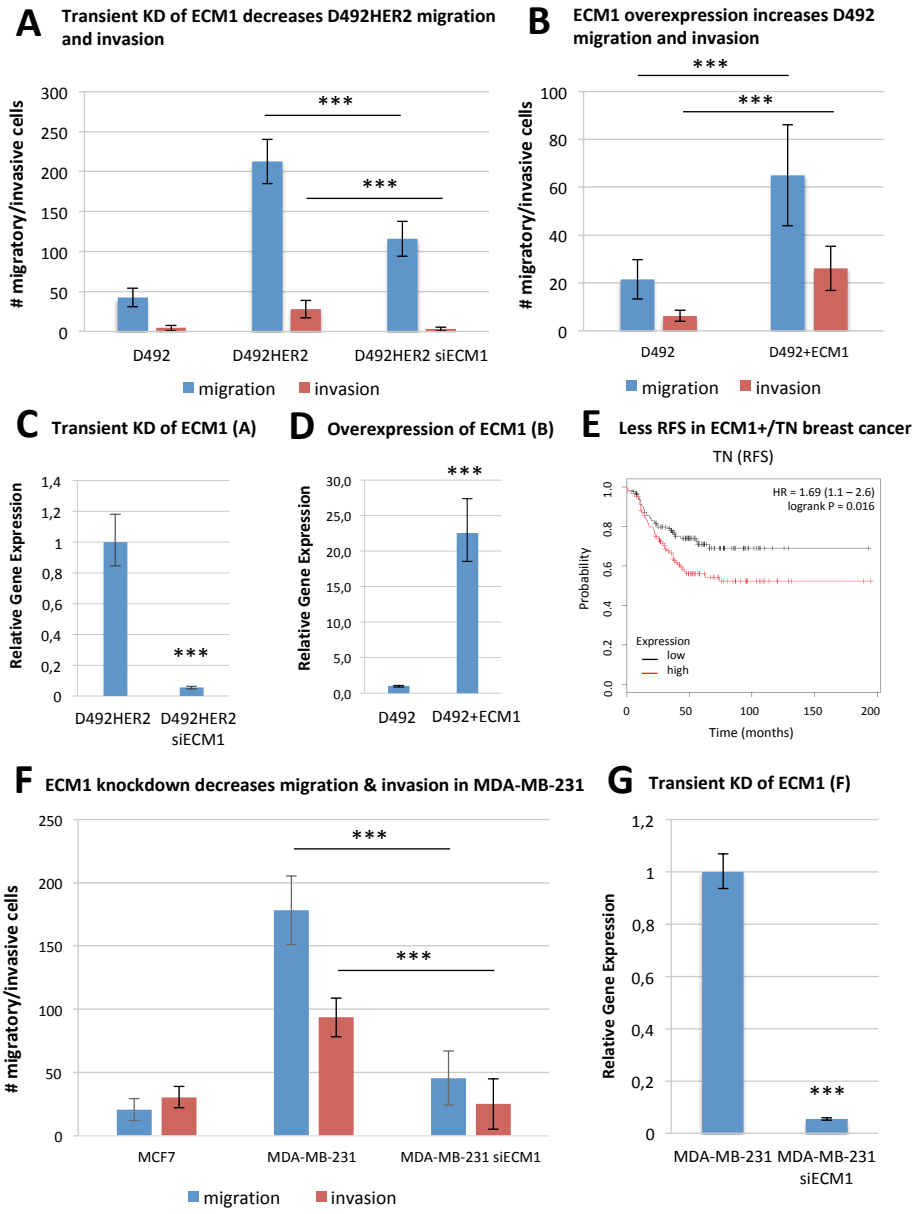


Figure 26. Transient KD of ECM1 decreases MDA-MB-231 and D492HER2 migration and invasion. A) Transient ECM1 knockdown decreases migration and invasion in D492HER2. Quantification of migratory and invasive D492HER2 cells upon transient ECM1 KD (n = 3). Student´s t-test, *** $p < 0.001$, ** $p < 0.01$, * $p < 0.05$. B) ECM1 overexpression in D492HER2 increases D492 migration and invasion. Quantification of migratory/invasive D492 cells upon ECM1 overexpression. Student´s t-test, *** $p < 0.001$, ** $p < 0.01$, * $p < 0.05$. C) Transient KD of ECM1. Quantification of transient ECM1 KD in D492HER2 on gene expression level using RT-qPCR (10nM siRNA). Student´s t-test, *** $p < 0.001$, ** $p < 0.01$, * $p < 0.05$. D) Overexpression of

ECM1. Quantification of ECM1 overexpression in D492 on gene expression level using RT-qPCR (CRISPR/a). Student´s t-test, *** $p < 0.001$, ** $p < 0.01$, * $p < 0.05$. E) Less RFS in ECM1+/TN breast cancer. Kaplan Meier survival plot for patient with ECM1+ triple-negative (TN) breast cancer (KM-plotter). F) ECM1 knockdown decreases migration and invasion in MDA-MB-231. Quantification of number of migratory and invasive MDA-MB-231 cells upon transient ECM1 KD (n = 3). Student´s t-test, *** $p < 0.001$, ** $p < 0.01$, * $p < 0.05$. G) Transient KD of ECM1. Quantification of transient ECM1 KD in MDA-MB-231 on gene expression level using RT-qPCR (10nM siRNA). Student´s t-test, *** $p < 0.001$, ** $p < 0.01$, * $p < 0.05$.

Quantification of migration and invasion in MDA-MB-231 with transient KD of ECM1 revealed significantly fewer migratory and invasive cells (Fig. 26F). These findings provide evidence that KD of ECM1 may improve outcome both for patients with HER2+ and TN breast cancer and that upregulation of GATA3 upon ECM1 KD may mediate the loss of basal marker expression, accompanied by a shift towards a luminal epithelial phenotype. Targeting ECM1 may therefore provide a novel possibility for cancer treatment, both through inhibiting cancer-induced endothelial feedback promoting tumor progression and by upregulation of GATA3 expression and luminal differentiation, correlating with better survival.

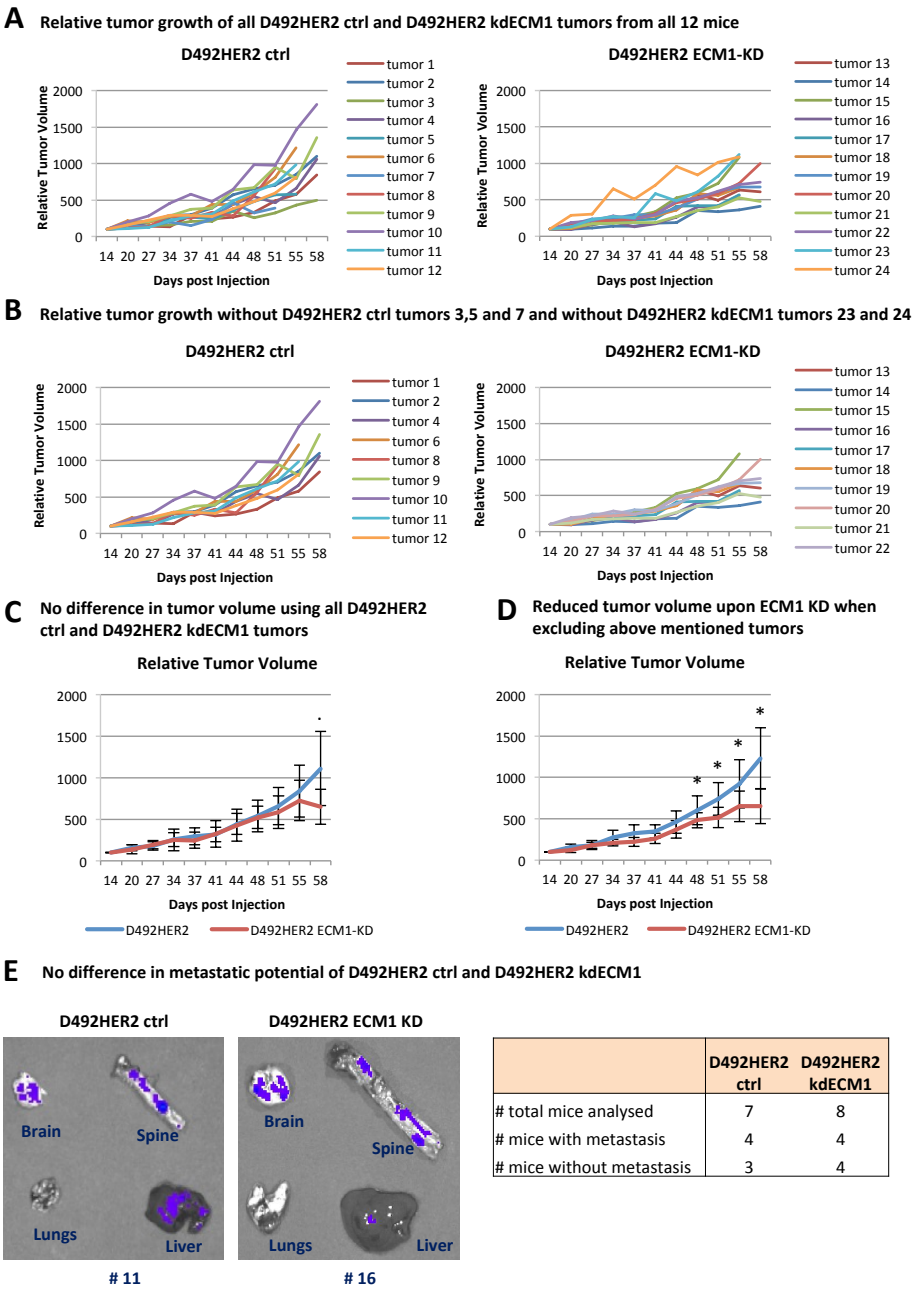
4.5 Role of ECM1 in tumor growth and metastatic potential *in vivo*

In order to determine the role of ECM1 in contributing to tumor growth and cancer progression *in vivo*, both tumorigenicity and metastasis assays have been performed with D492HER2 ctrl and D492HER2 with KD of ECM1 in NSG mice.

4.5.1 ECM1 in tumor growth

For tumorigenicity, cells were injected subcutaneously, tumor growth was measured 2-3 times per week and mice were sacrificed between day 46 and 62, depending on tumor burden according to FELASA ethical regulations. However, analysis of tumor volume revealed no significant difference between D492HER2 ctrl tumors and D492HER2 KD ECM1 tumors (Fig. 27A and C). However, when looking at the raw data several tumors from both D492HER2 ctrl (tumors #3, 5 and 7) and D492HER2 kdECM1 (tumors #23 and 24) could be noticed that show visible differences in tumor volume compared to the other 19 tumors in each group. Generally, cancer cells were injected in both sites of each mouse, so tumors #1, #3 etc. present tumors from one site whereas tumors #2, #4 etc. present tumors from the other site. Notably, D492HER2 ctrl tumors #3, 5 and 7, all tumors from the same site, showed significantly lower volume compared to the corresponding tumors

from the other site (#4, 6 and 8) and the other D492HER2 ctrl tumors. D492HER2 kdECM1 tumors #23 and 24 originate from the same mouse and show higher volume compared to the other tumors throughout all timepoints with tumor #23 being a significant outlier at day 51. Therefore, I reanalyzed the data excluding these tumors in order to compare the result to the whole dataset. Indeed, when excluding these tumors there was a significant difference in tumor volume with tumors having less volume upon ECM1 KD in D492HER2 cells injected (Fig. 27B and D). However, in order to exclude these tumors, one would need to have a reasonable justification such as obvious differences in behaviour or physiology of these mice, which could not clearly be confirmed. Due to this uncertainty, these data have not been used in manuscripts #I and #II. However, based on the *in vitro* data in the cellular system of D492 ECM1 rather affected migration and invasion. Therefore, a possible effect *in vivo* might also be better visible in a metastasis formation assay rather than in tumor growth. Therefore, metastasis assay was performed in the next step.



	D492HER2 ctrl	D492HER2 kdECM1
# total mice analysed	7	8
# mice with metastasis	4	4
# mice without metastasis	3	4

Figure 27. Role of ECM1 in tumor growth and metastatic potential. A) Relative tumor growth of all D492HER2 ctrl and D492HER2 kdECM1 tumors from all 12 mice. Relative tumor growth between day 14 and 58 after injection is plotted for all individual tumors (two tumors per mouse (1+2, 3+4, etc.) for D492HER2 ctrl and D492HER2 kdECM1. B) Relative tumor growth without D492HER2 ctrl tumors 3, 5 and 7 and without D492HER2 kdECM1 tumors 15, 23 and 24. Relative tumor growth between

day 14 and 58 after injection plotted for all tumors except #3, 5 and 7 (D492HER2 ctrl) and 15, 23 and 24 (D492HER2 kdECM1). C) No difference in tumor volume using all D492HER2 ctrl and D492HER2 kdECM1 tumors. Mean tumor volume (+/- SD) between day 14 and 58 after injection for D492HER2 ctrl and D492HER2 kdECM1 tumors including all samples. Student´s t-test, *** $p < 0.001$, ** $p < 0.01$, * $p < 0.05$, · $p < 0.1$. D) Reduced tumor volume upon ECM1 KD when excluding above-mentioned tumors. Mean tumor volume (+/- SD) between day 14 and 58 after injection for D492HER2 ctrl and D492HER2 kdECM1 tumors except mentioned tumors. Student´s t-test, *** $p < 0.001$, ** $p < 0.01$, * $p < 0.05$, · $p < 0.1$. E) No difference in metastatic potential of D492HER2 ctrl and D492HER2 kdECM1. Right: Representative IVIS images of metastatic organs (lungs, spine, liver, brain) from D492HER2 ctrl and D492HER2 kdECM1 mice. Left: Quantification of D492HER2 ctrl and D492HER2 kdECM1-injected mice with and without metastasis.

4.5.2 ECM1 in metastasis formation

For metastasis assay, D492HER2 cells with and without KD of ECM1 were injected by LV injection and mice were sacrificed after 65 days. Brain, spine, lungs and liver were dissected and imaged *ex vivo* for GFP fluorescence using the IVIS *in vivo* imaging system (Fig. 27E). However, analysis revealed no difference in metastatic burden between D492HER2 and D492HER2 with KD of ECM1 (Fig. 27E). In this context, it is important to mention that IVIS imaging of metastasis using only GFP as fluorescent marker is less sensitive than imaging of luminescence by e.g. luciferase and therefore may be less reliable. Therefore, repeating the assay with D492HER2 cells with insertion of a luciferase vector would be important to address this issue. Furthermore, the growth period had to be limited to 65 day due to regulatory matters. An extended growth period of up to 120 day could have given further insights in potential development of metastasis. As a third point it is to mention that the injection type (left ventricle (LV) injection) has been chosen based on a pilot study indicating that D492HER2 preferably metastasizes to the brain. However, in this experiment no brain metastasis could be detected. Therefore, repeating the assay with tail vain injection could give insight in metastasis formation specifically to lung and liver. In order to draw reliable conclusions about the role of ECM1 in metastasis formation *in vivo*, it would therefore be essential to repeat the assay and adjust the mentioned parameters.

In the last part of this chapter, I will now summarize our findings on the role of YKL-40 in D492HER2 tumorigenic properties in contrast to D492M with regard to oncogene- vs. endothelial-induced EMT (manuscript #III). Manuscript III is the main part of another PhD project (Erika Morera) focusing on the differences between D492M as endothelial-induced EMT cell line and D492HER2 as oncogene-induced EMT cell line.

4.6 YKL-40/CHI3L1 facilitates migration and invasion in HER2 overexpressing breast epithelial progenitor cells and generates a niche for capillary-like network formation (manuscript III, Morera et al.)

In the previously described secretome analysis, YKL-40 has been identified along with ECM1 as highly secreted in the D492HER2 CM. Both ECM1 and YKL-40 are members of a functional group of proteins involved in regulating angiogenesis. Comparison of D492M and D492HER2 secretomes specifically revealed YKL-40 as a protein with particularly high fold-difference in secretion (Fig. 28B). Upregulation of YKL-40 was confirmed on gene and protein levels (Fig. 28A).

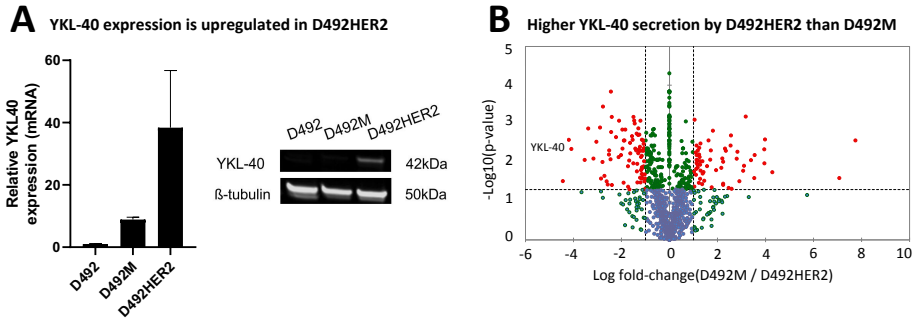


Figure 28. YKL-40 is higher expressed and secreted by D492HER2. A) YKL-40 expression is upregulated in D492HER2. Quantification of YKL-40 gene expression (RT-qPCR) and protein expression (western blot). B) Higher YKL-40 secretion by D492HER2 than D492M. Volcano blot representing proteins with at least 2-fold secretion difference and p-value of 0.05 (dotted lines) between D492M and D492HER2 (red).

In order to clarify the role of YKL-40 in tumorigenicity of D492HER2 and crosstalk with ECs, YKL-40 blocking antibody (mAY) as well as recombinant YKL-40 (rY) has been used. Additionally, transient and stable KD of YKL-40 has been performed in D492HER2 and stable overexpression in D492 and D492M.

4.6.1 YKL-40 expression in D492HER2 is linked to vascular network formation

The effect of blocking or adding YKL-40 as well as CM from D492 cell lines with or without YKL-40 expression on endothelial network formation has been analyzed after 24 h. First, ECs were treated with CM from D492HER2 ctrl cells and D492HER2 that had been treated with mAY. Blocking YKL-40 in D492HER2 resulted in decreased endothelial network formation upon treatment with D492HER2-CM, compared to untreated D492HER2-CM (Fig.

29A). This decrease could be rescued by addition of recombinant YKL-40 (rY) (Fig. 29A). Further, treatment of ECs with CM from D492 and D492M overexpressing YKL-40 led to an increase in network formation with the strongest effect observed for CM from D492 overexpressing YKL-40 (Fig. 29B). In agreement with these results, CM from D492HER2 with KD of YKL-40 showed decreased capability to induce endothelial network formation compared to CM from ctrl D492HER2 (Fig. 29B).

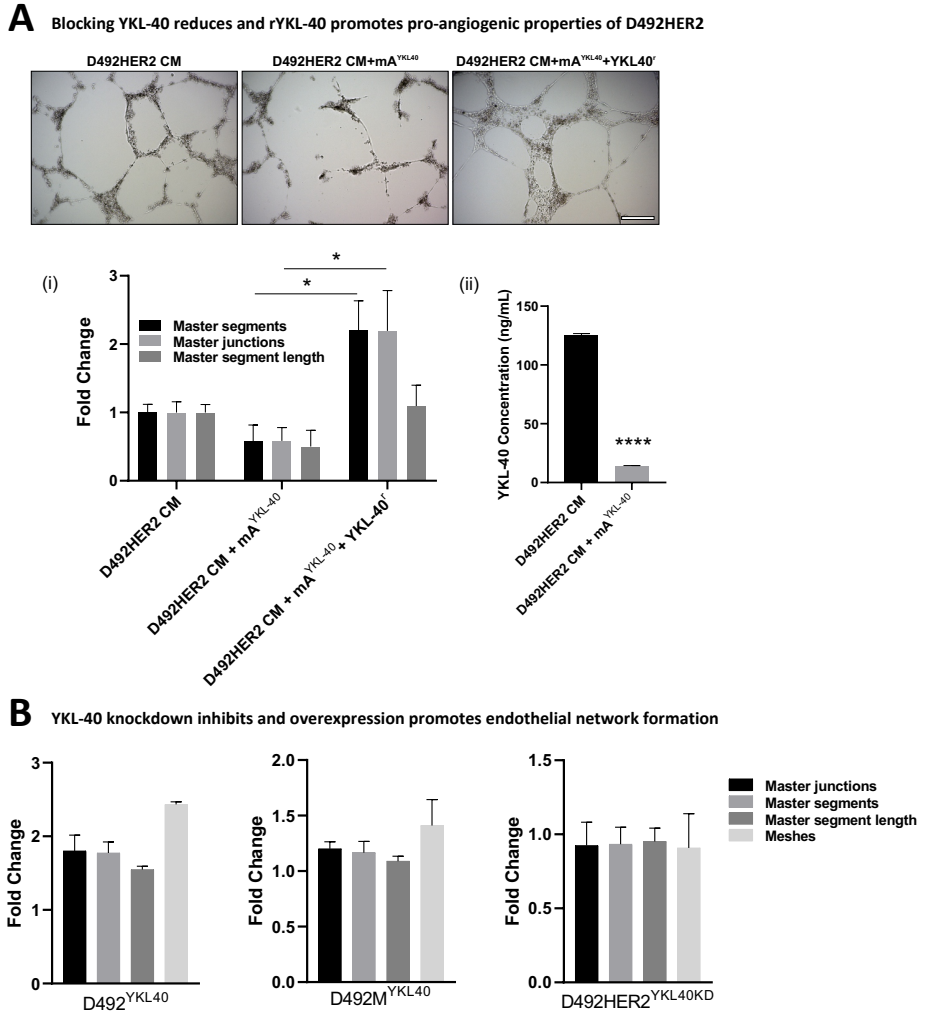


Figure 29. YKL-40 increases endothelial network formation. A) Blocking YKL-40 reduces and rYKL-40 promotes pro-angiogenic properties of D492HER2. Conditioned medium (CM) from D492HER2 stimulates angiogenesis in an *in vitro* angiogenesis assay. This effect was abrogated upon YKL-40 neutralization by monoclonal antibody (mAY) but rescued by the addition of recombinant YKL-40 protein (rY) (Scalebar = 200 µm). Parameters of angiogenesis were measured and analyzed by ImageJ

angiogenesis analyzer (i) and significance was assessed with one-way ANOVA and Tukey's multiple comparison test, * $p < 0.05$. Decreased concentration of YKL-40 upon incubation of cells with mAYKL40 was verified with ELISA (ii) Significance was tested with an unpaired t-test, **** $p < 0.0001$, *** $p < 0.001$, ** $p < 0.01$, * $p < 0.05$. B) When YKL-40 was overexpressed in D492 and D492M there was an increase in the capillary network formation, whereas stable knockdown of YKL-40 in D492HER2 showed a tendency to reduced capillary network formation.

These data suggest an involvement of YKL-40 in addition to ECM1 in the observed endothelial network-promoting properties of D492HER2. This concurs with previous studies showing pro-angiogenic properties of YKL-40 (Faibish et al., 2011; Riabov et al., 2014; Rusak et al., 2018; Shao, 2013). Shao and colleagues suggest that YKL-40 secreted by tumor-associated macrophages (TAMs) promotes tumor angiogenesis and therefore cancer progression (Shao, 2013). Faibish and colleagues further suggest that neutralizing YKL-40 might offer a new treatment option in brain cancer since it blocks tumor progression by inhibiting tumor angiogenesis (Faibish et al., 2011).

Gene expression analysis further showed that KD of YKL-40 leads to a decrease of VEGF-A and VEGF-C in D492HER2 (Fig. 30A). This suggests that the pro-angiogenic effect of YKL-40 might potentially be connected to VEGF signaling, one of the major pathways regulating angiogenesis (Hovey et al., 2001). Indeed, previous studies provide evidence for a mediating role of YKL-40 in VEGF signaling (Francescone et al., 2011; Shao, 2013). Francescone and research group reported that inhibition of YKL-40 resulted in decreased VEGF levels in brain tumor cells. VEGF-A and VEGF-C proteins bind to endothelial VEGFR2, activating a downstream signaling cascade inducing angiogenesis (Carmeliet & Jain, 2000). Therefore, quantifying VEGFR2 expression in YKL-40-induced ECs would be important in order to further clarify the relation between YKL-40 and VEGF signaling in D492HER2. However, the potential connection of YKL-40 with VEGF signaling suggests that YKL-40 probably acts in a different way than ECM1 in inducing angiogenesis.

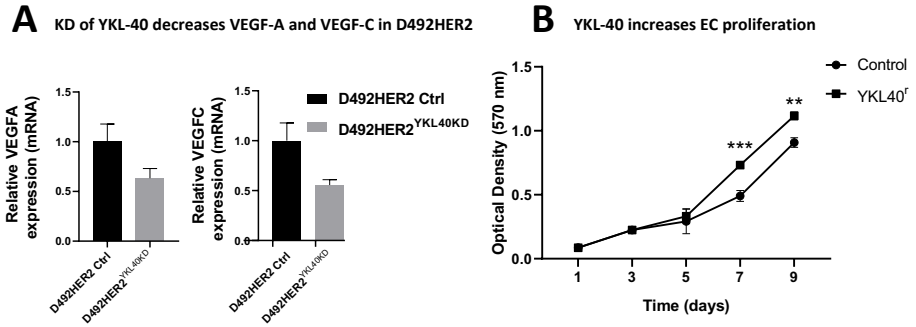


Figure 30. YKL-40 mediates VEGF-A and VEGF-C expression and increases endothelial proliferation. A) KD of YKL-40 decreases VEGF-A and VEGF-C in D492HER2. RT-qPCR quantification of VEGF-A and VEGF-C relative gene expression in D492HER2 ctrl and D492HER2 upon YKL-40 KD. B) YKL-40 increases EC proliferation. Proliferation curve of EC treated with rY vs untreated ECs. OD (at 570 nm) of crystal violet stained ECs blotted for days 1, 3, 5, 7 and 9. Student´s t-test, *** $p < 0.001$, ** $p < 0.01$, * $p < 0.05$.

Interestingly and also in contrast to ECM1, treatment of ECs with rY not only resulted in increased network formation but also proliferation (Fig. 30B). YKL-40 has previously been linked to increased proliferation of epithelial cells as well as increased migration of endothelial cells (Low et al., 2015; Shao, 2013). However, a role in increasing endothelial proliferation as well has not been reported yet. With regard to ECM1, previous studies have reported an involvement in regulation of proliferation (Lee et al., 2014c). However in the cellular model of D492, I could not confirm an increase of endothelial proliferation mediated by ECM1. Taken together, these data further support the idea of a functionally independent role of YKL-40 and ECM1 in the context of cancer-endothelial interaction. Looking into whether there might be a synergistic collaboration between both molecules would be of interest to further elucidate their role during cancer progression. Further experimental data suggest an involvement of YKL-40 in D492HER2 tumorigenic properties and 3D phenotype.

4.6.2 Knockdown of YKL-40 in D492HER2 inhibits migration and invasion

In order to assess the involvement of YKL-40 in tumorigenic properties of D492HER2, migration and invasion capacity of D492HER2 with YKL-40 KD and D492/D492M with YKL-40 overexpression was quantified using transwell assays. Transient and stable KD of YKL-40 in D492HER2 was confirmed on both mRNA and protein levels using RT-qPCR and western blot as well as overexpression in D492 and D492M using IF staining (Fig. 31A, C, E and F).

Both transient KD using 2 different siRNAs and stable KD of YKL-40 in D492HER2 resulted in significantly decreased numbers of migratory and invasive cells, hence reduced migration and invasion capacity of D492HER2 (Fig. 31B and D). In accordance with these results, D492 and D492M overexpressing YKL-40 showed a significantly increased migrative and invasive phenotype as indicated by higher numbers of migratory and invasive cells (Fig. 31E and F).

Taken together, these data demonstrate that high YKL-40 expression is associated with increased migration and invasion capacity and therefore suggest a possible role of YKL-40 in tumorigenicity. This is in line with previous studies on prostate cancer, cholangiocarcinoma and non-small cell lung cancer supporting a promoting effect of YKL-40 on cancer cell migration and invasion and therefore tumor progression (Hao et al., 2017; Jefri et al., 2015; Rusak et al., 2018; Thongsom et al., 2016). Therefore, targeting YKL-40 might not only be beneficial for cancer treatment through inhibition of YKL-40-induced angiogenesis but also through reducing tumorigenic properties of cancer cells. To further support the beneficial potential of YKL-40 KD, *in vivo* analysis of tumor and metastasis formation of D492HER2 upon KD of YKL-40 would be essential as next step.

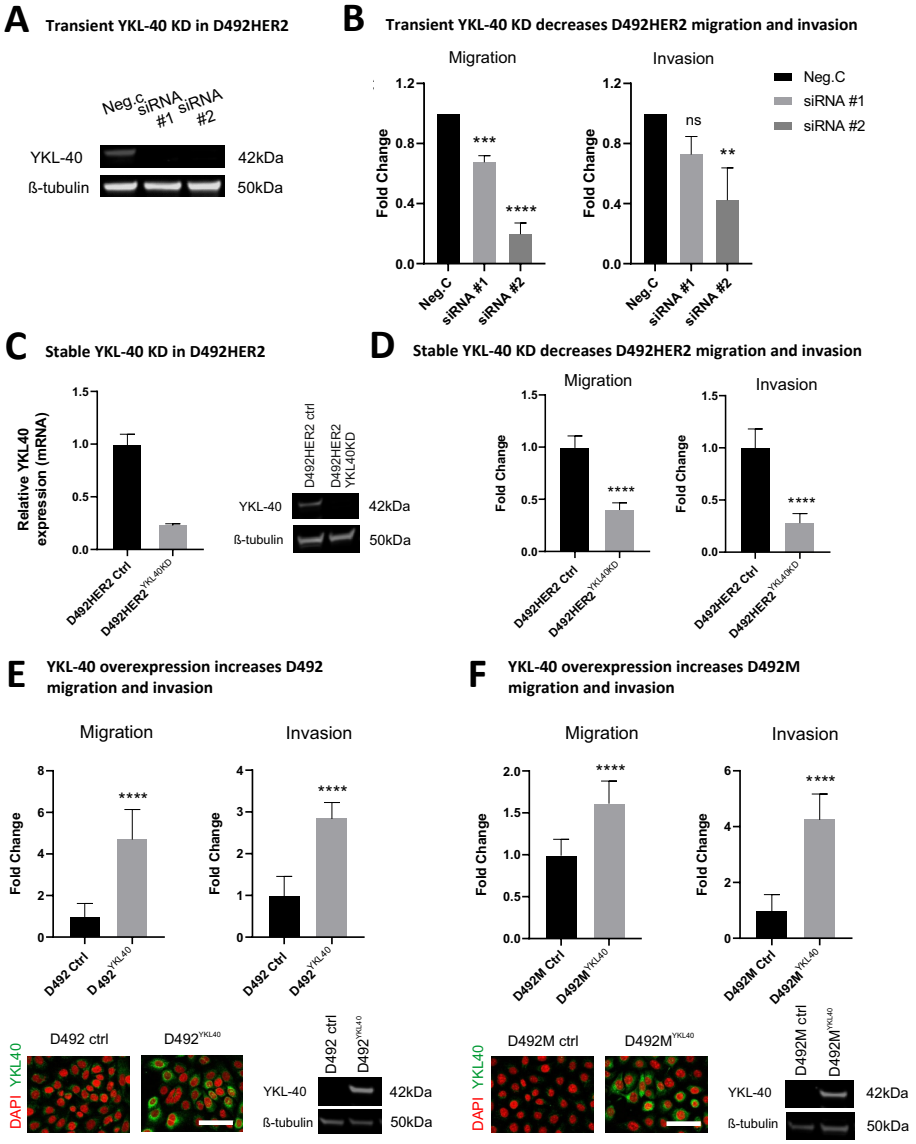


Figure 31. YKL-40 expression is associated with increased migration and invasion *in vitro*. A) Transient YKL-40 KD in D492HER2. Confirmation of transient KD of YKL-40 (red) in D492HER2 on protein level using western blot. B) Transient YKL-40 KD decreases D492HER2 migration and invasion. Transwell migration/invasion assay of D492HER2 negative ctrl and KD YKL-40 (siRNA #1 and #2). Number of migratory/invasive cells analysed as described previously. One-way ANOVA, **** p < 0.0001, *** *p* < 0.001, ** *p* < 0.01, * *p* < 0.05. C) Stable YKL-40 KD in D492HER2. Confirmation of stable KD of YKL-40 in D492HER2 on gene and protein level using RT-qPCR and western blot. D) Stable YKL-40 KD decreases D492HER2 migration and invasion. Transwell migration/invasion assay of D492HER2 ctrl and KD YKL-40. Number of migratory/invasive cells analysed as described previously. Student´s t-test, **** p < 0.0001, *** *p* < 0.001, ** *p* < 0.01, * *p* < 0.05. E) YKL-40

overexpression increases D492 migration and invasion. Transwell migration/invasion assay of D492 ctrl and with YKL-40 OE. Number of migratory/invasive cells analysed as described previously. Student´s t-test, **** p < 0.0001, *** *p* < 0.001, ** *p* < 0.01, * *p* < 0.05. Bottom: Confirmation of YKL-40 OE using IF staining and WB. Scale bar = 100 µm. F) YKL-40 overexpression increases D492M migration and invasion. Transwell migration/invasion assay of D492M ctrl and with YKL-40 OE. Number of migratory/invasive cells analysed as described previously. Student´s t-test, **** p < 0.0001, *** *p* < 0.001, ** *p* < 0.01, * *p* < 0.05. Bottom: Confirmation of YKL-40 OE with IF staining and WB. Scale bar = 100µm.

4.6.3 YKL-40 affects morphology of D492 cell lines when cultured in 3D culture

In addition to reduced tumorigenic properties of D492HER2 upon KD of YKL-40, the data also indicate changes in its 3D phenotype, further supporting a possible effect of YKL-40 KD *in vivo*.

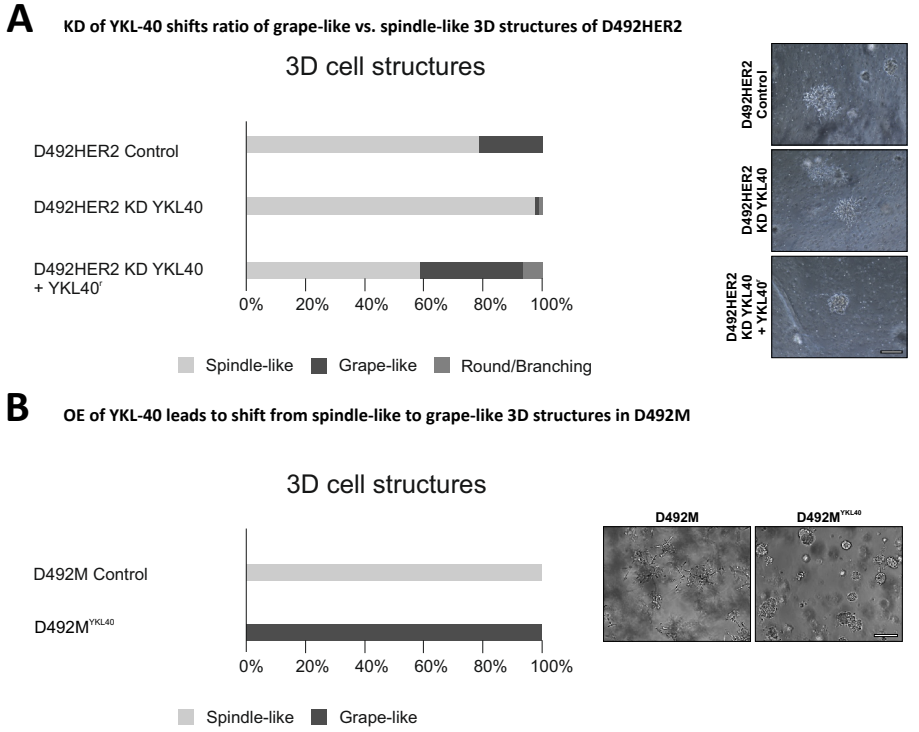


Figure 32. KD of YKL-40 affects D492HER2 3D phenotype. A) KD of YKL-40 shifts ratio of grape-like vs. spindle-like 3D structures of D492HER2. Quantification of grape-like and spindel-like structures in 3D culture (rBM) of D492HER2 ctrl, D492HER2 with KD of YKL-40 and D492HER2 KD YKL-40 +rY. Right: Phase contrast images of 3D structures. Scale bar = 200 µm. B) OE of YKL-40 leads to shift from spindle-like to grape-like 3D structures in D492M. Quantification of grape-like and spindel-like structures in 3D culture (rBM) of D492M ctrl and D492M with OE of YKL-40. Right: Phase contrast images of 3D structures. Scale bar = 200 µm.

In a previous study, D492HER2 was shown to form two types of structures in 3D culture, spindle-like and grape-like structures, whereas non-tumorigenic D492M form solely spindle-like structures (Ingthorsson et al., 2015). Interestingly, KD of YKL-40 in D492HER2 resulted in a clear change in the ratio of spindle-like vs. grape-like structures, with the proportion of grape-like structures being reduced from 21,4% to 1% (Fig. 32A+B). Thus, KD of YKL-40 shifts the 3D phenotype of D492HER2 more towards the non-tumorigenic D492M. Addition of recombinant YKL-40 is able to rescue the original D492HER2 and recovers the percentage of grape-like structures back to 32.8% of total 3D structures (Fig. 32A). In line with this, D492M overexpressing YKL-40 show higher numbers of grape-like structure in 3D culture compared to ctrl D492M with only spindle-like structures (Fig. 32B), calling for further studies on a possible role of YKL-40 in tumor and metastasis formation *in vivo*. Interestingly, these phenotype changes are only observed in a 3-dimensional environment but not in regular 2D culture, suggesting that a potential effect of YKL-40 KD may only be observed in a more natural-like culture condition than monolayer culture. This underlines the importance of performing *in vivo* studies to further clarify the potential of targeting YKL-40 in terms of improving cancer treatment.

5 Technical considerations

One of the main challenges during the experimental phase of a PhD study is to encounter difficulties and learning to find ways to solve them. When conducting research, it is crucial to pay attention to both the potential and the limitations of the methods to be used. In this chapter, I would like to address a number of experimental procedures performed in this study and their challenges. Being aware of context-dependent advantages and disadvantages of different methods may help to improve planning and conducting experiments and therefore improve the quality of scientific study.

5.1 Conditioned medium

When working with cell-conditioned medium and investigating its effect on another cell type, there are a number of issues that need to be considered. Several factors affect the quality of the medium and therefore the experimental outcome. I will discuss here how culture conditions, preparation of medium and growth factors as well as storage conditions affect consistency and reproducibility of achieved results.

5.1.1 Controlled conditions and consistency

On one hand, it is essential to efficiently control for consistency of external factors such as temperature, CO_2 and humidity when culturing cells in order to collect their conditioned medium. Variations in external conditions may cause cellular stress such as temperature stress or hypoxia and lead to activation of molecular stress-response mechanisms altering expression of stress-responsive genes and therefore also the secretome of the cells. In particular hypoxia is a process that itself also plays a role in the context of different types of cancer and therefore variations in external O_2 and CO_2 levels may bias the analysis of secreted factors and interpretation of experimental results.

On the other hand, internal factors such as cell confluence also need to be taken into account. When cells reach close to 100% confluence, expression levels of genes involved in cell proliferation decrease resulting in a different gene expression profile when compared to cells that are in the exponential stage of proliferation. Therefore, it is essential to avoid too high

confluence when collecting conditioned medium as well as keeping consistency between collections. In this study, we therefore changed the growth medium to fresh medium once the confluence reached 70%, which was then collected after 48 h of incubation, ensuring maximal amount of secreted factors. Furthermore, for collection we decided to only add half the original culture volume of medium in order to enrich 2x for secreted factors while reducing the amount of externally added growth factors by half. An upside of our cellular system is the possibility to work with a completely serum-free culture medium supplemented with specifically optimized amounts of selected growth factors. The downside of using serum as supplement for culture medium is that its exact composition is not clearly definable, making the analysis of a cellular secretome difficult. Therefore, using a culture medium with clearly defined additives is of advantage for secretome analysis.

5.1.2 Growth factors

However, also the quality and consistency in the preparation of growth factors is an essential factor for conditioned medium quality. The growth factors added to the DMEM:F12 base medium are essential for establishing and maintaining suitable growth conditions for the cells and avoiding stress. Variability among and lack of growth factors can result in altered cell proliferation rates and cause cellular stress, which eventually also leads to an altered secretome of the cells. In the first year of my PhD I encountered difficulties in reproducing results previously achieved using conditioned medium from D492HER2. After initial difficulties determining the problem we then noticed reduced proliferation rates and it turned out to be related to reduced quality of added EGF. EGF is one of the most essential factors to be added to the medium for culturing cells of the D492 lines. Inappropriate storage or variation in preparation of the working aliquots can therefore affect cell proliferation rates and eventually cellular secretome. For the work with CM it is very important to keep in mind how factors like that can have significant effects on the experimental outcome.

5.1.3 Storage conditions

Another factor influencing conditioned medium quality is its storage. In some studies, working with conditioned medium, it is stored at -80°C. However, the comparison of fresh CM vs. CM stored at -80°C in our study showed differences in quality. Some secreted signaling molecules may break down after only a few hours. For that reason, it is not suitable to store CM for

a long time. Even though storage at -80°C may delay this process it still cannot fully prevent it. Especially when investigating the effect of CM on another cell type, not loosing signal quality is of major importance. Therefore, we decided to only work with fresh CM in order to ensure reliable results.

To summarize, it is important to keep in mind how many small factors taken together can have a major influence on the condition of the cells and may significantly alter their growth and stress levels. Altered cellular processes can then result in affected secretion of factors and therefore lead to variability in the effects observed with conditioned medium. In order to ensure reliability and reproducibility of experimental data, it is therefore of highest importance first to be aware of this high sensitivity and second to keep consistency regarding external and internal conditions.

5.2 Endothelial network formation

One of the major readouts for the effect of cancer cells on the vascular niche throughout my study was the ability of ECs to form vascular network-like structures on top of a consistent Matrigel layer. The main advantage of this assay is that it offers a relatively straight-forward way to assess endothelial network formation in an *in vitro* setting, which limits the use of laboratory animals and is therefore in agreement with the guidelines and recommendations of the Federation of European Laboratory Animal Science Associations (FELASA) from 2012. However, I want to address a number of issues that need to be taken into consideration for this assay.

5.2.1 Endothelial model system

In many studies, human umbilical vein endothelial cells (HUVECs) are used as model system to look at effects of cancer cells on the endothelium. However, there is evidence that using organ-specific ECs could give more reliable results when studying cell-cell interactions (Rafii et al., 2016; Uwamori et al., 2019). Studies have shown that ECs from different organs differ in their response to stimuli from other cells. For example, whereas breast ECs respond to stimuli from breast cancer cells, other ECs may not show the same response (Rafii et al., 2016). The difficulty though with obtaining primary breast ECs is to efficiently eliminate fibroblasts in the culture after isolation of ECs from mammary tissue. One way is repeated magnetic sorting for the endothelial marker CD31. However, even very few fibroblasts left in the culture are sufficient to again take over the culture and overgrow the ECs. For that reason, we eventually decided to use HUVECs as

a main model in this study. Working with HUVECs, there are generally 2 possibilities of how to obtain the cells. One can either choose to work with primary cells in low passage or purchase immortalized cells. Both options have up- and downsides. Working with immortalized cells offers the advantage of being able to culture them for a much longer time period allowing more opportunity to perform experiments. However, there is an ongoing discussion on whether immortalized ECs actually still reflect a natural endothelium showing reliable and realistic responses in experimental research. Alternatively, primary HUVECs are non-modified and might therefore reflect a more original and natural response to stimuli. However, the downside of primary HUVECs in addition to their limited life span *in vitro* is the variability between different batches from different donors, which can affect reproducibility of experimental data. In this study we mainly used primary HUVECs as a model system. Nevertheless, using primary breast ECs throughout the entire study would have been more ideal. Therefore, there is urgent need for the development of a more efficient method to establish pure cultures of primary breast endothelial cells without fibroblast contamination.

5.2.2 Matrigel lot variability

In order to study endothelial network formation *in vitro*, the cells need to be seeded on top of some sort of scaffold since plastic is not sufficient for the cell to form these structures. One material commonly used for that purpose is Matrigel. Matrigel is a gelatinous protein mix resembling the basement membrane matrix and can provide the necessary environment for endothelial cells to form network-like structures. However, not only for endothelial cell culture Matrigel represents a useful 3-dimensional culture matrix. In our laboratory, the use of Matrigel for 3-dimensional culture of breast epithelial cells inside the gel is well established. 3D mono- and co-culture systems represent an environment more similar to the cells´ natural environment than a monolayer culture can be. This is essential for studying e.g. branching morphogenesis *in vitro*, which is one of the core competences in our group. However, one downside of using Matrigel as culture matrix is the variability in stiffness, protein concentration and endotoxin levels between production lots. The stiffness for example has an influence on whether epithelial cells are able to move inside the gel, which is necessary in order for them to form branching structures. When ordering a new lot, we therefore first validate whether it is suitable for epithelial cells to form branching colonies. To get back to endothelial network formation, the lot variability is less problematic

though since in that case the cells are seeded on top of the gel and not inside. Nevertheless, differences between Matrigel lots is an important issue to be aware of when performing experiments involving Matrigel cultures and when analyzing the experimental data.

5.2.3 Conditioned medium treatment

One of the main parts of this study was to investigate the effect of cancer cell-conditioned medium on ECs with endothelial network formation being one of the main readouts. When treating cells with CM from another cell type it needs to be taken into account that the cells used to condition the medium not only add factors to it by secretion but also reduce or deplete the amount of other factors, which they take up for their own metabolism (e.g. glucose). To account for this effect, it is often necessary to mix the CM to a certain ratio with fresh culture medium. When optimizing the use of CM in our study, I therefore tested different ratios of CM vs. fresh endothelial medium in order to determine the best ratio to be used in this system. Since the culture medium for endothelial cells (EGM supplemented with 5% FBS) contains serum, it was important to determine the ratio that allowed the best possible detection of CM-mediated effects while still being sufficient for the endothelial cells to proliferate without causing starvation. Based on the test outcome we decided to mix CM and fresh EGM5 in a ratio of 1:1 and kept this ratio consistent throughout the entire study. It is important to be aware that the literature can only give indications but cannot provide a ready-to-use protocol for working with CM. The use of CM, whether alone or mixed in a certain ratio with fresh medium is always system-dependent and needs to be optimized and adjusted in every study system.

5.3 Western Blotting

Up to now, western blotting has been one of the most common methods to quantify protein expression of cellular or secreted proteins. In order to achieve reliable and reproducible results, it is crucial to optimize both the protein extraction method depending on what kinds of proteins are to be investigated and the use of primary antibody for the protein of interest.

5.3.1 Protein isolation

Choosing and optimizing the method of isolation of proteins is essential for quantitative analysis and comparison between samples. In this study, this has played a role especially for the protein samples from conditioned

medium. After blotting the concentrated samples at first, I realized that not all protein from the larger fraction had transferred from the gel to the membrane after the standard transfer time that was usually used for intracellular protein samples. During the concentration of conditioned medium samples it can occasionally occur that proteins form aggregates that can be too large to be transferred in the regular transfer time. However, if not all protein is transferred, a reliable quantification cannot be ensured. Therefore, it is necessary to adjust the protocol in order to break up formed protein aggregates. I therefore increased the incubation time of the samples with ß-mercaptoethanol from 10 to 20 minutes and added a vortexing step of 1 minute. Using these optimization steps, I could overcome the issue of aggregate formation in the concentrated conditioned medium samples.

5.3.2 Antibody optimization

One very labor and time-consuming task is the primary antibody optimization for the quantification of protein expression of a protein of interest by western blotting. When testing an antibody for the first time, it is always recommended to compare different concentrations within the recommended range in the data sheet. In order to be sure that the antibody is functioning properly, it is important to include a positive control sample in addition to the samples to be analyzed for the testing, which can be e.g. a cell line known to express high levels of the protein of interest. Also, it is important to be aware of different splice variants resulting in different sizes of a protein that can lead to the appearance of more than one protein band on the membrane. This was the case with the first antibody for ECM1 that I tested for western blot (Origene Technologies, #TA318977). Therefore, I compared the sizes of all visible bands on the membrane. However, while some of the bands matched the known splice variants of ECM1 in size, others could not be related to splice variants indicating unspecific binding of the antibody. Therefore, I decided to test a different antibody (Santa Cruz Biotechnology, #sc-515843). Using this antibody, there was a band visible of the correct size and no unspecific binding occurred.

Here, I was working both with intracellular protein extract from the D492 cell lines as well as concentrated conditioned medium to quantify protein expression and secretion of ECM1. Even though there was no significant difference in protein band size between intracellular and secreted protein samples in case of ECM1, one needs to be aware that a protein could have a different size once it is secreted out of the cell due to posttranslational modifications during extracellular transport.

5.4 CRISPRa and CRISPRi

In recent years, gene-editing techniques have become important tools in cancer research for manipulating expression of selected genes with high precision and thereby identify new ways for treatment. One of the most widely used techniques is the CRISPR-Cas9 system (clustered regulatory interspaced short palindromic repeats-CRISPR-associated protein 9), originally derived from the bacterial adaptive immune system (Dominguez et al., 2016). It consists of two components, the Cas9 endonuclease and an RNA complex consisting of the target gene-identifying CRISPR RNA (crRNA) and the *trans*-activating crRNA (tracr-RNA), engineered into a single-guide RNA (sgRNA). The Cas9 can induce a DNA double-strand break within the target sequence, which can be used to introduce mutations or completely inactivate a gene of interest due to error-prone repair of the host DNA repair pathway (Dominguez et al., 2016). By providing a repair template, the CRISPR-Cas9 system can also be used to insert precise insertions or mutations (Dominguez et al., 2016; Mali et al., 2013).

In this study, we used a modified version of the CRISPR-Cas9 system in order to repress (CRISPRi) and enhance (CRISPRa) target gene expression on the transcriptional level. To use the system for expression activation, the nuclease activity of the Cas9 enzyme has been deactivated and the resulting deactivated Cas9 (dCas9) has been fused to an external transcription factor that either activates or represses gene transcription. One commonly used transcriptional activator in this system is the VP64 activator, which is able to either activate silent genes or upregulate expression of already active genes (Dominguez et al., 2016; La Russa & Qi, 2015). This system is a two-step system, where the cells of interest are first transfected with the dCAS9-VP64 plasmid, followed by a second transfection step where the sgRNA for the target system is inserted. The advantage of this system is that, in contrast to other systems, we have here an upregulation in expression of the actual endogenous gene in the cell to be studied and not of an exogenously inserted gene template. This is particularly important for minimizing off-target effects (La Russa & Qi, 2015).

The observed upregulation of target gene expression in mammalian cells however is with 2-5 fold on average only moderate. This also applied to our study, where ECM1 expression was only upregulated around 2.5-fold in D492 and 4-fold in D492M, using the dCas9-VP64 system alone. For that reason, we decided to use the novel synergistic activation mediator (SAM) system. In the SAM system, multiple transcriptional activators such as HSF1 and p65

are combined to achieve a synergistic effect together with VP64 and thereby increase transcriptional activation (La Russa & Qi, 2015). Using this method, we could increase the overexpression to 23-fold in both cell lines. Therefore, the CRISPRa system has proven a valuable tool with regard to generation of stable overexpression cell lines for ECM1 in our study.

For transcriptional repression, dCas9 is fused with an inhibitory KRAB (Krüppel-associated box) repressor domain. Depending on the efficacy of the sgRNA, a transcriptional repression of 90-99% can be achieved (La Russa & Qi, 2015). Using this system, we achieved a stable 90% knockdown of ECM1 in D492HER2. The CRISPRi system does not offer the option of generating an absolute knockout of a target gene. However, since the generation of a knockout cell line usually requires single-cell cloning, it is much more time consuming than the CRISPRi system. Additionally, for knocking down long non-coding and miRNAs the CRISPRi system showed better knockdown efficiency than other knockdown methods. Similar to the CRISPRa system, the reduction of off-target effects is an important advantage here as well (La Russa & Qi, 2015).

5.5 Summary

To summarize this chapter, there are a significant number of points that one needs to be aware of while conducting a study like this. Extensive literature research before starting the actual experimental work can help to avoid mistakes that other people already made and give important hints for trouble shooting.

If I would have the chance to repeat the project with the knowledge I have achieved during the time, I would probably perform the mass spectrometry analysis of the cell secretome and the RNA microarray of induced endothelial cells at an earlier point. These types of analyses offer a broader and less biased overview about the processes that are happening than investigating chosen genes or proteins based on already performed studies. Also, looking at targets that have already been described in the context to be investigated might actually limit the possibility to identify novel candidates involved on different levels in breast cancer progression and metastasis formation.

6 Summary and Conclusions

To summarize the outcome of this PhD project, I have identified ECM1 as cancer-secreted protein inducing endothelial network formation and an endothelial feedback response promoting tumorigenic properties of cancer cells. Treatment of ECs with CM from ECM1-expressing D492HER2 and MDA-MB-231 significantly increased network formation *in vitro* and induced an endothelial feedback accelerating cancer cell migration and invasion whereas knockdown of ECM1 reduced both effects (Fig. 33).

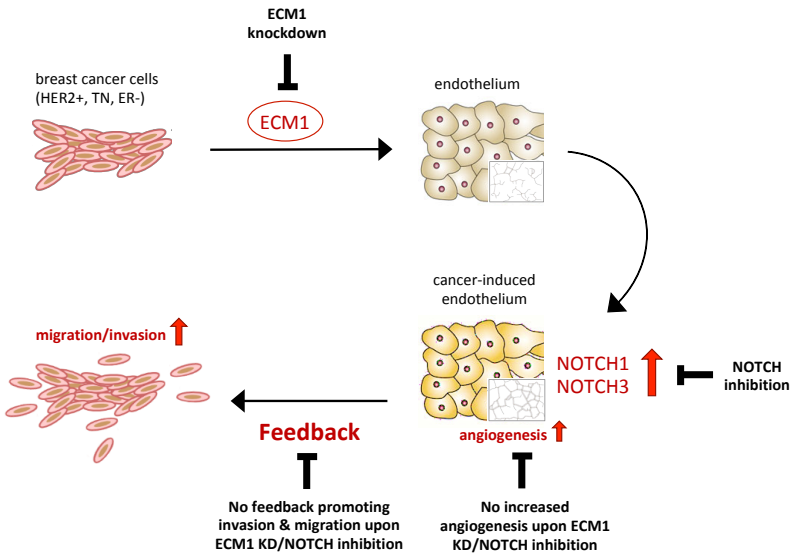


Figure 33. Schematic summary of ECM1 inducing an endothelial feedback promoting cancer cell migration and invasion. ECM1 secreted by HER2+, TN or ER- breast cancer cells increases endothelial network formation and induces endothelial feedback promoting cancer cell migration and invasion through upregulation of NOTCH1 and NOTCH3 expression. Knockdown of ECM1 in cancer cells and NOTCH inhibition in ECs inhibits the network formation increase and the feedback induction.

Only recently, research has put focus on cancer-associated ECs with regard to their potential role in supporting cancer progression. Ferraro and colleagues reported that supernatant from subconfluent ECs promotes migration of HER2-positive SKBR3 breast cancer cells (Ferraro et al., 2019). Lee and research group showed that by increased IL-6 secretion triple-negative breast cancer cells induce secretion of CCL5 in lymphatic

endothelial cells (LEC), which in turn enhances cancer cell migration (Lee et al., 2014a). ECM1 itself has previously been linked to breast cancer progression by increasing adhesion and invasion properties of circulating cancer cells (Wu et al., 2018). However, a role in cancer progression by inducing a tumorigenicity-promoting feedback in ECs has not been shown before. Therefore, my data point out a novel role of ECM1 in the context of cancer and might open up new possibilities for targeting the cancer microenvironment and eventually improve cancer treatments.

My data further indicate that endothelial NOTCH signaling plays a mediating role in ECM1-induced network formation as well as cancer-promoting feedback. NOTCH1 and NOTCH3 expression was upregulated in ECs treated with ECM1 and blocking endothelial NOTCH signaling prevented the increase in network formation and the feedback induction (Fig. 33). Previous studies have connected NOTCH signaling not only to increased angiogenesis but also to tumorigenicity-promoting features of ECs. Wieland and colleages have shown that increased NOTCH1 activity in cancer-associated ECs promoted neutrophil infiltration, tumor cell adhesion to the endothelium and intravasation, lung colonization and postsurgical metastasis (Wieland et al., 2017). As activators of NOTCH signaling, NOTCH ligands e.g. from the Delta-like or Jagged families are known and well studied. Mullendore and team detected overexpression of NOTCH ligand transcripts DLL4 and JAGGED2 in a majority of pancreatic cancer cell lines (Mullendore et al., 2009). However, the precise mechanisms of NOTCH activation in tumor-associated ECs is still largly unknown. ECM1 has been linked to several signaling pathways previously (Gan et al., 2017; Gomez-Contreras et al., 2017; Lee et al., 2015b; Wu et al., 2018). However, a connection of ECM1 and endothelial NOTCH expression has not been reported before. Therefore, with the data of this study I provide evidence for a potential novel role of ECM1 in mediating endothelial NOTCH signaling, contributing to the generation of a cancer-supporting vasculature.

In addition to its role in mediating cancer-endothelial crosstalk, ECM1 also directly affects cancer cell tumorigenicity and the luminal/basal epithelial marker expression profile. Knockdown of ECM1 in D492HER2 resulted in decreased expression of basal markers whereas luminal markers showed upregulated expression. One of the upregulated luminal markers was transcription factor GATA3 (as well as numerous downstream targets of GATA3). The transcription factor GATA3 is a key regulator of luminal differentiation (Kouros-Mehr et al., 2008), which expression is associated with improved survival in patients with HER2+ breast cancer. Indeed, D492HER2

cells show decreased tumorigenic properties in terms of less migration and invasion upon ECM1 knockdown (Fig. 34). Previous studies have shown that GATA3 expression is associated with inhibited cancer progression and metastasis formation (Yan et al., 2010; Yoon et al., 2010). However, a reverse correlation between ECM1 and GATA3 expression has not been shown previously. Therefore, my data provide evidence for a novel connection between ECM1 and GATA3 signaling in the context of luminal differentiation.

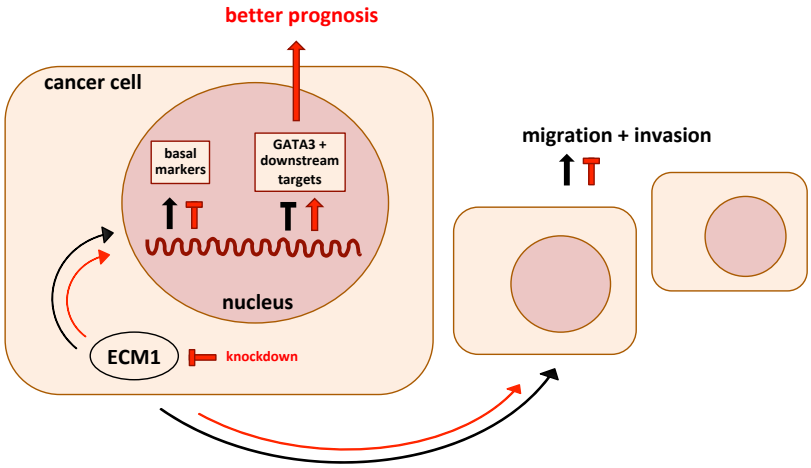


Figure 34. Schematic summary of ECM1 knockdown decreasing tumorigenic properties of D492HER2. Schematic overview of the role of ECM1 in mediating basal marker expression as well as GATA3 and downstream target expression and in mediating tumorigenic characteristics. Knockdown of ECM1 results in loss of basal markers and gain of GATA3 expression, as well as decreased migration and invasion.

However, to further support this hypothesis, it would be important to verify GATA3 upregulation upon ECM1 knockdown in other breast cancer cell lines expressing ECM1 as well as *in vivo*. Additionally, overexpression of GATA3 in D492HER2 as well as other cell lines could provide further insights regarding its role in reducing tumorigenicity and therefore improved clinical outcome. Moreover, the question of how overexpression of HER2 in D492 leads to upregulation of ECM1 is still open. Elucidating the molecular mechanism through which HER2 regulates ECM1 expression in tumor cells would be of great importance in order to fully understand the role of ECM1 in HER2-induced tumorigenicity.

In addition to ECM1, YKL-40 has further been identified as D492HER2-secreted protein involved in D492HER2 tumorigenicity and pro-angiogenic properties. Knockdown of YKL-40 resulted in reduced migration and invasion

capacity of D492HER2 and decreased pro-angiogenic properties of D492HER2-CM. However, in contrast to ECM1, treatment of ECs with recombinant YKL-40 resulted in increased endothelial proliferation. Furthermore, D492HER2 showed a more spindle-like 3D phenotype and decreased expression of VEGF-A and VEGF-C upon knockdown of YKL-40, supporting previous research connecting YKL-40 with VEGF signaling (Francescone et al., 2011; Shao, 2013). These data indicate that ECM1 and YKL-40 appear to function through different - either complementary or synergistic - mechanisms rather than playing similar roles in the context of endothelial crosstalk in breast cancer. In this context, generating a double knockdown of both ECM1 and YKL-40 in D492HER2 could be of high value in order to determine the impact on tumorigenicity and endothelial interaction *in vitro* and *in vivo*. However, to fully elucidate in what way ECM1 and YKL-40 differ in their function with regard to cancer progression, further studies are needed, including to determine whether or not YKL-40 could be involved in endothelial feedback induction as well. Clarifying the molecular connection between HER2 overexpression and YKL-40 upregulation would also be of value in this context.

In conclusion, ECM1 and YKL-40 have been identified as cancer-secreted pro-angiogenic factors. ECM1 is involved in inducing the endothelial niche to support cancer progression through increased cancer cell migration and invasion. Moreover, our data indicate a novel, mediating role of ECM1 in endothelial NOTCH signaling, which appears to be involved in mediating the induction of the cancer-promoting endothelial feedback. Additionally, KD of ECM1 results in decreased basal marker expression and upregulation of GATA3, which is correlated with significantly better prognosis in patients with HER2+ breast tumors. YKL-40 may provide D492HER2 with increased aggressiveness, supporting cancer progression and angiogenesis. Taken together, these findings might open up new possibilities for cancer treatment by better understanding of how an activated vascular niche provides positive feedback to the cancer and targeting this interaction between cancer cells and their microenvironment. Targeting ECM1 and YKL-40 may provide opportunities for development of novel therapies to reduce metastases and inhibit cancer progression.

References

Aparicio, S., Sawant, S., Lara, N., Barnstable, C. J., & Tombran-Tink, J. (2005). Expression of angiogenesis factors in human umbilical endothelial cells and their regulation by PEDF. *Biochemical and Biophysical Research Communications, 326*, 387-394. doi: 10.1016/j.bbrc.2004.11.041

Artavanis-Tsakonas, S., Rand, M. D., & Lake, R. J. (1999). Notch Signaling: Cell Fate Control and Signal Integration in Development. *Science, 284*(5415), 770-776. doi: 10.1126/science.284.5415.770

Arteaga, C. L., Sliwkowski, M. X., Osborne, C. K., Perez, E. A., Puglisi, F., & Gianni, L. (2011). Treatment of HER2-positive breast cancer: current status and future perspectives. *Nat Rev Clin Oncol, 9*(1), 16-32. doi: 10.1038/nrclinonc.2011.177

Baselga, J., Norton, L., Albanell, J., Kim, Y. M., & Mendelsohn, J. (1998). Recombinant humanized anti-HER2 antibody (Herceptin) enhances the antitumor activity of paclitaxel and doxorubicin against HER2/neu overexpressing human breast cancer xenografts. *Cancer Res, 58*(13), 2825-2831.

Benton, G., Crooke, E., & George, J. (2009). Laminin-1 induces E-cadherin expression in 3-dimensional cultured breast cancer cells by inhibiting DNA methyltransferase 1 and reversing promoter methylation status. *Faseb j, 23*(11), 3884-3895. doi: 10.1096/fj.08-128702

Bissell, M. J., Hall, H. G., & Parry, G. (1982). How Does the Extracellular Matrix Direct Gene Expression? *Journal of theoretical Biology, 99*, 31-68.

Brazil, D. P., Church, R. H., Surae, S., Godson, C., & Martin, F. (2015). BMP signalling: agony and antagony in the family. *Trends Cell Biol, 25*(5), 249-264. doi: 10.1016/j.tcb.2014.12.004

Briem, E., Ingthorsson, S., Traustadottir, G. A., Hilmarsdottir, B., & Gudjonsson, T. (2019). Application of the D492 Cell Lines to Explore Breast Morphogenesis, EMT and Cancer Progression in 3D Culture. *J Mammary Gland Biol Neoplasia*. doi: 10.1007/s10911-018-09424-w

Bustin, S. A., Benes, V., Garson, J. A., Hellemans, J., Huggett, J., Kubista, M., . . . Wittwer, C. T. (2009). The MIQE guidelines: minimum information for publication of quantitative real-time PCR experiments. *Clin Chem, 55*(4), 611-622. doi: 10.1373/clinchem.2008.112797

Carmeliet, P., & Jain, R. K. (2000). Angiogenesis in cancer and other diseases. *Nature, 407*(6801), 249-257. doi: 10.1038/35025220

Chen, H., Jia, W., & Li, J. (2016). ECM1 promotes migration and invasion of hepatocellular carcinoma by inducing epithelial-mesenchymal transition. *World J Surg Oncol, 14*(1), 195. doi: 10.1186/s12957-016-0952-z

De Francesco, E. M., Maggiolini, M., & Musti, A. M. (2018). Crosstalk between Notch, HIF-1alpha and GPER in Breast Cancer EMT. *Int J Mol Sci, 19*(7). doi: 10.3390/ijms19072011

Dominguez, A. A., Lim, W. A., & Qi, L. S. (2016). Beyond editing: repurposing CRISPR-Cas9 for precision genome regulation and interrogation. *Nat Rev Mol Cell Biol, 17*(1), 5-15. doi: 10.1038/nrm.2015.2

Egeblad, M., Rasch, M. G., & Weaver, V. M. (2010). Dynamic interplay between the collagen scaffold and tumor evolution. *Curr Opin Cell Biol, 22*(5), 697-706. doi: 10.1016/j.ceb.2010.08.015

Erler, J. T., Bennewith, K. L., Cox, T. R., Lang, G., Bird, D., Koong, A., . . . Giaccia, A. J. (2009). Hypoxia-induced lysyl oxidase is a critical mediator of bone marrow cell recruitment to form the premetastatic niche. *Cancer Cell, 15*(1), 35-44. doi: 10.1016/j.ccr.2008.11.012

Erler, J. T., & Weaver, V. M. (2009). Three-dimensional context regulation of metastasis. *Clin Exp Metastasis, 26*(1), 35-49. doi: 10.1007/s10585-008-9209-8

Espinosa Neira, R., & Salazar, E. P. (2012). Native type IV collagen induces an epithelial to mesenchymal transition-like process in mammary epithelial cells MCF10A. *Int J Biochem Cell Biol, 44*(12), 2194-2203. doi: 10.1016/j.biocel.2012.08.018

Fabregat, I., Malfettone, A., & Soukupova, J. (2016). New Insights into the Crossroads between EMT and Stemness in the Context of Cancer. *J Clin Med, 5*(3). doi: 10.3390/jcm5030037

Faibish, M., Francescone, R., Bentley, B., Yan, W., & Shao, R. (2011). A YKL-40-neutralizing antibody blocks tumor angiogenesis and progression: a potential therapeutic agent in cancers. *Mol Cancer Ther, 10*(5), 742-751. doi: 10.1158/1535-7163.MCT-10-0868

Ferraro, D. A., Patella, F., Zanivan, S., Donato, C., Aceto, N., Giannotta, M., . . . Buess, M. (2019). Endothelial cell-derived nidogen-1 inhibits migration of SK-BR-3 breast cancer cells. *BMC Cancer, 19*(1), 312. doi: 10.1186/s12885-019-5521-8

Francescone, R. A., Scully, S., Faibish, M., Taylor, S. L., Oh, D., Moral, L., . . . Shao, R. (2011). Role of YKL-40 in the angiogenesis, radioresistance, and progression of glioblastoma. *J Biol Chem, 286*(17), 15332-15343. doi: 10.1074/jbc.M110.212514

Franses, J. W., Baker, A. B., Chitalia, V. C., & Edelman, E. R. (2011). Stromal endothelial cells directly influence cancer progression. *Sci Transl Med, 3*(66), 66ra65. doi: 10.1126/scitranslmed.3001542

Franses, J. W., Drosu, N. C., Gibson, W. J., Chitalia, V. C., & Edelman, E. R. (2013). Dysfunctional endothelial cells directly stimulate cancer inflammation and metastasis. *Int J Cancer, 133*(6), 1334-1344. doi: 10.1002/ijc.28146

Gan, L., Meng, J., Xu, M., Liu, M., Qi, Y., Tan, C., . . . Wang, Z. (2017). Extracellular matrix protein 1 promotes cell metastasis and glucose metabolism by inducing integrin beta4/FAK/SOX2/HIF-1alpha signaling pathway in gastric cancer. *Oncogene*. doi: 10.1038/onc.2017.363

Gazinska, P., Grigoriadis, A., Brown, J. P., Millis, R. R., Mera, A., Gillett, C. E., . . . Pinder, S. E. (2013). Comparison of basal-like triple-negative breast cancer defined by morphology, immunohistochemistry and transcriptional profiles. *Mod Pathol, 26*(7), 955-966. doi: 10.1038/modpathol.2012.244

Ghajar, C. M. (2015). Metastasis prevention by targeting the dormant niche. *Nat Rev Cancer, 15*(4), 238-247. doi: 10.1038/nrc3910

Ghajar, C. M., Peinado, H., Mori, H., Matei, I. R., Evason, K. J., Brazier, H., . . . Bissell, M. J. (2013). The perivascular niche regulates breast tumour dormancy. *Nat Cell Biol, 15*(7), 807-817. doi: 10.1038/ncb2767

Gomez-Contreras, P., Ramiro-Diaz, J. M., Sierra, A., Stipp, C., Domann, F. E., Weigel, R. J., & Lal, G. (2017). Extracellular matrix 1 (ECM1) regulates the actin cytoskeletal architecture of aggressive breast cancer cells in part via S100A4 and Rho-family GTPases. *Clin Exp Metastasis, 34*(1), 37-49. doi: 10.1007/s10585-016-9827-5

Gouon-Evans, V., Lin, E. Y., & Pollard, J. W. (2002). Requirement of macrophages and eosinophils and their cytokines/chemokines for mammary gland development. *Breast Cancer Res, 4*(4), 155-164.

Gudjonsson, T., Ronnov-Jessen, L., Villadsen, R., Bissell, M. J., & Petersen, O. W. (2003). To create the correct microenvironment: three-dimensional heterotypic collagen assays for human breast epithelial morphogenesis and neoplasia. *Methods, 30*(3), 247-255.

Gudjonsson, T., Villadsen, R., Nielsen, H. L., Ronnov-Jessen, L., Bissell, M. J., & Petersen, O. W. (2002). Isolation, immortalization, and characterization of a human breast epithelial cell line with stem cell properties. *Genes Dev, 16*(6), 693-706. doi: 10.1101/gad.952602

Guo, D., Li, C., Teng, Q., Sun, Z., Li, Y., & Zhang, C. (2013). Notch1 overexpression promotes cell growth and tumor angiogenesis in myeloma. *Neoplasma, 60*(1), 33-40. doi: 10.4149/neo_2013_005

Han, Z., Ni, J., Smits, P., Underhill, C. B., Xie, B., Chen, Y., . . . Zhang, L. (2001). Extracellular matrix protein 1 (ECM1) has angiogenic properties and is expressed by breast tumor cells. *The FASEB Journal, 15*, 988-994.

Hao, H., Wang, L., Chen, H., Xie, L., Bai, T., Liu, H., & Wang, D. (2017). YKL-40 promotes the migration and invasion of prostate cancer cells by regulating epithelial mesenchymal transition. *Am J Transl Res, 9*(8), 3749-3757.

Harjes, U., Bridges, E., Gharpure, K. M., Roxanis, I., Sheldon, H., Miranda, F., . . . Harris, A. L. (2017). Antiangiogenic and tumour inhibitory effects of downregulating tumour endothelial FABP4. *Oncogene, 36*(7), 912-921. doi: 10.1038/onc.2016.256

Henninghausen, L., & Robinson, G. W. (2001). Signaling Pathways in Mammary Gland Development. *Developmental Cell, 1*, 467-475.

Hilmarsdottir, B., Briem, E., Sigurdsson, V., Franzdottir, S. R., Ringner, M., Arason, A. J., . . . Gudjonsson, T. (2015). MicroRNA-200c-141 and Np63 are required for breast epithelial differentiation and branching morphogenesis. *Dev Biol, 403*(2), 150-161. doi: 10.1016/j.ydbio.2015.05.007

Hoshino, A., Costa-Silva, B., Shen, T. L., Rodrigues, G., Hashimoto, A., Tesic Mark, M., . . . Lyden, D. (2015). Tumour exosome integrins determine organotropic metastasis. *Nature, 527*(7578), 329-335. doi: 10.1038/nature15756

Hovey, R. C., Goldhar, A. S., Baffi, J., & Vonderhaar, B. K. (2001). Transcriptional regulation of vascular endothelial growth factor expression in epithelial and stromal cells during mouse mammary gland development. *Mol Endocrinol, 15*(5), 819-831. doi: 10.1210/mend.15.5.0635

Hoye, A. M., & Erler, J. T. (2016). Structural ECM components in the premetastatic and metastatic niche. *Am J Physiol Cell Physiol, 310*(11), C955-967. doi: 10.1152/ajpcell.00326.2015

Huang, M., Narita, S., Inoue, T., Koizumi, A., Saito, M., Tsuruta, H., . . . Habuchi, T. (2017). Fatty acid binding protein 4 enhances prostate cancer progression by upregulating matrix metalloproteinases and stromal cell cytokine production. *Oncotarget, 8*(67), 111780-111794. doi: 10.18632/oncotarget.22908

Ingthorsson, S., Andersen, K., Hilmarsdottir, B., Maelandsmo, G. M., Magnusson, M. K., & Gudjonsson, T. (2015). HER2 induced EMT

and tumorigenicity in breast epithelial progenitor cells is inhibited by coexpression of EGFR. *Oncogene*. doi: 10.1038/onc.2015.489

Ingthorsson, S., Sigurdsson, V., Fridriksdottir, A., Jr., Jonasson, J. G., Kjartansson, J., Magnusson, M. K., & Gudjonsson, T. (2010). Endothelial cells stimulate growth of normal and cancerous breast epithelial cells in 3D culture. *BMC Res Notes, 3*, 184. doi: 10.1186/1756-0500-3-184

Insua-Rodriguez, J., & Oskarsson, T. (2016). The extracellular matrix in breast cancer. *Adv Drug Deliv Rev, 97*, 41-55. doi: 10.1016/j.addr.2015.12.017

Jang, B. G., Kim, H. S., Chang, W. Y., Bae, J. M., Oh, H. J., Wen, X., . . . Kang, G. H. (2017). Prognostic significance of stromal GREM1 expression in colorectal cancer. *Hum Pathol, 62*, 56-65. doi: 10.1016/j.humpath.2016.12.018

Jefri, M., Huang, Y. N., Huang, W. C., Tai, C. S., & Chen, W. L. (2015). YKL-40 regulated epithelial-mesenchymal transition and migration/invasion enhancement in non-small cell lung cancer. *BMC Cancer, 15*, 590. doi: 10.1186/s12885-015-1592-3

Kalluri, R. (2003). Basement membranes: structure, assembly and role in tumour angiogenesis. *Nat Rev Cancer, 3*(6), 422-433. doi: 10.1038/nrc1094

Kalluri, R., & Weinberg, R. A. (2009). The basics of epithelial-mesenchymal transition. *J Clin Invest, 119*(6), 1420-1428. doi: 10.1172/jci39104

Kalucka, J., Bierhansl, L., Conchinha, N. V., Missiaen, R., Elia, I., Bruning, U., . . . Carmeliet, P. (2018). Quiescent Endothelial Cells Upregulate Fatty Acid beta-Oxidation for Vasculoprotection via Redox Homeostasis. *Cell Metab, 28*(6), 881-894.e813. doi: 10.1016/j.cmet.2018.07.016

Karagiannis, G. S., Musrap, N., Saraon, P., Treacy, A., Schaeffer, D. F., Kirsch, R., . . . Diamandis, E. P. (2015). Bone morphogenetic protein antagonist gremlin-1 regulates colon cancer progression. *Biol Chem, 396*(2), 163-183. doi: 10.1515/hsz-2014-0221

Kastrup, J. (2012). Can YKL-40 be a new inflammatory biomarker in cardiovascular disease? *Immunobiology, 217*(5), 483-491. doi: 10.1016/j.imbio.2011.04.007

Kleinman, H. K., Philp, D., & Hoffman, M. P. (2003). Role of the extracellular matrix in morphogenesis. *Curr Opin Biotechnol, 14*(5), 526-532.

Komohara, Y., Jinushi, M., & Takeya, M. (2014). Clinical significance of macrophage heterogeneity in human malignant tumors. *Cancer Sci, 105*(1), 1-8. doi: 10.1111/cas.12314

Komohara, Y., & Takeya, M. (2017). CAFs and TAMs: maestros of the tumour microenvironment. *J Pathol, 241*(3), 313-315. doi: 10.1002/path.4824

Kouros-Mehr, H., Kim, J. W., Bechis, S. K., & Werb, Z. (2008). GATA-3 and the regulation of the mammary luminal cell fate. *Curr Opin Cell Biol, 20*(2), 164-170. doi: 10.1016/j.ceb.2008.02.003

Kumar, R., & Yarmand-Bagheri, R. (2001). The role of HER2 in angiogenesis. *Semin Oncol, 28*(5 Suppl 16), 27-32.

La Russa, M. F., & Qi, L. S. (2015). The New State of the Art: Cas9 for Gene Activation and Repression. *Mol Cell Biol, 35*(22), 3800-3809. doi: 10.1128/MCB.00512-15

Laughner, E., Taghavi, P., Chiles, K., Mahon, P. C., & Semenza, G. L. (2001). HER2 (neu) signaling increases the rate of hypoxia-inducible factor 1alpha (HIF-1alpha) synthesis: novel mechanism for HIF-1-mediated vascular endothelial growth factor expression. *Mol Cell Biol, 21*(12), 3995-4004. doi: 10.1128/MCB.21.12.3995-4004.2001

Lee, E., Fertig, E. J., Jin, K., Sukumar, S., Pandey, N. B., & Popel, A. S. (2014a). Breast cancer cells condition lymphatic endothelial cells within pre-metastatic niches to promote metastasis. *Nat Commun, 5*, 4715. doi: 10.1038/ncomms5715

Lee, E., Pandey, N. B., & Popel, A. S. (2014b). Lymphatic endothelial cells support tumor growth in breast cancer. *Sci Rep, 4*, 5853. doi: 10.1038/srep05853

Lee, E., Pandey, N. B., & Popel, A. S. (2015a). Crosstalk between cancer cells and blood endothelial and lymphatic endothelial cells in tumour and organ microenvironment. *Expert Rev Mol Med, 17*, e3. doi: 10.1017/erm.2015.2

Lee, G. Y., Kenny, P. A., Lee, E. H., & Bissell, M. J. (2007). Three-dimensional culture models of normal and malignant breast epithelial cells. *Nat Methods, 4*(4), 359-365. doi: 10.1038/nmeth1015

Lee, K. M., Nam, K., Oh, S., Lim, J., Kim, R. K., Shim, D., . . . Shin, I. (2015b). ECM1 regulates tumor metastasis and CSC-like property through stabilization of beta-catenin. *Oncogene, 34*(50), 6055-6065. doi: 10.1038/onc.2015.54

Lee, K. M., Nam, K., Oh, S., Lim, J., Kim, Y. P., Lee, J. W., . . . Shin, I. (2014c). Extracellular matrix protein 1 regulates cell proliferation and trastuzumab resistance through activation of epidermal growth factor signaling. *Breast Cancer Res, 16*(6), 479. doi: 10.1186/s13058-014-0479-6

Lefort, S., Thuleau, A., Kieffer, Y., Sirven, P., Bieche, I., Marangoni, E., . . . Mechta-Grigoriou, F. (2017). CXCR4 inhibitors could benefit to HER2

but not to triple-negative breast cancer patients. *Oncogene, 36*(9), 1211-1222. doi: 10.1038/onc.2016.284

Li, G., Zheng, J., Xu, B., Ling, J., Qiu, W., & Wang, Y. (2017). Simvastatin inhibits tumor angiogenesis in HER2-overexpressing human colorectal cancer. *Biomed Pharmacother, 85*, 418-424. doi: 10.1016/j.biopha.2016.11.045

Low, D., Subramaniam, R., Lin, L., Aomatsu, T., Mizoguchi, A., Ng, A., . . . Mizoguchi, E. (2015). Chitinase 3-like 1 induces survival and proliferation of intestinal epithelial cells during chronic inflammation and colitis-associated cancer by regulating S100A9. *Oncotarget, 6*(34), 36535-36550. doi: 10.18632/oncotarget.5440

Lowy, C. M., & Oskarsson, T. (2015). Tenascin C in metastasis: A view from the invasive front. *Cell Adh Migr, 9*(1-2), 112-124. doi: 10.1080/19336918.2015.1008331

Macias, H., & Hinck, L. (2012). Mammary gland development. *Wiley Interdiscip Rev Dev Biol, 1*(4), 533-557. doi: 10.1002/wdev.35

Mali, P., Yang, L., Esvelt, K. M., Aach, J., Guell, M., DiCarlo, J. E., . . . Church, G. M. (2013). RNA-guided human genome engineering via Cas9. *Science, 339*(6121), 823-826. doi: 10.1126/science.1232033

Martin-Castillo, B., Oliveras-Ferraros, C., Vazquez-Martin, A., Cufi, S., Moreno, J. M., Corominas-Faja, B., . . . Menendez, J. A. (2013). Basal/HER2 breast carcinomas: integrating molecular taxonomy with cancer stem cell dynamics to predict primary resistance to trastuzumab (Herceptin). *Cell Cycle, 12*(2), 225-245. doi: 10.4161/cc.23274

Mathieu, E., Meheus, L., Raymackers, J., & Merregaert, J. (1994). Characterization of the Osteogenic Stromal Cell Line MN7: Identification of Secreted MN7 Proteins Using Two-Dimensional I'olyacrylamide Gel Electrophoresis, Western Blotting, and Microsequencing. *JOURNAL OF BONE AND MINERAL RESEARCH, 9*(6), 903-913.

Mi, H., Muruganujan, A., Casagrande, J. T., & Thomas, P. D. (2013). Large-scale gene function analysis with the PANTHER classification system. *Nat Protoc, 8*(8), 1551-1566. doi: 10.1038/nprot.2013.092

Mitola, S., Ravelli, C., Moroni, E., Salvi, V., Leali, D., Ballmer-Hofer, K., . . . Presta, M. (2010). Gremlin is a novel agonist of the major proangiogenic receptor VEGFR2. *Blood, 116*(18), 3677-3680. doi: 10.1182/blood-2010-06-291930

Morsing, M., Klitgaard, M. C., Jafari, A., Villadsen, R., Kassem, M., Petersen, O. W., & Ronnov-Jessen, L. (2016). Evidence of two distinct

functionally specialized fibroblast lineages in breast stroma. *Breast Cancer Res, 18*(1), 108. doi: 10.1186/s13058-016-0769-2

Moser, M., Binder, O., Wu, Y., Aitsebaomo, J., Ren, R., Bode, C., . . . Patterson, C. (2003). BMPER, a Novel Endothelial Cell Precursor-Derived Protein, Antagonizes Bone Morphogenetic Protein Signaling and Endothelial Cell Differentiation. *Molecular and Cellular Biology, 23*(16), 5664-5679. doi: 10.1128/mcb.23.16.5664-5679.2003

Mullendore, M. E., Koorstra, J. B., Li, Y. M., Offerhaus, G. J., Fan, X., Henderson, C. M., . . . Feldmann, G. (2009). Ligand-dependent Notch signaling is involved in tumor initiation and tumor maintenance in pancreatic cancer. *Clin Cancer Res, 15*(7), 2291-2301. doi: 10.1158/1078-0432.ccr-08-2004

Murtas, D., Piras, F., Minerba, L., Maxia, C., Ferreli, C., Demurtas, P., . . . Perra, M. T. (2015). Activated Notch1 expression is associated with angiogenesis in cutaneous melanoma. *Clin Exp Med, 15*(3), 351-360. doi: 10.1007/s10238-014-0300-y

Muschler, J., & Streuli, C. H. (2010). Cell-matrix interactions in mammary gland development and breast cancer. *Cold Spring Harb Perspect Biol, 2*(10), a003202. doi: 10.1101/cshperspect.a003202

Naylor, M. J., Li, N., Cheung, J., Lowe, E. T., Lambert, E., Marlow, R., . . . Streuli, C. H. (2005). Ablation of beta1 integrin in mammary epithelium reveals a key role for integrin in glandular morphogenesis and differentiation. *J Cell Biol, 171*(4), 717-728. doi: 10.1083/jcb.200503144

Oskarsson, T., Acharyya, S., Zhang, X. H., Vanharanta, S., Tavazoie, S. F., Morris, P. G., . . . Massague, J. (2011). Breast cancer cells produce tenascin C as a metastatic niche component to colonize the lungs. *Nat Med, 17*(7), 867-874. doi: 10.1038/nm.2379

Oyama, N., & Merregaert, J. (2017). The Extracellular Matrix Protein 1 (ECM1) in Molecular-Based Skin Biology. 91-110. doi: 10.1007/978-3-662-47398-6_8

Perou, C. M. (2011). Molecular stratification of triple-negative breast cancers. *Oncologist, 16 Suppl 1*, 61-70. doi: 10.1634/theoncologist.2011-S1-61

Perou, C. M., Sorlie, T., Eisen, M. B., van de Rijn, M., Jeffrey, S. S., Rees, C. A., . . . Botstein, D. (2000). Molecular portraits of human breast tumours. *Nature, 406*(6797), 747-752. doi: 10.1038/35021093

Pollard, J. W. (2008). Macrophages define the invasive microenvironment in breast cancer. *J Leukoc Biol, 84*(3), 623-630. doi: 10.1189/jlb.1107762

Rafii, S., Butler, J. M., & Ding, B. S. (2016). Angiocrine functions of organ-specific endothelial cells. *Nature, 529*(7586), 316-325. doi: 10.1038/nature17040

Rakha, E. A., & Ellis, I. O. (2009). Triple-negative/basal-like breast cancer: review. *Pathology, 41*(1), 40-47. doi: 10.1080/00313020802563510

Ralston, A., Cox, B. J., Nishioka, N., Sasaki, H., Chea, E., Rugg-Gunn, P., . . . Rossant, J. (2010). Gata3 regulates trophoblast development downstream of Tead4 and in parallel to Cdx2. *Development, 137*(3), 395-403. doi: 10.1242/dev.038828

Riabov, V., Gudima, A., Wang, N., Mickley, A., Orekhov, A., & Kzhyshkowska, J. (2014). Role of tumor associated macrophages in tumor angiogenesis and lymphangiogenesis. *Front Physiol, 5*, 75. doi: 10.3389/fphys.2014.00075

Rosenblat, J. D., Brietzke, E., Mansur, R. B., Maruschak, N. A., Lee, Y., & McIntyre, R. S. (2015). Inflammation as a neurobiological substrate of cognitive impairment in bipolar disorder: Evidence, pathophysiology and treatment implications. *J Affect Disord, 188*, 149-159. doi: 10.1016/j.jad.2015.08.058

Rossiter, H., Barresi, C., Ghannadan, M., Gruber, F., Mildner, M., Fodinger, D., & Tschachler, E. (2007). Inactivation of VEGF in mammary gland epithelium severely compromises mammary gland development and function. *Faseb j, 21*(14), 3994-4004. doi: 10.1096/fj.07-8720com

Roswall, P., Bocci, M., Bartoschek, M., Li, H., Kristiansen, G., Jansson, S., . . . Pietras, K. (2018). Microenvironmental control of breast cancer subtype elicited through paracrine platelet-derived growth factor-CC signaling. *Nat Med, 24*(4), 463-473. doi: 10.1038/nm.4494

Rouillard, A. D., Gundersen, G. W., Fernandez, N. F., Wang, Z., Monteiro, C. D., McDermott, M. G., & Ma'ayan, A. (2016). The harmonizome: a collection of processed datasets gathered to serve and mine knowledge about genes and proteins. *Database (Oxford), 2016*. doi: 10.1093/database/baw100

Rusak, A., Jablonska, K., Piotrowska, A., Grzegrzolka, J., Nowak, A., Wojnar, A., & Dziegiel, P. (2018). The Role of CHI3L1 Expression in Angiogenesis in Invasive Ductal Breast Carcinoma. *Anticancer Res, 38*(6), 3357-3366. doi: 10.21873/anticanres.12602

Sage, H., & Bornstein, P. (1982). Endothelial cells from umbilical vein and a hemangioendothelioma secrete basement membrane largely to the exclusion of interstitial procollagens. *Arteriosclerosis, 2*(1), 27-36.

Sage, H., Pritzl, P., & Bornstein, P. (1982). Endothelial cells secrete a novel collagen type in vitro independently of prolyl hydroxylation. *Coll Relat Res, 2*(6), 465-479.

Saitoh, M. (2018). Involvement of partial EMT in cancer progression. *J Biochem, 164*(4), 257-264. doi: 10.1093/jb/mvy047

Santamaria, P. G., Moreno-Bueno, G., Portillo, F., & Cano, A. (2017). EMT: Present and future in clinical oncology. *Mol Oncol, 11*(7), 718-738. doi: 10.1002/1878-0261.12091

Sato, M., Kawana, K., Fujimoto, A., Yoshida, M., Nakamura, H., Nishida, H., . . . Fujii, T. (2016). Clinical significance of Gremlin 1 in cervical cancer and its effects on cancer stem cell maintenance. *Oncol Rep, 35*(1), 391-397. doi: 10.3892/or.2015.4367

Schwertfeger, K. L., Rosen, J. M., & Cohen, D. A. (2006). Mammary gland macrophages: pleiotropic functions in mammary development. *J Mammary Gland Biol Neoplasia, 11*(3-4), 229-238. doi: 10.1007/s10911-006-9028-y

Sercu, S., Zhang, L., & Merregaert, J. (2008a). The extracellular matrix protein 1: its molecular interaction and implication in tumor progression. *Cancer Invest, 26*(4), 375-384. doi: 10.1080/07357900701788148

Sercu, S., Zhang, M., Oyama, N., Hansen, U., Ghalbzouri, A. E., Jun, G., . . . Merregaert, J. H. (2008b). Interaction of extracellular matrix protein 1 with extracellular matrix components: ECM1 is a basement membrane protein of the skin. *J Invest Dermatol, 128*(6), 1397-1408. doi: 10.1038/sj.jid.5701231

Shan, T., Chen, S., Chen, X., Lin, W. R., Li, W., Ma, J., . . . Kang, Y. (2017). Cancer-associated fibroblasts enhance pancreatic cancer cell invasion by remodeling the metabolic conversion mechanism. *Oncology Reports, 37*, 1971-1979.

Shao, R. (2013). YKL-40 acts as an angiogenic factor to promote tumor angiogenesis. *Front Physiol, 4*, 122. doi: 10.3389/fphys.2013.00122

Shibata, A., Nagaya, T., Imai, T., Funahashi, H., Nakao, A., & Seo, H. (2002). Inhibition of NF-kB activity decreases the VEGF mRNA expression in MDA-MB-231 breast cancer cells. *Breast Cancer Research and Treatment, 73*, 237-243.

Sigurdsson, V., Hilmarsdottir, B., Sigmundsdottir, H., Fridriksdottir, A. J., Ringner, M., Villadsen, R., . . . Gudjonsson, T. (2011). Endothelial induced EMT in breast epithelial cells with stem cell properties. *PLoS One, 6*(9), e23833. doi: 10.1371/journal.pone.0023833

Sorlie, T., Perou, C. M., Tibshirani, R., Aas, T., Geisler, S., Johnsen, H., . . . Borresen-Dale, A. L. (2001). Gene expression patterns of breast carcinomas distinguish tumor subclasses with clinical implications. *Proc Natl Acad Sci U S A, 98*(19), 10869-10874. doi: 10.1073/pnas.191367098

Sorlie, T., Tibshirani, R., Parker, J., Hastie, T., Marron, J. S., Nobel, A., . . . Botstein, D. (2003). Repeated observation of breast tumor subtypes in independent gene expression data sets. *Proc Natl Acad Sci U S A, 100*(14), 8418-8423. doi: 10.1073/pnas.0932692100

Sternlicht, M. D. (2006). Key stages in mammary gland development: the cues that regulate ductal branching morphogenesis. *Breast Cancer Res, 8*(1), 201. doi: 10.1186/bcr1368

Thiery, J. P. (2002). Epithelial-mesenchymal transitions in tumour progression. *Nat Rev Cancer, 2*(6), 442-454. doi: 10.1038/nrc822

Thiery, J. P., Acloque, H., Huang, R. Y., & Nieto, M. A. (2009). Epithelial-mesenchymal transitions in development and disease. *Cell, 139*(5), 871-890. doi: 10.1016/j.cell.2009.11.007

Thongsom, S., Chaocharoen, W., Silsirivanit, A., Wongkham, S., Sripa, B., Choe, H., . . . Talabnin, C. (2016). YKL-40/chitinase-3-like protein 1 is associated with poor prognosis and promotes cell growth and migration of cholangiocarcinoma. *Tumour Biol, 37*(7), 9451-9463. doi: 10.1007/s13277-016-4838-z

Tran, H. D., Luitel, K., Kim, M., Zhang, K., Longmore, G. D., & Tran, D. D. (2014). Transient SNAIL1 expression is necessary for metastatic competence in breast cancer. *Cancer Res, 74*(21), 6330-6340. doi: 10.1158/0008-5472.can-14-0923

Traustadottir, G. A., Jensen, C. H., Thomassen, M., Beck, H. C., Mortensen, S. B., Laborda, J., . . . Andersen, D. C. (2016). Evidence of non-canonical NOTCH signaling: Delta-like 1 homolog (DLK1) directly interacts with the NOTCH1 receptor in mammals. *Cell Signal, 28*(4), 246-254. doi: 10.1016/j.cellsig.2016.01.003

Tsai, J. H., Donaher, J. L., Murphy, D. A., Chau, S., & Yang, J. (2012). Spatiotemporal regulation of epithelial-mesenchymal transition is essential for squamous cell carcinoma metastasis. *Cancer Cell, 22*(6), 725-736. doi: 10.1016/j.ccr.2012.09.022

Turajlic, S., Swanton, C., & (2016). Metastasis as an evolutionary process. *Science, 352*(6282), 169-175.

Ucar, A., Vafaizadeh, V., Jarry, H., Fiedler, J., Klemmt, P. A., Thum, T., . . . Chowdhury, K. (2010). miR-212 and miR-132 are required for epithelial stromal interactions necessary for mouse mammary gland development. *Nat Genet, 42*(12), 1101-1108. doi: 10.1038/ng.709

Ucuzian, A. A., Gassman, A. A., East, A. T., & Greisler, H. P. (2010). Molecular mediators of angiogenesis. *J Burn Care Res, 31*(1), 158-175. doi: 10.1097/BCR.0b013e3181c7ed82

Uwamori, H., Ono, Y., Yamashita, T., Arai, K., & Sudo, R. (2019). Comparison of organ-specific endothelial cells in terms of

microvascular formation and endothelial barrier functions. *Microvasc Res, 122*, 60-70. doi: 10.1016/j.mvr.2018.11.007

Vignon, E. (2001). Is glycoprotein YKL40 a new marker for joint disorders? *Joint Bone Spine, 68*(6), 454-456.

Villadsen, R., Fridriksdottir, A. J., Ronnov-Jessen, L., Gudjonsson, T., Rank, F., LaBarge, M. A., . . . Petersen, O. W. (2007). Evidence for a stem cell hierarchy in the adult human breast. *J Cell Biol, 177*(1), 87-101. doi: 10.1083/jcb.200611114

Wang, L., Yu, J., Ni, J., Xu, X.-M., Wang, J., Ning, H., . . . Zhang, L. (2003). Extracellular matrix protein 1 (ECM1) is over-expressed in malignant epithelial tumors. *Cancer Letters, 200*(1), 57-67. doi: 10.1016/s0304-3835(03)00350-1

Wang, X., Zheng, M., Liu, G., Xia, W., McKeown-Longo, P. J., Hung, M. C., & Zhao, J. (2007). Kruppel-like factor 8 induces epithelial to mesenchymal transition and epithelial cell invasion. *Cancer Res, 67*(15), 7184-7193. doi: 10.1158/0008-5472.can-06-4729

Wieland, E., Rodriguez-Vita, J., Liebler, S. S., Mogler, C., Moll, I., Herberich, S. E., . . . Fischer, A. (2017). Endothelial Notch1 Activity Facilitates Metastasis. *Cancer Cell, 31*(3), 355-367. doi: 10.1016/j.ccell.2017.01.007

Wiesen, J. F., Young, P., Werb, Z., & Cunha, G. R. (1999). Signaling through the stromal epidermal growth factor receptor is necessary for mammary ductal development. *Development, 126*(2), 335-344.

Wu, Q., Chen, D., Luo, Q., Yang, Q., Zhao, C., Zhang, D., . . . Qi, Z. (2018). Extracellular matrix protein 1 recruits moesin to facilitate invadopodia formation and breast cancer metastasis. *Cancer Lett, 437*, 44-55. doi: 10.1016/j.canlet.2018.08.022

Xiao, Q., Jiang, Y., Liu, Q., Yue, J., Liu, C., Zhao, X., . . . Ge, G. (2015). Minor Type IV Collagen alpha5 Chain Promotes Cancer Progression through Discoidin Domain Receptor-1. *PLoS Genet, 11*(5), e1005249. doi: 10.1371/journal.pgen.1005249

Yan, W., Cao, Q. J., Arenas, R. B., Bentley, B., & Shao, R. (2010). GATA3 inhibits breast cancer metastasis through the reversal of epithelial-mesenchymal transition. *J Biol Chem, 285*(18), 14042-14051. doi: 10.1074/jbc.M110.105262

Yang, J., & Weinberg, R. A. (2008). Epithelial-mesenchymal transition: at the crossroads of development and tumor metastasis. *Dev Cell, 14*(6), 818-829. doi: 10.1016/j.devcel.2008.05.009

Yin, M., Tissari, M., Tamminen, J., Ylivinkka, I., Ronty, M., von Nandelstadh, P., . . . Koli, K. (2017). Gremlin-1 is a key regulator of the invasive

cell phenotype in mesothelioma. *Oncotarget, 8*(58), 98280-98297. doi: 10.18632/oncotarget.21550

Yoon, N. K., Maresh, E. L., Shen, D., Elshimali, Y., Apple, S., Horvath, S., . . . Goodglick, L. (2010). Higher levels of GATA3 predict better survival in women with breast cancer. *Hum Pathol, 41*(12), 1794-1801. doi: 10.1016/j.humpath.2010.06.010

Yu, W., Datta, A., Leroy, P., O'Brien, L. E., Mak, G., Jou, T. S., . . . Zegers, M. M. (2005). Beta1-integrin orients epithelial polarity via Rac1 and laminin. *Mol Biol Cell, 16*(2), 433-445. doi: 10.1091/mbc.e04-05-0435

Zhang, K., Corsa, C. A., Ponik, S. M., Prior, J. L., Piwnica-Worms, D., Eliceiri, K. W., . . . Longmore, G. D. (2013). The collagen receptor discoidin domain receptor 2 stabilizes SNAIL1 to facilitate breast cancer metastasis. *Nat Cell Biol, 15*(6), 677-687. doi: 10.1038/ncb2743

Zhang, Z., Li, X., Sun, W., Yue, S., Yang, J., Li, J., . . . Dou, K. (2017). Loss of exosomal miR-320a from cancer-associated fibroblasts contributes to HCC proliferation and metastasis. *Cancer Lett, 397*, 33-42. doi: 10.1016/j.canlet.2017.03.004

Zhu, J., Xiong, G., Trinkle, C., & Xu, R. (2014). Integrated extracellular matrix signaling in mammary gland development and breast cancer progression. *Histol Histopathol, 29*(9), 1083-1092. doi: 10.14670/hh-29.1083

Original publications

Paper I

ECM1 secreted by HER2-overexpressing breast cancer cells promotes formation of a vascular niche accelerating cancer cell migration and invasion

Running title: ECM1 induces vascular niche promoting cancer

Sophie Sarah Steinhäuser[1], Erika Morera[1], Zuzana Budkova[1], Qiong Wang[3], Ottar Rolfsson[3], Angela Riedel[4,5], Aileen Krueger[4,5], Bylgja Hilmarsdóttir[7], Gunhild M Maelandsmo[7], Bjarni Agnar Agnarsson[8,9], Jon Gunnlaugur Jonasson[8,9], Saevar Ingthorsson[1], Gunnhildur Asta Traustadottir[1], Thordur Oskarsson[4,5,6], and Thorarinn Gudjonsson[1,2,3]

[1]Stem Cell Research Unit, Biomedical Center, Department of Anatomy, Faculty of Medicine, School of Health Sciences, University of Iceland, Iceland
[2]Department of Laboratory Hematology, University Hospital, Iceland
[3]Center for Systems Biology, University of Iceland, Reykjavik, Iceland
[4]Heidelberg Institute for Stem Cell Technology and Experimental Medicine (HI-STEM gGmbH), 69120 Heidelberg, Germany.
[5]Division of Stem Cells and Cancer, German Cancer Research Center (DKFZ), 69120 Heidelberg, Germany.
[6]German Cancer Consortium (DKTK), 69120 Heidelberg, Germany.
[7]Department of Tumor Biology, Institute for cancer research, The Norwegian Radium Hospital, Oslo, Norway.
[8]Department of Pathology, Landspitali - University Hospital, Reykjavik, Iceland
[9]Faculty of Medicine, University of Iceland, Reykjavik, Iceland.

Correspondence: Thorarinn Gudjonsson, Stem Cell Research Unit, Department of Anatomy, Medical Faculty, Biomedical Center, University of Iceland, Vatnsmyrarvegi 16, 101 Reykjavík, Iceland. Tel: +354-5254827; Fax: +354 -4884. E-mail: tgudjons@hi.is

Abstract

The tumor microenvironment is increasingly recognized as key player in cancer progression. Investigating heterotypic interactions between cancer cells and their microenvironment is important for understanding how specific cell types support cancer. Forming the vasculature, endothelial cells (ECs) are a prominent cell type in the microenvironment of both normal and neoplastic breast gland. Here, we sought out to analyze epithelial-endothelial crosstalk in the breast using isogenic non-tumorigenic vs. tumorigenic breast epithelial cell lines and primary ECs. The cellular model used here consists of D492, a breast epithelial cell line with stem cell properties, and two isogenic D492-derived EMT cell lines, D492M and D492HER2. D492M was generated by endothelial-induced EMT and is non-tumorigenic while D492HER2 is tumorigenic, expressing the ErbB2/HER2 oncogene. To investigate cellular crosstalk, we used both conditioned medium (CM) and 2D/3D co-culture systems. Secretome analysis of D492 cell lines was performed using mass spectrometry and candidate knockdown (KD) and overexpression (OE) was done using siRNA and CRISPRi/CRISPRa technology. D492HER2 directly enhances endothelial network formation and activates a molecular axis in ECs promoting D492HER2 migration and invasion, suggesting an endothelial feedback response. Secretome analysis identified extracellular matrix protein 1 (ECM1) as potential angiogenic inducer in D492HER2. Confirming its involvement, KD of ECM1 reduced the ability of D492HER2-CM to increase endothelial network formation and induce the endothelial feedback, while recombinant ECM1 (rECM1) increased both. Interestingly, NOTCH1 and NOTCH3 expression was upregulated in ECs upon treatment with D492HER2-CM or rECM1 but not by CM from D492HER2 with ECM1 KD. Blocking endothelial NOTCH signaling inhibited the increase in network formation and the ability of ECs to promote D492HER2 migration and invasion. In summary, our data demonstrate that cancer-secreted ECM1 induces a NOTCH-mediated endothelial feedback promoting cancer progression by enhancing migration and invasion. Targeting this interaction may provide a novel possibility to improve cancer treatment.

Key words

HER2 breast cancer, ECM1, angiogenesis, endothelial feedback, NOTCH

Organ morphogenesis is dependent on heterotypic interactions between multiple cell types. In breast morphogenesis, the epithelial compartment generates branching ducts that result in terminal duct lobular units (TDLU) [1]. Ducts and TDLUs are surrounded by a basement membrane, embedded in stroma consisting of extracellular matrix (ECM) as well as multiple cell types including fibroblasts, immune cells and endothelial cells (ECs) forming the microvessels [1, 2]. Formation of TDLU is highly dependent on heterotypic interactions between the epithelial cells and the surrounding vascular rich stroma. Multiple studies have shown that the stromal compartment plays a fundamental role when it comes to epithelial morphogenesis [2-6]. For example, the ability of breast epithelial cells to form TDLU-like structures in a 3-dimensional environment *in vitro* is strongly enhanced by the presence of breast ECs [2]. In addition to its role in normal development, recent studies provide evidence that proliferation and migration of cancer cells is also largely dependent on interactions with the surrounding stroma [3, 7-9].

The tumor microenvironment is composed of a plethora of different cell types and extra cellular matrix (ECM) [10]. The interaction between cancer cells and cells of the microenvironment is a crucial determinant of cancer progression. Co-evolution of cancer cells and tumor stroma can lead to the generation of niches that support tumor growth, both at the primary site and at distant metastatic sites [11]. In this context, many studies have been focusing on identifying the role of tumor-associated macrophages (TAMs) and cancer-associated fibroblasts (CAFs) in cancer progression [16-20].

Recent research, however, suggests that endothelial cells of blood vessels play a role in cancer progression that is far beyond delivering oxygen and nutrients [7, 21-24]. There is evidence that the endothelium can impact cancer progression by either preventing or supporting tumor growth and metastasis formation. An intact vasculature can keep metastatic cells in a dormant and non-proliferative state whereas a sprouting vasculature rather supports metastatic outgrowth [7, 25, 26]. Ghajar and colleagues found that endothelial-derived thrombospondin-1 (TSP1) induces cancer cell dormancy

in breast cancer and therefore prevents outgrowth of metastasis in lung and bones [7]. However, in the presence of sprouting neovasculature this suppressive effect was lost and the endothelium now appeared to promote tumor outgrowth via TGF-b1 and periostin [7]. Therefore, an essential question to ask is how cancer cells interact with ECs in order to promote the generation of a vascular niche promoting tumor growth and cancer progression. Presently, a number of molecular mediators of angiogenesis have been identified [27]. The most commonly described candidates include VEGF, FGF2, TNF-a, TGF-b1, PDGF as well as angiopoietins. Laughner et al. were able to show that HER2 signaling in breast cancer cells could increase HIF1a-mediated VEGF expression resulting in increased tumor angiogenesis [30]. Lee et al. showed that increased IL-6 secretion in breast cancer cells induces secretion of CCL5 in lymphatic endothelial cells (LEC), which in return enhances cancer cell migration [22]. Furthermore, cancer cell-secreted IL-6 increases VEGF expression in LECs, which enhances lung vascular permeability and lymph node angiogenesis and thereby promotes metastatic outgrowth [22, 23]. In addition, the NOTCH signaling pathway has recently been linked to angiogenesis [27-29]. Murtas and colleagues report increased NOTCH1 expression by tumor endothelium in cutaneous melanoma that was linked to increasing microvascular density [28]. This suggests that targeting the interaction between cancer cells and their niches may provide additional means to inhibit progression of cancer. However, our understanding of the generation of vascular niches and molecular interactions within the niches is generally still rudimentary.

We have previously established a breast epithelial cell line with stem cell properties, referred to as D492 [32-35]. D492 can generate both luminal- and myoepithelial cells and in 3D rBM culture it forms branching structures reminiscent of TDLU *in vivo*. When D492 was co-cultured with ECs in an organoid culture, a subpopulation of D492 underwent EMT and such a structure isolated gave rise to D492M [32]. D492HER2 was generated by overexpressing the ErbB2/HER2 oncogene in D492, which then underwent oncogene-induced EMT [36]. In contrast to D492M, D492HER2 has

tumorigenic properties, as evidenced by injection of cells in the mammary fat pads of NSG mice. The different tumorigenicities of these two isogenic EMT derivatives of D492 present an interesting research platform to study tumorigenicity, especially with regard to interaction with the endothelium.

In this study, we show that conditioned medium (CM) from D492HER2 increases endothelial network formation *in vitro* and induces an endothelial feedback promoting D492HER2 migration. Secretome identified ECM1 as potential pro-angiogenic factor in D492HER2. Recombinant ECM1 (rECM1) increases endothelial network formation while knockdown (KD) of ECM1 reduces the ability of D492HER2-CM to increase the endothelial network. ECM1 has previously been associated with decreased overall and distant metastasis-free survival when expressed in HER2+ breast tumors [37-39]. A role in angiogenesis and cancer cell migration and invasion has been suggested in laryngeal carcinoma, cholangiocarcinoma, gastric cancer, bladder cancer and breast cancer [37, 40-43]. However, the mechanism through which ECM1 induces a pro-tumorigenic vascular niche promoting cancer progression is still unknown. Finally, increased expression of NOTCH1 and NOTCH3 in ECs treated with D492HER2-CM or indicates a possible modulatory role of ECM1 in NOTCH signaling during angiogenesis and cancer.

Materials and Methods

Cell culture

D492, D492M and D492HER2 cells were maintained in H14 medium in tissue culture treated T25 Falcon flasks (BD Biosciences (BD), Franklin Lakes, NJ, USA) coated with collagen I (Advanced Biomatrix, San Diego, CA, USA), as described previously [32, 36]. The cells were grown at 37°C and 5% CO2 and subcultured into new flasks 1-2 times per week in a ratio of 1:10 (D492), 1:5 (D492M) or 1:15 (D492HER2). MDA-MB-231 was cultured in Gibco™ RPMI 1640 medium containing 10% fetal bovine serum (FBS) (Invitrogen), further referred to as R10F, and MCF-7 in Gibco™ DMEM:F-12 medium with

10% FBS. Both cell lines were subcultured 1-2 times per week at a ratio of 1:10. HUVEC primary ECs were obtained from the National University Hospital (Landspitali) Reykjavik and cultured up to passage 8 in EBM2 medium (Lonza) supplemented with growth factors and 5% FBS, further referred to as EGM5. HUVECs were subcultured 1-2 times per week at a ratio of 1:10. Culture medium was changed three times per week and routinely checked for mycoplasma contamination.

Conditioned medium (CM) and mass spectrometry

D492, D492M and D492HER2 were grown in H14 medium until 70-80% confluence. Cells were washed with 1x PBS and half of the original volume of fresh H14 was added in order to enrich for secreted factors. After 48h incubation at 37°C conditioned medium (CM) was collected, centrifuged at 2000 rpm for 3 minutes and sterile filtered through 0.22 µm filter unit. For endothelial network formation in 3D culture, 10.000 HUVECs were seeded in freshly collected CM (or unconditioned control H14) and fresh EGM5 medium (ratio 1:1) in a 96-well angiogenesis plate (#89646, Ibidi) on top of 10 µl solidified rBM Matrigel (#354230, Corning). For recombinant protein experiments, rECM1 (#TP723147, Origene) was added to the medium in a final concentration of 15, 30, 60 or 120 ng/ml. 60 ng/ml was then chosen as concentration for further experiments. For endothelial NOTCH inhibition, gamma-secretase inhibitor DAPT (#D5942, Sigma-Aldrich) was added to the medium in a final concentration of 20 µM. Phase contrast images of the establishing endothelial network were taken after 4 h, 24 h and 48 h. Images were converted to RGB color and analyzed using ImageJ Angiogenesis Analyzer macro. For mass spectrometry, D492 lines were grown in T175 flasks and CM was collected as described above, concentrated for 55 minutes using EMD Millipore Amicon™ Ultra-15 Centrifugal Filter Units (#UFC900324, Merck Millipore) followed by buffer exchange to 100 mM TRIS/HCL buffer. Samples (triplicates) were stored at -80°C. Label Free relative protein quantification by nLC MS/MS after trypsin digestion was performed at the FingerPrints Proteomics Facility, University of Dundee, UK and raw data were analyzed using MaxQuant software (version 1.6.2.1).

Quantitative and statistical analysis was performed using XLStat (version 2018.1). Data were p-value corrected (significance level 0.05) and sorted based on ≥2-fold higher secretion (LFQ intensity) by D492HER2 compared to both D492 and D492M. The resulting candidate list of 77 proteins was used for GO term analysis using PANTHER database (statistical overrepresentation test). As annotation data set we used “GO biological process complete” with Bonferroni correction for multiple testing. To investigate feedback effects of conditioned/induced ECs, CM from D492 lines was added to 40-50% confluent HUVECs (as described above) and incubated for 48 h. Cells were washed with 1x PBS and fresh EGM5 (half volume) was added to collect conditioned endothelial-secreted factors. After 48 h, CM from induced vs. non-induced HUVECs was collected, centrifuged (2000 rpm, 3 minutes) and filtered (0.22 µm) and added to 40% confluent D492HER2 together with fresh H14 (ratio 1:1) for 48 h.

Migration and invasion assay

Migration was analyzed using transwell-filter units for 24-well plates with 8 µm pore size ((#353097, Corning). 30.000 cells were seeded on top of the filter in 250 µl culture medium. For invasion assay, filters were pre-coated with 1:10 rBM in H14 for 30 minutes at 37°C. For migration assay, cells were incubated for 24 h and for 48 h in invasion assay. Recombinant ECM1 and NOTCH inhibitor DAPT were used in the concentrations as described before. For migration towards ECs, HUVECs were grown in 500 µl EGM5 to 80% confluence in 24-well plate. Then, medium was changed to H14+EGM5 (1:1) and D492 line cells were seeded on top of filter units (triplicates) in H14+EGM5 (1:1). As positive control, 10% FBS was added to the medium below the filter instead of HUVECs and as negative control, medium above and below the filter unit was identical (H14+EGM5, 1:1). For migration and invasion of D492HER2 treated with CM of induced vs. non-induced ECs, 30.000 D492HER2 cells were seeded in 250 µl H14 on top of the non-coated or rBM-coated filter units (triplicates) and 500 µl H14 containing 10% FBS as attractant was added below. For MDA-MB-231, R10F was used instead of H14 while keeping the same experimental setup. After 24 h or 48 h, non-

migratory or non-invasive cells were removed from the top of the filter using Q-tips, migratory cells below the filter were fixed for 10 minutes with 4% PFA (#252549, Sigma-Aldrich) and stained for 30 minutes with 1:5000 diluted DAPI nuclear staining (20mg/ml) (#D9542, Sigma-Aldrich). Using an EVOS FL Auto 2 Cell Imaging System (Thermo Fisher Scientific), three images per replicate were taken at 10x magnification. Images were converted to 8-bit in ImageJ (version 2.0.0), threshold-adjusted and binary-converted. Migratory cells were counted using the "analyze particles" function.

Transient knockdown (KD) using siRNA

Knockdown was performed in 24-well plate using pre-designed Silencer® Select human ECM1 siRNA (#s4441, Thermo Fisher Scientific) compared to a scrambled negative control (Silencer Select negative control No. 1, Thermo Fisher Scientific, #4390843). Cells were reverse transfected for 48 h according to the manufacturer's protocol using a siRNA concentration of 10 nM. Proliferation was monitored using an IncuCyte ZOOM 2016B System. Knockdown was confirmed using RT-qPCR and western blotting. After 48 h, medium was changed to normal H14 and incubated for another 48 h for collection of conditioned medium as described above. Endothelial network formation was analyzed as previously described for HUVECs treated with CM from D492HER2^{siECM1}compared to control D492HER2.

Generation of stable knockdown and overexpression cell lines using CRISPRi/CRISPRa

In order to generate stable ECM1 knockdown in D492HER2 and overexpression in D492 and D492M, we used the novel CRISPRi (inhibition) and CRISPRa (activation) system. sgRNA plasmids were purchased from Genscript; For ECM1 overexpression and knockdown, a combination of two sgRNAs were used. Overexpression sgRNAs were pre-design and located between 1-200 bp upstream of the ECM1 transcription start site and knockdown sgRNAs custom-designed to bind between 1-200 bp downstream. sgRNAs were cloned into the plenti sgRNA(MS2)_zeo plasmid (Genscript). As negative control, an empty plenti sgRNA(MS2)_zeo plasmid

was used (Genscript). For production of lentiviral particles, HEK293T cells were used and virus was collected 48 h and 72 h after transfection. D492 and D492M were first transduced with plenti dCAS9-VP64-Blast plasmid for transcriptional activation and selected with blasticidin at a concentration of 2 µg/ml for 7 days. D492HER2 were transduced with pHR-SFFV-KRAB-dCas9-P2A-mCherry plasmid for repression and sorted for mCherry expression. Next, transduction with lentivirus containing sgRNA plasmids for overexpression (D492 and D492M containing dCas9-VP64 cassette) and knockdown (D492HER2 containing dCas9-KRAB cassette) was performed. For both KD and OE, two different gRNAs were pooled (KD: ECM1 custom gRNA 1 and 2 (GTGGTCAGTTGCCCCAGGAT, GCCGGCCACTGAAGCTTGTC) and OE: ECM1 SAM guide RNA 1 and 2 (CATCTACAGGCTGCCTTCTG, GAAACTGAGGCACAAACTAG)). Cells were selected with 400 µg/ml (D492, D492M) or 600 µg/ml (D492HER2) zeocin (Invitrogen) for 14 days. For enhancement of ECM1 OE, D492 and D492M were then transduced with lenti MS2-P65-HSF1 Hygro plasmid, containing enhancer domains MS2, P65 and HSP1 that bind to VP64 and enhance its activation activity. Cells were selected with 100 µg/ml hygromycin (Sellekchem, #S2908) for 10-12 days (Fig. 7). ECM1 KD or OE were validated on gene expression level using RT-qPCR.

RNA microarray

For RNA microarray analysis, D492, D492M and D492HER2 with and without ECM1 overexpression/knockdown were grown until 80% confluence, fresh H14 medium was added and CM was collected after 48 h. HUVECs were grown to 40% confluence, washed with 1x PBS and CM was added together with fresh EGM5 (ratio 1:1). After 24 h, RNA was extracted using the RNeasy Mini Kit (Qiagen). Sample concentration and quality was analyzed using the Agilent 2100 Bioanalyzer System (Agilent). As RNA microarray, Affimetrix human Clariom S Assay was performed at the sequencing core facility, German Cancer Research Center (DKFZ) Heidelberg, Germany. Raw data were analyzed using Chipster high-throughput data analysis software v3.12.

RNA, cDNA and RT-qPCR

Total RNA was extracted with Trizol (Life Technologies) and reverse transcribed with hexanucleotides using the SuperScript® IV First-Strand Synthesis System (Invitrogen). Resulting cDNA (10 ng per reaction) was used for quantitative real-time PCR, in master mix (Life Technologies) with pre-designed primer pairs ECM1 (Hs.PT.58.20438560), NOTCH1 (Hs.PT.58.23074795), NOTCH3 (Hs.PT.58.38492200) and beta-2-microglobulin (B2M) as reference gene (Hs.PT.58v.18759587). Experiments were carried out in triplicate on 7500 Real Time PCR System (Life Technologies). Expression levels were normalized to the reference gene and relative mRNA differences were calculated with the ΔΔCt method according to the MIQE guidelines [44].

Protein isolation and western blotting

Protein was isolated using RIPA lysis buffer supplemented with phosphatase and protease inhibitor cocktails (Life Technologies). For western blotting, 5-10 µg protein was used per lane, unless otherwise stated. Samples were denatured using 10% mercaptoethanol at 95 °C for 5 min and run on NuPage 10% Bis-Tris gels (Life Technologies) in 2-(N-morpholino)ethanesulfonic acid (MES) running buffer. Samples were then transferred to Immobilon FL PVDF membranes (Millipore). Membranes were blocked in Li-Cor blocking buffer and primary antibodies (ECM1: sc-515843 (Santa Cruz), beta tubulin: ab6046 (Abcam)) were incubated overnight at 4°C. Near-infrared fluorescence visualization was measured using Odyssey CLx scanner (Li-Cor, Cambridge, UK).

Immunofluorescence (IF) staining

HUVECs were grown to 80% confluence on 8-well chamber slides (#354108, Falcon), fixed with 3.7% PFA, permeabilized with 0.1% Triton X-100 and unspecific background was blocked using 10% FBS in 1xPBS. Incubation with primary antibodies for ECM1 (Sigma Aldrich, #HPA027241), NOTCH1 (#sc-376403, Santa Cruz) and NOTCH3 (#ab23426, Abcam) was done overnight at 4°C, followed by incubation with secondary antibodies

conjugated with Alexa Fluor-488, -546 or -647 for one hour at RT. For nuclei staining DAPI was used together with secondary antibodies at a concentration of 1:5000. Imaging was done using FV1200 Olympus inverted confocal microscope. For IHC staining, paraffin-embedded tumor tissue samples were processed in xylene and ethanol in order to remove paraffin and then rehydrated in dH2O. Following rehydration, high-temperature antigen retrieval in 1x T/E buffer was performed and samples were stained as described above. Counterstaining was performed with filtered hematoxylin for 1-2 minutes.

Statistical analysis

All experiments were performed at minimum in triplicate. Graphs were generated in Microsoft Excel 2015. Error bars represent the standard deviation of the mean. Statistical analysis was performed in R 3.3.3. (R Development Core team, 2013). Data were checked for normal distribution and Students t-test or ANOVA followed by Tukey's honest significant difference test on linear models (lm) was performed when normally distributed whereas Kruskal-Wallis chi-squared test was used when not normally distributed. The significance level was 0.05.

Results

Conditioned medium from D492HER2 promotes endothelial network formation

Initially, we aimed to analyze the heterotypic interactions between normal and cancerous epithelial cells of the mammary gland and endothelial cells (ECs). To address this, we used isogenic normal- and cancerous cell lines derived from the D492 breast epithelial progenitor cell line [33, 35]. We collected conditioned medium (CM) from D492, D492M and D492HER2 and analyzed the effect on endothelial network formation *in vitro*. ECs were seeded in CM from D492, D492M and D492HER2 on top of rBM and endothelial network formation was analyzed after 4 h, 24 h and 48 h (Fig. 1A and B, suppl. Fig. S1). The established network of ECs treated with CM from D492HER2 but

not from D492 and D492M showed significantly higher numbers of master junctions, master segments, meshes and higher total master segment length after 4 h (Fig. 1A and B). This indicates that D492HER2-CM enhances early endothelial network formation *in vitro*. All quantified parameters were also significantly higher upon treatment with D492HER2-derived CM after 24 h and 48 h indicating stability and persistence of the observed pro-angiogenic effect of D492HER2-CM over time (suppl. Fig. S1).

D492HER2-induced ECs feed back on D492HER2 by promoting migration and invasion

After identifying D492HER2 as a cell line enhancing endothelial network formation, we collected CM from D492HER2-induced ECs and treated D492HER2 (Fig. 1C) in order to investigate a possible feedback response through cellular cross talk. Interestingly, we observed that treatment with CM from D492HER2-induced ECs stimulated increased migration and invasion of D492HER2, in contrast to CM from untreated ECs and D492-induced ECs (Fig. 1D), suggesting a positive feedback. To identify whether migration of D492HER2 cells was specifically directed towards the endothelium rather than being general, we performed indirect co-culture of D492, D492M and D492HER2 in a transwell assay with or without ECs present below the filter (Fig. 1E). When analyzing the number of migratory cells, D492HER2 in particular showed an increased migratory phenotype towards ECs below the filter (Fig. 1F), supporting the hypothesis that migration is increased towards the endothelium mediated by induced ECs. In line with this, we could see significantly more D492HER2 than D492 or D492M cells directly associated with ECs in 2D and 3D co-culture with ECs (suppl. Fig. S2).

Enrichment of angiogenesis-regulating proteins and identification of ECM1 in D492HER2 secretome

In order to identify secreted factors from D492HER2 that are mediating the observed pro-angiogenic effect, we performed label-free mass spectrometry on concentrated CM from all three D492 cell lines. In order to determine candidates involved in tumorigenicity rather than EMT phenotype, we

focused on proteins higher secreted by D492HER2 compared to both D492 and D492M. We used RT-qPCR and transcriptomic data to verify secretome candidates. After correction of the data for significance (0.05 significance level) and at least 2-fold difference in secretion, we received a list of a total of 77 proteins more highly secreted by D492HER2 compared to D492 and D492M (Fig. 2A). GO term analysis showed 6.7-fold enrichment for GO term group “regulation of angiogenesis” (GO:0045765) among D492HER2-secreted candidates (Fig. 2B), consisting of 7 gene members (Fig. 2C). We then compared secretion levels of these 7 candidates in our secretome data set and identified extracellular matrix protein 1 (ECM1) and chitinase-3-like 1 (CHI3L1) as the two proteins with the most prominent secretion profile (Fig. 2D). Interestingly, secretion levels of commonly recognized angiogenesis inducers such as VEGFa, FGF2 or PDGF were not significantly elevated in our cell lines, suggesting a different mechanism behind the observed pro-angiogenic effect of D492HER2 secretome (Fig. 2D). CHI3L1, also known as YKL-40, is a secreted glycoprotein, which is associated with a number of biological functions and also plays a role in chronic inflammation diseases and cancer [45-47]. Recently, it has been linked to idiopathic pulmonary fibrosis (48). Previous studies provide evidence for a role of YKL-40 in tumor angiogenesis by mediating VEGF signaling (49, 50). ECM1 is a secreted glycoprotein, which was first identified in the mouse osteogenic stromal cell line MN7 (51). It was initially described as modulator of proliferation and differentiation of epidermal keratinocytes and basement membrane reconstitution in the skin (52). However, it has also been linked to angiogenesis and malignant transformation (37-39, 42, 52-54). Interestingly, analysis to determine correlation to different gene modules using GOBO Gene set analysis database (University of Lund, Sweden) revealed a significant spearman correlation of ECM1 to the gene module “stroma” (Fig. 2E). Kaplan-Maier survival analysis revealed for both CHI3L1 and ECM1 a significant correlation of gene expression with decreased survival (suppl. Fig. S4). However, whereas in case of CHI3L1 this correlation is not specifically associated with a certain cancer subtype, ECM1 expression is significantly

correlated with decreased distant metastasis-free survival (DMSF) when expressed in HER2+ and ER- breast tumors (Fig. 2F and G, suppl. Fig. S3 and S4) [48]. These data put together led our focus on ECM1 as the main candidate for further investigation in the context of stromal interaction.

ECM1 enhances endothelial network and induces endothelial feedback

To verify that ECM1 is involved in the inducing effects of D492HER2 on endothelial network formation and positive feedback, we investigated whether recombinant ECM1 is capable of inducing network formation and feedback as well. We treated ECs with 15, 30, 60 and 120 ng/ml of rECM1 and quantified network formation as described previously. Indeed, rECM1 had significantly increased the endothelial network formed after 4 h and 24 h as quantified by numbers of master junctions, meshes, master segments and total master segment length (Fig. 3A and B). Hereby, the strongest effect was seen for treatment with 30 and 60 ng/ml rECM1 (Fig. 3B). This indicates that the system may already be saturated at these concentrations rather than rECM1 having a dose-dependent effect. To look at the endothelial feedback, we induced ECs with 60 ng/ml rECM1 and treated D492HER2 with CM of ECM1-induced ECs (Fig. 3C). CM of ECM1-induced ECs significantly increased D492HER2 migration and invasion (Fig. 3D), confirming that ECM1 does play a role in inducing the endothelial feedback induced by D492HER2.

To verify the activity of ECM1, we induced stable overexpression of ECM1 in D492 and D492M. CM from D492 and D492M stably overexpressing ECM1 showed pro-angiogenic properties (Fig. 4A and B). Furthermore, D492 and D492M overexpressing ECM1 show increased migration towards ECs, similar as observed for D492HER2 (suppl. Fig. S6). Next, we generated transient KD of ECM1 in D492HER2 using siRNA (suppl. Fig S5) and stable KD using CRISPRi. Both transient and stable KD were successful (over 90% KD), as verified on gene as well as protein level (suppl. Fig. S5 and 6). In accordance with the observed effects of rECM1 and ECM1 overexpression, treatment with CM from D492HER2-kdECM1 resulted in significantly lower endothelial network formation compared to control D492HER2 (Fig. 4A+B).

Similar results were obtained with CM from D492HER2 with transient ECM1 KD (suppl. Fig. S5). Analysis of the endothelial feedback showed that treatment of ECs with CM from D492HER2-kdECM1 did not induce an endothelial response to D492HER2 increasing cell migration and invasion (Fig. 4C and D). Also, the observed increased migration of D492HER2 towards ECs (Fig. 4C) could be depleted upon KD of ECM1, supporting the role of ECM1 in mediating the endothelial feedback and promoting migration towards the endothelium (Fig. 4E and F). These data suggest ECM1 as a specific mediator of endothelial response promoting cancer progression.

Triple-negative MDA-MB-231 cells also show high ECM1 expression and are capable of increasing endothelial network formation and inducing endothelial feedback

When analyzing the correlation of ECM1 and prognosis, we noted that high expression of ECM1 was not only correlated to worse survival in HER2+ breast cancer patients but also in triple-negative (TN) and generally estrogen receptor-negative (ER-) tumor patients (suppl. Fig. S4 and S8B). In addition, correlation analysis using the Metabric discovery data set showed a significant positive correlation between ECM1 expression and CD31 as established endothelial marker in ER- breast cancer (suppl. Fig S8E). Therefore, we decided to include MDA-MB-231 as triple-negative and MCF-7 as ER+ cell line in our study. Interestingly, CM from MDA-MB-231 but not MCF-7 also increased endothelial network formation after 4 h, 24 h and 48 h (suppl. Figs. S8C and D, S9). Similar to D492HER2, MDA-MB-231 expresses high levels of ECM1 in contrast to MCF-7 (suppl. Fig. S8A). Treating ECs with rECM1 also induced an endothelial feedback promoting MDA-MB-231 migration, as seen for ECM1-expressing D492HER2 (suppl. Fig. S8F and G). Upon transient ECM1 knockdown in MDA-MB-231 (RT-qPCR confirmation of ECM1 KD see suppl. Fig. S8H), its ability to increase endothelial network formation was significantly decreased (suppl. Fig. S8I). This suggests that ECM1 might play a role in cancer progression through endothelial crosstalk in a broader range of breast cancer subtypes than just HER2+.

ECM1 upregulates endothelial NOTCH1 and NOTCH3

To investigate whether treatment with D492HER2-CM upregulates commonly known angiogenesis modulators in ECs, we examined gene expression levels of endothelial VEGFa, VEGFR2 and PDGFb. However, none of these markers showed increased expression upon treatment with D492HER2-CM (suppl. Fig. S7A).

In order to determine transcriptional changes occurring in ECs specifically in response to cancer-secreted ECM1, we performed RNA microarray analysis of ECs treated with CM from D492HER2 and D492HER2 with ECM1 knockdown. After p-value correction and setting the fold change cut-off to 2-fold, analysis revealed 18 genes upregulated in ECs treated with D492HER2-CM compared to ECs treated with CM from D492HER2-kdECM1 (suppl. Fig. S7). However, the observed changes in genes expression were rather mild. One of the mildly higher expressed genes in ECs treated with D492HER2-CM was fatty acid binding protein 4 or FABP4. FABP4 itself could not be confirmed as upregulated compared to untreated ECs, however it led our attention to the NOTCH pathway since its expression is regulated by NOTCH1 [49-51]. When investigating the expression of the NOTCH receptors 1-4 in ECs, we observed increased NOTCH1 and NOTCH3 gene and protein expression in ECs treated with D492HER2-CM and rECM1 but not with CM from D492HER2-kdECM1 (Fig. 5A).

Blocking endothelial NOTCH signaling interrupts the increase in network formation and feedback induction

Next, we wanted to investigate whether endothelial NOTCH signaling was implicated in the observed increase in endothelial network formation and the induction of an endothelial feedback promoting cancer cell migration and invasion. By blocking endothelial NOTCH using gamma-secretase inhibitor DAPT, interruption in both the increase in network formation and the feedback induction was observed. While treatment with rECM1 resulted in significantly increased numbers of master junctions, master segments, total master segment length and number of meshes, this effect was no longer

visible upon addition of DAPT (Fig. 5B and C). Furthermore, CM of rECM1-induced ECs stimulated an increase in cancer cell migration and invasion whereas the addition of DAPT inhibited the induction of this feedback (Fig. 5D and E). Blocking endothelial NOTCH signaling therefore appears to interrupt both cancer-increased network formation as well as feedback induction.

Discussion

In this study, we have demonstrated that the HER2-overexpressing breast cancer cell line, D492HER2, stimulates endothelial network formation *in vitro* and is capable of inducing an endothelial feedback promoting cancer cell migration towards the endothelium and invasion. We have further identified ECM1 as a secreted factor in D492HER2 that plays a role in mediating both the pro-angiogenic effect of D492HER2 and the feedback induction. Recombinant ECM1 increases endothelial network formation and induces the feedback while knockdown of ECM1 interrupts both. Furthermore, D492HER2 no longer show an increased migrative phenotype towards ECs upon ECM1 knockdown.

ECM1 is a secreted glycoprotein and was first identified in the mouse osteogenic stromal cell line MN7 [52]. It was initially described as modulator of proliferation and differentiation of epidermal keratinocytes and basement membrane reconstitution in the skin [53]. However, it has also been linked to angiogenesis and malignant transformation [37-39, 42, 43, 48, 53, 54]. Han et al. (2001) demonstrated that recombinant ECM1 stimulated proliferation and blood vessel formation in the chorioallantoic membrane of chicken embryos [37] and Wang et al. (2003) found it to be expressed particularly in highly malignant breast epithelial tumors [39]. Recently, Wu et al. (2018) linked ECM1 to breast cancer progression by suggesting a role of ECM1 in facilitating metastasis through increased invasion and adhesion capacity of ECM1-expressing cancer cells [55]. These data are in line with our findings in the current study. Ferraro et al. (2019) recently showed that ECs are capable

of increasing migration and invasion of SKBR3 breast cancer cells [56]. However, a direct involvement of cancer-secreted ECM1 in cancer progression through induction of an endothelial feedback supporting cancer migration and invasion has not been reported yet. Here, we show that the increased migration is directed towards the endothelium, suggesting that ECM1 may play a mediating role in inducing ECs to promote cancer cell migration from the primary tumor towards the vasculature and therefore support metastasis formation and tumor progression.

Survival analysis shows that expression of ECM1 in HER2+ breast tumors is associated with significantly reduced distant-metastasis-free-survival (DMFS). Therefore, targeting ECM1 in tumors overexpressing HER2 could lead to better patient prognosis. This is supported by a study of Lee et al. (2014), which showed that ECM1 regulates resistance to trastuzumab, a recombinant antibody targeting HER2 and the most common drug used in treatment of HER2+ breast cancer [48]. Interestingly, the triple-negative (TN) breast cancer cell line MDA-MB-231 also expresses high levels of ECM1 and is capable of inducing endothelial network formation in the present study and previous studies [22, 23, 55]. Knockdown of ECM1 in MDA-MB-231 inhibits these pro-angiogenic effects, supporting the mediating role of ECM1 in increasing the endothelial network. We also report that rECM1 is capable of inducing a positive endothelial feedback on MDA-MB-231 migration. Since expression of ECM1 also correlates with worse outcome in TN and generally ER- breast cancer, its molecular involvement in breast cancer progression might be more general rather than only limited to HER2+ cancer. Silencing of ECM1 in MDA-MB-231 led to a decrease in cancer cell migration and invasion capacity, linking its expression to increased tumor progression aggressiveness [55, 57]. Therefore, ECM1 might represent a possible therapeutic target for a broader range of breast cancer patients than just HER2+ individuals. However, the specific relationship between HER2 overexpression and ECM1 still needs to be elucidated. ECM1 expression is upregulated in several HER2+ breast cancer cell lines including ZR7530, SUM44PE and HCC202. However, other HER2+ cell lines such as SKBR3 or

BT474 show no ECM1 upregulation. However, among the breast cancer cell lines with strong ECM1 upregulation according to the GOBO database there are numerous ER- cell lines (e.g. HCC1143, HBL100, SUM1315MO2, MDAMB435, MDAMB231). Lee et al. report that high ECM1 expression in HER2+ breast cancer is correlated with poor prognosis and trastuzumab resistance (53). They suggest that ECM1 may interact with EGFR family receptors that interact with HER2, attenuating therapeutic action by trastuzumab. However, the mechanisms of ECM1 expression regulation itself are not very well understood in HER2+ breast cancer. Smits et al. (1999) identified conserved potential binding sites for transcription factors of the Ap1, Ets and Sp1 family in the human ECM1 gene in MN7 cells (61). Ye et al. (2016) provide evidence that ECM1 is a target of miR-486-3p in cervical cancer. Overexpression of miR-486-3p thereby inhibited cell growth and metastasis by targeting ECM1 (62). However, we could not detect differential expression of miR-486-3p between D492, D492M and D492HER2, suggesting that ECM1 might be regulated through a different mechanism in our HER2+ breast cancer system. Generally, investigating the involvement of epigenetic regulation in modulating ECM1 expression and downstream signaling could be of great interest though as it could potentially give novel insights also in the context of cellular crosstalk.

In our model, ECM1 was identified as cancer-secreted protein with pro-angiogenic properties that is capable of inducing an endothelial feedback promoting cancer cell migration towards ECs and invasion (Fig. 6). However, the molecular mechanism through which ECM1 mediates this feedback of the vascular niche on cancer progression has not been described previously. Here, we identified an upregulation of NOTCH1 and NOTCH3 receptor expression in ECs upon treatment with D492HER2-CM and rECM1 but not CM from D492HER2 with ECM1 knockdown. However, the initial microarray candidate, FABP4, could not be confirmed in further experiments, indicating that the subsequent downstream signaling may not involve FABP4. This would coincide with the findings that in addition to NOTCH1, also VEGFa, bFGF and FOXO1 play potential roles in regulation of FABP4 expression

(63). So far, ECM1 has been associated with EGF signaling [48], ITGB4/FAK/SOX2/HIF1a [41] and WNT1/ß-catenin [42] pathways but a mediating role in NOTCH signaling has not been described. NOTCH signaling is very complex and plays a role in a large number of biological processes [58, 59]. Nevertheless, recent studies suggest NOTCH1 as a key player in inducing tumor angiogenesis and therefore promoting tumor progression in cutaneous melanoma and myeloma [28, 29]. Kalucka et al. have shown that NOTCH1 is involved in endothelial barrier function and angiogenesis by controlling fatty acid metabolism [51]. These data would support a possible involvement of endothelial NOTCH in mediating the increase in endothelial network and possibly the induction of the pro-cancerous feedback in breast cancer. Indeed, upon inhibition of endothelial NOTCH signaling, the enhancing effect of ECM1 on network formation and feedback was no longer observed, indicating the existence of a ECM1/NOTCH axis involved in mediating the crosstalk between cancer cells and endothelium in terms of promoting cancer progression (Fig. 6).

In conclusion, we have identified ECM1 as a cancer-secreted pro-angiogenic factor involved in inducing the endothelial niche to support cancer progression through increased cancer cell migration and invasion. Moreover, our data indicate a novel, mediating role of ECM1 in endothelial NOTCH signaling, which appears to be involved in mediating the induction of the cancer-promoting endothelial feedback (Fig. 6). Taken together, our findings might open up new possibilities for cancer treatment by understanding how an activated vascular niche provides positive feedback to the cancer and targeting this interaction between cancer cells and their microenvironment.

Acknowledgements

We thank the FingerPrints Proteomics Facility at the University of Dundee for performing the mass spectrometry and the Center for Systems Biology at the University of Iceland for the technical support during mass spectrometry data analysis. Further, we want to thank the HI-STEM laboratory and the

sequencing core facility at the German Cancer Research Center, DKFZ Heidelberg, Germany, for technical support and performing of the RNA microarray. Finally, we thank Prof. Dr. Haraldur Haraldsson, University of Iceland for providing primary human umbilical vascular endothelial cells. Human umbilical vascular endothelial cells were obtained from umbilical chords at the childbirth department, University Hospital Iceland (ethical application nr. 35/2013). This work was supported by Grants from Landspitali University Hospital Science Fund, University of Iceland Research Fund (Grant of Excellence: #152144051 Doctoral Grant: #185042051), and Icelandic Science and Technology Policy.

Disclosure/Conflict of interests

The authors declare that they have no conflict of interest. The funding body had no role in the design of the study and collection, analysis, and interpretation of data and in writing the manuscript.

Supplementary information is available at Laboratory Investigation's website.

References

1. Hassiotou F, Geddes D. Anatomy of the human mammary gland: Current status of knowledge. Clinical anatomy (New York, NY). 2013;26(1):29-48.

2. Sigurdsson V, Fridriksdottir AJ, Kjartansson J, Jonasson JG, Steinarsdottir M, Petersen OW, et al. Human breast microvascular endothelial cells retain phenotypic traits in long-term finite life span culture. In Vitro Cell Dev Biol Anim. 2006;42(10):332-40.

3. Ingthorsson S, Sigurdsson V, Fridriksdottir A, Jr., Jonasson JG, Kjartansson J, Magnusson MK, et al. Endothelial cells stimulate growth of normal and cancerous breast epithelial cells in 3D culture. BMC Res Notes. 2010;3:184.

4. Gudjonsson T, Ronnov-Jessen L, Villadsen R, Bissell MJ, Petersen OW. To create the correct microenvironment: three-dimensional heterotypic collagen assays for human breast epithelial morphogenesis and neoplasia. Methods. 2003;30(3):247-55.

5. Bergthorsson JT, Magnusson MK, Gudjonsson T. Endothelial-rich microenvironment supports growth and branching morphogenesis of prostate epithelial cells. Prostate. 2013;73(8):884-96.

6. Bissell MJ, Hall HG, Parry G. How Does the Extracellular Matrix Direct Gene Expression? Journal of theoretical Biology. 1982;99:31-68.

7. Ghajar CM, Peinado H, Mori H, Matei IR, Evason KJ, Brazier H, et al. The perivascular niche regulates breast tumour dormancy. Nat Cell Biol. 2013;15(7):807-17.

8. Erler JT, Weaver VM. Three-dimensional context regulation of metastasis. Clin Exp Metastasis. 2009;26(1):35-49.

9. Hoye AM, Erler JT. Structural ECM components in the premetastatic and metastatic niche. Am J Physiol Cell Physiol. 2016;310(11):C955-67.

10. Hanahan D, Coussens LM. Accessories to the crime: functions of cells recruited to the tumor microenvironment. Cancer Cell. 2012;21(3):309-22.

11. Oskarsson T, Batlle E, Massague J. Metastatic stem cells: sources, niches, and vital pathways. Cell stem cell. 2014;14(3):306-21.
12. Oskarsson T, Acharyya S, Zhang XH, Vanharanta S, Tavazoie SF, Morris PG, et al. Breast cancer cells produce tenascin C as a metastatic niche component to colonize the lungs. Nat Med. 2011;17(7):867-74.
13. Lowy CM, Oskarsson T. Tenascin C in metastasis: A view from the invasive front. Cell Adh Migr. 2015;9(1-2):112-24.
14. Insua-Rodríguez J, Pein M, Hongu T, Meier J, Descot A, Lowy CM, et al. Stress signaling in breast cancer cells induces matrix components that promote chemoresistant metastasis. EMBO Molecular Medicine. 2018.
15. Erler JT, Bennewith KL, Cox TR, Lang G, Bird D, Koong A, et al. Hypoxia-induced lysyl oxidase is a critical mediator of bone marrow cell recruitment to form the premetastatic niche. Cancer Cell. 2009;15(1):35-44.
16. Pollard JW. Macrophages define the invasive microenvironment in breast cancer. J Leukoc Biol. 2008;84(3):623-30.
17. Komohara Y, Jinushi M, Takeya M. Clinical significance of macrophage heterogeneity in human malignant tumors. Cancer Sci. 2014;105(1):1-8.
18. Komohara Y, Takeya M. CAFs and TAMs: maestros of the tumour microenvironment. J Pathol. 2017;241(3):313-5.
19. Shan T, Chen S, Chen X, Lin WR, Li W, Ma J, et al. Cancer-associated fibroblasts enhance pancreatic cancer cell invasion by remodeling the metabolic conversion mechanism. Oncology Reports. 2017;37:1971-9.
20. Zhang Z, Li X, Sun W, Yue S, Yang J, Li J, et al. Loss of exosomal miR-320a from cancer-associated fibroblasts contributes to HCC proliferation and metastasis. Cancer Lett. 2017;397:33-42.
21. Ghajar CM. Metastasis prevention by targeting the dormant niche. Nat Rev Cancer. 2015;15(4):238-47.
22. Lee E, Fertig EJ, Jin K, Sukumar S, Pandey NB, Popel AS. Breast cancer cells condition lymphatic endothelial cells within pre-metastatic niches to promote metastasis. Nat Commun. 2014;5:4715.

23. Lee E, Pandey NB, Popel AS. Crosstalk between cancer cells and blood endothelial and lymphatic endothelial cells in tumour and organ microenvironment. Expert Rev Mol Med. 2015;17:e3.
24. Lee E, Pandey NB, Popel AS. Lymphatic endothelial cells support tumor growth in breast cancer. Sci Rep. 2014;4:5853.
25. Franses JW, Baker AB, Chitalia VC, Edelman ER. Stromal endothelial cells directly influence cancer progression. Sci Transl Med. 2011;3(66):66ra5.
26. Franses JW, Drosu NC, Gibson WJ, Chitalia VC, Edelman ER. Dysfunctional endothelial cells directly stimulate cancer inflammation and metastasis. Int J Cancer. 2013;133(6):1334-44.
27. Ucuzian AA, Gassman AA, East AT, Greisler HP. Molecular mediators of angiogenesis. J Burn Care Res. 2010;31(1):158-75.
28. Murtas D, Piras F, Minerba L, Maxia C, Ferreli C, Demurtas P, et al. Activated Notch1 expression is associated with angiogenesis in cutaneous melanoma. Clinical and experimental medicine. 2015;15(3):351-60.
29. Guo D, Li C, Teng Q, Sun Z, Li Y, Zhang C. Notch1 overexpression promotes cell growth and tumor angiogenesis in myeloma. Neoplasma. 2013;60(1):33-40.
30. Laughner E, Taghavi P, Chiles K, Mahon PC, Semenza GL. HER2 (neu) signaling increases the rate of hypoxia-inducible factor 1alpha (HIF-1alpha) synthesis: novel mechanism for HIF-1-mediated vascular endothelial growth factor expression. Mol Cell Biol. 2001;21(12):3995-4004.
31. Hoshino A, Costa-Silva B, Shen TL, Rodrigues G, Hashimoto A, Tesic Mark M, et al. Tumour exosome integrins determine organotropic metastasis. Nature. 2015;527(7578):329-35.
32. Sigurdsson V, Hilmarsdottir B, Sigmundsdottir H, Fridriksdottir AJ, Ringner M, Villadsen R, et al. Endothelial induced EMT in breast epithelial cells with stem cell properties. PLoS One. 2011;6(9):e23833.
33. Gudjonsson T, Villadsen R, Nielsen HL, Ronnov-Jessen L, Bissell MJ, Petersen OW. Isolation, immortalization, and characterization of a human

787 breast epithelial cell line with stem cell properties. Genes Dev.
788 2002;16(6):693-706.
789 34. Villadsen R, Fridriksdottir AJ, Ronnov-Jessen L, Gudjonsson T, Rank
790 F, LaBarge MA, et al. Evidence for a stem cell hierarchy in the adult human
791 breast. J Cell Biol. 2007;177(1):87-101.
792 35. Briem E, Ingthorsson S, Traustadottir GA, Hilmarsdottir B,
793 Gudjonsson T. Application of the D492 Cell Lines to Explore Breast
794 Morphogenesis, EMT and Cancer Progression in 3D Culture. Journal of
795 mammary gland biology and neoplasia. 2019.
796 36. Ingthorsson S, Andersen K, Hilmarsdottir B, Maelandsmo GM,
797 Magnusson MK, Gudjonsson T. HER2 induced EMT and tumorigenicity in
798 breast epithelial progenitor cells is inhibited by coexpression of EGFR.
799 Oncogene. 2015.
800 37. Han Z, Ni J, Smits P, Underhill CB, Xie B, Chen Y, et al. Extracellular
801 matrix protein 1 (ECM1) has angiogenic properties and is expressed by
802 breast tumor cells. The FASEB Journal. 2001;15:988-94.
803 38. Sercu S, Zhang L, Merregaert J. The extracellular matrix protein 1: its
804 molecular interaction and implication in tumor progression. Cancer Invest.
805 2008;26(4):375-84.
806 39. Wang L, Yu J, Ni J, Xu X-M, Wang J, Ning H, et al. Extracellular
807 matrix protein 1 (ECM1) is over-expressed in malignant epithelial tumors.
808 Cancer Letters. 2003;200(1):57-67.
809 40. Chen H, Jia W, Li J. ECM1 promotes migration and invasion of
810 hepatocellular carcinoma by inducing epithelial-mesenchymal transition.
811 World J Surg Oncol. 2016;14(1):195.
812 41. Gan L, Meng J, Xu M, Liu M, Qi Y, Tan C, et al. Extracellular matrix
813 protein 1 promotes cell metastasis and glucose metabolism by inducing
814 integrin beta4/FAK/SOX2/HIF-1alpha signaling pathway in gastric cancer.
815 Oncogene. 2017.
816 42. Lee KM, Nam K, Oh S, Lim J, Kim RK, Shim D, et al. ECM1
817 regulates tumor metastasis and CSC-like property through stabilization of
818 beta-catenin. Oncogene. 2015;34(50):6055-65.

819 43. Wang Z, Zhou Q, Li A, Huang W, Cai Z, Chen W. Extracellular matrix
820 protein 1 (ECM1) is associated with carcinogenesis potential of human
821 bladder cancer. OncoTargets and therapy. 2019;12:1423-32.
822 44. Bustin SA, Benes V, Garson JA, Hellemans J, Huggett J, Kubista M,
823 et al. The MIQE guidelines: minimum information for publication of
824 quantitative real-time PCR experiments. Clin Chem. 2009;55(4):611-22.
825 45. Rosenblat JD, Brietzke E, Mansur RB, Maruschak NA, Lee Y,
826 McIntyre RS. Inflammation as a neurobiological substrate of cognitive
827 impairment in bipolar disorder: Evidence, pathophysiology and treatment
828 implications. Journal of affective disorders. 2015;188:149-59.
829 46. Kastrup J. Can YKL-40 be a new inflammatory biomarker in
830 cardiovascular disease? Immunobiology. 2012;217(5):483-91.
831 47. Vignon E. Is glycoprotein YKL40 a new marker for joint disorders?
832 Joint, bone, spine : revue du rhumatisme. 2001;68(6):454-6.
833 48. Zhou Y, Peng H, Sun H, Peng X, Tang C, Gan Y, et al. Chitinase 3-
834 like 1 suppresses injury and promotes fibroproliferative responses in
835 Mammalian lung fibrosis. Sci Transl Med. 2014;6(240):240ra76.
836 49. Francescone RA, Scully S, Faibish M, Taylor SL, Oh D, Moral L, et
837 al. Role of YKL-40 in the angiogenesis, radioresistance, and progression of
838 glioblastoma. The Journal of biological chemistry. 2011;286(17):15332-43.
839 50. Shao R. YKL-40 acts as an angiogenic factor to promote tumor
840 angiogenesis. Frontiers in physiology. 2013;4:122.
841 51. Mathieu E, Meheus L, Raymackers J, Merregaert J. Characterization
842 of the Osteogenic Stromal Cell Line MN7: Identification of Secreted MN7
843 Proteins Using Two-Dimensional I'olyacrylamide Gel Electrophoresis,
844 Western Blotting, and Microsequencing. JOURNAL OF BONE AND
845 MINERAL RESEARCH. 1994;9(6):903-13.
846 52. Oyama N, Merregaert J. The Extracellular Matrix Protein 1 (ECM1) in
847 Molecular-Based Skin Biology. 2017:91-110.
848 53. Lee KM, Nam K, Oh S, Lim J, Kim YP, Lee JW, et al. Extracellular
849 matrix protein 1 regulates cell proliferation and trastuzumab resistance

through activation of epidermal growth factor signaling. Breast Cancer Res. 2014;16(6):479.
54. Sercu S, Zhang M, Oyama N, Hansen U, Ghalbzouri AE, Jun G, et al. Interaction of extracellular matrix protein 1 with extracellular matrix components: ECM1 is a basement membrane protein of the skin. J Invest Dermatol. 2008;128(6):1397-408.
55. Harjes U, Bridges E, Gharpure KM, Roxanis I, Sheldon H, Miranda F, et al. Antiangiogenic and tumour inhibitory effects of downregulating tumour endothelial FABP4. Oncogene. 2017;36(7):912-21.
56. Bruning U, Morales-Rodriguez F, Kalucka J, Goveia J, Taverna F, Queiroz KCS, et al. Impairment of Angiogenesis by Fatty Acid Synthase Inhibition Involves mTOR Malonylation. Cell metabolism. 2018;28(6):866-80.e15.
57. Kalucka J, Bierhansl L, Conchinha NV, Missiaen R, Elia I, Bruning U, et al. Quiescent Endothelial Cells Upregulate Fatty Acid beta-Oxidation for Vasculoprotection via Redox Homeostasis. Cell metabolism. 2018;28(6):881-94.e13.
58. Wu Q, Chen D, Luo Q, Yang Q, Zhao C, Zhang D, et al. Extracellular matrix protein 1 recruits moesin to facilitate invadopodia formation and breast cancer metastasis. Cancer Lett. 2018;437:44-55.
59. Ferraro DA, Patella F, Zanivan S, Donato C, Aceto N, Giannotta M, et al. Endothelial cell-derived nidogen-1 inhibits migration of SK-BR-3 breast cancer cells. BMC cancer. 2019;19(1):312.
60. Gomez-Contreras P, Ramiro-Diaz JM, Sierra A, Stipp C, Domann FE, Weigel RJ, et al. Extracellular matrix 1 (ECM1) regulates the actin cytoskeletal architecture of aggressive breast cancer cells in part via S100A4 and Rho-family GTPases. Clin Exp Metastasis. 2017;34(1):37-49.
61. Smits P, Bhalerao J, Merregaert J. Molecular cloning and characterization of the mouse Ecm1 gene and its 5' regulatory sequences. Gene. 1999;226(2):253-61.
62. Ye H, Yu X, Xia J, Tang X, Tang L, Chen F. MiR-486-3p targeting ECM1 represses cell proliferation and metastasis in cervical cancer.

Biomedicine & pharmacotherapy = Biomedecine & pharmacotherapie. 2016;80:109-14.

63. Furuhashi M, Saitoh S, Shimamoto K, Miura T. Fatty Acid-Binding Protein 4 (FABP4): Pathophysiological Insights and Potent Clinical Biomarker of Metabolic and Cardiovascular Diseases. Clinical Medicine Insights Cardiology. 2014;8(Suppl 3):23-33.

64. Traustadottir GA, Jensen CH, Thomassen M, Beck HC, Mortensen SB, Laborda J, et al. Evidence of non-canonical NOTCH signaling: Delta-like 1 homolog (DLK1) directly interacts with the NOTCH1 receptor in mammals. Cellular signalling. 2016;28(4):246-54.

65. Artavanis-Tsakonas S, Rand MD, Lake RJ. Notch Signaling: Cell Fate Control and Signal Integration in Development. Science. 1999;284(5415):770-6

Figure Legends

Fig. 1: CM from D492HER2 enhances endothelial network and induces endothelial feedback increasing D492HER2 migration/invasion. A) Enhanced endothelial network formation in D492HER2-CM after 4 h. Top: Representative phase-contrast images of HUVEC endothelial network after 4 h on top of rBM in control (unconditioned) medium and conditioned medium from D492, D492M and D492HER2. Each condition included 4-6 wells as replicates and 1-2 images were taken per well at 10x magnification (scale bar = 100 µm). Bottom: Corresponding angiogenesis images (ImageJ, angiogenesis analyzer plugin) showing branches, junctions, master junctions, master segments and meshes. B) Endothelial network formation - Quantification. Quantification of master junctions, master segments total master segment length and meshes for each image using angiogenesis analyzer plugin (average and standard deviation per condition). Statistical analysis performed in R, one-way ANOVA, *** $p < 0.001$, ** $p < 0.01$, * $p < 0.05$, ▪ < 0.1. C) Endothelial feedback - schematic overview. Schematic work-flow of conditioning of ECs (see methods). D) D492HER2-induced ECs promote D492HER2 migration & invasion. Transwell-migration & invasion assays of D492HER2 treated with unconditioned medium, unconditioned HUVEC-CM, D492-conditioned HUVEC-CM and D492HER2-conditioned HUVEC-CM. Number of migratory/invasive cells is shown for the different treatments (Student´s t-Test, *** $p < 0.001$, ** $p < 0.01$, * $p < 0.05$, ▪ < 0.1). E) Migration towards ECs - schematic overview. Schematic setup of transwell-migration assay of D492, D492M and D492HER2 towards HUVECs seeded below the transwell filter. Migration towards HUVECs (in H14 + EGM1) was compared with migration towards 10% FBS in H14 + EGM5 (pos. ctrl) and plain H14 + EGM5 (neg. ctrl). F) Increased D492HER2 migration towards ECs. Migration of D492, D492M and D492HER2 towards HUVECs. Number

of migratory cells is shown for the different treatments (Student´s t-Test, *** p < 0.001, ** p < 0.01, * p < 0.05, ▪ < 0.1).

Fig. 2: Identification of ECM1 as pro-angiogenic candidate in D492HER2. A) 77 candidates. Heat map of 77 proteins higher secreted by D492HER2 compared to both D492 and D492M (label-free mass spectrometry secretome data, p < 0.05, threshold fold change ≥ 2-fold). B) Enrichment of angiogenesis-regulating genes in D492HER2 secretome (GO terms). Enrichment of „Regulation of Angiogenesis“ GO term group GO:0045765 among D492HER2 secretome. Statistical overrepresentation test (Panther DB) was performed using “GO biological process complete” as annotation data set with Bonferroni correction for multiple testing. C) GO:0045765 gene members. Proteins part of GO term group GO:0045765 (Regulation of Angiogenesis). D) Highest secretion levels of ECM1 & CHI3L1. Secretion levels (label-free quantification LFQ) of the 7 candidates from C (left of dotted line) compared to secretion levels of commonly known angiogenesis inducers (right of dotted line). E) Correlation of ECM1 to 8 gene modules. Spearman correlation of ECM1 expression to different gene modules in breast tumor samples (GOBO Genset analysis, Lund University). F) DMFS in ECM1+/HER2+ patients. Kaplan-Meier plot of ECM1 in HER2+ tumors showing correlation of high expression with decreased distant metastasis-free survival (DMFS). G) ECM1 expression in HER2+ tumors. ECM1 expression in representative HER2+ tumor samples showing low and high expression. Cells were counterstained with hemotoxilyn. scale bar = 100 µm.

Fig. 3: Recombinant ECM1 enhances endothelial network and induces endothelial feedback increasing D492HER2 migration/invasion. A) Increased endothelial tube formation with recombinant ECM1. Top: HUVEC endothelial network on top of matrigel in different concentrations of recombinant ECM1 (after 24 h). 4-6 wells as replicates per condition and 1-2 images taken per well at 10x magnification (scale bar = 100 µm). Bottom: Corresponding angiogenesis images (ImageJ angiogenesis analyzer). B) Endothelial network formation - quantification. Quantification of master

junctions, master segments, total master segment length and meshes for each image using angiogenesis analyzer plugin. One-way ANOVA, *** $p < 0.001$, ** $p < 0.01$, * $p < 0.05$, ▪ < 0.1. C) Endothelial feedback by rECM1 - schematic overview. Schematic work-flow of conditioning of ECs using 60 ng/ml rECM1. D) rECM1-induced ECs promote D492HER2 migration & invasion. Transwell migration & invasion assays of D492HER2 treated with unconditioned medium, unconditioned HUVEC-CM and 60ng rECM1 treated HUVEC-CM. Number of migratory/invasive cells shown for different treatments (Student´s t-Test, *** $p < 0.001$, ** $p < 0.01$, * $p < 0.05$, ▪ < 0.1).

Fig. 4: ECM1 knockdown inhibits pro-angiogenic effect of D492HER2-CM and endothelial feedback on D492HER2 migration/invasion. A) Reduced pro-angiogenic properties of D492HER2-CM upon ECM1 knockdown. Top: HUVEC endothelial network on top of matrigel in CM from D492 and D492M with ECM1 overexpression and D492HER2 with ECM1 knockdown compared to empty vector control (after 4 h). 4-6 wells as replicates per condition and 1-2 images taken per well at 10x magnification (scale bar = 100 µm). Bottom: Corresponding angiogenesis images (ImageJ angiogenesis analyzer). B) Endothelial network formation - quantification. Quantification of master junctions, master segments, total master segment length and meshes for each image using angiogenesis analyzer plugin. One-way ANOVA, *** $p < 0.001$, ** $p < 0.01$, * $p < 0.05$, ▪ < 0.1. C) Endothelial feedback reduction - schematic overview. Schematic work flow of conditioning of ECs using CM from D492HER2-kdECM1. D) No endothelial feedback on D492HER2 migration upon ECM1 knockdown. Transwell migration and invasion assays of D492HER2 treated with unconditioned medium, unconditioned HUVEC-CM, D492HER2-conditioned HUVEC-CM and D492HER2-kdECM1 conditioned HUVEC-CM. Student´s t-Test, *** $p < 0.001$, ** $p < 0.01$, * $p < 0.05$, ▪ < 0.1. E) Migration towards ECs - schematic overview. Schematic setup of transwell-migration assay of D492HER2 empty ctrl. and D492HER2-kdECM1 towards HUVECs compared to pos. ctrl (10% FBS) and neg. ctrl (plain H14 + EGM5). F) No increased migration towards ECs upon ECM1 knockdown. Migration of D492HER2 empty ctrl and

D492HER2-kdECM1 towards HUVECs. Number of migratory cells for different treatments (Student´s t-Test, *** $p < 0.001$, ** $p < 0.01$, * $p < 0.05$, ▪ < 0.1).

Fig. 5: Inhibition of endothelial NOTCH signaling prevents increased tube formation and feedback induction. A) ECM1 increases endothelial NOTCH1 & NOTCH3. Increased NOTCH1 and NOTCH3 expression in HUVECs treated with D492HER2-CM and rECM1 but not D492HER2-kdECM1-CM on gene expression level (left) & protein expression level (IF staining, scale bar = 50 µm). Kruskal-Wallis Test, *** $p < 0.001$, ** $p < 0.01$, * $p < 0.05$ ▪ < 0.1. B) NOTCH inhibition blocks ECM1-induced increase of endothelial network formation. Top: HUVEC endothelial network in H14 (ctrl), 60 ng/ml rECM1, 60 ng/ml rECM1 + DMSO & 60 ng/ml rECM1 + DAPT (20 µM) after 4 h. 4-6 wells as replicates per condition and 1-2 images taken per well at 10x magnification (scale bar = 100 µm). Bottom: Corresponding angiogenesis images (ImageJ angiogenesis analyzer). C) Endothelial network formation - quantification. Quantification of master junctions, master segments, total master segment length and meshes for each image using angiogenesis analyzer plugin. One-way ANOVA, *** $p < 0.001$, ** $p < 0.01$, * $p < 0.05$ ▪ < 0.1. D) Endothelial feedback reduction - schematic overview. Schematic work-flow of treating ECs using 60 ng/ml rECM1 and blocking NOTCH signaling using DAPT (20 µM). E) NOTCH inhibition blocks rECM1-induced endothelial feedback on migration & invasion. Transwell migration & invasion assays of D492HER2 treated with unconditioned medium, unconditioned HUVEC-CM and 60 ng rECM1 treated HUVEC-CM, 60 ng rECM1 + DMSO treated HUVEC-CM and 60 ng rECM1 + DAPT treated HUVEC-CM (NOTCH inhibition). Number of migratory/invasive cells for different treatments (Student´s t-Test, *** $p < 0.001$, ** $p < 0.01$, * $p < 0.05$ ▪ < 0.1).

Fig. 6: Schematic summary of ECM1 inducing an endothelial feedback promoting cancer cell migration/invasion. ECM1 secreted by HER2+, TN or ER- breast cancer cells increases endothelial network formation and

induces endothelial feedback promoting cancer cell migration & invasion through upregulation of NOTCH1 & NOTCH3 expression. Knockdown of ECM1 in cancer cells and NOTCH inhibition in ECs inhibits the network formation increase and the feedback induction.

Supplementary material

Fig. S1: CM of D492HER2 enhanced endothelial network - 24 h and 48 h. A) Enhanced endothelial network formation in D492HER2-CM after 24 h. Top: Phase-contrast images of HUVEC endothelial network after 24 h on top of matrigel in H14, D492-CM, D492M-CM and D492HER2-CM, 10x magnification (scale bar = 100 µm). Bottom: Corresponding angiogenesis images (ImageJ, angiogenesis analyzer) showing branches, junctions, master junctions, master segments and meshes. B) Endothelial network formation 24 h - Quantification. Quantification of master junctions, master segments, total master segment length and meshes (angiogenesis analyzer). Statistical analysis performed in R, one-way ANOVA, *** $p < 0.001$, ** $p < 0.01$, * $p < 0.05$, · < 0.1 . C) Enhanced endothelial network formation in D492HER2-CM after 48 h. Top: HUVEC endothelial network after 48 h (phase contrast). Bottom: Angiogenesis images. D) Endothelial network formation 24 h - Quantification. Quantification of master junctions, master segments total master segment length and meshes. One-way ANOVA, *** $p < 0.001$, ** $p < 0.01$, * $p < 0.05$, · < 0.1 .

Fig. S2: D492HER2 has increased affinity to ECs in 2D and 3D. A) Increased endothelial cell contact of D492HER2 in 3D. 3D co-culture of D492 and D492HER2 with HUVEC on top of matrigel. Red arrows mark cells attached to branching points fo the endothelial network. Scale bar = 100 µm. B) Increased endothelial cell contact of D492HER2 in 2D. 2D co-culture of

D492, D492M and D492HER2 with HUVEC (brown: DAB staining for CD31) for 24 h. Red arrows mark cells attached to brown endothelial cells. Sclae bar = 50 µm. C) Quantification of B. Mean number of cells attached to HUVEC. Statistical analyses for C) performed in R, one-way ANOVAs, *** $p < 0.001$, ** $p < 0.01$, * $p < 0.05$, · < 0.1 .

Fig. S3: Decreased DMFS when ECM1 but not CHI3L1 is expressed in HER2+ tumors (breastmark). Analysis of distant metastasis-free survival (DMFS) for ECM1 and CHI3L1 expression in different breast cancer subtypes (database breastmark).

Fig. S4: Differential survival pattern for ECM1 and CHI3L1 in HER2+ and ER- tumors (KM plotter). Comparison of distant metastasis-free survival (DMFS) and relapse-free survival (RFS) for ECM1 and CHI3L1 between ER-, triple-negative (TN), HER2+ and HER2+ ER- PR- samples.

Fig. S5: Transient knockdown of ECM1 inhibits pro-angiogenic effect of D492HER2-CM. A) ECM1 knockdown. Confirmation of transient ECM1 knockdown at gene expression level (Relative Gene Expression) and protein expression level (IF staining), scale bar = 50 µm. siRNA used at a concentration of 10 nM (Student´s t-Test *** $p < 0.001$, ** $p < 0.01$, * $p < 0.05$, · < 0.1). B) Reduced endothelial network formation in D492HER2siECM1-CM. Top: HUVEC endothelial network after 4 h in H14, D492-CM, ctrl D492HER2-CM, siRNA neg. ctrl D492HER2-CM and siECM1 D492HER2-CM (phase contrast), 10x magnification (scale bar = 100 µm). Bottom: Angiogenesis images showing branches, junctions, master junctions, master segments and meshes. C) Endothelial network formation - Quantification. Quantification of master junctions, master segments total master segment length and meshes. One-way ANOVA, *** $p < 0.001$, ** $p < 0.01$, * $p < 0.05$, · < 0.1 .

Fig. S6: Increased migration of D492 and D492M overexpressing ECM1 towards ECs. A) Confirmation of stable ECM1 overexpression and knockdown (gene and protein level). Confirmation in stable knockdown cell lines (D492+ECM1, D492M+ECM1, D492HER2-kdECM1). Left: gene expression level (relative expression), right: protein expression (western blot) and quantification. B) Increased migration of ECM1-overexpressing D492 and D492M towards ECs. Transwell-migration assay of D492 empty vector ctrl and D492HER2 with ECM1 overexpression as well as D492M empty and D492M overexpressing ECM1 towards HUVECs (80% confluent) seeded below the transwell filter. Migration towards HUVECs (in H14 + EGM1) was compared with migration towards 10% FBS in H14 + EGM5 (pos. ctrl) and plane H14 + EGM5 (neg. ctrl). Student´s t-Test (R), *** $p < 0.001$, ** $p < 0.01$, * $p < 0.05$, · < 0.1 .

Fig. S7: Mildly increased gene expression of candidates in ECs upon treatment with D492HER2-CM compared to CM from D492HER2 with ECM1 KD. A) No upregulation of VEGFa, VEGFR2 or PDGFb in HUVECs treated with D492HER2-CM. RT-qPCR testing of common endothelial angiogenesis-regulating genes in response to CM treatment. B) Top 10 up- and downregulated genes in HUVECs treated with CM from D492HER2 vs. CM from D492HER2-kdECM1. Affymetrix human Clariom S microarray, 2-fold change threshold, p-value adjusted. C) RT-qPCR validation of candidates from A. Kruskal-Wallis Test (R), *** p < 0.001, ** p < 0.01, * p < 0.05, · < 0.1.

Fig. S8: CM from MDA-MB-231 enhances endothelial network and induces endothelial feedback increasing MDA-MB-231 migration. A) High ECM1 expression in MDA-MB-231. Relative Gene expression of ECM1 in MDA-MB-231 and MCF7 compared to D492, D492M and D492HER2. B) DMFS & RFS in ECM1+/TN & ECM1+/ER- breast cancer. ECM1 expression

correlates with worse relapse-free survival (RFS) in triple-negative (TN) breast cancer patients & with worse distant metastasis-free survival (DMFS) in ER- breast cancer patients. C) Enhanced endothelial tube formation in MDA-MB-231 CM. Top: HUVEC endothelial network after 4 h in R10F, MCF7-CM and MDA-MB-231-CM (phase contrast). 10x magnification, scale bar = 100 µm. Bottom: Angiogenesis images. D) Endothelial tube formation - Quantification. Quantification of master junctions, master segments total master segment length and meshes. One-way ANOVA, *** $p < 0.001$, ** $p < 0.01$, * $p < 0.05$, · < 0.1 . E) ECM1/CD31 expression correlation in ER- breast cancer. Correlation analysis of ECM1 and CD31 gene expression using Metabric discovery data set showing significant positive correlation (p = 0.0181) in ER- breast cancer. F) Endothelial feedback by rECM1 - schematic overview. Schematic work flow of conditioning of ECs using 60 ng/ml rECM1. G) ECM1-induced ECs promote MDA-MB-231 migration. Transwell-migration assay of MDA-MB-231 treated with unconditioned medium (R10F), unconditioned HUVEC-CM and 60 ng rECM1-treated HUVEC-CM. Number of migratory cells is shown for the different treatments. Student´s t-Test (R), *** $p < 0.001$, ** $p < 0.01$, * $p < 0.05$, · < 0.1 . H) ECM1 KD. Confirmation of ECM1 knockdown on gene expression level (RT-qPCR). Student´s t-Test (R), *** $p < 0.001$, ** $p < 0.01$, * $p < 0.05$, · < 0.1 . I) Decreased endothelial tube formation upon ECM1 knockdown in MDA-MB-231. Quantification HUVEC endothelial network after 4 h in ctrl media (R10F), MCF7-CM, ctrl MDA-MB-231-CM, siRNA neg. ctrl MDA-MB-231-CM and siECM1 MDA-MB-231-CM. One-way ANOVA, *** $p < 0.001$, ** $p < 0.01$, * $p < 0.05$, · < 0.1.

Fig. S9: CM of MDA-MB-231 enhanced endothelial network - 24 h and 48 h. A) Top: HUVEC endothelial network after 24 h in R10F, MCF7-CM and MDA-MB-231-CM (phase contrast), 10x magnification. Bottom: Angiogenesis images showing branches, junctions, master junctions, master segments and meshes. B) Quantification of master junctions, master segments total master segment length and meshes. One-way ANOVA, *** p < 0.001, ** p < 0.01, * p

< 0.05, · < 0.1. C) Top: HUVEC endothelial network after 48 h (phase contrast). Bottom: Angiogenesis images. D) Quantification of master junctions, master segments total master segment length and meshes. One-way ANOVA, *** p < 0.001, ** p < 0.01, * p < 0.05, · < 0.1.

Figure 1: Conditioned medium from D492HER2 enhances endothelial network and induces endothelial feedback increasing D492HER2 migration/invasion.

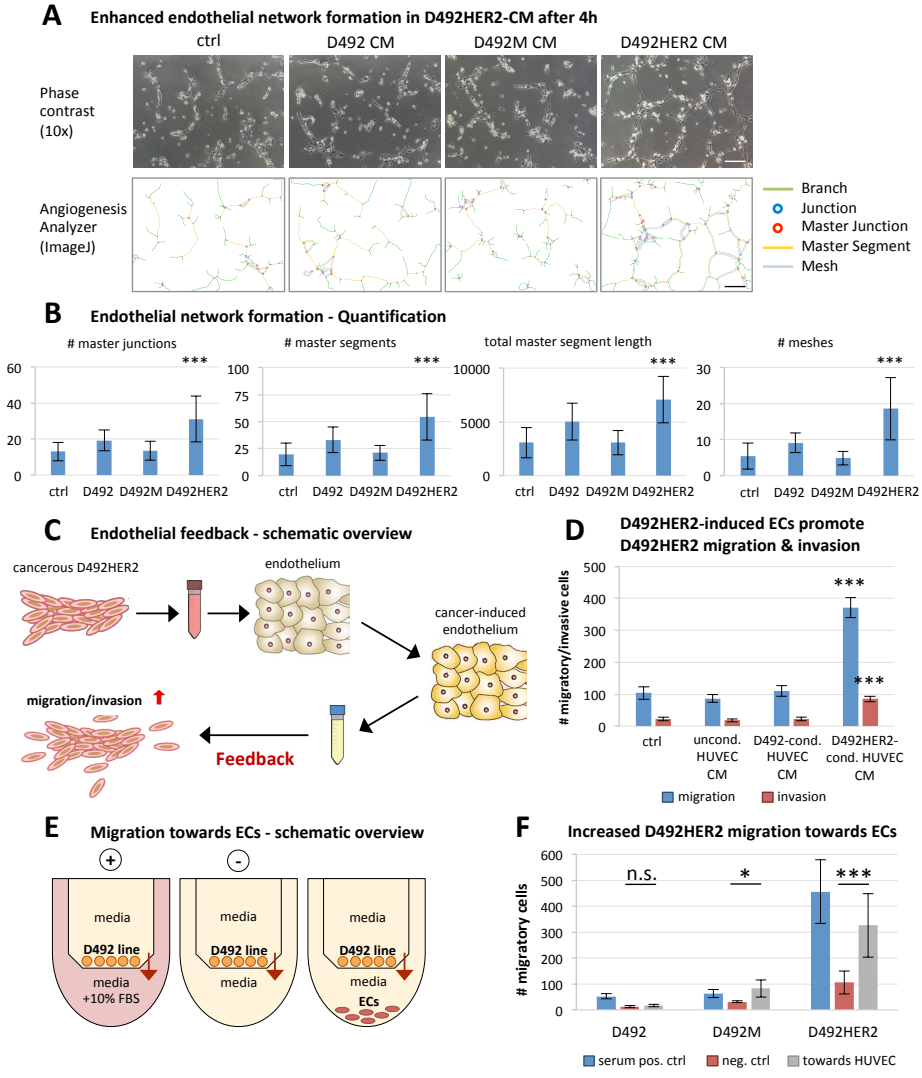
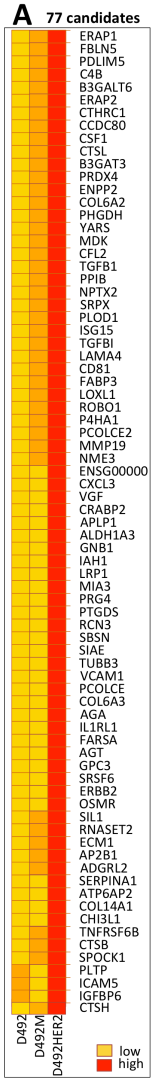


Figure 2: Identification of ECM1 as pro-angiogenic candidate in D492HER2.

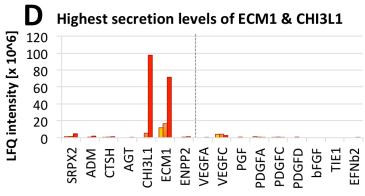


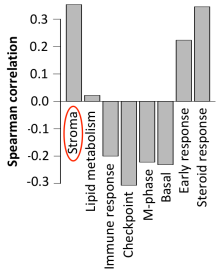
B Enrichment of angiogenesis-regulating genes in D492HER2 secretome (GO terms)

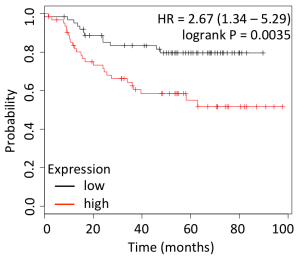
GO biological process complete	Expected Genes	Present Genes	Fold Enrichment	P-value
ossification involved in bone remodeling (GO:0043932)	0,01	2	> 100	2,00E-04
positive regulation of protein catabolic process in the vacuole (GO:1904352)	0,02	2	> 100	2,79E-04
cellular response to thyroid hormone stimulus (GO:0097067)	0,06	3	50,58	4,50E-05
chondrocyte morphogenesis (GO:0090171)	0,07	3	44,96	6,14E-05
growth plate cartilage chondrocyte morphogenesis (GO:0003429)	0,07	3	44,96	6,14E-05
chondrocyte morphogenesis involved in endochondral bone morphogenesis (GO:0003414)	0,07	3	44,96	6,14E-05
growth plate cartilage morphogenesis (GO:0003422)	0,07	3	42,6	7,09E-05
chondrocyte development involved in endochondral bone morphogenesis (GO:0003433)	0,09	3	35,19	1,19E-04
growth plate cartilage chondrocyte differentiation (GO:0003418)	0,09	3	33,72	1,33E-04
response to thyroid hormone (GO:0097066)	0,1	3	31,13	1,65E-04
cartilage morphogenesis (GO:0060536)	0,1	3	28,9	2,02E-04
chondrocyte differentiation involved in endochondral bone morphogenesis (GO:0003413)	0,11	3	27,91	2,23E-04
peptide catabolic process (GO:0043171)	0,11	3	26,98	2,44E-04
regulation of superoxide metabolic process (GO:0090322)	0,12	3	25,29	2,91E-04
aorta development (GO:0035904)	0,18	4	22,48	4,07E-05
collagen metabolic process (GO:0032963)	0,21	4	19,27	7,17E-05
chondrocyte differentiation (GO:0002062)	0,3	5	16,45	1,76E-05
positive regulation of animal organ morphogenesis (GO:0110110)	0,32	5	15,68	2,19E-05
organ growth (GO:0035265)	0,34	5	14,5	3,13E-05
artery development (GO:0060840)	0,3	4	13,32	2,78E-04
extracellular matrix organization (GO:0030198)	1,17	15	12,85	1,06E-12
extracellular structure organization (GO:0043062)	1,33	17	12,77	2,95E-14
regulation of morphogenesis of an epithelium (GO:1905330)	0,49	5	10,3	1,49E-04
regulation of animal organ morphogenesis (GO:2000027)	0,79	8	10,18	1,53E-06
cartilage development (GO:0051216)	0,64	6	9,36	5,28E-05
connective tissue development (GO:0061448)	0,82	7	8,51	2,21E-05
negative regulation of peptidase activity (GO:0010466)	0,89	7	7,87	3,58E-05
regulation of peptidase activity (GO:0052547)	1,55	11	7,12	4,79E-07
blood vessel development (GO:0001568)	1,77	12	6,77	2,30E-07
regulation of angiogenesis (GO:0045765)	1,05	7	6,7	9,63E-05
vasculature development (GO:0001944)	1,86	12	6,46	3,76E-07
cardiovascular system development (GO:0072358)	1,9	12	6,32	4,71E-07
regulation of vasculature development (GO:1901342)	1,15	7	6,09	1,70E-04
cellular amino acid metabolic process (GO:0006520)	1,18	7	5,94	1,99E-04
blood vessel morphogenesis (GO:0048514)	1,47	8	5,45	1,22E-04
inflammatory response (GO:0006954)	1,73	9	5,21	6,29E-05
circulatory system development (GO:0072359)	3,11	16	5,14	7,40E-08
tube morphogenesis (GO:0035239)	2,35	12	5,11	4,16E-06

C GO:0045765 gene members

Regulation of angiogenesis (GO:0045765)		
UniProtKB	**Gene name**	**PANTHER family**
O60687	SRPX2	Sushi repeat-containing protein
P35318	ADM	ADM
P09668	CTSH	Pro-cathepsin H
P01019	AGT	Angiotensinogen
P36222	CHI3L1	Chitinase-3-like protein 1
Q16610	ECM1	Extracellular matrix protein 1
Q13822	ENPP2	Ectonucleotide pyrophosphatase/ phosphodiesterase family member 2







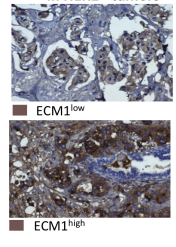


Figure 3: Recombinant ECM1 enhances endothelial network and induces endothelial feedback increasing D492HER2 migration/invasion.

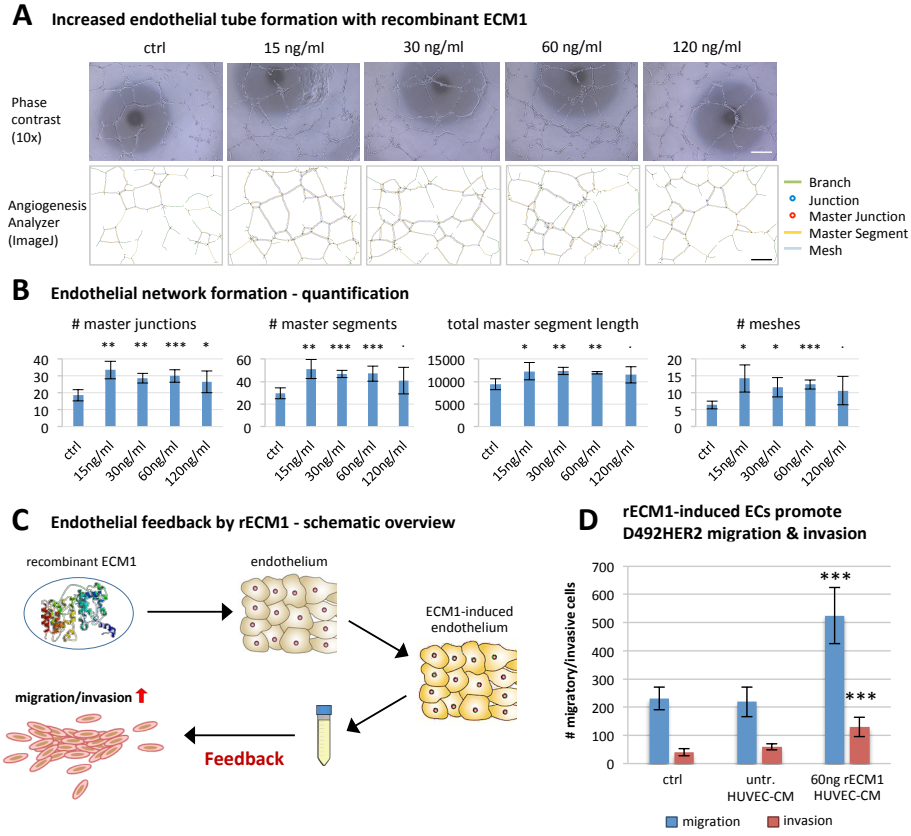


Figure 4: ECM1 knockdown inhibits pro-angiogenic effect of D492HER2-CM and endothelial feedback on D492HER2 migration/invasion.

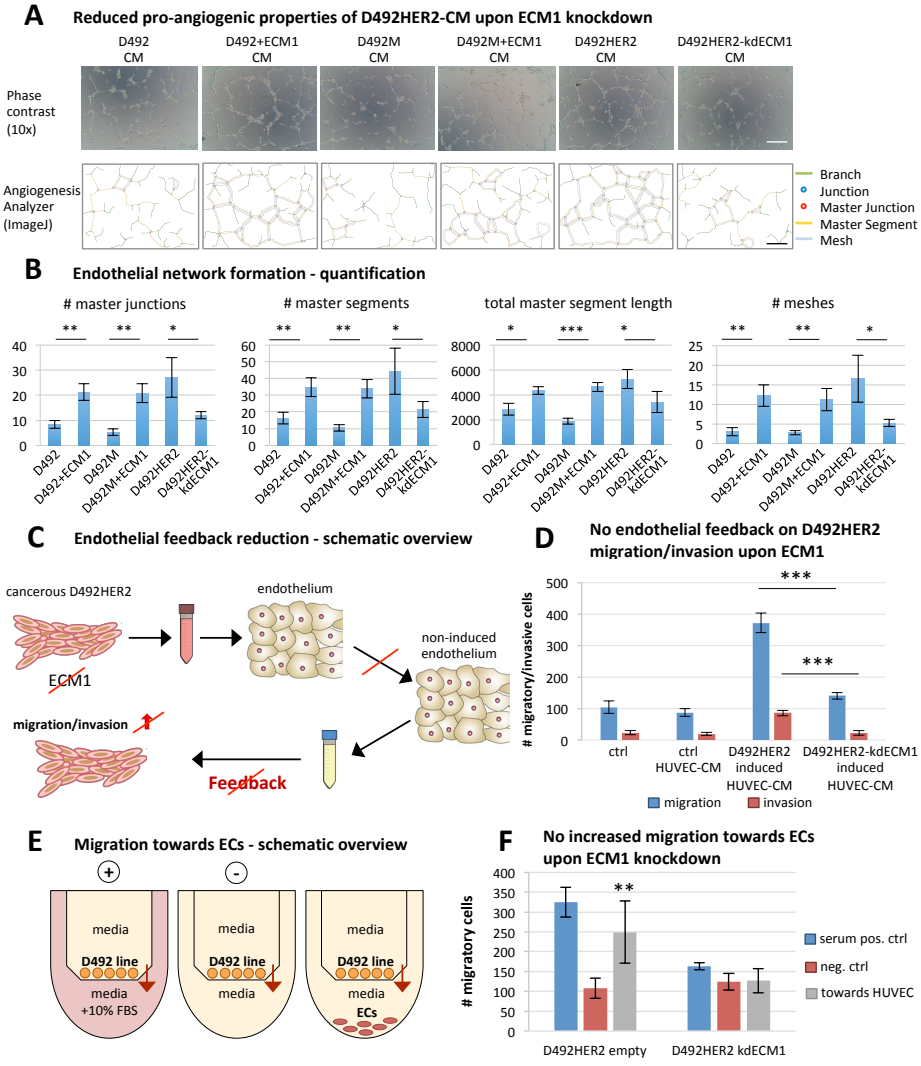


Figure 5: Inhibition of endothelial NOTCH signaling prevents increased tube formation and feedback induction.

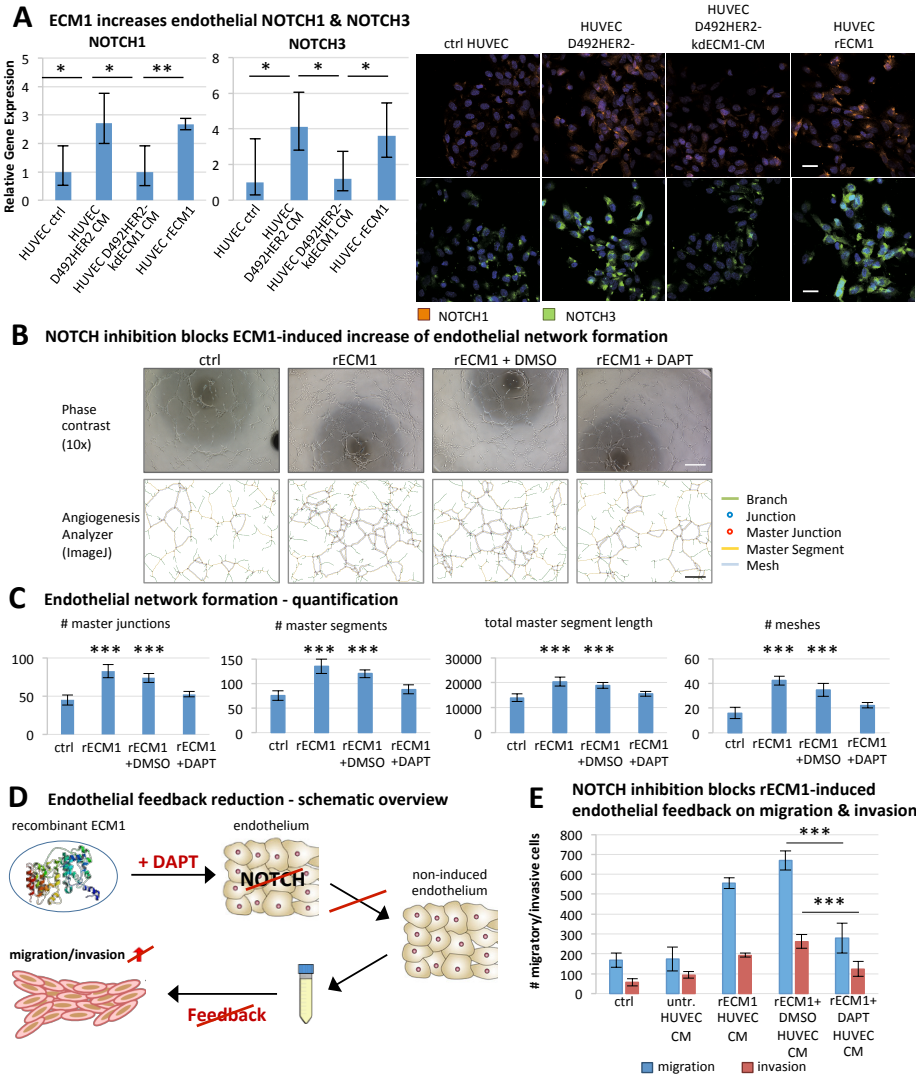
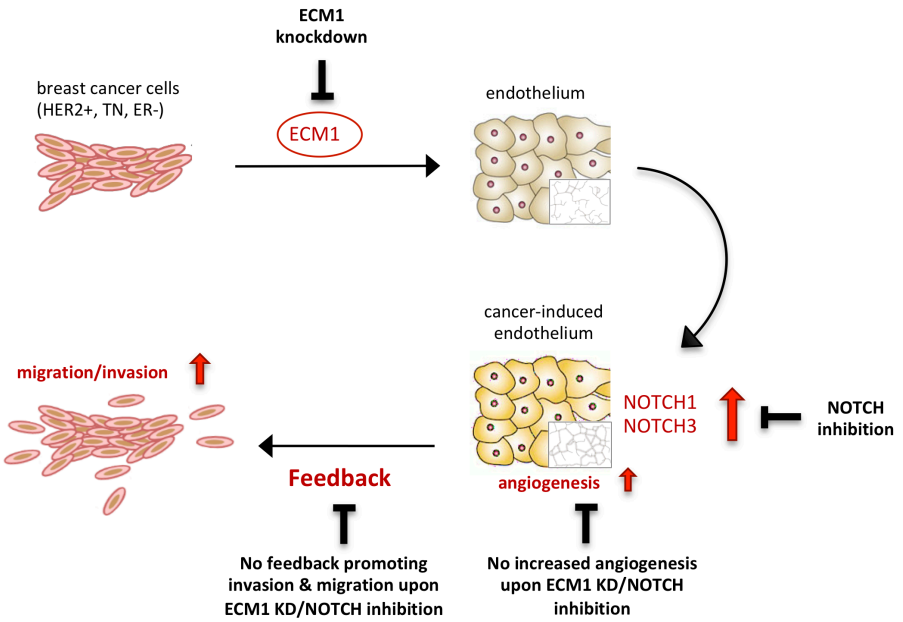
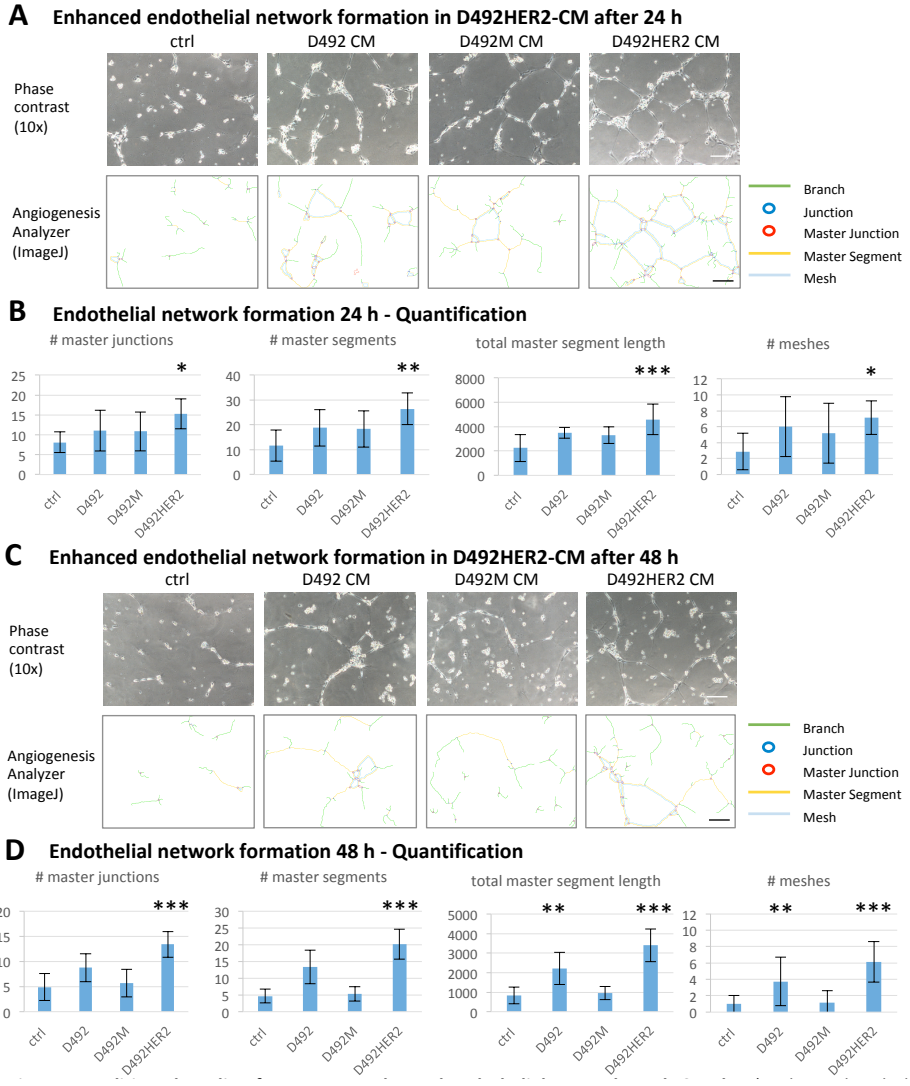


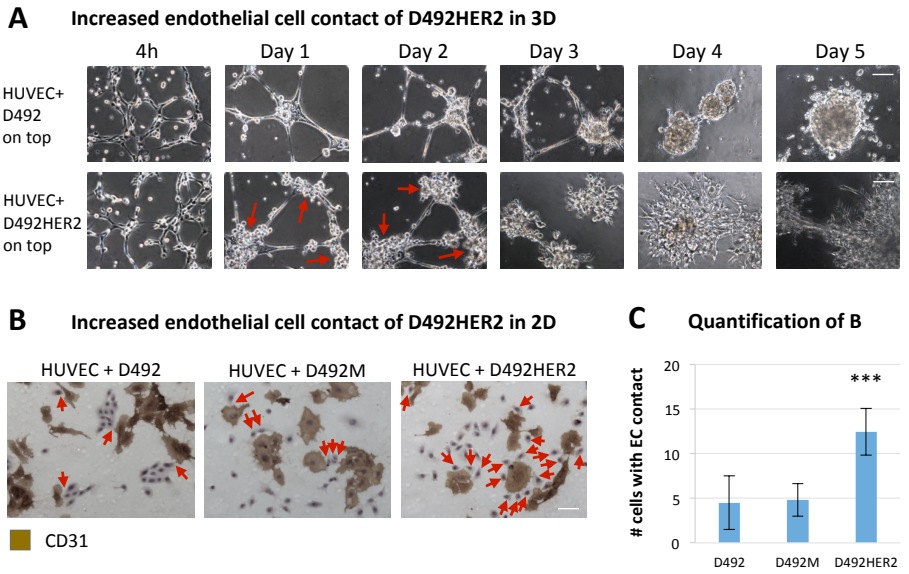
Figure 6: Schematic summary of ECM1 inducing an endothelial feedback promoting cancer cell migration/invasion.



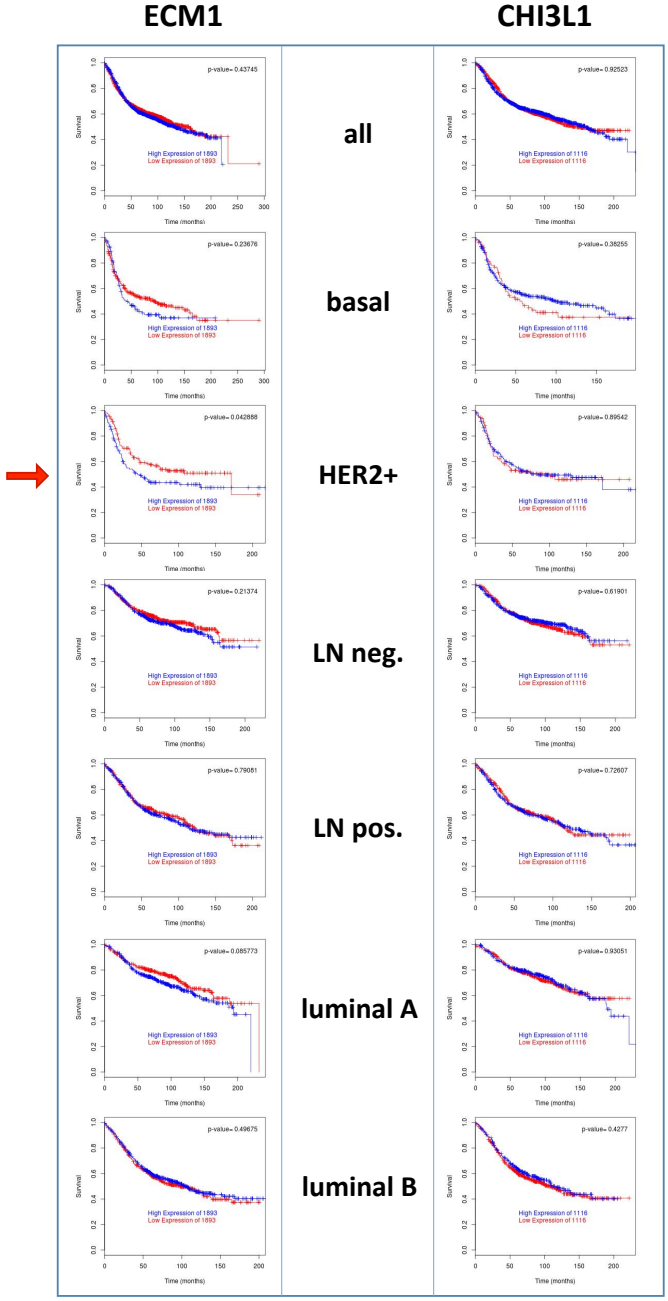
Suppl. Figure S1: CM of D492HER2 enhanced endothelial network - 24 h and 48 h.



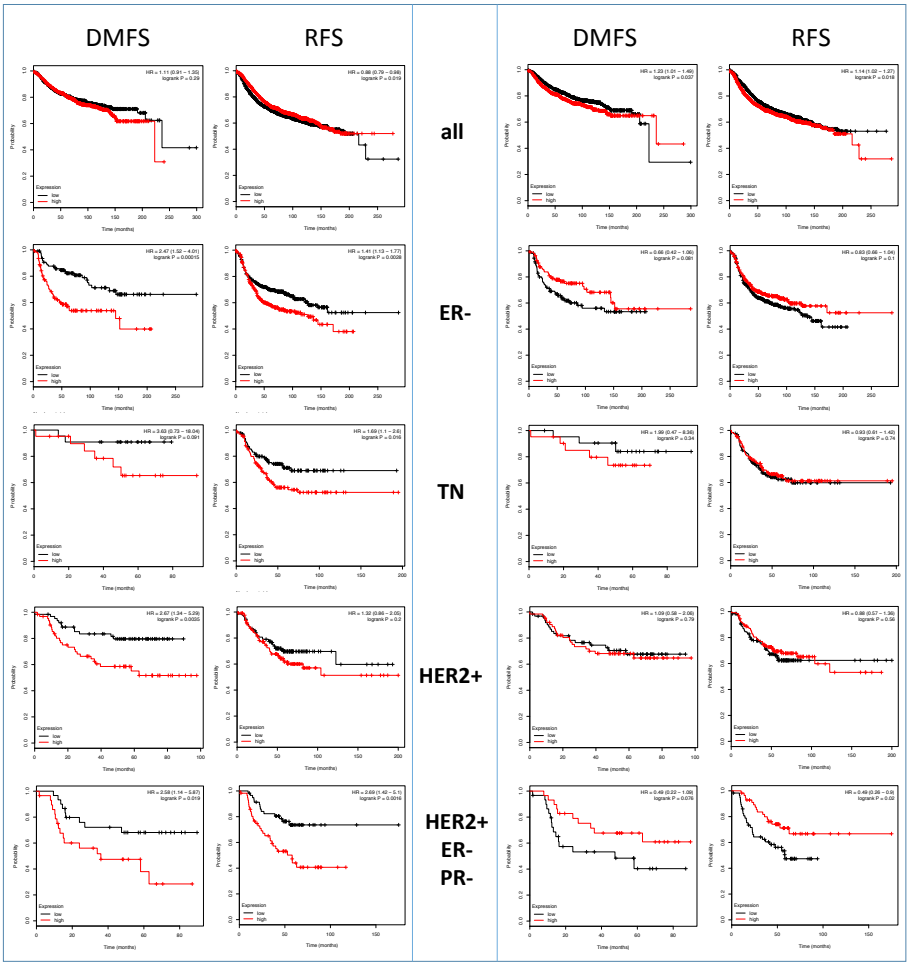
Suppl. Figure S2: D492HER2 has increased affinity to ECs in 2D and 3D.



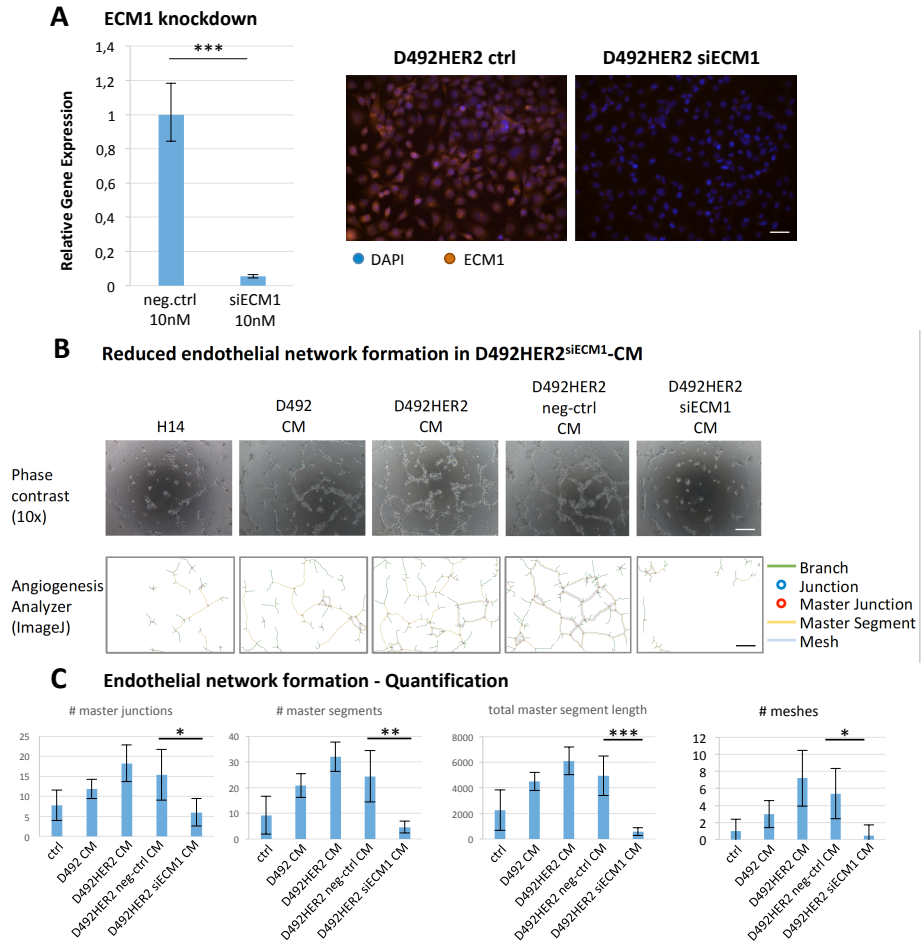
Suppl. Figure S3: Decreased DMFS when ECM1 but not CHI3L1 is expressed in HER2+ tumors (breastmark).



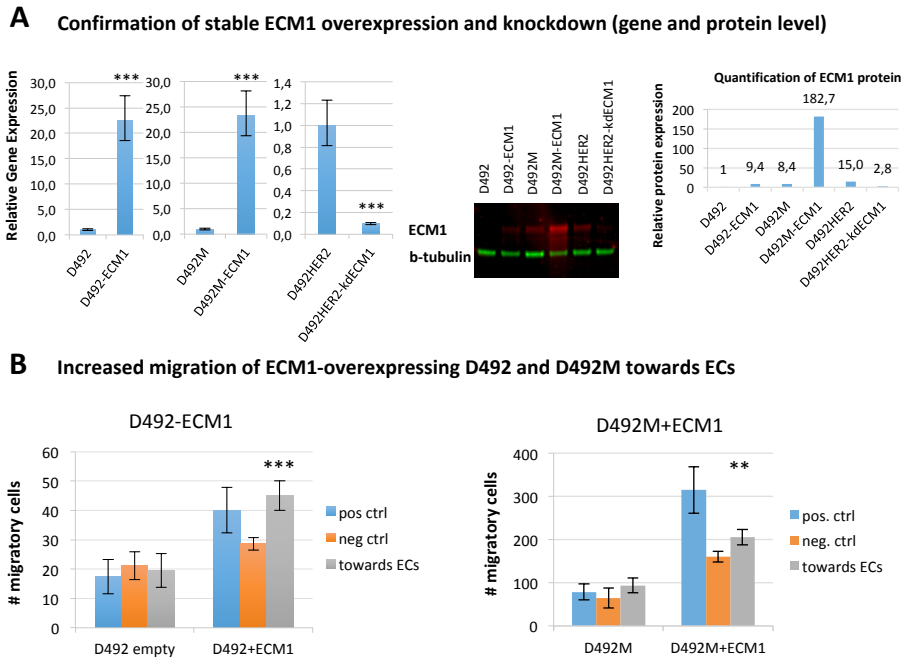
Suppl. Figure S4: Differential survival pattern for ECM1 and CHI3L1 in HER2+ and ER- tumors (KM plotter).



Suppl. Figure S5: Transient knockdown of ECM1 inhibits pro-angiogenic effect of D492HER2-CM.

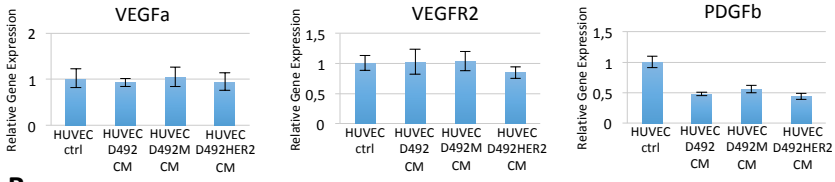


Suppl. Figure S6: Increased migration of D492 and D492M overexpressing ECM1 towards ECs.



Suppl. Figure S7: Mildly increased gene expression of candidates in ECs upon treatment with D492HER2-CM compared to CM from D492HER2 with ECM1 KD.

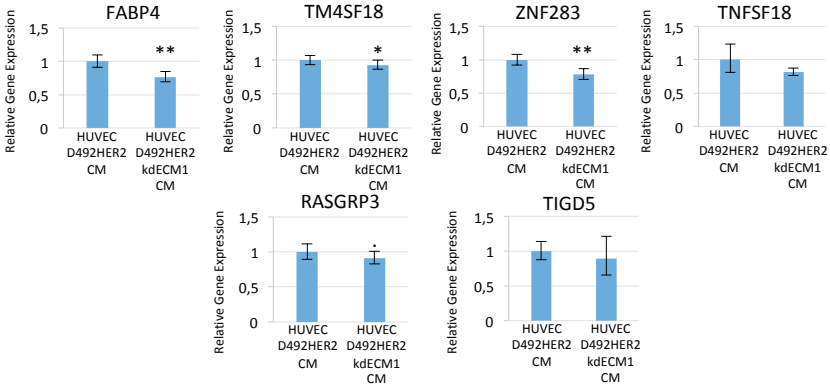
A **No upregulation of VEGFa, VEGFR2 or PDGFb in HUVECs treated with D492HER2-CM**



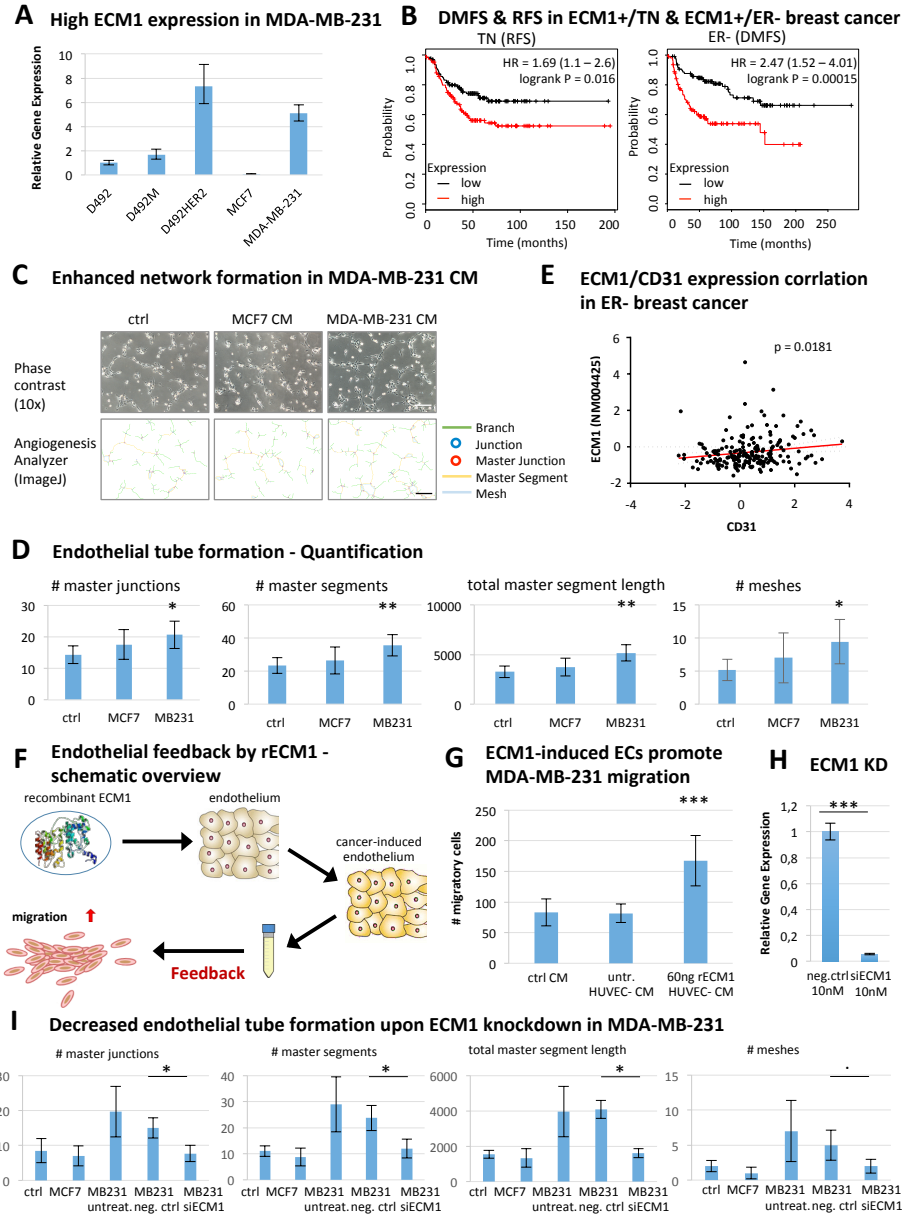
B **Top 10 up- and downregulated genes in HUVECs treated with D492HER2/D492HER2-kdECM1 CM**

chip.microarray 001.cel	Gene Symbol	Description	D492HER 2 CM	D492HER2-kdECM1 CM	p-value adjusted	log2 FC	FC
100287728_at	**LOC100287728**	uncharacterized LOC100287728	↑	↓	0	-1,06	0,48
2167_at	**FABP4**	fatty acid binding protein 4, adipocyte	↑	↓	5,00E-06	-0,85	0,56
84948_at	**TIGD5**	tigger transposable element derived 5	↑	↓	0,000565	-0,71	0,61
116441_at	**TM4SF18**	transmembrane 4 L six family member 18	↑	↓	0,009003	-0,61	0,65
25780_at	**RASGRP3**	RAS guanyl releasing protein 3 (calcium and DAG-regulated)	↑	↓	0,018059	-0,58	0,67
135924_at	**OR9A2**	olfactory receptor, family 9, subfamily A, member 2	↑	↓	0,018059	-0,58	0,67
8995_at	**TNFSF18**	tumor necrosis factor (ligand) superfamily, member 18	↑	↓	0,019042	-0,58	0,67
56911_at	**MAP3K7CL**	MAP3K7 C-terminal like	↑	↓	0,02629	-0,56	0,68
284349_at	**ZNF283**	zinc finger protein 283	↑	↓	0,029553	-0,56	0,68
359787_at	**DPPA3**	developmental pluripotency associated 3	↑	↓	0,030925	-0,55	0,68
597_at	**BCL2A1**	BCL2-related protein A1	↓	↑	0,015665	0,59	1,51
51351_at	**ZNF117**	zinc finger protein 117	↓	↑	0,015046	0,59	1,51
3078_at	**CFHR1**	complement factor H-related 1	↓	↑	0,011634	0,60	1,52
6407_at	**SEMG2**	semenogelin II	↓	↑	0,009003	0,61	1,53
414189_at	**AGAP6**	ArfGAP with GTPase domain, ankyrin repeat and PH domain 6	↓	↑	0,008609	0,62	1,54
256586_at	**LYSMD2**	LysM, putative peptidoglycan-binding, domain containing 2	↓	↑	0,007606	0,63	1,54
345778_at	**MTX3**	metaxin 3	↓	↑	0,002965	0,66	1,58
56999_at	**ADAMTS9**	ADAM metallopeptidase with thrombospondin type 1 motif, 9	↓	↑	0,000989	0,69	1,61
79324_at	**OR51G1**	olfactory receptor, family 51, subfamily G, member 1 (gene/pseudogene)	↓	↑	0,00061	0,71	1,63
5473_at	**PPBP**	pro-platelet basic protein (chemokine (C-X-C motif) ligand 7)	↓	↑	0,000565	0,72	1,64

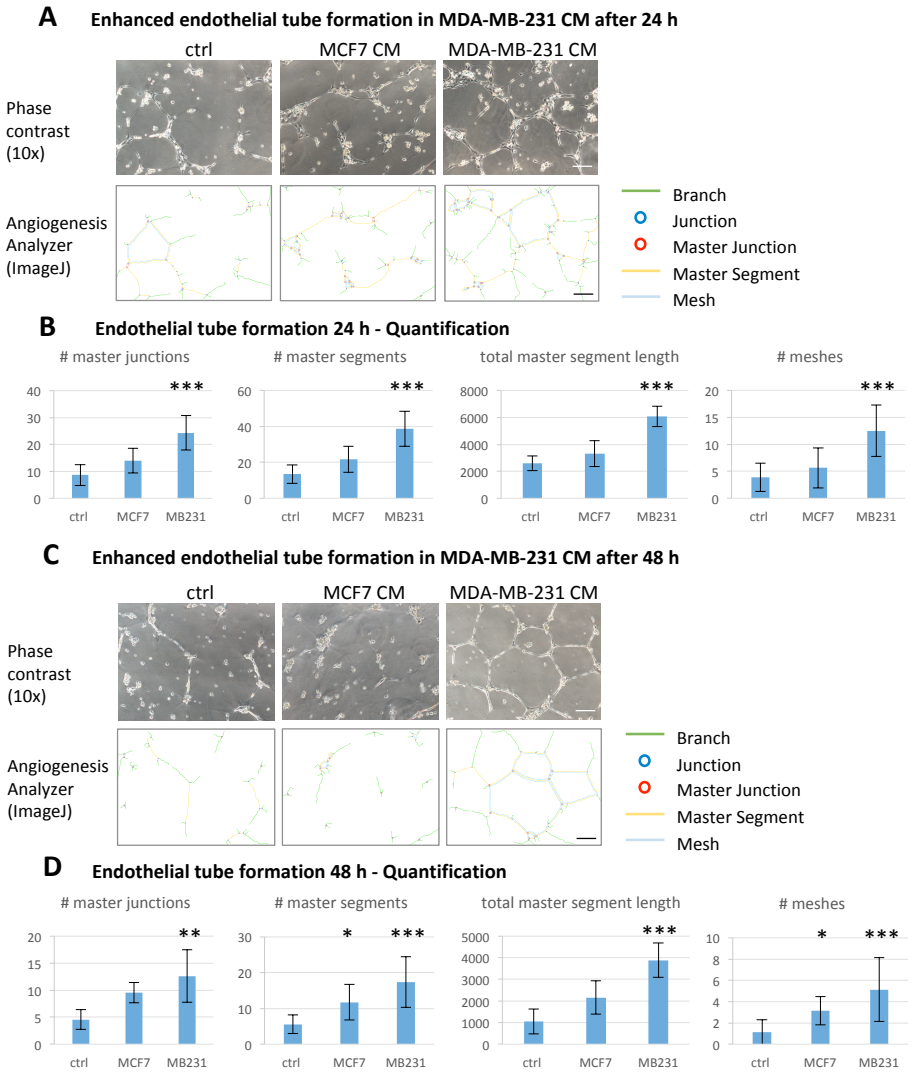
C **Validation of candidates from B with RT-qPCR**



Suppl. Figure S8: CM from MDA-MB-231 enhances endothelial network and induces endothelial feedback increasing MDA-MB-231 migration.



Suppl. Figure S9: Conditioned medium of MDA-MB-231 enhanced endothelial network - 24 h and 48 h.



Paper II

ECM1 knockdown in HER2-expressing breast cancer promotes loss of basal characteristics and re-expression of GATA3

Sophie S. Steinhäuser[1], Anna Karen Sigurdarsdottir[1], Zuzana Budkova[1], Bylgja Hilmarsdottir[3], Gunnhildur A. Traustadottir[1], Gunhild Maelandsmo[3], Thorarinn Gudjonsson[1,2]

[1]Stem Cell Research Unit, Department of Anatomy, Faculty of Medicine, School of Health Sciences, Biomedical Center, University of Iceland, Iceland

[2]Department of Laboratory Hematology, Landspitali - University Hospital, Iceland

[3]Department of Tumor Biology, Institute for Cancer Research, Oslo University Hospital, Norway

Correspondence: T Gudjonsson, Stem Cell Research Unit, Department of Anatomy, Faculty of Medicine, School of Health Sciences, Biomedical Center, University of Iceland, Vatnsmyrarvegi 16, 101 Reykjavík, Iceland.

Tel: +354-5254827; Fax: +354 5254884. E-mail: tgudjons@hi.is

Abstract

Despite increasing understanding in molecular and cellular mechanisms of breast cancer, it is still one of the major causes of death worldwide. Understanding the process of breast cancer progression and the factors driving metastases formation is therefore of major importance.

Here, we use D492 as a normal breast epithelial cell line with stem cell properties and its derivative D492HER2 with overexpression of the HER2/ERBB2 oncogene, which has tumorigenic characteristics and metastasizes *in vivo*.

We found that expression of ECM1 is upregulated in D492HER2 and correlates with decreased survival in HER2+ patient tumor samples. Knockdown of ECM1 leads to downregulated gene expression of basal markers such as CDH3, ITGB4, KRT14 and KRT17 whereas luminal differentiation marker GATA3 and downstream targets show upregulated expression. Survival analysis suggests that re-expression of GATA3 in HER2+ patient tumor samples correlates with better outcome. Indeed, knockdown of ECM1 in D492HER2 leads to decreased migration and invasion ability *in vitro*.

In conclusion, we identified ECM1 as potential candidate contributing to migrative and invasive properties of D492HER2 and our data suggest ECM1 as novel mediator of GATA3 expression. Targeting ECM1 might offer novel opportunities to reduce tumorigenic characteristics that contribute to metastasis formation and therefore cancer progression.

Introduction

According to the World Health Organization, cancer is one of the leading causes of death worldwide being responsible for 9.6 million deaths in the year 2018 (https://www.who.int/news-room/fact-sheets/detail/cancer, 4.2.2019). For women, breast cancer is the most common type of cancer and the most frequent cause of cancer-related deaths, as reported by The Cancer Atlas (http://canceratlas.cancer.org/the-burden/breast-cancer/, 4.2.2019). Despite new methods in assessing the genetic background of cancers (next-generation sequencing), metastatic diseases remain largely incurable and are still one of the main causes of cancer related deaths (Rankin & Giaccia, 2016). Metastases are the final result of a complex process involving migration and tissue invasion of primary tumor cells followed by intravasation, circulation and survival in the blood and/or lymphatic system, extravasation and colonization in distant organs (Rankin & Giaccia, 2016; Valastyan & Weinberg, 2011). Therefore, determining factors regulating e.g. migration and invasion capacity in cancer cells and how they drive metastases formation in particular is of major importance for improving cancer treatment.

There are multiple ways of subtyping breast cancer. Using cDNA microarrays derived from primary tumor samples, Perou and Sorlie grouped breast tumors using hierarchical clustering into distinct subgroups (Perou et al., 2000; Sorlie et al., 2001; Sorlie et al., 2003). The most prominent groups thereafter are Luminal A, Luminal B, triple-negative (TN), HER2-enriched and Normal-like breast cancer, resembling in signature to that of normal breast gland. Whereas luminal A and B tumors are estrogen receptor (ER) positive, HER2-enriched tumors show high expression of the HER2/ERBB2 receptor. HER2-enriched tumors are usually ER-negative and tend to be more prone to form metastasis due to high heterogeneity. They can be treated using Trastuzumab (Herceptin), a monoclonal antibody inhibiting the function of the HER2 receptor, which can drastically increase survival of HER2 breast cancer patients. However, in many cases tumor cells can require resistance

against trastuzumab, which leads to relapse after initial improvement (Lee, K. M. et al., 2014).

TN tumors are characterized by low expression of epithelial cadherins and keratins and are believed to originate from the least differentiated progenitor populations of the breast (Perou, 2011). The majority of TN breast cancers show basal characteristics and is referred to as basal-like (Gazinska et al., 2013; Rakha & Ellis, 2009). Basal-like breast cancer is more common in younger women and has high rates of metastasis due to cancer cells being more invasive. Due to lack of targetable receptor expression, basal-like breast cancer has been difficult to treat and therefore has a worse prognosis. However, basal characteristics are not only in TN breast cancer associated with worse outcome. Martin-Castillo and colleagues suggest the existence of a subpopulation of HER2+ cancer cells with increased basal or stem-like signature that is prone to require trastuzumab resistance in contrast to a more luminal trastuzumab-sensitive subpopulation (Martin-Castillo et al., 2013). Through high heterogeneity, HER2+ cells are able to enter or exit the trastuzumab-sensitive stage and therefore escape therapy (Martin-Castillo et al., 2013). Being able to target basal subpopulations both among HER2+ and TN breast cancer may therefore be beneficial for improving treatment options and patient outcome.

We have previously established a breast epithelial cell line with stem cell properties, referred to as D492 (Gudjonsson et al., 2002; Sigurdsson et al., 2011; Villadsen et al., 2007). D492 can generate both luminal- and myoepithelial cells and in 3D rBM culture it forms branching structures reminiscent of TDLU in vivo. Using artificial overexpression of the ErbB2/HER2 oncogene, the cell line D492HER2 was generated, which then underwent oncogene-induced EMT (Ingthorsson et al., 2015) and has tumorigenic properties.

In this study, we show that extracellular matrix protein 1 (ECM1) was among the genes upregulated in D492HER2 and that its expression in HER2+ breast tumors correlates with decreased patient survival. Knockdown of ECM1 in

D492HER2 resulted in upregulation of luminal transcription factor GATA3 and downstream targets, accompanied by loss of basal marker expression. GATA3 is associated with better outcome when expressed in patients with HER2+ breast tumors, which can be confirmed by decreased migration and invasion capacity of D492HER2 upon ECM1 knockdown.

Material and Methods

Cell culture

D492 and D492HER2 cells were maintained in H14 medium in tissue culture treated T25 Falcon flasks (BD Biosciences (BD), Franklin Lakes, NJ, USA) coated with collagen I (Advanced Biomatrix, San Diego, CA, USA), as described previously (Ingthorsson et al., 2015; Sigurdsson et al., 2011). The cells were grown at 37°C and 5% CO2 and subcultured into new flasks 1-2 times per week in a ratio of 1:10 (D492) or 1:15 (D492HER2). MDA-MB-231 cells were cultured in Gibco™ RPMI 1640 media containing 10% fetal bovine serum (FBS) (Invitrogen) and subcultured 1-2 per week at a ratio of 1:10. Culture medium was changed three times per week and routinely checked for mycoplasma contamination.

Migration and invasion assay

Migration was analyzed using transwell-filter units for 24-well plates with 8 µm pore size ((#353097, Corning). For invasion assay, filters were pre-coated with 1:10 rBM in H14 for 30 minutes at 37°C. For migration assay, cells were incubated for 24 h and for 48 h in invasion assay. 30.000 D492HER2 cells were seeded in 250 µl H14 on top of the non-coated or rBM-coated filter units (triplicates) and 500 µl H14 containing 10% FBS as attractant was added below. For MDA-MB-231, R10F was used instead of H14 while keeping the same experimental setup. After 24 h or 48 h, non-migratory or non-invasive cells were removed from the top of the filter using Q-tips, migratory cells below the filter were fixed for 10 minutes with 3.7% PFA (#252549, Sigma-Aldrich) and stained for 30 minutes with 1:5000 diluted

DAPI nuclear staining (20 mg/ml) (#D9542, Sigma-Aldrich). Using an EVOS FL Auto 2 Cell Imaging System (Thermo Fisher Scientific), three images per replicate were taken at 10x magnification. Images were converted to 8-bit in ImageJ (version 2.0.0), threshold-adjusted and binary-converted. Migratory cells were counted using the “analyze particles” function.

Transient knockdown (KD) using siRNA

Knockdown was performed in 24-well plate using pre-designed Silencer® Select human ECM1 siRNA (#s4441, Thermo Fisher Scientific). Cells were reverse transfected for 48 h according to the manufacture’s protocol using a siRNA concentration of 10nM. Proliferation was monitored using an IncuCyte ZOOM 2016B System. Knockdown was confirmed using RT-qPCR and western blotting. After 48 h, media was changed to normal H14 and incubated for another 48h for collection of conditioned media as described above. Endothelial network formation was analyzed as previously described for HUVECs treated with CM from D492HER2siECM1 compared to control D492HER2.

Generation of stable knockdown cell line using CRISPRi

In order to generate stable ECM1 knockdown in D492HER2, we used the novel CRISPRi (inhibition) system. sgRNA plasmid were purchased from Genscript; For ECM1 knockdown, a combination of two sgRNAs were used. Knockdown sgRNAs were custom-designed to bind between 1-200 bp downstream. sgRNAs were cloned into the plenti sgRNA(MS2)_zeo plasmid (Genscript). As negative control, an empty plenti sgRNA(MS2)_zeo plasmid was used (Genscript). For production of lentiviral particles, HEK231 cells were used and virus was collected 48 h and 72 h after transfection. D492HER2 was transduced with pHR-SFFV-KRAB-dCas9-P2A-mCherry plasmid for repression and sorted for mCherry expression. Next, transduction with lentivirus containing sgRNA plasmids for knockdown (D492HER2 containing dCas9-KRAB cassette) was performed. Cells were selected with 600µg/ml (D492HER2) zeocin (Invitrogen) for 14 days.

RNA, cDNA and RT-qPCR

Total RNA was extracted with Trizol (Life Technologies) and reverse transcribed with hexanucleotides using the SuperScript® IV First-Strand Synthesis System (Invitrogen). Resulting cDNA (10 ng per reaction) was used for quantitative real-time PCR, in master mix (Life Technologies) with pre-designed primer pairs ECM1 (Hs.PT.58.20438560), CDH3 (Hs.PT.58.39234242), ITGB4 (Hs.PT.58.3714621), KRT14 (Hs.PT.58.4592110), KRT17 (Hs.PT.58.20464487), GATA3 (Hs.PT.58.19431110), KRT7 (Hs.PT.58.3835469), KRT19 (Hs.PT.58.4188708), LAMA1 (Hs.PT.58.15231709), FN (Hs.PT.58.40005963), NOTCH2 (Hs.PT.58.28296019), HEY1 (Hs.PT.58.4299267), HEY2 (Hs.PT.58.582440) and beta-2-microglobulin (B2M) as reference gene (Hs.PT.58v.18759587). Experiments were carried out in triplicate on 7500 Real Time PCR System (Life Technologies). Expression levels were normalized to the reference gene and relative mRNA differences were calculated with the ΔΔCt method according to the MIQE guidelines (Bustin et al., 2009).

Immunofluorescence (IF) and immunohistochemistry (IHC) staining

HUVECs were grown to 80% confluence on 8-well chamber slides (#354108, Falcon), fixed with 3.7% PFA, permeabilized with 0.1% Triton X-100 and unspecific background was blocked using 10% FBS in 1xPBS. Incubation with primary antibodies for ECM1 (Sigma Aldrich, #HPA027241), GATA3 (Cell Signaling, #CS5852), CK19 (Abcam, #ab7754) and FN (Abcam, #ab6328) was done overnight at 4°C, followed by incubation with secondary antibodies conjugated with Alexa Fluor-488, 546 or 647 for one hour in RT. For nuclei staining DAPI was used together with secondary antibodies at a concentration of 1:5000. Imaging was done using FV1200 Olympus inverted confocal microscope. For IHC staining, paraffin-embedded tumor tissue samples were processed in xylene and ethanol in order to remove paraffin and then rehydrated in dH2O. Following rehydration, high-temperature antigen retrieval was performed and samples were stained as described above. Counterstaining was performed with filtered hematoxylin for 1-2 minutes.

Statistical analysis

All experiments were performed at minimum in triplicate. Graphs were generated in Microsoft Excel 2015. Error bars represent the standard deviation of the mean. Statistical analysis was performed in R 3.3.3. (R Development Core team, 2013). Data were checked for normal distribution and Students t-test or ANOVA followed by Tukey's honest significant difference test on linear models (lm) was performed when normally distributed whereas Kruskal-Wallis chi-squared test was used when not normally distributed. The significance level was 0.05.

Results

ECM1 is upregulated in D492HER2 and correlates with worse outcome in HER2+ patient tumor samples

In this study, we compared the tumorigenic breast epithelial cell line D492HER2 with its epithelial parental cell line D492. In vivo, D492HER2 forms solid breast tumors in NSG mice after mammary fat pad injection (Ingthorsson et al., 2015). Using previously generated transcriptomic and secretome data, we identified extracellular matrix protein 1 (ECM1) that appeared to be significantly upregulated in D492HER2 compared to D492, both on gene and protein expression level (Fig. 1A and B). We also confirmed strong ECM1 expression in mouse xenografts generated by D492HER2 but not D492 (Fig. 1C). Survival analysis revealed expression of ECM1 in HER2+ breast tumors is correlated with significantly worse distant metastasis-free survival (DMFS) (Fig. 1D) (Lee, K. M. et al., 2014). Therefore, we wanted to further investigate the role of ECM1 in our cellular model and whether it may offer a new therapeutic target in HER2+ breast cancer.

ECM1 knockdown leads to loss of basal characteristics and gain of GATA3 expression, associated with better outcome

In order to clarify its role in D492HER2, we generated transient and stable knockdown (KD) of ECM1 in D492HER2 (Fig. 3A). Interestingly, gene expression analysis D492HER2 with KD of ECM1 revealed significant downregulation of basal markers CDH3, ITGB4, KRT14 and KRT17 whereas luminal markers showed upregulated expression (Fig. 2A). Among the upregulated luminal markers was transcription factor GATA3 (Fig. 2A and B). Therefore, we decided to analyze expression of GATA3 downstream targets in order to confirm activation of GATA3 downstream pathways. Indeed, among upregulated downstream targets were KRT19, LAMA1, FN, NOTCH2 as well as HEY1 and HEY2 as NOTCH downstream targets (Fig. 2B). Upregulation of GATA3, KRT19 and FN in D492HER2 upon KD of ECM1 was confirmed on protein level using immunofluorescence (IF) staining (Fig.

2C). Remarkably, survival analysis revealed that expression of GATA3 in HER2+ breast tumors correlates with an increase in relapse-free survival (RFS) and therefore a better prognosis (Fig. 2D).

ECM1 knockdown decreased D492HER2 migration and invasion

In order to determine the effect of ECM1 KD on tumorigenic traits in D492HER2 *in vitro*, we performed transwell-migration and invasion assay. Interestingly, stable KD of ECM1 significantly reduced the ability of D492HER2 to migrate and invade (Fig. 3B and C). This could be confirmed using siRNA for transient KD of ECM1 both for D492HER2 and for MDA-MB-231, which also expresses high levels of ECM1 (suppl. Fig. S1). We further confirmed the involvement of ECM1 in migration and invasion using D492 with stable overexpression of ECM1, which showed an increased migrative and invasive phenotype compared to the empty control D492 cell line.

In summary, we identified as potential tumorigenic candidate ECM1 with overexpression in D492HER2. ECM1 expression correlates with worse outcome in patients with HER2+ breast tumors. Here we have shown that knockdown of ECM1 leads to increased expression of luminal GATA3, which correlates with better outcome and reduction of basal characteristics. Indeed, D492HER2 with KD of ECM1 showed significantly decreased migration and invasion ability.

Discussion

Here, we identify ECM1 as potential tumorigenic candidate in D492HER2. ECM1 is a secreted glycoprotein and was first identified in the mouse osteogenic stromal cell line MN7 (Mathieu et al., 1994). It was initially described as modulator of proliferation and differentiation of epidermal keratinocytes and basement membrane reconstitution in the skin (Oyama & Merregaert, 2017). However, recently it has also been linked to malignant transformation (Han et al., 2001; Lee, K. M. et al., 2015; Lee, K. M. et al., 2014; Oyama & Merregaert, 2017; Sercu, Zhang, & Merregaert, 2008; Sercu, Zhang, Oyama, et al., 2008; Wang et al., 2003). Wang et al. (2003) found it to be expressed particularly in highly malignant breast epithelial tumors (Wang et al., 2003). Wu et al. (2018) very recently linked ECM1 to breast cancer progression by suggesting a role in facilitating metastasis through increased invasion and adhesion capacity of ECM1-expressing cancer cells (Wu et al., 2018).

Survival analysis shows that expression of ECM1 in HER2+ breast tumors is associated with significantly reduced distant-metastasis-free-survival (DMFS). Therefore, targeting ECM1 in tumors overexpressing HER2 could lead to better patient prognosis. This is supported by a study of Lee et al. (2014), which showed that ECM1 regulates resistance to trastuzumab, the major agent for chemotherapeutical treatment of HER2+ breast cancer (Lee, K. M. et al., 2014). Interestingly, the triple-negative (TN) breast cancer cell line MDA-MB-231 also expresses high levels of ECM1 and shows a strong migrative and invasive phenotype (Lee, E. et al., 2014; Lee, E. et al., 2015; Wu et al., 2018). Similar to D492HER2, knockdown of ECM1 also results in decreased migration and invasion in MDA-MB-231 (Gomez-Contreras et al., 2017; Wu et al., 2018). Since expression of ECM1 also correlates with worse outcome in TN breast cancer, its molecular involvement in breast cancer progression might actually be more general rather than only limited to HER2+ cancer. Therefore, ECM1 might represent a possible therapeutic target for a broader range of breast cancer patients than just HER2+ individuals.

However, the specific relationship between HER2 overexpression and ECM1 still needs to be elucidated.

So far, ECM1 has been associated with EGF signaling (Lee, K. M. et al., 2014), ITGB4/FAK/SOX2/HIF1a (Gan et al., 2017) and WNT1/ß-catenin (Lee, K. M. et al., 2015) pathways. However, a mediating role on GATA3 expression and therefore involvement in GATA3 downstream signaling has not been described. The transcription factor GATA3 is one of the key players in luminal differentiation of breast epithelial progenitor cells during breast development (Kouros-Mehr et al., 2008). However, very often breast tumors originate from the basal fraction and lack expression of luminal markers as well as GATA3 (Chu et al., 2013; Wei et al., 2017). In breast cancer, mutation or loss of GATA3 expression has been associated with increased invasiveness and poor prognosis (Asch-Kendrick & Cimino-Mathews, 2016; Takaku et al., 2015). In a breast cancer mouse model, enforced GATA3 expression led to increased differentiation and decreased metastasis formation (Takaku et al., 2015). Here, we show that KD of ECM1 results in upregulation of GATA3 both on gene and protein expression level, which is accompanied by expression loss of numerous basal markers. Survival analysis showed that expression of GATA3 in HER2+ breast tumors is correlated with significantly better patient prognosis.

Targeting ECM1 led to significant reduction of tumorigenic traits such as migration and invasion and may therefore provide opportunities for development of novel therapies in order to reduce metastases and cancer progression.

Literature

Asch-Kendrick, R., & Cimino-Mathews, A. (2016). The role of GATA3 in breast carcinomas: a review. Hum Pathol, 48, 37-47. doi: 10.1016/j.humpath.2015.09.035

Bustin, S. A., Benes, V., Garson, J. A., Hellemans, J., Huggett, J., Kubista, M., . . . Wittwer, C. T. (2009). The MIQE guidelines: minimum information for publication of quantitative real-time PCR experiments. Clin Chem, 55(4), 611-622. doi: 10.1373/clinchem.2008.112797

Chu, I. M., Lai, W. C., Aprelikova, O., El Touny, L. H., Kouros-Mehr, H., & Green, J. E. (2013). Expression of GATA3 in MDA-MB-231 triple-negative breast cancer cells induces a growth inhibitory response to TGFss. PLoS One, 8(4), e61125. doi: 10.1371/journal.pone.0061125

Gan, L., Meng, J., Xu, M., Liu, M., Qi, Y., Tan, C., . . . Wang, Z. (2017). Extracellular matrix protein 1 promotes cell metastasis and glucose metabolism by inducing integrin beta4/FAK/SOX2/HIF-1alpha signaling pathway in gastric cancer. Oncogene. doi: 10.1038/onc.2017.363

Gazinska, P., Grigoriadis, A., Brown, J. P., Millis, R. R., Mera, A., Gillett, C. E., . . . Pinder, S. E. (2013). Comparison of basal-like triple-negative breast cancer defined by morphology, immunohistochemistry and transcriptional profiles. Mod Pathol, 26(7), 955-966. doi: 10.1038/modpathol.2012.244

Gomez-Contreras, P., Ramiro-Diaz, J. M., Sierra, A., Stipp, C., Domann, F. E., Weigel, R. J., & Lal, G. (2017). Extracellular matrix 1 (ECM1) regulates the actin cytoskeletal architecture of aggressive breast cancer cells in part via S100A4 and Rho-family GTPases. Clin Exp Metastasis, 34(1), 37-49. doi: 10.1007/s10585-016-9827-5

Gudjonsson, T., Villadsen, R., Nielsen, H. L., Ronnov-Jessen, L., Bissell, M. J., & Petersen, O. W. (2002). Isolation, immortalization, and characterization of a human breast epithelial cell line with stem cell properties. Genes Dev, 16(6), 693-706. doi: 10.1101/gad.952602

Han, Z., Ni, J., Smits, P., Underhill, C. B., Xie, B., Chen, Y., . . . Zhang, L. (2001). Extracellular matrix protein 1 (ECM1) has angiogenic properties and is expressed by breast tumor cells. The FASEB Journal, 15, 988-994.

Ingthorsson, S., Andersen, K., Hilmarsdottir, B., Maelandsmo, G. M., Magnusson, M. K., & Gudjonsson, T. (2015). HER2 induced EMT and tumorigenicity in breast epithelial progenitor cells is inhibited by coexpression of EGFR. Oncogene. doi: 10.1038/onc.2015.489

Kouros-Mehr, H., Kim, J. W., Bechis, S. K., & Werb, Z. (2008). GATA-3 and the regulation of the mammary luminal cell fate. Curr Opin Cell Biol, 20(2), 164-170. doi: 10.1016/j.ceb.2008.02.003

Lee, E., Fertig, E. J., Jin, K., Sukumar, S., Pandey, N. B., & Popel, A. S. (2014). Breast cancer cells condition lymphatic endothelial cells within pre-metastatic niches to promote metastasis. Nat Commun, 5, 4715. doi: 10.1038/ncomms5715

Lee, E., Pandey, N. B., & Popel, A. S. (2015). Crosstalk between cancer cells and blood endothelial and lymphatic endothelial cells in tumour and organ microenvironment. Expert Rev Mol Med, 17, e3. doi: 10.1017/erm.2015.2

Lee, K. M., Nam, K., Oh, S., Lim, J., Kim, R. K., Shim, D., . . . Shin, I. (2015). ECM1 regulates tumor metastasis and CSC-like property through stabilization of beta-catenin. Oncogene, 34(50), 6055-6065. doi: 10.1038/onc.2015.54

Lee, K. M., Nam, K., Oh, S., Lim, J., Kim, Y. P., Lee, J. W., . . . Shin, I. (2014). Extracellular matrix protein 1 regulates cell proliferation and trastuzumab resistance through activation of epidermal growth factor signaling. Breast Cancer Res, 16(6), 479. doi: 10.1186/s13058-014-0479-6

Martin-Castillo, B., Oliveras-Ferraros, C., Vazquez-Martin, A., Cufi, S., Moreno, J. M., Corominas-Faja, B., . . . Menendez, J. A. (2013). Basal/HER2 breast carcinomas: integrating molecular taxonomy with cancer stem cell dynamics to predict primary resistance to trastuzumab (Herceptin). Cell Cycle, 12(2), 225-245. doi: 10.4161/cc.23274

Mathieu, E., Meheus, L., Raymackers, J., & Merregaert, J. (1994). Characterization of the Osteogenic Stromal Cell Line MN7: Identification of Secreted MN7 Proteins Using Two-Dimensional I'olyacrylamide Gel Electrophoresis, Western Blotting, and Microsequencing. JOURNAL OF BONE AND MINERAL RESEARCH, 9(6), 903-913.

Oyama, N., & Merregaert, J. (2017). The Extracellular Matrix Protein 1 (ECM1) in Molecular-Based Skin Biology. 91-110. doi: 10.1007/978-3-662-47398-6_8

Perou, C. M. (2011). Molecular stratification of triple-negative breast cancers. Oncologist, 16 Suppl 1, 61-70. doi: 10.1634/theoncologist.2011-S1-61

Perou, C. M., Sorlie, T., Eisen, M. B., van de Rijn, M., Jeffrey, S. S., Rees, C. A., . . . Botstein, D. (2000). Molecular portraits of human breast tumours. Nature, 406(6797), 747-752. doi: 10.1038/35021093

Rakha, E. A., & Ellis, I. O. (2009). Triple-negative/basal-like breast cancer: review. Pathology, 41(1), 40-47. doi: 10.1080/00313020802563510

Rankin, E. B., & Giaccia, A. J. (2016). Metastasis as an evolutionary process. Science, 352(6282), 169-175.

Sercu, S., Zhang, L., & Merregaert, J. (2008). The extracellular matrix protein 1: its molecular interaction and implication in tumor progression. Cancer Invest, 26(4), 375-384. doi: 10.1080/07357900701788148

Sercu, S., Zhang, M., Oyama, N., Hansen, U., Ghalbzouri, A. E., Jun, G., . . . Merregaert, J. H. (2008). Interaction of extracellular matrix protein 1 with extracellular matrix components: ECM1 is a basement membrane protein of the skin. J Invest Dermatol, 128(6), 1397-1408. doi: 10.1038/sj.jid.5701231

Sigurdsson, V., Hilmarsdottir, B., Sigmundsdottir, H., Fridriksdottir, A. J., Ringner, M., Villadsen, R., . . . Gudjonsson, T. (2011). Endothelial induced EMT in breast epithelial cells with stem cell properties. PLoS One, 6(9), e23833. doi: 10.1371/journal.pone.0023833

Sorlie, T., Perou, C. M., Tibshirani, R., Aas, T., Geisler, S., Johnsen, H., . . . Borresen-Dale, A. L. (2001). Gene expression patterns of breast carcinomas distinguish tumor subclasses with clinical implications. Proc Natl Acad Sci U S A, 98(19), 10869-10874. doi: 10.1073/pnas.191367098

Sorlie, T., Tibshirani, R., Parker, J., Hastie, T., Marron, J. S., Nobel, A., . . . Botstein, D. (2003). Repeated observation of breast tumor subtypes in independent gene expression data sets. Proc Natl Acad Sci U S A, 100(14), 8418-8423. doi: 10.1073/pnas.0932692100

Takaku, M., Grimm, S. A., & Wade, P. A. (2015). GATA3 in Breast Cancer: Tumor Suppressor or Oncogene? Gene Expr, 16(4), 163-168. doi: 10.3727/105221615x14399878166113

Valastyan, S., & Weinberg, R. A. (2011). Tumor metastasis: molecular insights and evolving paradigms. Cell, 147(2), 275-292. doi: 10.1016/j.cell.2011.09.024

Villadsen, R., Fridriksdottir, A. J., Ronnov-Jessen, L., Gudjonsson, T., Rank, F., LaBarge, M. A., . . . Petersen, O. W. (2007). Evidence for a stem cell hierarchy in the adult human breast. J Cell Biol, 177(1), 87-101. doi: 10.1083/jcb.200611114

Wang, L., Yu, J., Ni, J., Xu, X.-M., Wang, J., Ning, H., . . . Zhang, L. (2003). Extracellular matrix protein 1 (ECM1) is over-expressed in malignant epithelial tumors. Cancer Letters, 200(1), 57-67. doi: 10.1016/s0304-3835(03)00350-1

Wei, S., Zhong, L., Wang, X., & Zhang, W. (2017). Low expression of GATA3 promotes cell proliferation and metastasis in gastric cancer. Cancer Manag Res, 9, 769-780. doi: 10.2147/CMAR.S147973

Wu, Q., Chen, D., Luo, Q., Yang, Q., Zhao, C., Zhang, D., . . . Qi, Z. (2018). Extracellular matrix protein 1 recruits moesin to facilitate invadopodia formation and breast cancer metastasis. Cancer Lett, 437, 44-55. doi: 10.1016/j.canlet.2018.08.022

Figure Legends

Fig. 1: ECM1 is upregulated in D492HER2 and correlates with worse outcome in HER2+ patient tumor samples. A) Upregulated ECM1 gene expression in D492HER2. Relative gene expression of ECM1 in D492 vs. D492HER2 (RT-qPCR). Statistical analysis performed in R, Student´s t-test, *** $p < 0.001$, ** $p < 0.01$, * $p < 0.05$. B) Upregulated ECM1 protein expression in D492HER2. IF staining for ECM1 (red) and DAPI (blue) in D492 vs. D492HER2. Scale bar = 50 µm. C) Increased ECM1 expression in D492HER2 mouse xenografts. IHC staining for ECM1 (brown) in mouse xenografts from D492 vs. D492HER2. Scale bar = 50 µm. D) Decreased DMFS in ECM1+/HER2+ patients. Kaplan-Meier plot (KM-plotter) showing distant metastasis-free survival in patients with HER2+ breast cancer with and without ECM1 expression.

Fig. 2: ECM1 knockdown leads to loss of basal characteristics and gain of GATA3 expression, associated with better outcome. A) Decrease of basal and increase of luminal markers in D492HER2 upon ECM1 knockdown. Relative gene expression of luminal and basal markers in D492HER2 empty ctrl vs. D492HER2-kdECM1 (RT-qPCR). Kruskal-Wallis Test, *** $p < 0.001$, ** $p < 0.01$, * $p < 0.05$. B) ECM1 knockdown upregulates gene expression of GATA3 and downstream targets. Relative gene expression of GATA3 and GATA3 downstream targets in D492HER2 empty ctrl vs. D492HER2-kdECM1 (RT-qPCR). Kruskal-Wallis Test, *** $p < 0.001$, ** $p < 0.01$, * $p < 0.05$. C) Upregulated protein expression of GATA3, CK19 and FN upon ECM1 knockdown. IF staining of GATA3 and selected downstream targets in D492HER2 empty ctrl vs. D492HER2-kdECM1. Scale bar = 50 µM. D) GATA3 expression in HER2+ tumors is associated with increased RFS. Kaplan-Meier plot (KM-plotter) showing relapse-free survival in patients with HER2+ breast cancer with and without GATA3 expression.

Fig. 3: ECM1 knockdown decreases D492HER2 migration and invasion. A) ECM1 knockdown. Relative gene expression of ECM1 in D492HER2 empty ctrl vs. D492HER2-kdECM1 as confirmation of successful stable knockdown (RT-qPCR). Student´s t-test, *** $p < 0.001$, ** $p < 0.01$, * $p < 0.05$. B) Transwell migration assay - setup. Top: Schematic setup of transwell migration and invasion assays. Bottom: Representative binary images of DAPI-stained migratory and invasive cells below the transwell filter after removal of non-migratory/non-invasive cells on top. C) ECM1 knockdown decreases migration and invasion in D492HER2. Quantification of number of migratory and invasive cells on images as shown in B) (n = 3). Student´s t-test, *** $p < 0.001$, ** $p < 0.01$, * $p < 0.05$.

Fig. 4: Schematic summary of ECM1 knockdown decreasing tumorigenic properties of D492HER2. Schematic overview of role of ECM1 in mediating basal marker expression as well as GATA3 and downstream target expression and mediating tumorigenic characteristics. Knockdown of ECM1 results in loss of basal markers and gain of GATA3 expression, as well as decreased migration and invasion capacity.

Supplementary files

Fig. S1: Transient ECM1-KD decreases MDA-MB-231 and D492HER2 migration and invasion. A) Transient ECM1 knockdown decreases migration and invasion in D492HER2. Quantification of number of migratory and invasive D492HER2 cells upon transient ECM1 KD (n = 3). Student´s t-test, *** $p < 0.001$, ** $p < 0.01$, * $p < 0.05$. B) ECM1 overexpression in D492HER2 increases D492 migration and invasion. Quantification of migratory/invasive D492 cells upon ECM1 overexpression. Student´s t-test, *** $p < 0.001$, ** $p < 0.01$, * $p < 0.05$. C) Transient KD of ECM1. Quantification of transient ECM1 KD in D492HER2 on gene expression level using RT-qPCR (10µM siRNA). Student´s t-test, *** $p < 0.001$, ** $p < 0.01$, * $p < 0.05$. D) Overexpression of ECM1. Quantification of ECM1 overexpression

in D492 on gene expression level using RT-qPCR (CRISPR/a). Student´s t-test, *** $p < 0.001$, ** $p < 0.01$, * $p < 0.05$. E) Less RFS in ECM1+/TN breast cancer. Kaplan Meier survival plot for patient with ECM1+ triple-negative (TN) breast cancer (KM-plotter). F) ECM1 knockdown decreases migration and invasion in MDA-MB-231. Quantification of number of migratory and invasive MDA-MB-231 cells upon transient ECM1 KD (n = 3). Student´s t-test, *** $p < 0.001$, ** $p < 0.01$, * $p < 0.05$. G) Transient KD of ECM1. Quantification of transient ECM1 KD in MDA-MB-231 on gene expression level using RT-qPCR (10 µM siRNA). Student´s t-test, *** $p < 0.001$, ** $p < 0.01$, * $p < 0.05$.

Figure 1: ECM1 is upregulated in D492HER2 and correlates with worse outcome in HER2+ patient tumor samples.

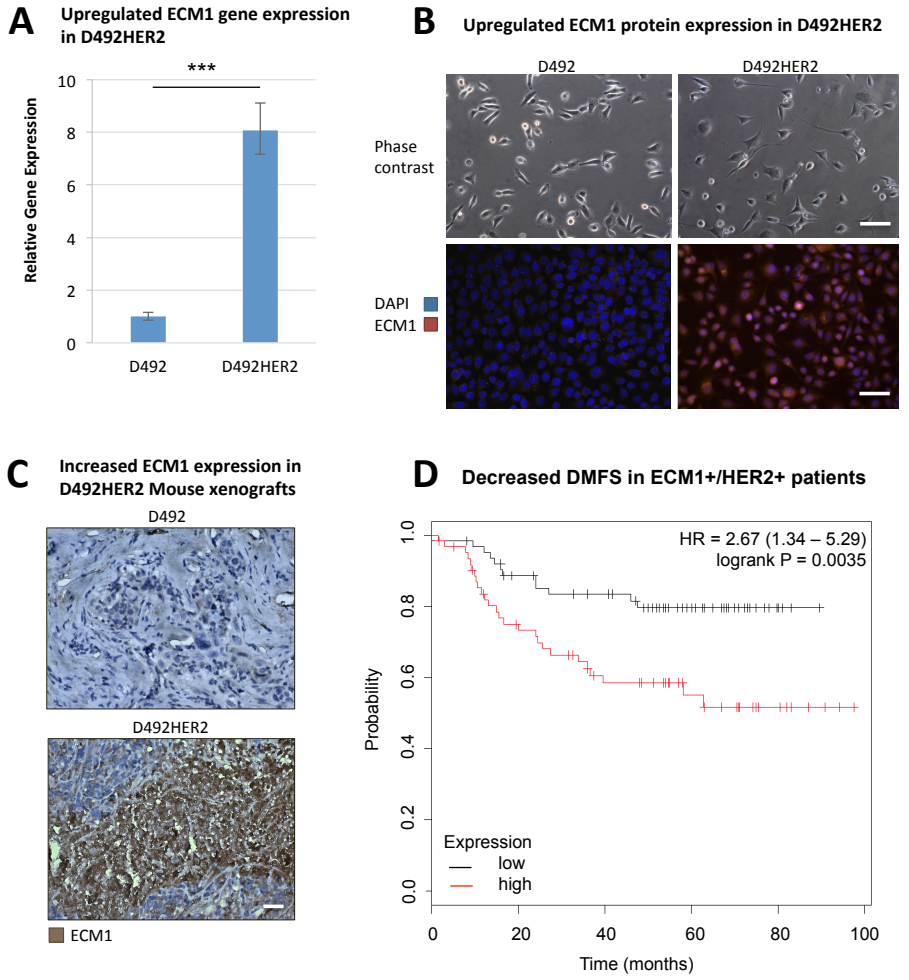


Figure 2: ECM1 knockdown leads to loss of basal characteristics and gain of GATA3 expression, associated with better outcome.

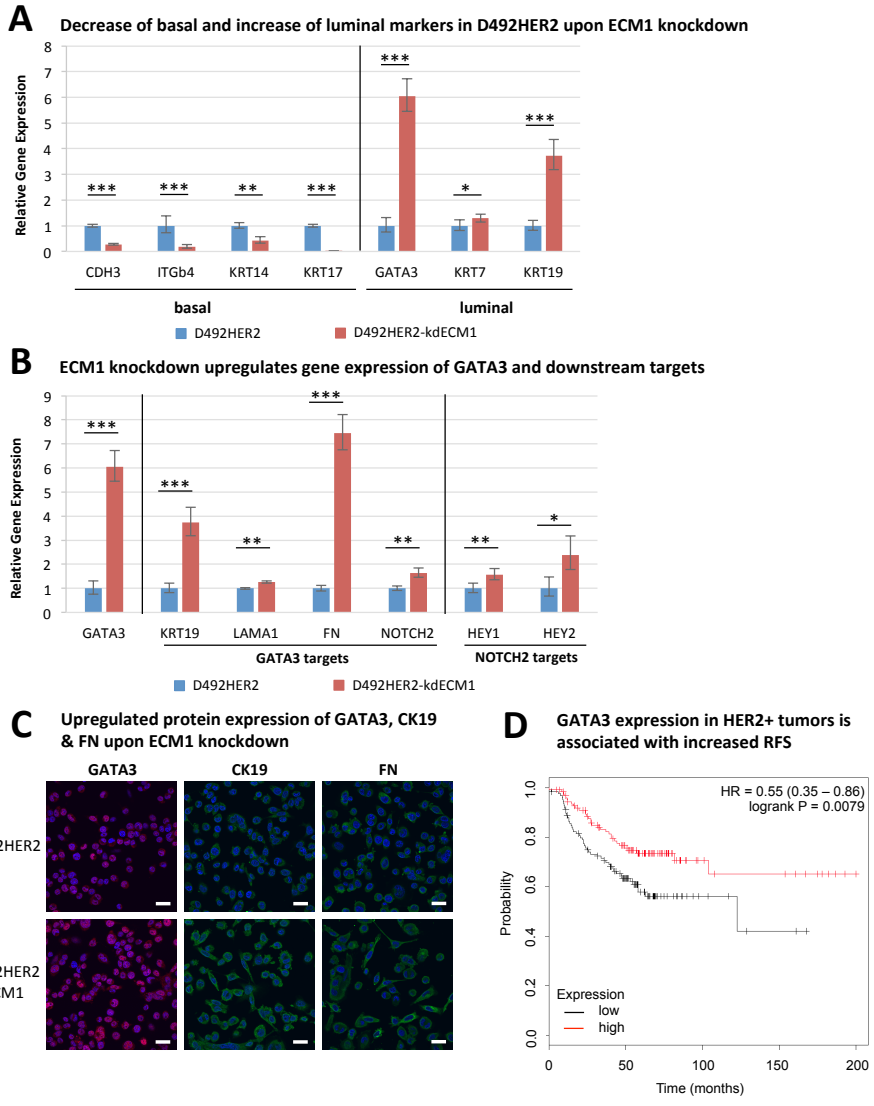


Figure 3: ECM1 knockdown decreases D492HER2 migration and invasion.

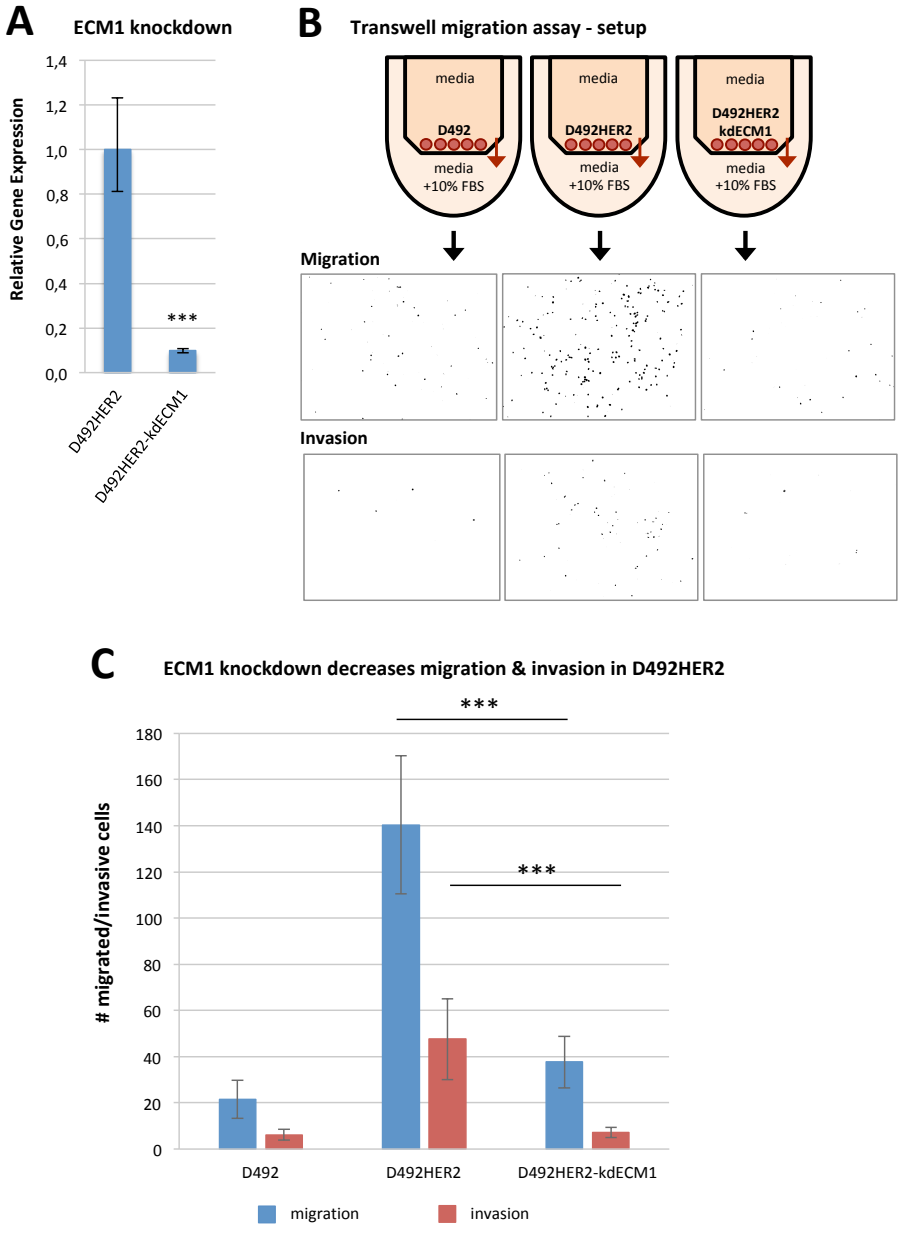
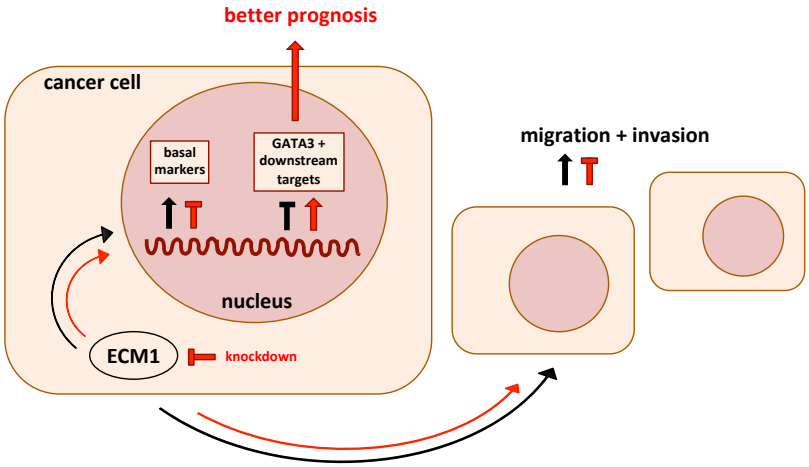
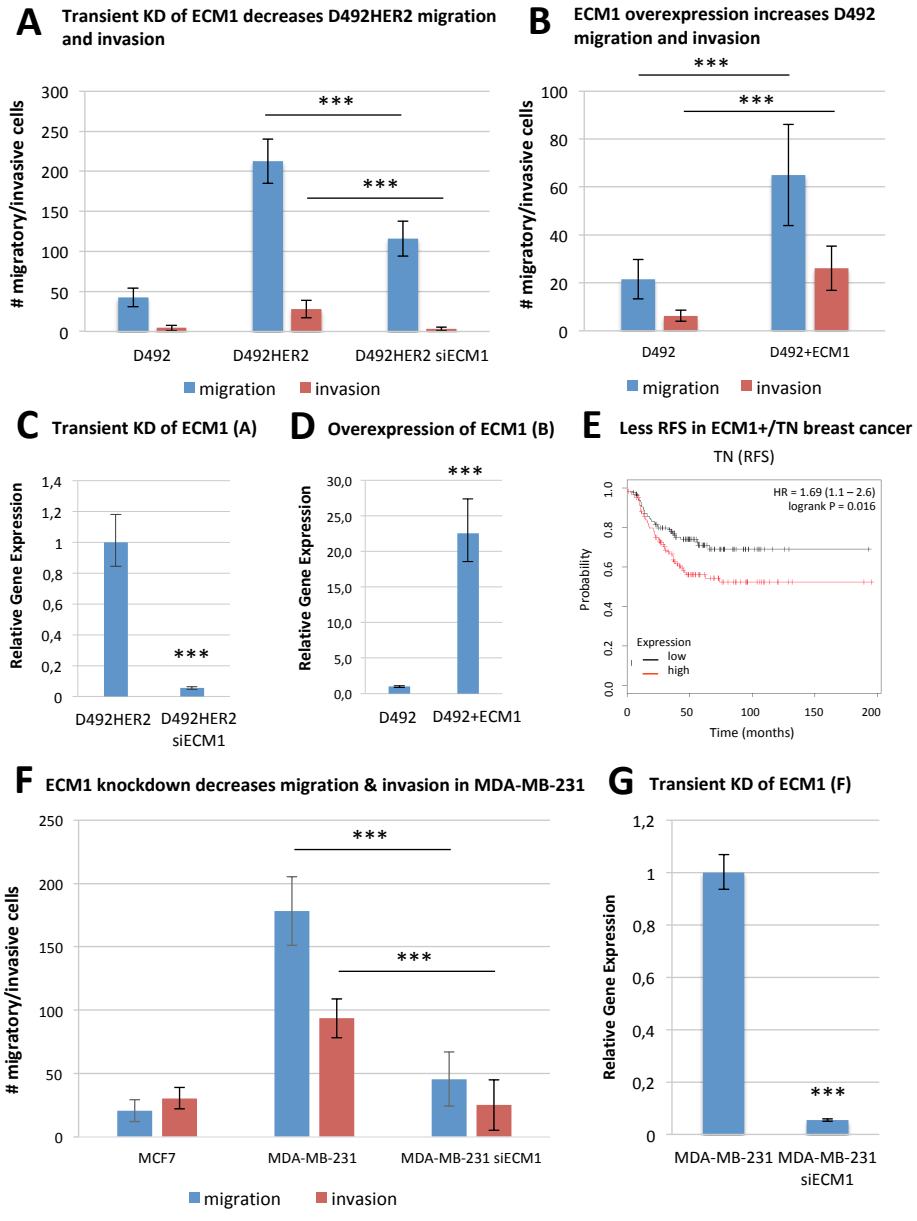


Figure 4: Schematic summary of ECM1 knockdown decreasing tumorigenic properties of D492HER2.



Suppl. Figure S1: Transient ECM1-KD decreases MDA-MB-231 and D492HER2 migration and invasion.



Paper III

In Vitro Cellular & Developmental Biology - Animal
https://doi.org/10.1007/s11626-019-00403-x

YKL-40/CHI3L1 facilitates migration and invasion in HER2 overexpressing breast epithelial progenitor cells and generates a niche for capillary-like network formation

Erika Morera[1] · Sarah Sophie Steinhäuser[1] · Zuzana Budkova[1] · Saevar Ingthorsson[1] · Jennifer Kricker[1] · Aileen Krueger[3] · Gunnhildur Asta Traustadottir[1] · Thorarinn Gudjonsson[1,2]

Received: 10 April 2019 / Accepted: 13 August 2019 / Editor: Tetsuji Okamoto
© The Author(s) 2019

Abstract
Epithelial to mesenchymal transition (EMT) is a developmental event that is hijacked in some diseases such as fibrosis and cancer. In cancer, EMT has been linked to increased invasion and metastasis and is generally associated with a poor prognosis. In this study, we have compared phenotypic and functional differences between two isogenic cell lines with an EMT profile: D492M and D492HER2 that are both derived from D492, a breast epithelial cell line with stem cell properties. D492M is non-tumorigenic while D492HER2 is tumorigenic. Thus, the aim of this study was to analyze the expression profile of these cell lines, identify potential oncogenes, and evaluate their effects on cellular phenotype. We performed transcriptome and secretome analyses of D492M and D492HER2 and verified expression of selected genes at the RNA and protein level. One candidate, YKL-40 (also known as CHI3L1), was selected for further studies due to its differential expression between D492M and D492HER2, being considerably higher in D492HER2. YKL-40 has been linked to chronic inflammation diseases and cancer, yet its function is not fully understood. Knock-down experiments of YKL-40 in D492HER2 resulted in reduced migration and invasion as well as reduced ability to induce angiogenesis in an in vitro assay, plus changes in the EMT-phenotype. In summary, our data suggest that YKL-40 may provide D492HER2 with increased aggressiveness, supporting cancer progression and facilitating angiogenesis.

Keywords YKL-40/CHI3L1 · Epithelial to mesenchymal transition (EMT) · Migration · Invasive breast cancer · Angiogenesis

Introduction

Epithelial to mesenchymal transition (EMT) is a developmental process that describes the plasticity of epithelial cells to change phenotype from compact adherent epithelium to mesenchymal-like cells that have lost their polarity and cell-cell adherence (Thiery *et al*. 2009). This is an important event in normal development, during gastrulation, neural crest formation, and wound healing, but also takes place in malignant processes like fibrosis and cancer (Thiery *et al*. 2009; Nieto 2013). In cancer, EMT is associated with increased aggressiveness and it is believed to be necessary for migration and invasion of cancer cells for the initial steps in the metastatic processes (Thiery *et al*. 2009).

The EMT process is accompanied by increased expression of mesenchymal markers such as vimentin, N-cadherin, α-smooth muscle actin, fibronectin, and/or Axl, as well as decreased or absent expression of epithelial markers like cytokeratins, yet the most referenced change in EMT is the loss of E-cadherin (Peinado *et al*. 2007; Gjerdrum *et al*. 2010). EMT is known to be induced by a number of factors. It can take place due to intrinsic factors such as genetic mutations or epigenetic changes or extrinsic factors like hypoxia or inflammation that stimulate the release of signals from the stroma (Yang *et al*. 2008; Kalluri and Weinberg 2009; Polyak and Weinberg 2009). Transforming growth factor beta (TGF-β) has been

Electronic supplementary material The online version of this article (https://doi.org/10.1007/s11626-019-00403-x) contains supplementary material, which is available to authorized users.

✉ Thorarinn Gudjonsson
tgudjons@hi.is

[1] Stem Cell Research Unit, Biomedical Center, Department of Anatomy, Faculty of Medicine, School of Health Sciences, University of Iceland, Vatnsmyrarvegi 16, 101 Reykjavik, Iceland

[2] Department of Laboratory Hematology, Landspitali - University Hospital, Reykjavik, Iceland

[3] Heidelberg Institute for Stem Cell Technology and Experimental Medicine, Heidelberg, Germany

Published online: 03 September 2019

Table 1. List of primers used in this study. List of gene IDs for all target genes used and their corresponding primer IDs and supplier

Primers	Cat. number	Company
miR-200c	No. YP00204482	Qiagen
miR-203	No. 205914	Exiqon
miR-205	No. 204487	Exiqon
VEGF-A	Hs.PT.58.21234833	IDT
VEGF-C	Hs.PT.58.14602240	IDT
GUCA1C	Hs.PT.58.680712	IDT
CITED1	Hs.PT.58.1567731	IDT
MYBPH	Hs.PT.58.39772389	IDT
YKL-40 /CHI3L1	Hs.PT.58.22570467	IDT
KCNQ1OT1	Hs.PT.58.4572396.g	IDT
ERBB2	Hs.PT.58.1330269	IDT
GPR27	Hs.PT.58.38722549.g	IDT
S100A9	Hs.PT.58.20989743	IDT
DLK1	Hs.PT.58.40622309	IDT
GDF6	Hs.PT.58.20193545	IDT
PXDN	Hs.PT.58.630748	IDT
TLR4	Hs.PT.58.38700156.g	IDT
BMP4	Hs.PT.56a.3848863	IDT
CDH2	Hs.PT.58.26024443	IDT

shown to be a powerful inducer of EMT in a number of cell types (Kasai *et al*. 2005; Willis and Borok 2007; Kalluri and Weinberg 2009). Tyrosine kinase receptors and their ligands like EGF, PDGF, FGF, and HGF have also been shown to induce EMT (Kalluri and Weinberg 2009). Recently, regulatory functions carried out by non-coding RNAs have attracted the attention of researchers. Downregulation of miRNAs, especially members of the miR-200 family, miR-203, and miR-205, have been linked to EMT (Wiklund *et al*. 2010; Moes *et al*. 2012; DeCastro *et al*. 2013; Hilmarsdottir *et al*. 2014, 2015). In epithelial cells, the expression of these miRs is high but is commonly reduced or absent during EMT. Interestingly, rescue of these miRs can revert the EMT phenotype in the process mesenchymal to epithelial transition (MET) (Burk *et al*. 2008; Korpal *et al*. 2008; Hilmarsdottir *et al*. 2014). Furthermore, EMT in cells is often accompanied by increased ability to migrate and invade, as well as increased resistance to apoptosis (Thiery *et al*. 2009). For this reason, EMT has been related to aggressiveness and metastasis in cancer (Thiery 2002; Nieto 2013; Tan *et al*. 2014). The concept of cancer stem cells (CSCs) has also been linked to EMT, where EMT is an integral part of CSC plasticity and survival (Mani *et al*. 2008). Like somatic stem cells, CSCs have the capability to self-renew and their EMT phenotype is believed to be protective against external damages, which could lead to resistance to cancer therapies (Al-Hajj *et al*. 2003; Stingl 2006). In addition, CSCs as a cell population could be the cells responsible for the dissemination of cancer cells and the heterogeneity evidenced in metastasis (Brabletz 2012). Therefore, it is vital to elucidate the role of CSCs in cancer progression in order to improve efficient treatments and targeted therapy.

In breast cancer, the subtype basal-like breast cancer (BLBC) is identified as having the most undifferentiated cells and heterogeneity, which has been linked to CSCs and interestingly has a higher incidence of EMT (Mani *et al*. 2008; Morel *et al*. 2008; Sarrio *et al*. 2008). However, EMT is not exclusively found in this subtype. In luminal and HER2 breast cancers, there is an EMT-derived phenotype, although at a lower percentage (Yu *et al*. 2013; Tan *et al*. 2014).

Resistance to drugs in breast cancer may be associated with EMT-phenotype and heterogeneity of cells in the tumor. It is important to note that states of EMT are not merely defined as completely epithelial or mesenchymal; there are intermediate states of EMT that provide plasticity and advantages to cells to adapt to their microenvironment. This program is referred as partial-EMT (p-EMT) (Huang *et al*. 2013; Nieto 2013; Tam and Weinberg 2013; Yu *et al*. 2013).

The epithelial cells that reside in the breast gland are under continuous remodeling due to hormonal cycling and interactions with the surrounding stroma. This crosstalk is required in normal development and differentiation, and is utilized by tumor cells during cancer progression. Resident fibroblasts and macrophages in the stroma are able to produce growth

Table 2. List of antibodies used in this study. List of primary antibodies (protein IDs, dilution, company, and order IDs) for western blotting and IF staining for candidate proteins

Antibodies	Assay	Cat. number	Company	Dilution
Actin	WB	ab3280	Abcam	1:5000
Axl	IF	CS no. 8661	Cell Signaling	1:100
CK14	WB	ab15461	Abcam	1:1000
CK19	IF	ab7754	Abcam	1:100
E-cadherin	WB	610182	BD Transduction Labs	1:1000
Tubulin	WB	ab6046	Abcam	1:5000
Vimentin	WB	M0725	DAKO	1:1000
YKL-40 /CHI3L1	IF	MABC196	Millipore	1:100
YKL-40 /CHI3L1	WB	MABC196	Millipore	1:500

Table 3. siRNAs used for transient YKL-40 knockdown. Catalog numbers of siRNAs used as negative control and transient knock-down of YKL-40

siRNAs	Product name	Cat. number	Company
Neg Ctrl siRNA	Silencer® Select Negative Control No. 1 siRNA	4390843	ThermoFisher Scientific
YKL-40 siRNA 1	Silencer® Select CHI3L1 siRNA 1	AM16708 (ID 119124)	ThermoFisher Scientific
YKL-40 siRNA 2	Silencer® Select CHI3L1 siRNA 2	AM16708 (ID 119126)	ThermoFisher Scientific

factors and pro-inflammatory molecules, but also pro-angiogenic molecules that support the creation of new blood vessels. Fibroblasts not only interact with epithelial cells, they also activate the action of immune cells like macrophages and promote angiogenesis by cell communication with endothelial cells. The vascular endothelial growth factor (VEGF) and TGF-β are secreted by fibroblasts and macrophages, and they are able to stimulate angiogenesis. TGF-β induces the expression of VEGF that is secreted to the ECM and stimulates endothelial cells to initiate angiogenesis (Relf *et al*. 1997; Carmeliet and Jain 2000).

There is also direct interaction between epithelial cells and endothelial cells. The vascular niche plays an important role in transporting oxygen and nutrients and releasing signals for its correct morphogenesis and development. Indeed, it has also been observed that endothelial cells increase growth and branching morphogenesis of breast epithelium (Shekhar *et al*. 2000; Sigurdsson *et al*. 2006; Ingthorsson *et al*. 2010) and induce EMT (Sigurdsson *et al*. 2011). In the context of cancer, the high proliferation rate of tumor cells can lead to a reduction in oxygen concentration resulting in acidification of the surrounding stroma. In order to survive, cancer cells are able to secrete signals that induce angiogenesis, such as VEGF (Hanahan and Weinberg 2011). Receptors on endothelial cells, such as VEGFR2, are induced to trigger activation of the transcriptional machinery of angiogenesis that involves the hypoxic inducible factor 1 (HIF1) and other factors like nuclear factor κB (NF-κB) (Vegran *et al*. 2011; Sonveaux *et al*. 2012). The increase in angiogenesis ensures oxygen and a nutrient supply and therefore results in a worse prognosis of the cancer, making it an important factor to study.

D492 is a breast progenitor epithelial cell line that was established by immortalization of a suprabasal subpopulation of breast tissue from a healthy donor (Gudjonsson *et al*. 2002). As reviewed in Briem *et al*. (2019), D492 can generate both luminal and myoepithelial cells, and in 3D culture forms branching terminal ductal lobular units (TDLU) like structures (Briem *et al*. 2019). We have previously demonstrated that when D492 is co-cultured with breast endothelial cells (BRENCs), a subpopulation of cells undergoes EMT. One such subpopulation was isolated, giving rise to the D492M cell line, which has a fixed mesenchymal phenotype (Sigurdsson *et al*. 2011). In addition, we have shown that D492 cells with forced overexpression of the HER2 oncogene (D492HER2) have lost their epithelial phenotype and gained a mesenchymal one (Ingthorsson *et al*. 2015).

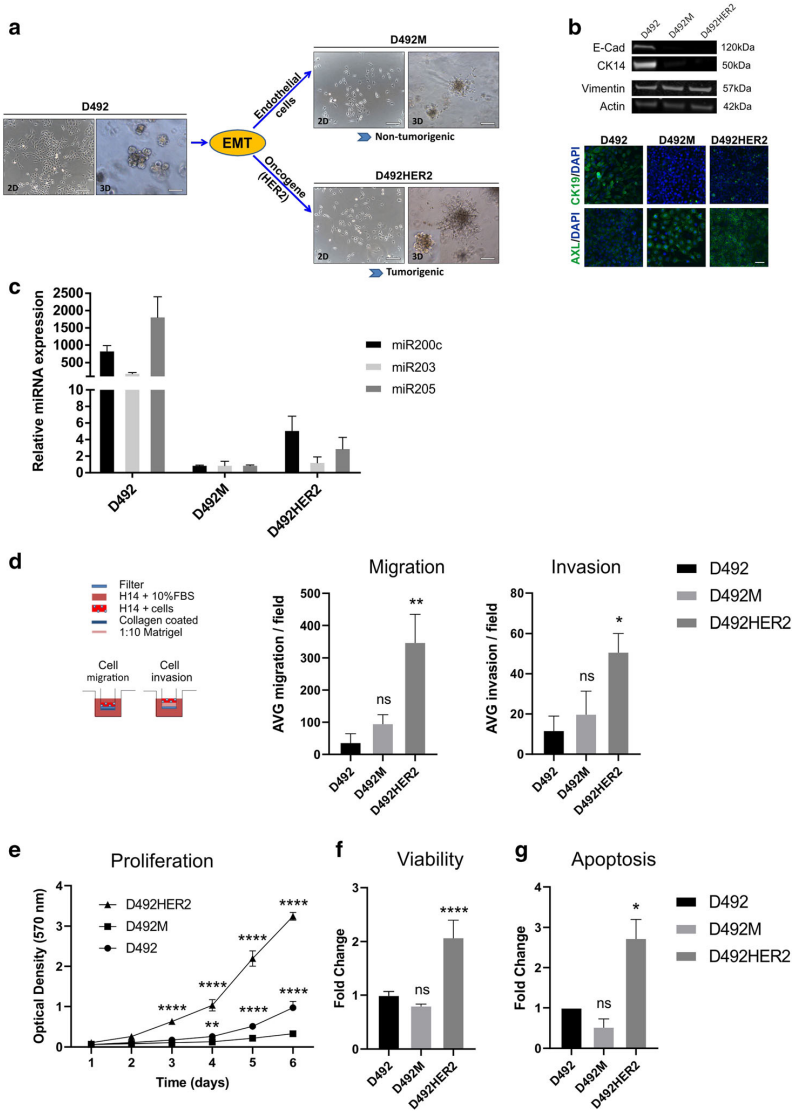
In this study, we have compared functional and phenotypic differences between D492M and D492HER2. We show here that D492HER2 proliferates, migrates, and invades faster than D492M. Furthermore, glucose metabolism is more dependent on glycolysis than oxidative phosphorylation in D492HER2. The comparative analysis of transcriptome revealed that a glycoprotein, YKL-40, also known as CHI3L1, is highly upregulated in D492HER2 and may contribute to the differences in tumorigenicity between the cell lines. YKL-40 has previously been linked to chronic inflammation diseases and cancer (Libreros *et al*. 2012; Jefri *et al*. 2015; Libreros and Iragavarapu-Charyulu 2015; Cohen *et al*. 2017); however, its function is not clearly understood yet. Functional studies using knockdown of YKL-40, recombinant protein, and overexpression experiments reveal that YKL-40 influences migration, invasion, and angiogenesis and induces changes in the EMT phenotype.

Material and Methods

Cell culture (2D and 3D) The main cell lines used in this project were D492 (Gudjonsson *et al*. 2002) and its EMT-phenotype-derived cell sublines D492M (Sigurdsson *et al*. 2011) and D492HER2 (Ingthorsson *et al*. 2015). For monolayer culture, flasks or plates were pre-coated with collagen I (2.2%) (no. 5005-B, Advanced BioMatrix, Carlsbad, CA). The medium used for culturing the cell lines was H14 (Blaschke *et al*. 1994), an enriched serum-free medium based on DMEM:F12 in which growth factors are added (insulin,

Table 4. gRNAs used for generating stable cell lines. Names and sequences of gRNAs used to either knockdown or overexpress YKL-40

gRNAs	Sequence	Action	Company
YKL-40/CHI3L1 KD	CCGCCATTTCTGCGCACCCA	Knockdown	
YKL-40/CHI3L1 SAM OV 1	AGTTTTGAAAACTTTGGGTC	Overexpress	Genscript
YKL-40/CHI3L1 SAM OV 2	CTGCCAGCAGAAGAGCCACT	Overexpress	Genscript



transferrin, EGF, sodium selenite (NaSel), estradiol, hydrocortisone, prolactin).

Human umbilical vein endothelial cells (HUVECs) were isolated from umbilical cords obtained from Landspitali University Hospital, Reykjavik, Iceland, with informed consent and approved by the Landspitali ethical committee (No. 35/2013). HUVECs were cultured in EGM2 + 5% FBS (no. CC-3162, Lonza).

In 3D cultures, cells were cultured in 300 μL of Matrigel (no. 354230, Corning, Corning, NY) per well, in 24-well plates (no. 353047, Corning, Corning, NY). In monoculture, 20,000 cells were embedded in reconstituted basement membrane, rBM, purchased as Matrigel (Corning no. 354230), with 500 μL of H14 media on top, while in co-cultures, 500 cells of D492 or its sublines were co-cultured with 150,000–200,000 HUVECs, embedded in Matrigel, with 500 μL of EGM2 + 5% FBS media on top.

Gene expression levels by qRT-PCR Total RNA was isolated with cold Tri-Reagent reagent (no. AM9738, Life Technologies, Carlsbad, CA). RNA precipitation was done using isopropanol and centrifugation at 14,000 rpm for 20 min.

◀ **Figure 1.** Phenotypic and functional characterization of D492M and D492HER2 cell lines. (*a*) D492M and D492HER2 are isogenic EMT-derived sublines of D492, a breast epithelial cell line with progenitor properties, which in 3D cell culture forms branching structures, resembling the TDLUs of the breast. D492M and D492HER2 were generated when D492 underwent endothelial-induced and oncogene (HER2)-induced EMT, respectively. D492M and D492HER2 show similar EMT-phenotype in 2D, but in 3D, D492M generate spindle-like colonies whereas D492HER2 generate spindle-like and grape-like colonies. D492M and D492HER2 also differ in their ability to generate tumors, as only D492HER2 is able to form tumors. *Scale bar* = 200 μm. (*b*) D492M and D492HER2 have lost expression of epithelial markers (E-cadherin, cytokeratin-14, and cytokeratin-19) and gained expression of mesenchymal markers (Axl and vimentin) as shown by western blotting and immunofluorescence. *Scale bar* = 100 μm. (*c*) D492M and D492HER2 show reduction in the expression of epithelial microRNAs such as miR-200c, miR-203, and miR-205 compared to D492. The lowest levels of expression are found in D492M (mean ± SD, $n = 2$). (*d*) In transwell migration and invasion assays, D492HER2 has an increased ability to migrate and invade compared to D492 and D492M. Results are shown as average number of cells per field (mean ± SEM, $n = 3$). One-way analysis of variance (ANOVA) and Dunnett's multiple comparison test were used to test significance ($*p \le 0.05$, $**p \le 0.01$). (*e*) D492HER2 cells proliferate at a higher rate than D492 and D492M cells as shown by staining with crystal violet. Results are shown as average of four replicates (mean ± SD). Statistical significance was assessed using multiple *t* tests (one per *row*) ($**p \le 0.01$, $****p \le 0.0001$). (*f*) Furthermore, increased proliferation rate of D492HER2 compared to D492 and D492M cells was demonstrated using PrestoBlue™ Cell Viability reagent. Results are shown as average of eight replicates normalized to D492 (mean ± SD). One-way analysis of variance (ANOVA) and Dunnett's multiple comparison test were used to test significance ($****p \le 0.0001$). (*g*) In addition, D492HER2 cells are more susceptible to chemically induced apoptosis as compared to D492 and D492M cells. Caspase 3/7 luciferase activity was measured by luminescence and normalized to D492 (mean ± SEM, $n = 2$). Significance was assessed with one-way analysis of variance (ANOVA) and Dunnett's multiple comparison test ($*p \le 0.05$).

Afterwards, RNA was washed with ethanol two times. The RNA pellet was diluted in RNAse free water. Concentration of RNA was measured using a NanoDrop® ND-1000 UV/Vis-Spectrophotometer (Thermo Fisher Scientific, Waltham, MA). For cDNA synthesis, SuperScript IV (no. 18090-200, Thermo Fisher Scientific) and random hexamer primers were used.

To quantify the expression level of genes, TaqMan (no. M3004L, NEB) or SYBR Green (no. M3003L, NEB) chemistries were used to detect gene expression. Comparative Ct values were determined using an ABI 7500 instrument (Applied Biosystems, Foster City, CA). All used primers are listed in Table 1. GAPDH was used as the reference gene.

Expression levels of miRNAs by qRT-PCR Total RNA was extracted with Tri-Reagent (no. AM9738, Thermo Fisher Scientific). The RNA was reverse transcribed using miRCURY LNA RT Kit (no. 339340, Qiagen, Hilden, Germany) for cDNA synthesis reactions. Quantitative RT-PCR analysis of miRNAs was performed using miRCURY LNA SYBR Green PCR Kit (no. 339346, Qiagen). Relative expression was calculated with the $2^{\Delta\Delta Ct}$ method. All used primers are listed in Table 1. Normalization was done with U6 (no. 203907, Exiqon, Vedbaek, Denmark).

Protein levels by Western Blot (WB) Protein isolation was done using RIPA buffer, and the concentration was measured by the colorimetric Bradford method. Equal amount of protein was loaded for each sample (5 μg) in precast NuPAGE 10% Bis-Tris gels (Invitrogen, Carlsbad, CA). Proteins were detected using IRDye secondary antibodies on an Odyssey imaging system (Li-Cor Biosciences, Lincoln, NE). Loading controls actin or tubulin were used for quantification. Antibodies used for WB are listed in Table 2.

Immunostaining Immunofluorescence (IF) was used to detect proteins and visualize their subcellular location. Cells were fixed with 3.7% paraformaldehyde (PFA) and permeabilized with 0.1% Triton X-100. Blocking with FBS was done prior to incubation with primary antibodies. Incubation was done overnight at 4°C and followed by incubation of secondary antibodies conjugated to fluorochromes Alexa Fluor-488, Fluor-546, or Fluor-647 for 1 h at room temperature. For nuclei staining, DAPI was used. Imaging was done using an EVOS FL Auto 2 Cell Imaging System (Thermo Fisher Scientific) or FV1200 Olympus inverted confocal microscope. Antibodies used for IF are listed in Table 2.

Transcriptome data analysis and classification Total RNA sequence profiles for D492, D492M, and D492HER2 were obtained from normal cell cultures and treated following the protocol detailed in Halldorsson *et al.* (2017).

Differentially expressed genes between cell lines were further classified into categories to see the biological processes that were enriched. Using a differential range from two fold change, genes were analyzed by the PANTHER analysis database (www.pantherdb.org) following instructions of Mi *et al.* (2013).

Secretome data analysis For mass spectrometry, D492 lines were grown in T175 flasks (no. 353112, Corning) and conditioned medium (CM) was collected, concentrated for 55 min using EMD Millipore Amicon™ Ultra-15 Centrifugal Filter Units (no. UFC900324, Merck Millipore, Darmstadt, Germany) followed by buffer exchange to 100 mM TRIS/HCl buffer. Triplicate samples were stored at − 80°C. Label-free relative protein quantification by nLC MS/MS after trypsin digestion was performed at the FingerPrints Proteomics Facility, University of Dundee, Dundee, UK and raw data were analyzed using MaxQuant software (version 1.6.2.1). Quantitative and statistical analyses were performed using XLStat (version 2018.1). Data were *P* value corrected (significance level 0.05)

a

Feature ID	D492 HER2 vs D492M Fold change	Higher/Lower expression confirmed by qPCR
GUCA1C	594.2	Almost not expressed
CITED1	306.1	D492HER2 > D492M
MYBPH	304.1	Similar expression
CHI3L1	199.2	D492HER2 > D492M
KCNQ1OT1	175.8	D492HER2 > D492M
ERBB2	136.1	D492HER2 > D492M
LINC00958	114.2	No
GPR27	73.3	D492HER2 > D492M
S100A9	71.0	D492M > D492HER2
DLK1	68.7	D492HER2 > D492M
More than 3.000 transcripts		
BMP4	-105.0	D492M > D492HER2
CDH2	-111.6	D492M > D492HER2
TLR4	-149.0	D492M > D492HER2
PXDN	-219.4	D492M > D492HER2
GDF6	-835.8	Similar expression

b

Enriched PANTHER GO Biological Processes in D492HER2 compared to D492M	Fold enrichment	P-value
D-aspartate transport (GO:0070777)	100	3.05E-02
inflammatory response (GO:0006954)	3.16	4.10E-04
cell chemotaxis (GO:0060326)	3.01	1.03E-02
cytokine-mediated signaling pathway (GO:0019221)	2.79	3.15E-02
regulation of neurotransmitter levels (GO:0001505)	2.72	4.02E-02
cellular response to cytokine stimulus (GO:0071345)	2.55	1.58E-02
organic anion transport (GO:0015711)	2.35	4.22E-02
cell proliferation (GO:0008283)	2.17	5.71E-03
defense response (GO:0006952)	2.09	4.70E-03
vasculature development (GO:0001944)	-2.02	4.95E-02
skeletal system development (GO:0001501)	-2.1	1.83E-02
circulatory system development (GO:0072359)	-2.23	1.84E-02
regulation of synapse structure or activity (GO:0050803)	-2.69	1.00E-02
sensory organ development (GO:0007423)	-2.77	2.85E-03
sensory organ morphogenesis (GO:0090596)	-3.54	1.44E-02
regulation of cartilage development (GO:0061035)	-4.5	3.96E-02
eye morphogenesis (GO:0048592)	-4.67	1.10E-02
negative regulation of embryonic development (GO:0045992)	-11.37	3.05E-02

c

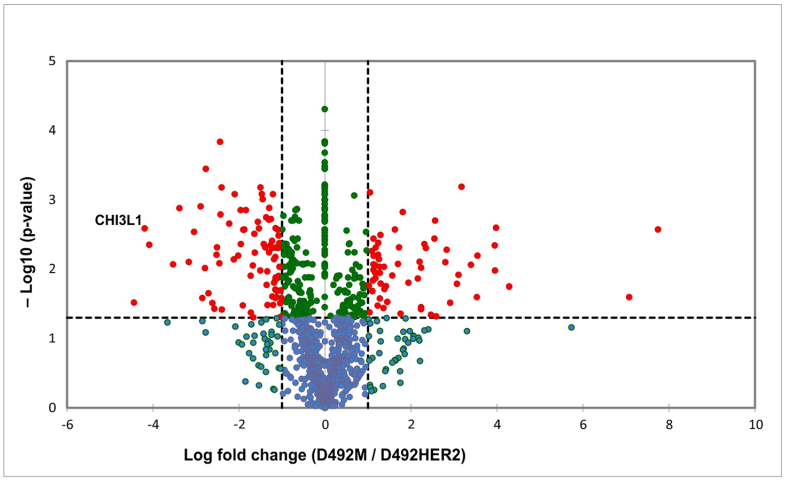


Figure 2. YKL-40 is enriched in D492HER2. *a* The analysis of transcriptome data comparing D492M and D492HER2 revealed more than 3000 transcripts differently expressed (more than two fold). YKL-40 (or CHI3L1) is more highly expressed in D492HER2 compared to D492M. *b* Classification of genes in biological processes shows an enrichment in D492HER2 compared to D492M in D-aspartate transport, inflammatory response, cell chemotaxis, cytokine-mediated signaling pathway, regulation of neurotransmitter levels, cellular response to cytokine stimulus, organic anion transport, cell proliferation, and defense response. YKL-40 is involved in the processes that require interaction with the stroma: inflammatory response, cell chemotaxis, cellular response to cytokine stimulus, and defense response (marked with *yellow*). *c* Mass spectrometry analysis of secreted proteins in CM revealed that YKL-40 is enriched in the secretome of D492HER2 compared to D492M (p value = 0.01).

and sorted based on ≥2-fold higher secretion (LFQ intensity) by D492HER2 compared to D492M.

Migration and invasion assays Migration and invasion assays were done in 24-well plates with transwell filter inserts (no. 353097, Corning) of 8 μm size pore diameter. Transwell inserts in the migration assay were pre-coated with collagen I (2.2%) and in the invasion assay; they were pre-coated with Matrigel diluted 1:10 in H14 media. Fifty thousand cells/transwell were seeded on the upper chamber in H14 media. In the bottom chamber, H14 was supplemented with 10% FBS as a chemoattractant. A cotton swab was used to remove non-migrated and non-invaded cells after 24 h and after 48 h, respectively. Thereafter, cells were fixed with 3.7% PFA and

stained with crystal violet (10%) or DAPI (1:5000 dilution) for 30 min. Three random pictures were taken per well and the number of cells was quantified. For DAPI-stained samples, images were converted to 8-bit in ImageJ (version 2.0.0), threshold-adjusted, and binary-converted and migratory/invasive cells were counted using the *analyze particles* function.

Proliferation assay Proliferation of cells was determined by seeding 10,000 cells/well in triplicate in 24-well plates in H14 (D492 cell lines) or EGM5 (HUVECS). Every day (2 d for HUVECs), cells were fixed and stained with crystal violet (10%). Crystal violet was diluted with acetic acid and the OD was measured at 570 nm wavelength. Alternatively, cell viability was assessed using PrestoBlue™ Cell Viability Reagent (ThermoFisher Scientific, Waltham, MA). Cells were seeded in H14 media in a 96-well plate at a density of 3000 cells/well and cultured for 4 d. PrestoBlue was added (1/10th of the total volume) to each well and incubated for 4 h, and absorbance was read on a plate reader at 570 nm and 595 nm.

Apoptosis assay To quantify apoptosis, cleavage of caspase 3/7 was measured by a luciferase assay (ApoTox-GloTM Triplex Assay, Promega, Madison, WI). Apoptosis was induced by incubating cells with 10 μM camptothecin (CPT) for 24 h according to the manufacturer's protocol. After cellular lysis, luciferase was measured with a microplate reader ModulusTM II (Turner Biosystems, Sunnyvale, CA).

Glucose consumption and lactate production measurements Glucose uptake was measured using Glucose Uptake-GloTM kit (no. J1341, Promega) following the manufacturer's protocol. Briefly, the analogue of glucose, 2-deoxyglucose (2DG), was added to the media and taken up by cells. When transported into cells, 2DG is phosphorylated to 2-deoxyglucose 6-phosphate (2DG6P) and further metabolization stimulates luciferase reactions and luminescence was measured by the microplate reader Modulus TM II (Turner Biosystems, Sunnyvale, CA).

Glucose consumption and lactate production were measured from the collected media when cells were in a high confluency. Metabolites were measured at the Analyzer machine (ABL90 FLEX Analyzer, Radiometer) at the Blood Bank of Landspitali (Reykjavik, Iceland).

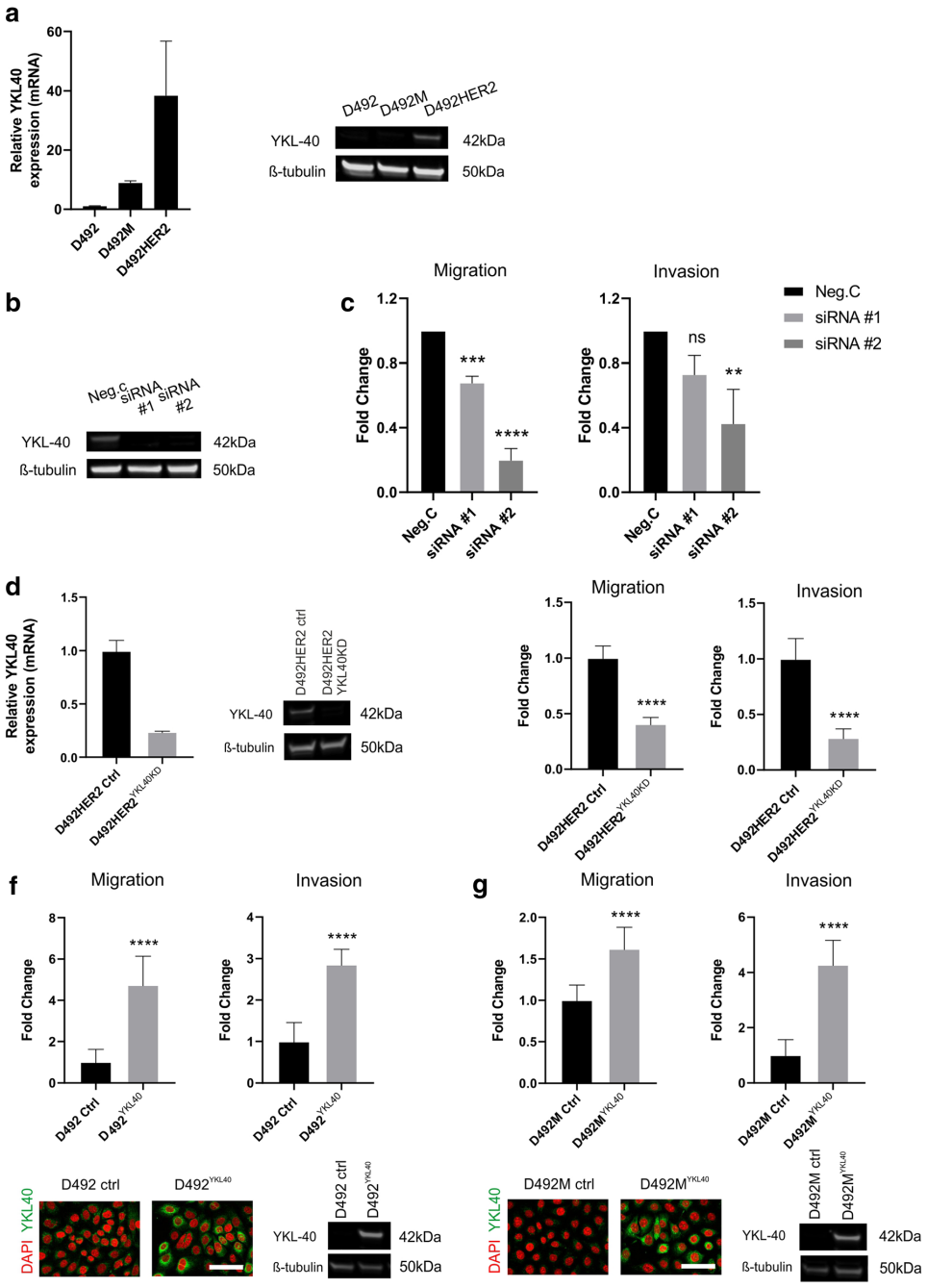
Neutralization assay of YKL-40 protein A monoclonal antibody against YKL-40 (mA^{YKL40}) (MABC196, Millipore) was used to block the secretion of YKL-40 in D492HER2. The antibody was diluted in fresh H14 medium at a concentration of 10 μg/mL. Medium from cells incubated for 24 h with mA^{YKL40} was collected, and medium from non-treated D492HER2 cells was used as control. Conditioned media (CM) were used for tube formation assays (described below).

Tube formation assay on endothelial cells (angiogenesis assay in vitro) To simulate angiogenesis in vitro, 10,000–12,000 HUVECs were seeded on top of 10 μL solidified rBM in a 96-well angiogenesis plate (no. 89646, Ibidi). Controls included HUVECs cultured in EGM5 media and a dilution of 1:1 EGM5 and conditioned media (CM). Recombinant YKL-40 protein (YKL-40^r) (no. 11227H08H5, Thermo Fisher Scientific, Waltham, MA) was added to the medium at a final concentration of 100 ng/mL. After incubation overnight, the endothelial network was imaged using the EVOS FL Auto 2 Cell Imaging System. Analysis and quantification were done using the *Angiogenesis analyzer* plug-in on ImageJ software (version 2.0.0).

Transient knockdown of YKL-40 by siRNA Pre-designed siRNAs (Silencer® Select Pre-Designed, Validated and Custom siRNA, Life Technologies) against YKL-40 were used at a concentration of 10 nM in D492HER2 cells to down-regulate YKL-40. First, cells were seeded on 6-well plate (no. 353046, Corning, Corning, NY) and after 24 h, cells were transfected with the siRNA using chemical transfection with Lipofectamine® RNAiMAX (no. 13778150, Life Technologies, Carlsbad, CA). For each experiment, two different siRNAs against YKL-40 and a negative control siRNA (no. 4390843, Life Technologies, Carlsbad, CA) were used. The siRNAs are listed in Table 3. After 48 h, the knockdown was confirmed by qRT-PCR and by WB.

Generation of stable cell line with knockdown of YKL-40 in D492HER2 by CRISPR Specific gRNAs to knockdown YKL-40 were designed with the publicly available online ATUM CRISPR tool (https://www.atum.bio/). Annealing of the forward and reverse gRNA oligos was followed by ligation with the backbone vector pMLM3636. High-efficiency competent bacteria (no. C2987H, NEB) were transformed, and confirmation of successful DNA insertion was done by colony PCR. Plasmids were sequenced to confirm correct gRNA sequences. Transfection of D492HER2 was done with four plasmid gRNAs and a plasmid with only a Cas9 cassette (pST1374) using Lipofectamine® 3000 (Thermo Fisher). The control cell line was generated by transfecting the cells with only the Cas9 cassette. Selection of cells with insertion of Cas9 was done using blasticidin. Knockdown of YKL-40 in D492HER2 was confirmed by qRT-PCR and WB. Subsequently, the cell line that gave the best efficiency of knockdown was selected for further work. The sequence of this gRNA is in Table 4. It should be noted that D492HER2 is a cell line not suitable for single-cell cloning; therefore, a pool of cells was used for confirmation of knockdown and further experiments.

Generation of stable cell lines overexpressing YKL-40 in D492 and D492M by CRISPRa Overexpression of YKL-40 in D492



and D492M was carried out using the modified CRISPR strategy, called CRISPRa (Zhang *et al*. 2015). Two specific SAM gRNAs for YKL-40 and one empty control were purchased from Genscript containing zeomycin resistance cassettes. The gRNA sequences are listed in Table 4. Transfection of HEK293T cells was done to produce viral particles including gRNAs. Viruses collected were used to infect D492 and D492M cells that were previously transfected with dCas9-

◀ **Figure 3.** YKL-40 affects migration and invasion in D492 cell lines. *a* YKL-40 is more highly expressed in D492HER2, compared to D492 and D492M, both at mRNA and protein level. *b*, *c* Transient siRNA knock-down of YKL40 reduced the ability of D492HER2 to migrate and invade in vitro (mean ± SD, $n = 3$). Statistical significance was tested using one-way analysis of variance (ANOVA) and Dunnett's multiple comparison test (**$p \leq 0.01$, ***$p \leq 0.001$, ****$p \leq 0.0001$). *d*, *e* Knock-down of YKL-40 in D492HER2 in stable cell lines generated by CRISPR/Cas9 technology reduced the ability of D492HER2 to migrate and invade similarly to transient transfection. *f*, *g* Accordingly, overexpression of YKL40 in D492 and D492M using CRISPRa system increased their ability to migrate and invade. Overexpression of YKL-40 was confirmed by immunofluorescence staining (*Scale bar* = 100 μm) and western blotting. Migration and invasion assay results are shown as average of eight replicates (mean ± SD). Unpaired *t* test was used to test significance (**$p \leq 0.01$, ***$p \leq 0.001$, ****$p \leq 0.0001$).

VP64 to activate the promoter and later induce overexpression of the selected gene. Transduction with gRNAs was performed and selection was done with zeocin (no. R25005, Thermo Fisher Scientific). Confirmation of overexpression of YKL-40 in D492 and D492M was done by qRT-PCR, WB, and IF.

Statistical analysis One-way analysis of variance (ANOVA) using Dunnett's multiple comparison test or unpaired *t* tests were performed using GraphPad Prism to test significance. *P* values below 0.05 were considered significant (*$p \leq 0.05$, **$p \leq 0.01$, ***$p \leq 0.001$, ****$p \leq 0.0001$).

Results

Phenotypic and functional characterization of D492M and D492HER2 D492M and D492HER2 are isogenic cell lines that share a partial-EMT phenotype but are different in terms of their ability to form tumors in mice (Sigurdsson *et al*. 2011; Ingthorsson *et al*. 2015). D492M and D492HER2 are both derived from D492, a breast epithelial progenitor cell line, through endothelial-induced EMT and oncogene-induced EMT, respectively (Fig. 1*a*). D492M and D492HER2 have lost the expression of epithelial markers like E-cadherin, CK14, and CK19 and gained expression of some mesenchymal markers like vimentin and Axl, (Fig. 1*b*). MicroRNAs (miRs) such as miR-200c, miR-203, and miR-205 are frequently down-regulated in epithelial cells undergoing EMT, and this was the case for D492M and D492HER2. While D492 showed high expression of miR-200c, miR-203, and miR-205, these microRNAs were greatly reduced in D492HER2 and relatively absent in D492M (Fig. 1*c*). The difference in expression levels between D492M and D492HER2 may have been due to a more intermediate state of EMT for D492HER2. This intermediate state was also supported by the glucose metabolism (Fig. S1). These data show D492HER2 is more comparable in glucose uptake to D492 than D492M.

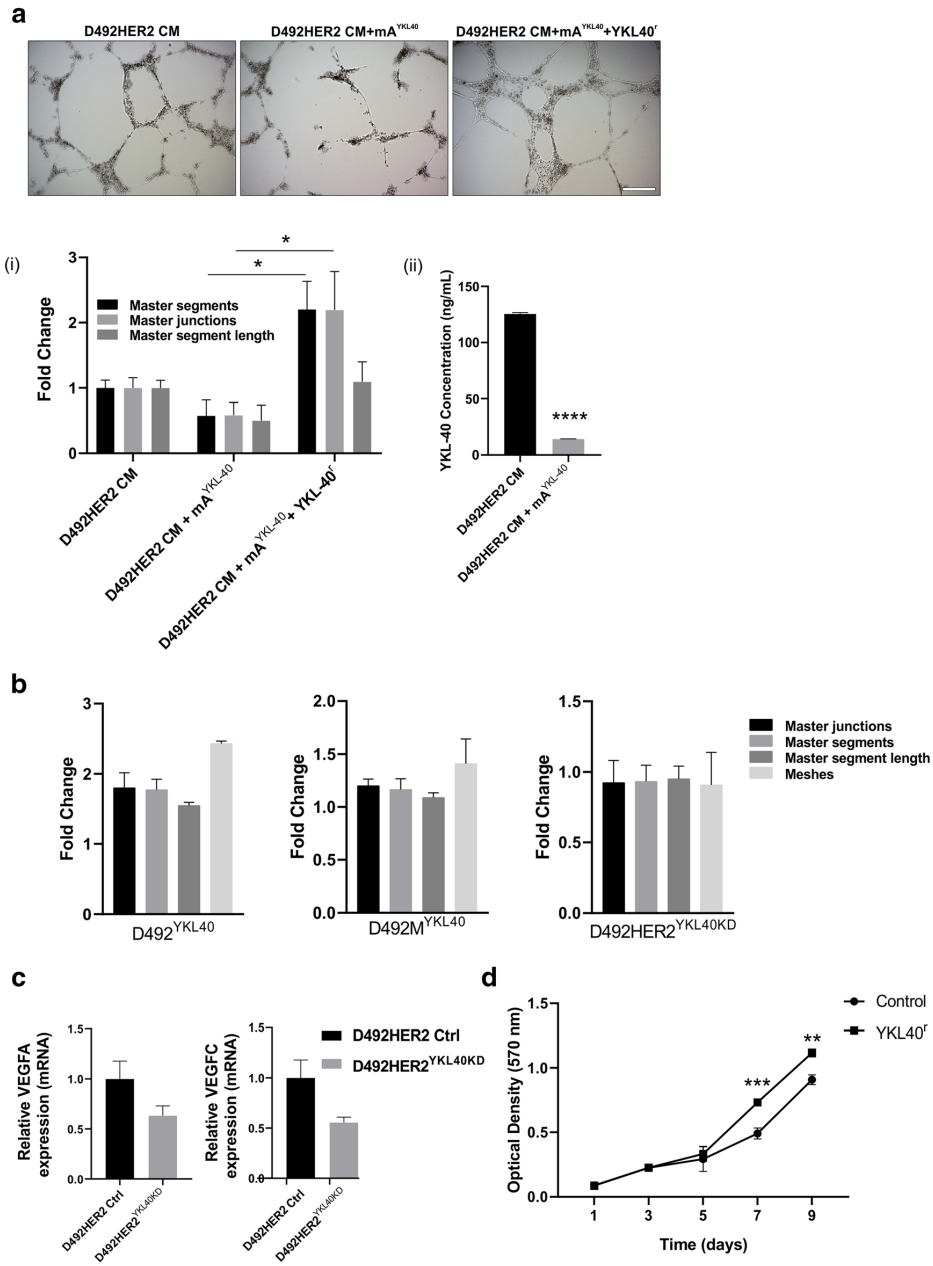
Further characterization demonstrated functional differences between the cell lines. Notably, D492HER2 cells migrated and invaded through transwell filters more efficiently than both D492M and D492 (Fig. 1*d*). The cell proliferation rate of D492HER2 cells was also significantly higher than in D492 and D492M cells (Fig. 1*e*, *f*). Furthermore, D492HER2 cells were more susceptible to chemically induced apoptosis than D492 and D492M cells (Fig. 1*g*), despite an apparent shift from oxidative phosphorylation to glycolysis as D492HER2 had higher glucose consumption and higher lactate production than either D492 or D492M cells (Fig. S1).

The functional differences between D492M and D492HER2 in terms of tumorigenicity prompted us to look into gene expression and secretome of D492M and D492HER2 to search for potential candidates responsible for these effects.

Transcriptome and secretome analyses show that YKL-40 is enriched in D492HER2 Next, we employed genome-wide analysis to reveal differences in gene expression in D492M and D492HER2. More than 40,000 transcripts were differentially expressed between D492M and D492HER2 and the most 15 differentially regulated genes were confirmed by qPCR (Fig. 2*a*). As expected, HER2 (ErbB2) has much higher expression in D492HER2 cells due to the ectopic overexpression of the gene (Ingthorsson *et al*. 2015). Although CITED1 was the first validated candidate, its absolute level of expression was low; thus, we focused our interest on a gene very highly expressed in D492HER2 compared to D492M (and also to D492), namely YKL-40 (also known as CHI3L1). The function of YKL-40 is not clearly understood but it has been suggested to be involved in cancer progression and other inflammation diseases (Libreros *et al*. 2012; Libreros and Iragavarapu-Charyulu 2015; Cohen *et al*. 2017) and even in EMT (Jefri *et al*. 2015).

Genes differentially expressed within the range of two fold change between D492M and D492HER2 were further classified using PANTHER analysis (Mi *et al*. 2013) in order to establish the biological processes that were enriched in each cell line. Genes more highly expressed in D492HER2 compared to D492M were shown to be involved in the following biological processes: D-aspartate transport, inflammatory response, cell chemotaxis, cellular response to cytokine stimulus, defense response, cellular response to cytokine stimulus, cell proliferation, and organic anion transport, among others (Fig. 2b). Interestingly, YKL-40 was found enriched in four of the 18 groups, as highlighted in yellow in Fig. 2b.

Complementing the gene expression data, we also measured by mass spectrometry the secretion of the proteins by D492M and D492HER2. Analysis of the total secreted



proteins in the conditioned media (CM) from D492M and D492HER2 revealed YKL-40 was found in much higher concentration in CM from D492HER2 (97.8 LFQ intensity) than D492M (5.4 LFQ intensity) (Fig. 2*c*). After these promising results, we strengthened our focus on YKL-40 as a firm candidate that could lead to differences between D492M and D492HER2.

Knockdown of YKL-40 in D492HER2 inhibits migration and invasion To explore the functional role of YKL-40 in

◀ **Figure 4.** YKL-40 expression in D492HER2 is linked to increased potential to stimulate angiogenesis. (*a*) Conditioned media (CM) from D492HER2 cells stimulates angiogenesis in an in vitro angiogenesis assay. This effect was abrogated upon YKL-40 neutralization by a monoclonal antibody (mA^{YKL40}) but rescued by the addition of recombinant YKL-40 protein ($YKL40^{r}$) (*Scalebar* = 200 μm). (i) Parameters of angiogenesis were measured and analyzed by ImageJ angiogenesis analyzer plug (mean ± SD) and significance was assessed with one-way analysis of variance (ANOVA) and Tukey's multiple comparison test ($*p \leq 0.05$). (ii) Decreased concentration of YKL-40 upon incubation of cells with mA^{YKL40} was verified with ELISA. Significance was tested with an unpaired t-test ($****p \leq 0.0001$). (*b*) When YKL-40 was overexpressed in D492 and D492M, there was an increase in the capillary network formation, whereas stable knockdown of YKL-40 in D492HER2 showed a tendency to reduced capillary network formation. (*c*) Knockdown of YKL-40 reduced the expression of other pro-angiogenic inducers, VEGFA and VEGFC. (*d*) Finally, recombinant YKL-40 protein ($YKL-40^{r}$) induced proliferation of endothelial cells when added to the media. Unpaired *t* test was used to test significance ($**p \leq 0.01$, $***p \leq 0.001$).

D492HER2, we did both transient and stable knockdown (KD). First, we confirmed the expression of YKL-40 at mRNA and protein level in D492, D492M, and D492HER2 demonstrating its abundant expression in D492HER2 (Fig. 3*a*). Transient knockdown with two different siRNAs greatly reduced YKL-40 expression in D492HER2 cells (Fig. 3*b*) and resulted in a significant decrease in migration and invasion (Fig. 3*c*). To further corroborate these effects, we generated stable YKL-40 KD using CRISPR technology in D492HER2 cells (Fig. 3*d*). Similar to transient KD of YKL-40, the stable KD cell line showed a reduction in migration and invasion compared to control D492HER2 cells (Fig. 3*e*). To analyze if overexpression of YKL-40 in D492 and D492M resulted in increased migration and invasion, we stably overexpressed YKL-40 in these cells and, indeed, this resulted in a large increase in both migration and invasion (Fig. 3*f*, *g*). No differences were seen with regard to cell proliferation regardless if YKL-40 was knocked down in D492HER2 or overexpressed in D492/D492M (data not shown). Collectively, these results demonstrate that in our cell system, YKL-40 increases migration and invasion.

YKL-40 expression in D492HER2 is linked to vascular network formation YKL-40 has previously been linked to angiogenesis (Shao *et al*. 2009, 2011). In order to see if increased expression of YKL-40 in D492HER2 was linked to increased potential to stimulate angiogenesis in an in vitro assay, we treated HUVECs on top of Matrigel with CM from D492HER2 with and without a functional blocking antibody against YKL-40 (mA^{YKL40}). Blocking YKL-40 directly reduced the ability of CM medium to induce HUVECs to form capillary-like networks. This blocking effect was reversed by adding recombinant YKL-40 protein ($YKL-40^{r}$) (Fig. 4*a*).

In agreement, CM from D492 and D492M stably overexpressing YKL-40 increased HUVEC network formation on top of Matrigel, whereas stable knockdown of YKL-40 in D492HER2 cells reduced HUVECs network formation (Fig. 4*b*). Additionally, the reduction of YKL-40 in the stable cell line revealed reduced expression of other pro-angiogenic genes, like VEGF-A and VEGF-C (Fig. 4*c*), suggesting a synergic pro-angiogenic effect induced in D492HER2. Furthermore, adding recombinant YKL-40 protein ($YKL-40^{r}$) to media not only stimulated tube formation on endothelial cells, but also increased proliferation rates of HUVECs (Fig. 4d).

YKL-40 affects phenotype of D492 cell lines when cultured in 3D culture When YKL-40 was downregulated in D492HER2 by transient or stable transfection, no phenotypic changes were seen in monolayer culture and EMT markers in immunostaining and western blot did not show any differences; thus, the EMT phenotype remained unaltered in 2D. Due to the transient nature of using siRNA, it was difficult to explore if there were any phenotypic changes occurring in 3D culture. In contrast, 3D culturing of cells with stable knockdown of YKL-40 revealed differences in phenotype of the D492 cell lines.

In 3D culture, D492HER2 formed two colony shapes, spindle-like and grape-like (Ingthorsson *et al*. 2015). Interestingly, when YKL-40 was knocked down, there was a dramatic change in the proportion of spindle-like and grape-like structures, with the proportion of grape-like structures being reduced from 21.4% to 1% (Fig. 5*a*). This subsequent change in the 3D phenotype of D492HER2 cells with knockdown of YKL-40 was similar to D492M cells that only showed a spindle-like phenotype (Sigurdsson *et al*. 2011). However, when the recombinant YKL-40 protein ($YKL-40^{r}$) was added to the media of D492HER2 with YKL-40 KD, the grape-like structures were rescued to 32.8% of the total 3D structures (Fig. 5*a*).

To confirm the shift to grape-like structures with the addition of YKL-40, D492M cells overexpressing YKL-40 were seeded in 3D cell culture. Remarkably, the entire cell population lost the ability to form spindle-like structures, and instead only grape-like structures were observed (Fig. 5*b*).

Discussion

In this study, we compared phenotypic and functional differences between two isogenic cell lines that share a partial-EMT phenotype but differ in terms of oncogenic properties. D492M is non-tumorigenic, whereas D492HER2 is tumorigenic. We identified YKL-40, also known as a chitinase-3-like protein 1 (CHI3L1), as a protein highly expressed and secreted in D492HER2 compared to D492M. Functional in vitro studies demonstrated that YKL-40 is involved in migration and invasion of D492HER2. Furthermore, blocking YKL-40 in conditioned media (CM) from D492HER2 reduced the ability of the

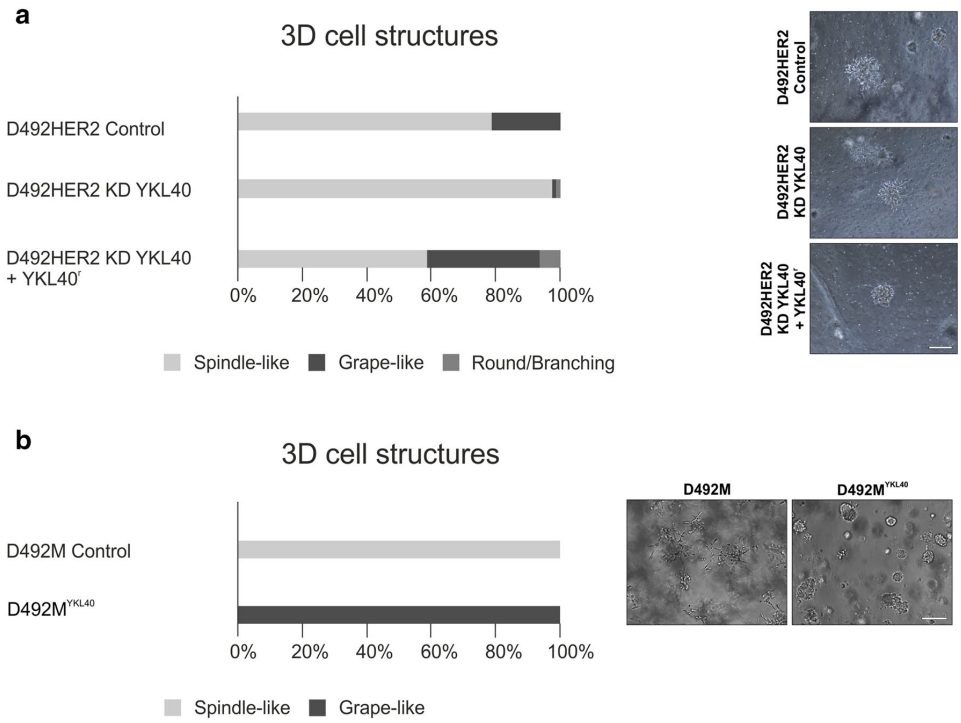


Figure 5. YKL-40 affects the phenotype of D492 cell lines in 3D. *a* CRISPR/Cas9-mediated knockdown of YKL-40 in D492HER2 cells, increased the number of spindle-like structures in a 3D culture, but grape-like structures were recovered with addition of recombinant YKL-40 protein ($YKL40^r$) to the media (*Scalebar* = 200 μm). *b* Overexpression of YKL-40 in D492M shifted the phenotype from spindle-like structures to grape-like structures in 3D (Scalebar = 200 μm).

D492HER2-derived CM to induce formation of capillary like network in an in vitro angiogenesis assay, which conversely can be rescued with the addition of recombinant YKL-40 protein. Finally, KD of YKL-40 in D492HER2 changed the ratio of spindle- and grape-like structures in favor of spindle-like structures, which could be reverted when the recombinant protein was added to the KD cells in 3D culture.

The term EMT is used for describing phenotypic changes where epithelial cells lose and gain epithelial and mesenchymal traits, respectively. Very rarely, a complete EMT occurs, and rather intermediate states are the most frequent phenotypes. Thus, it is common that traces of epithelial traits remain and a full mesenchymal phenotype is often incomplete resulting in a large spectrum of EMT phenotypes (Nieto 2013).

D492M and D492HER2 share some EMT properties such as loss of E-cadherin and cytokeratins and formation of a spindle-shaped phenotype in monolayer. D492M has a more fixed EMT phenotype with low or absent expression of epithelial markers, including microRNAs, and gain of mesenchymal markers (Sigurdsson *et al*. 2011; Hilmarsdottir *et al*. 2015). In a recent paper, we demonstrated that reintroduction of miR-200c-141 into D492M was sufficient to revert the phenotype to epithelial lineage, albeit only to luminal epithelial cells. Further studies demonstrated that the basal cell transcription factor P63 was necessary to recover the basal/myoepithelial phenotype. Co-transfection of miR-200c-141 and P63 into D492M was sufficient to regain the original phenotype of D492 (Hilmarsdottir *et al*. 2015). On the other hand, D492HER2 shows more intermediate EMT phenotype than D492M and could be defined as a cell line with partial-EMT (Ingthorsson *et al*. 2015). Even though D492HER2 migrates, invades, and proliferates more, it is more susceptible to apoptosis, its glucose metabolism is more similar to the one in the epithelial cell line (D492), and the expression levels of the regulatory epithelial miRNAs are reduced but not as dramatic as in the case of D492M. Moreover, there are evident phenotypic differences between these two cell lines when cultured in 3D in reconstituted basement membrane matrix, as D492M forms exclusively spindle-shaped EMT-like colonies in contrast to D492HER2 that forms mixture of spindle-shape and grape-like colonies.

Triple-negative breast cancer cell lines are often spindle-shaped with more prominent EMT phenotype in 3D rBM while cell lines with high HER2 expression are associated with grape-like phenotype (Han *et al*. 2010). We have previously shown that D492M and D492HER2 form spindle-shaped and grape-like structures in 3D rBM, respectively (Sigurdsson *et al*. 2011; Ingthorsson *et al*. 2016). That overexpression of YKL-40 in D492M shifts the phenotype toward grape-like structures may indicate that YKL-40 confers increased plasticity to D492M. Further studies in our laboratory aim to unravel whether YKL-40 expression is associated with tumorigenic potential of D492M and D492HER2.

Comparing and analyzing gene-wide expression and protein-wide secretion of D492M and D492HER2, YKL-40 was the most relevant candidate to study the differences between the cell lines. YKL-40 is a secreted glycoprotein of a still unclear function. The protein belongs to the chitinase family, but it lacks hydrolase activity (Renkema *et al*. 1998). It is expressed by several cell types including macrophages, neutrophils, epithelial cells, synovial cells, chondrocytes, smooth muscle cells, and some cancer cells (Recklies *et al*. 2002; Johansen *et al*. 2006). It is suggested to be involved in inflammation and angiogenesis, as well as survival and growth in tumors (Johansen *et al*. 2006). It is highly secreted in inflammation diseases (Roslind and Johansen 2009; Bonneh-Barkay *et al*. 2010) and some cancers, such as breast cancer, melanoma, glioblastoma, or small cell lung carcinoma (Johansen *et al*. 2006; Shao *et al*. 2011; Jefri *et al*. 2015; Libreros and Iragavarapu-Charyulu 2015). Recently, it has been linked to idiopathic pulmonary fibrosis (Zhou *et al*. 2014) and immunosuppressive effects by cancer-associated fibroblasts in breast cancer (Cohen *et al*. 2017).

We have confirmed here that changes in intrinsic expression of YKL-40 in D492HER2 lead to differences in migration and invasion behavior of the cells. When YKL-40 is downregulated by transient or stable knockdown, D492HER2 becomes less migrative and invasive. Migration and invasion are important processes that support cancer development and progression (Hanahan and Weinberg 2011) what indicates that YKL-40 may play a key role in invasiveness and dissemination of cancer cells.

YKL-40 has been previously linked to EMT in non-small cell lung cancer (Jefri *et al*. 2015), yet in our study, when YKL-40 was downregulated in D492HER2, its EMT phenotype in monolayer remained unaltered and there were no differences in expression of EMT markers. Nevertheless, high expression of YKL-40 or the addition of the recombinant protein has been related to an increase in the grape-shaped colonies in 3D cell cultures of the EMT-derived cell lines. This fact suggests that YKL-40 may have been involved in the plasticity of the cells, as the phenotype in 3D was changed when its expression was reduced in D492HER2 and then rescued when the recombinant protein was added. This is also interesting, since the grape-like structures are often associated with HER2-expressing cell lines (Kenny *et al*. 2007).

A number of papers have shown association between YKL-40 and HER2 expression in breast cancer. Wang *et al*. showed by meta-analysis of existing databases that YKL-40 is associated with poor prognosis in breast cancer patients (Wan *et al*. 2017). Kang *et al*. have demonstrated that YKL-40 expression in breast cancer is associated with Her-2 and basal-like molecular subtype of breast cancer (Kang *et al*. 2014). Also, Shao *et al*. showed an association between YKL-40 and Her2 subtype (Shao *et al*. 2011). Although, the association between YKL-40 and HER2 has been demonstrated, it is, however, to our best knowledge, still not clear if there are any direct or indirect molecular interactions between these two proteins in breast cancer. Using the breast mark database (Madden *et al*. 2013), we were however not able to link high or low expression of CHI3L1 in distinct subtype of breast cancer to increased or reduced survival.

PANTHER classification of the differentially regulated genes showed that YKL-40 is in enriched in biological processes related to interactions with the microenvironment that can support the development of tumors by cancer cells (inflammatory response, cell chemotaxis, cellular response to cytokine stimulus, and defense response). We demonstrate here that YKL-40 interacts with the microenvironment and more concretely is contributing to the angiogenesis-inducing effect of D492HER2.

We have demonstrated that YKL-40 secreted by D492HER2 has a role in angiogenesis. When YKL-40 protein is reduced in the media by a specific YKL-40 blocking antibody or stable knockdown in D492HER2, angiogenesis is decreased. Conversely, increased levels of YKL-40 in the CM by the addition of recombinant YKL-40 protein or secreted by the cell line reverted the effects to standard tube formation parameters.

Interestingly, the reduction of YKL-40 in D492HER2 by the stable knockdown cell line revealed the reduction of the expression of other pro-angiogenic genes, including VEGF-A and VEGF-C. These genes encode protein ligands that bind and activate VEGF receptor 2 (VEGFR2, Flk-1/KDR), one of the main receptors implicated in the induction of angiogenesis in endothelial cells (Carmeliet and Jain 2000; Harper and Bates 2008). Indeed, it has been shown that a monoclonal antibody against YKL-40 abolishes YKL-40-induced activation of the membrane VEGF receptor 2 and intracellular signaling mitogen-activated protein (MAP) kinase extracellular signal-regulated kinase (Erk) 1 and Erk 2 (Faibish *et al*. 2011).

However, the role of YKL-40 in cancer progression may not be exclusively derived from cancer cells and not limited to promote interactions with endothelial cells. Recently, it has been described that YKL-40 is highly secreted by fibroblasts

associated to cancer (CAFs) in breast-promoting tumor growth and facilitating metastasis. Moreover, YKL-40 released by CAFs supports recruitment of macrophages and promotes the switch to tumor-associated macrophages (TAMs) (Cohen *et al.* 2017). Furthermore, TAMs in breast cancer express YKL-40 where the secreted protein increases inflammation and angiogenesis leading to a worse prognosis and conceivably to metastasis (Shao 2013). Collectively, this suggests that YKL-40 has a complex role in malignancy that may provide the signals for further progression involving changes within cancer cells to migrate and invade and interact with cells of the surrounding stroma. Moreover, it also may provide feedback from the microenvironment to support cancer development, tumor growth, and incrementation of dissemination of cancer cells in metastasis.

Conclusion

In conclusion, our data suggest that YKL-40 may provide D492HER2 with increased aggressiveness, evidenced by enhanced migration and invasion. Furthermore, YKL-40 may also support cancer progression by facilitating angiogenesis and may therefore be of interest as a potential novel therapeutic target in HER2-positive breast cancer.

Acknowledgments This work was supported by Grants from Landspitali University Hospital Science Fund, University of Iceland Research Fund, and Icelandic Science and Technology Policy—Grant of Excellence: 152144051. 'Göngum saman,' a supporting group for breast cancer research in Iceland (www.gongumsaman.is). The funders had no role in study design, data collection and analysis, decision to publish, or preparation of the manuscript.

Open Access This article is distributed under the terms of the Creative Commons Attribution 4.0 International License (http://creativecommons.org/licenses/by/4.0/), which permits unrestricted use, distribution, and reproduction in any medium, provided you give appropriate credit to the original author(s) and the source, provide a link to the Creative Commons license, and indicate if changes were made.

References

Al-Hajj M, Wicha MS, Benito-Hernandez A, Morrison SJ, Clarke MF (2003) Prospective identification of tumorigenic breast cancer cells. Proc Natl Acad Sci U S A 100(7):3983–3988

Blaschke RJ, Howlett AR, Desprez PY, Petersen OW, Bissell MJ (1994) Cell differentiation by extracellular matrix components. Methods Enzymol 245:535–556

Bonneh-Barkay D, Wang G, Starkey A, Hamilton RL, Wiley CA (2010) In vivo CHI3L1 (YKL-40) expression in astrocytes in acute and chronic neurological diseases. J Neuroinflammation 7:34

Brabletz T (2012) EMT and MET in metastasis: where are the cancer stem cells? Cancer Cell 22(6):699–701

Briem E, Ingthorsson S, Traustadottir GA, Hilmarsdottir B, Gudjonsson T (2019) Application of the D492 cell lines to explore breast morphogenesis, EMT and cancer progression in 3D culture. J Mammary Gland Biol Neoplasia 24(2):139–147

Burk U, Schubert J, Wellner U, Schmalhofer O, Vincan E, Spaderna S, Brabletz T (2008) A reciprocal repression between ZEB1 and members of the miR-200 family promotes EMT and invasion in cancer cells. EMBO Rep 9(6):582–589

Carmeliet P, Jain RK (2000) Angiogenesis in cancer and other diseases. Nature 407(6801):249–257

Cohen N, Shani O, Raz Y, Sharon Y, Hoffman D, Abramovitz L, Erez N (2017) Fibroblasts drive an immunosuppressive and growth-promoting microenvironment in breast cancer via secretion of chitinase 3-like 1. Oncogene 36(31):4457–4468

DeCastro AJ, Dunphy KA, Hutchinson J, Balboni AL, Cherukuri P, Jerry DJ, DiRenzo J (2013) MiR203 mediates subversion of stem cell properties during mammary epithelial differentiation via repression of DeltaNP63alpha and promotes mesenchymal-to-epithelial transition. Cell Death Dis 4:e514

Faibish M, Francescone R, Bentley B, Yan W, Shao R (2011) A YKL-40-neutralizing antibody blocks tumor angiogenesis and progression: a potential therapeutic agent in cancers. Mol Cancer Ther 10(5):742–751

Gjerdrum C, Tiron C, Hoiby T, Stefansson I, Haugen H, Sandal T, Collett K, Li S, McCormack E, Gjertsen BT, Micklem DR, Akslen LA, Glackin C, Lorens JB (2010) Axl is an essential epithelial-to-mesenchymal transition-induced regulator of breast cancer metastasis and patient survival. Proc Natl Acad Sci U S A 107(3):1124–1129

Gudjonsson T, Villadsen R, Nielsen HL, Ronnov-Jessen L, Bissell MJ, Petersen OW (2002) Isolation, immortalization, and characterization of a human breast epithelial cell line with stem cell properties. Genes Dev 16(6):693–706

Halldorsson S, Rohatgi N, Magnusdottir M, Choudhary KS, Gudjonsson T, Knutsen E, Barkovskaya A, Hilmarsdottir B, Perander M, Mælandsmo GM, Gudmundsson S, Rolfsson Ó (2017) Metabolic re-wiring of isogenic breast epithelial cell lines following epithelial to mesenchymal transition. Cancer Lett 396:117–129

Han, J., et al., Molecular predictors of 3D morphogenesis by breast cancer cell lines in 3D culture. PLoS Comput Biol, 2010. 6(2): p. e1000684.

Hanahan D, Weinberg RA (2011) Hallmarks of cancer: the next generation. Cell 144(5):646–674

Harper SJ, Bates DO (2008) VEGF-A splicing: the key to anti-angiogenic therapeutics? Nat Rev Cancer 8(11):880–887

Hilmarsdottir B, Briem E, Bergthorsson JT, Magnusson MK, Gudjonsson T (2014) Functional role of the microRNA-200 family in breast morphogenesis and neoplasia. Genes (Basel) 5(3):804–820

Hilmarsdottir B, Briem E, Sigurdsson V, Franzdottir SR, Ringner M, Arason AJ, Bergthorsson JT, Magnusson MK, Gudjonsson T (2015) MicroRNA-200c-141 and Np63 are required for breast epithelial differentiation and branching morphogenesis. Dev Biol 403(2):150–161

Huang RY, Wong MK, Tan TZ, Kuay KT, Ng AH, Chung VY, Chu YS, Matsumura N, Lai HC, Lee YF, Sim WJ, Chai C, Pietschmann E, Mori S, Low JJ, Choolani M, Thiery JP (2013) An EMT spectrum defines an anoikis-resistant and spheroidogenic intermediate mesenchymal state that is sensitive to e-cadherin restoration by a src-kinase inhibitor, saracatinib (AZD0530). Cell Death Dis 4:e915

Ingthorsson, S., et al., HER2 induced EMT and tumorigenicity in breast epithelial progenitor cells is inhibited by coexpression of EGFR. Oncogene, 2016. 35(32): p. 4244–55.

Ingthorsson S *et al* (2015) HER2 induced EMT and tumorigenicity in breast epithelial progenitor cells is inhibited by coexpression of EGFR. Oncogene 35(32):4244–4255

Ingthorsson S, Andersen K, Hilmarsdottir B, Maelandsmo GM, Magnusson MK, Gudjonsson T (2016) HER2 induced EMT and tumorigenicity in breast epithelial progenitor cells is inhibited by coexpression of EGFR. Oncogene 35(32):4244–4255

Ingthorsson S, Sigurdsson V, Fridriksdottir AJ, Jonasson JG, Kjartansson J, Magnusson MK, Gudjonsson T (2010) Endothelial cells stimulate growth of normal and cancerous breast epithelial cells in 3D culture. BMC Res Notes 3(1):184

Jefri M, Huang YN, Huang WC, Tai CS, Chen WL (2015) YKL-40 regulated epithelial-mesenchymal transition and migration/invasion enhancement in non-small cell lung cancer. BMC Cancer 15:590

Johansen JS, Jensen BV, Roslind A, Nielsen D, Price PA (2006) Serum YKL-40, a new prognostic biomarker in cancer patients? Cancer Epidemiol Biomark Prev 15(2):194–202

Kalluri R, Weinberg RA (2009) The basics of epithelial-mesenchymal transition. J Clin Invest 119(6):1420–1428

Kang EJ, Jung H, Woo OH, Park KH, Woo SU, Yang DS, Kim AR, Lee JB, Kim YH, Kim JS, Seo JH (2014) YKL-40 expression could be a poor prognostic marker in the breast cancer tissue. Tumour Biol 35(1):277–286

Kasai H, Allen JT, Mason RM, Kamimura T, Zhang Z (2005) TGF-beta1 induces human alveolar epithelial to mesenchymal cell transition (EMT). Respir Res 6:56

Kenny PA, Lee GY, Myers CA, Neve RM, Semeiks JR, Spellman PT, Lorenz K, Lee EH, Barcellos-Hoff MH, Petersen OW, Gray JW, Bissell MJ (2007) The morphologies of breast cancer cell lines in three-dimensional assays correlate with their profiles of gene expression. Mol Oncol 1(1):84–96

Korpal M, Lee ES, Hu G, Kang Y (2008) The miR-200 family inhibits epithelial-mesenchymal transition and cancer cell migration by direct targeting of E-cadherin transcriptional repressors ZEB1 and ZEB2. J Biol Chem 283(22):14910–14914

Libreros S, Garcia-Areas R, Shibata Y, Carrio R, Torroella-Kouri M, Iragavarapu-Charyulu V (2012) Induction of proinflammatory mediators by CHI3L1 is reduced by chitin treatment: decreased tumor metastasis in a breast cancer model. Int J Cancer 131(2):377–386

Libreros S, Iragavarapu-Charyulu V (2015) YKL-40/CHI3L1 drives inflammation on the road of tumor progression. J Leukoc Biol 98(6):931–936

Madden SF, Clarke C, Gaule P, Aherne ST, O'Donovan N, Clynes M, Crown J, Gallagher WM (2013) BreastMark: an integrated approach to mining publicly available transcriptomic datasets relating to breast cancer outcome. Breast Cancer Res 15(4):R52

Mani SA, Guo W, Liao MJ, Eaton EN, Ayyanan A, Zhou AY, Brooks M, Reinhard F, Zhang CC, Shipitsin M, Campbell LL, Polyak K, Brisken C, Yang J, Weinberg RA (2008) The epithelial-mesenchymal transition generates cells with properties of stem cells. Cell 133(4):704–715

Mi H, Muruganujan A, Casagrande JT, Thomas PD (2013) Large-scale gene function analysis with the PANTHER classification system. Nat Protoc 8:1551–1566

Moes M, Le Bechec A, Crespo I, Laurini C, Halavatyi A, Vetter G, del Sol A, Friederich E (2012) A novel network integrating a miRNA-203/SNAI1 feedback loop which regulates epithelial to mesenchymal transition. PLoS One 7(4)

Morel AP, Lievre M, Thomas C, Hinkal G, Ansieau S, Puisieux A (2008) Generation of breast cancer stem cells through epithelial-mesenchymal transition. PLoS One 3(8):e2888

Nieto MA (2013) Epithelial plasticity: a common theme in embryonic and cancer cells. Science 342(6159):1234850

Peinado H, Olmeda D, Cano A (2007) Snail, Zeb and bHLH factors in tumour progression: an alliance against the epithelial phenotype? Nat Rev Cancer 7(6):415–428

Polyak K, Weinberg RA (2009) Transitions between epithelial and mesenchymal states: acquisition of malignant and stem cell traits. Nat Rev Cancer 9(4):265–273

Recklies AD, White C, Ling H (2002) The chitinase 3-like protein human cartilage glycoprotein 39 (HC-gp39) stimulates proliferation of human connective-tissue cells and activates both extracellular signal-regulated kinase- and protein kinase B-mediated signalling pathways. Biochem J 365(1):119–126

Relf M, LeJeune S, Scott PA, Fox S, Smith K, Leek R, Moghaddam A, Whitehouse R, Bicknell R, Harris AL (1997) Expression of the angiogenic factors vascular endothelial cell growth factor, acidic and basic fibroblast growth factor, tumor growth factor beta-1, platelet-derived endothelial cell growth factor, placenta growth factor, and pleiotrophin in human primary breast cancer and its relation to angiogenesis. Cancer Res 57(5):963–969

Renkema GH, Boot RG, Au FL, Donker-Koopman WE, Strijland A, Muijsers AO, Hrebicek M, Aerts JM (1998) Chitotriosidase, a chitinase, and the 39-kDa human cartilage glycoprotein, a chitin-binding lectin, are homologues of family 18 glycosyl hydrolases secreted by human macrophages. Eur J Biochem 251(1–2):504–509

Roslind A, Johansen JS (2009) YKL-40: a novel marker shared by chronic inflammation and oncogenic transformation. Methods Mol Biol 511:159–184

Sarrio D, Rodriguez-Pinilla SM, Hardisson D, Cano A, Moreno-Bueno G, Palacios J (2008) Epithelial-mesenchymal transition in breast cancer relates to the basal-like phenotype. Cancer Res 68(4):989–997

Shao R (2013) YKL-40 acts as an angiogenic factor to promote tumor angiogenesis. Front Physiol 4:122

Shao R, Cao QJ, Arenas RB, Bigelow C, Bentley B, Yan W (2011) Breast cancer expression of YKL-40 correlates with tumour grade, poor differentiation, and other cancer markers. Br J Cancer 105(8):1203–1209

Shao R, Hamel K, Petersen L, Cao QJ, Arenas RB, Bigelow C, Bentley B, Yan W (2009) YKL-40, a secreted glycoprotein, promotes tumor angiogenesis. Oncogene 28(50):4456–4468

Shekhar MP, Werdell J, Tait L (2000) Interaction with endothelial cells is a prerequisite for branching ductal-alveolar morphogenesis and hyperplasia of preneoplastic human breast epithelial cells: regulation by estrogen. Cancer Res 60(2):439–449

Sigurdsson V, Fridriksdottir AJ, Kjartansson J, Jonasson JG, Steinarsdottir M, Petersen OW, Ogmundsdottir HM, Gudjonsson T (2006) Human breast microvascular endothelial cells retain phenotypic traits in long-term finite life span culture. In Vitro Cell Dev Biol Anim 42(10):332–340

Sigurdsson V, Hilmarsdottir B, Sigmundsdottir H, Fridriksdottir AJ, Ringner M, Villadsen R, Borg A, Agnarsson BA, Petersen OW, Magnusson MK, Gudjonsson T (2011) Endothelial induced EMT in breast epithelial cells with stem cell properties. PLoS One 6(9):e23833

Sonveaux P, Copetti T, De Saedeleer CJ, Vegran F, Verrax J, Kennedy KM, Moon EJ, Dhup S, Danhier P, Frerart F, Gallez B, Ribeiro A, Michiels C, Dewhirst MW, Feron O (2012) Targeting the lactate transporter MCT1 in endothelial cells inhibits lactate-induced HIF-1 activation and tumor angiogenesis. PLoS One 7(3):e33418

Stingl J (2006) Purification and unique properties of mammary epithelial stem cells. Nature 439:993–997

Tam WL, Weinberg RA (2013) The epigenetics of epithelial-mesenchymal plasticity in cancer. Nat Med 19(11):1438–1449

Tan TZ, Miow QH, Miki Y, Noda T, Mori S, Huang RY, Thiery JP (2014) Epithelial-mesenchymal transition spectrum quantification and its efficacy in deciphering survival and drug responses of cancer patients. EMBO Mol Med 6(10):1279–1293

Thiery JP (2002) Epithelial-mesenchymal transitions in tumour progression. Nat Rev Cancer 2(6):442–454

Thiery JP, Acloque H, Huang RY, Nieto MA (2009) Epithelial-mesenchymal transitions in development and disease. Cell 139(5):871–890

Vegran F, Boidot R, Michiels C, Sonveaux P, Feron O (2011) Lactate influx through the endothelial cell monocarboxylate transporter MCT1 supports an NF-kappaB/IL-8 pathway that drives tumor angiogenesis. Cancer Res 71(7):2550–2560

Wan G, Xiang L, Sun X, Wang X, Li H, Ge W, Cao F (2017) Elevated YKL-40 expression is associated with a poor prognosis in breast cancer patients. Oncotarget 8(3):5382–5391

Wiklund ED, Bramsen JB, Hulf T, Dyrskjot L, Ramanathan R, Hansen TB, Villadsen SB, Gao S, Ostenfeld MS, Borre M, Peter ME, Orntoft TF, Kjems J, Clark SJ (2010) Coordinated epigenetic repression of the miR-200 family and miR-205 in invasive bladder cancer. Int J Cancer 128(6):1327–1334

Willis BC, Borok Z (2007) TGF-beta-induced EMT: mechanisms and implications for fibrotic lung disease. Am J Physiol Lung Cell Mol Physiol 293(3):L525–L534

Yang MH, Wu MZ, Chiou SH, Chen PM, Chang SY, Liu CJ, Teng SC, Wu KJ (2008) Direct regulation of TWIST by HIF-1alpha promotes metastasis. Nat Cell Biol 10(3):295–305

Yu M, Bardia A, Wittner BS, Stott SL, Smas ME, Ting DT, Isakoff SJ, Ciciliano JC, Wells MN, Shah AM, Concannon KF, Donaldson MC, Sequist LV, Brachtel E, Sgroi D, Baselga J, Ramaswamy S, Toner M, Haber DA, Maheswaran S (2013) Circulating breast tumor cells exhibit dynamic changes in epithelial and mesenchymal composition. Science 339(6119):580–584

Zhang, Y., Yin, C., Zhang, T., Li, F., Yang, W., Kaminski, R. et al. (2015). CRISPR/gRNA-directed synergistic activation mediator (SAM) induces specific, persistent and robust reactivation of the HIV-1 latent reservoirs. Scientific Reports, 5(1). https://doi.org/10.1038/srep16277

Zhou Y, Peng H, Sun H, Peng X, Tang C, Gan Y, Chen X, Mathur A, Hu B, Slade MD, Montgomery RR, Shaw AC, Homer RJ, White ES, Lee CM, Moore MW, Gulati M, Lee CG, Elias JA, Herzog EL (2014) Chitinase 3-like 1 suppresses injury and promotes fibroproliferative responses in Mammalian lung fibrosis. Sci Transl Med 6(240):240ra276

Supplemental data.

Figure S1

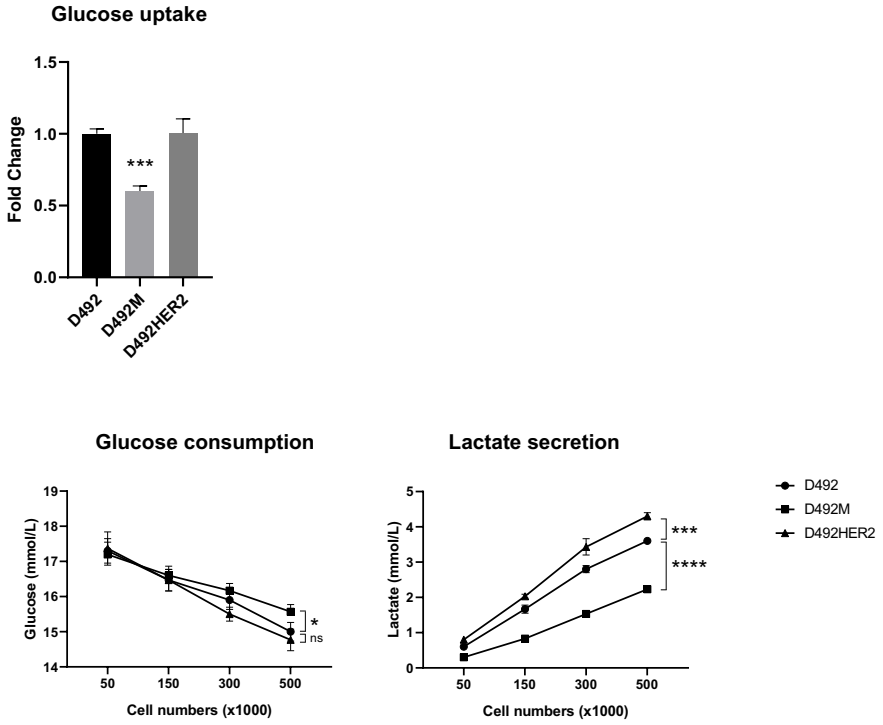


Figure S1. Glucose metabolism in D492HER2 is more comparable to D492, rather than D492M. Analysis of glucose metabolism in D492, D492M and D492HER2 reveals a shift from oxidative phosphorylation to glycolysis in D492HER2 compared to D492M, as it takes up and consumes more glucose and produces and secretes more lactate than D492M. Thus, glucose metabolism of D492HER2 is more similar to D492, suggesting a more intermediate partial EMT phenotype than D492M. Statistical significance was tested using one-way analysis of variance (ANOVA) followed by Dunnett's multiple comparison test and multiple t-test to assess statistical difference between D492 and other two cell lines, D492M and D492HER2 (*$p \leq 0.05$, ***$p \leq 0.001$, ****$p \leq 0.0001$).